DISSERTATION

Characterization of amicarbalide derivatives as new antimalarial compounds:

Investigation of the mode of action and the mechanism of resistance

submitted to the

Combined Faculties for the Natural Sciences and for Mathematics

of the Ruperto-Carola University of Heidelberg, Germany

for the degree of Doctor of Natural Sciences

presented by

Maëlle Duffey (M. Sc.)

Referees: *Prof. Dr. Michael Lanzer*

Prof. Dr. Christine Clayton

Dissertation

submitted to the

Combined Faculties for the Natural Sciences and for Mathematics

of the Ruperto-Carola University of Heidelberg, Germany

for the degree of

Doctor of Natural Sciences

presented by

Maëlle Duffey (M. Sc.)

born in Poissy, France

Date of oral examination: ……..

Characterization of amicarbalide derivatives as new antimalarial compounds:

Investigation of the mode of action and the mechanism of resistance

Referees: *Prof. Dr. Michael Lanzer*

Prof. Dr. Christine Clayton

Ich erkläre hiermit, dass ich die vorliegende Doktorarbeit selbstständig unter Anleitung verfasst und keine anderen als die angegebenen Quellen und Hilfsmittel benutzt habe.

Ich erkläre hiermit, dass ich an keiner anderen Stelle ein Prüfungsverfahren beantragt bzw. die Dissertation in dieser oder anderer Form bereits anderweitig als Prüfungsarbeit verwendet oder einer anderen Fakultät als Dissertation vorgelegt habe.

Die vorliegende Arbeit wurde am Department für Infektiologie, Abteilung Parasitologie des Universitätsklinikum Heidelberg in der Zeit von August 2014 bis Februar 2018 unter der Leitung von Prof. Dr. Michael Lanzer ausgeführt.

…… ……

Datum Maëlle Duffey

Les graines sont invisibles. Elles dorment dans le secret de la terre jusqu'à ce qu'il prenne fantaisie à l'une d'entre elle de se réveiller.

Antoine de Saint-Exupéry

Le Petit Prince (1946)

Table of contents

Acknowledgements ..... **I**
Summary ..... **III**
Zusammenfassung ..... **IV**
Abbreviations ..... **V**
1. Introduction **1**
1.1. Malaria – a major human infectious disease 1
1.1.1. Origin and history 1
1.1.2. Clinical manifestations 1
1.1.3. Global impact and eradication strategy 2
1.2. *Plasmodium falciparum´*s biology 4
1.2.1. Life cycle of *Plasmodium falciparum* 4
1.2.2. Calcium homeostasis in *P. falciparum*: the role of PfATP6 6
1.2.2.1. Calcium homeostasis in *Plasmodium* 6
1.2.2.2. PfATP6: the *P. falciparum* SERCA 8
1.2.2.3. The PfATP6 - artemisinin controversy 9
1.2.3. Editing *P. falciparum´*s genome 10
1.3. Antimalarial chemotherapies and drug resistance 12
1.3.1. Antimalarial drugs and their mode of action 12
1.3.1.1. Quinolines 13
1.3.1.2. Antifolates 14
1.3.1.3. Inhibitor of the respiratory chain 14
1.3.1.4. Artemisinins and Artemisinin-based Combination Therapies 15
1.3.2. Drug resistance mechanisms 16
1.3.3. Future perspectives for antimalarial drugs 19
1.4. Development of the drug candidate SC83288 for the treatment of severe malaria 21
1.5. Aim of the study 23
2. Materials and methods **25**
2.1. Materials 25
2.1.1. Equipment 25
2.1.2. Disposables 28
2.1.3. Chemicals 29
2.1.4. Biological material 30
2.1.5. Buffers, media and solutions 36
2.2. Methods 43

2.2.1. Cell culture of *Plasmodium falciparum* parasites 43
2.2.1.1. *In vitro* culture conditions 43
2.2.1.2. Morphological monitoring of parasites and determination of parasitemia 43
2.2.1.3. Parasites synchronization with sorbitol 44
2.2.1.4. Cryopreservation and thawing of the parasites 44
2.2.1.5. Magnetic purification of the parasites 45
2.2.1.6. Plasmid DNA transfection of parasites 45
2.2.1.7. Cloning parasites by limiting dilution 46
2.2.2. Microbiological methods 47
2.2.2.1. Preparation of electro-competent PMC 103 *E. coli* bacteria 47
2.2.2.2. Preparation of chemo-competent XL-1-Blue *E. coli* bacteria 48
2.2.2.3. Transformation of electro-competent PMC 103 *E. coli* bacteria 48
2.2.2.4. Transformation of chemo-competent XL1-Blue cells 48
2.2.2.5. Transformation of chemo-competent XL10-Gold Ultracompetent Cells 49
2.2.2.6. Isolation of plasmid DNA from bacteria (Miniprep) 49
2.2.2.7. Isolation of plasmid DNA from bacteria (Maxiprep) 49
2.2.3. Molecular Biology 50
2.2.3.1. Genomic DNA isolation from *P. falciparum* parasites 50
2.2.3.2. RNA isolation from *P. falciparum* parasites 50
2.2.3.3. DNase treatment of the isolated RNA 51
2.2.3.4. Reverse transcription 51
2.2.3.5. Polymerase chain reaction (PCR) 52
2.2.3.6. Quantitative real-time PCR (qRT-PCR) 53
2.2.3.7. Agarose gel electrophoresis and nucleic acids 54
2.2.3.8. Agarose gel extraction and PCR product purification 55
2.2.3.9. Photometric determination of DNA/RNA concentration 55
2.2.3.10. Restriction digestion of DNA 55
2.2.3.11. Dephosphorylation of DNA with alkaline phosphatase 56
2.2.3.12. Ligation of digested DNA fragments 56
2.2.3.13. DNA sequencing 58
2.2.3.14. Pyrosequencing 58
2.2.4. Protein Biochemistry 59
2.2.4.1. Preparation of *P. falciparum* protein extract 59
2.2.4.2. SDS-PAGE electrophoresis 60
2.2.4.3. Visualization of proteins by Coomassie staining 60
2.2.4.4. Western blotting 60
2.2.4.5. Western blot striping 61
2.2.4.6. [^{35}S]-methionine incorporation assay during protein synthesis 61
2.2.5. Growth inhibition assay and determination of IC_{50} values 62

2.2.6. *In vitro* speed of action or “killing speed” experiments....63
2.2.6.1. Relative speed of action assay....64
2.2.6.2. Recrudescence assay....64
2.2.6.3. Dual-color flow cytometry assay....66
2.2.7. *In vitro* drug combination assays....66
2.2.8. Ring Survival assay (RSA)....69
2.2.9. Fitness assay....69
2.2.10. Progression of *P. falciparum* through the life cycle....69
2.2.11. Flow cytometry analysis....70
2.2.12. Microscopy techniques....70
2.2.12.1. Live Fluorescence microscopy....70
2.2.12.2. Immunofluorescence analysis (IFA)....72
2.2.13. Untargeted metabolomics analysis sample preparation....72
2.2.14. Data and statistical analysis....73
3. Results....75
3.1. Characterization of the *in vitro* antiplasmodial activity of SC81458 and SC83288....75
3.1.1. Susceptibility of *P. falciparum* to SC81458 and SC83288....75
3.1.2. SC81458 and SC83288 *in vitro* speed of action in *P. falciparum*....76
3.1.3. Progression of *P. falciparum* over its life cycle upon SC83288 treatment....79
3.1.4. Profiling the SC-lead compounds against artemisinins....82
3.1.4.1. The SC-lead compounds do not interact with artemisinin....82
3.1.4.2. The SC-lead compounds show no cross-resistance with artemisinins....83
3.2. Investigation of the role of PfTAP6 and calcium homeostasis with respect to the SC-lead compounds mode of action and resistance mechanism....86
3.2.1. PfATP6 is not a direct molecular target of the SC-lead compounds....88
3.2.2. Use of the CRISPR/Cas9 system for genetically engineering PfATP6....90
3.2.3. Characterization of the 3D7 PfATP6 ^{F972Y} mutant line....93
3.2.3.1. *P. falciparum* 3D7 PfATP6 ^{F972Y} susceptibility to SC81458 and SC83288....93
3.2.3.2. The PfATP6 ^{F972Y} mutation gives rise to a fitness cost related to calcium homeostasis....96
3.2.4. Overexpression of the PfATP6 T108, T109 variant in *P. falciparum* is altering the susceptibility to SC83288....102
3.2.5. The *pfatp6* amplified locus in Dd2^{SC83288} *P. falciparum* does not carry genes coding for proteins involved in the resistance mechanism to the SC-lead compounds....105
4. Discussion....107
4.1. Characterization of SC83288 *in vitro* antiplasmodial activity as a candidate for clinical development....107
4.2. PfTAP6 is a component of resistance to SC83288....111
5. Conclusion and outlooks....119

6. References 121
7. Appendix I: DNA and proteins sequences 141
8. Appendix II: Plasmid maps 153
9. Appendix III 160
10. Publications and Conference presentations 161

Acknowledgements

Many people contributed in various ways to the completion of this thesis, and I will do my best not to leave anyone out.

I would first like to thank Prof. Dr. Michael Lanzer for giving me the opportunity to join his laboratory and work on such an interesting topic for my PhD thesis. I would like to further thank Prof. Dr. Christine Clayton and Dr. Marcel Deponte for their valuable contributions during my TAC meetings, and Dr. Silvia Portugal and Prof. Dr. Dirk Grimm for their participation in my defense committee. I am also grateful for the help of Dr. Cecilia Sanchez who contributed to the progress of my lab work by providing me with helpful information.

A special thanks to all my lab mates over these years, for creating such a friendly and intellectually stimulating working atmosphere. Thanks to Marina, Stefan, Adi, Sonia, Tina, Britta, Sebastiano, Isa, Clemens, Marvin, Mailin, Hani and Marek. Thanks in particular to Monika for her countless brainstormings with me, and to Nick for correcting my English in all of my reports. Thank you to Dr. Markus Ganter for his fruitful discussions about DNA replication. Thank you to all the practical, bachelor's and master's student who joined us over these years with their refreshing enthusiasm and motivation, especially at times when mine failed me.

Thank you to Miriam and Sandra for helping me through the maze of the German administration system, always with a welcoming smile.

I would also like to thank Verena Schwarz and Gabriella Gatto from the Department for Human Genetics at the Universitätsklinikum Heidelberg for always gracefully letting me use their qPCR systems. I thank Chiatali Chakraborty from the ZMBH for introducing me to the [^{35}S]-methionine incorporation assay. Thank you to our collaborators Dr. Henry Staines and Hatoon Abdullah Niyazi at St George's University in London for performing the complementation assay.

Thank you to Dr. Vibor Laketa for kindly introducing me to the Leica SP5 confocal microscope and always being available for any of my microscopy issue.

Thank you to all my friends, from France, Switzerland, Germany or elsewhere around the world for their moral support during this challenging time. Particularly, thanks to Harmonie and Anne, who proofread this manuscript, and with whom the long skype conversations made me feel like we were not so far away. Thank you to Maro, whose permanent enthusiasm and constant belief in my own abilities made me want to live up to them. Thanks

to Florent, for accompanying me over this journey in Heidelberg, his never-failing support and the countless existential (or not) conversations over beers.

A deep thank you to my former supervisor during my master's thesis at the Institute for Cell Biology and Immunology at the Universität Stuttgart, Dr. Roman Fischer who pushed me early on to learn and work in an independent manner, and without whom I most likely would have never even started as a PhD student.

A great thank to Jam, for his patience and understanding and for pushing me out of the lab to explore (part of) the world with me.

Enfin, un dernier, mais non des moindres, merci à ma famille, tout particulièrement à mes parents Françoise et Jean-Louis pour leur soutien inconditionnel tout au long de mes études et de ces années de doctorat. Bien qu'ils m'aient toujours poussée à me surpasser, ils, ainsi que le reste de ma famille (mes sœurs Aurélie et Céline, beaux-frères Mathieu et Guillaume, ainsi que mes neveux Casimir et Archibald) n'ont jamais hésité à me rappeler, consciemment ou non, que la vie de ne résume pas uniquement à son aspect professionnel.

Summary

Despite the tremendous progress in the fight against malaria during the last two decades, it remains one of the most important infectious diseases worldwide, leading to approximately 500 000 lethal cases annually, mostly among young children. The emergence and spread of resistance of the *Plasmodium* parasites to all the drugs currently available on the market are a major threat to its control and eradication. It moreover emphasizes the dire need for new antimalarial agents with distinct modes of action. Previously, the medicinal chemistry team at the biotechnology company 4SC AG, Munich, presented a series of promising antimalarial compounds, optimized around an amicarbalide backbone. Two agents were selected out of this series as lead-compounds for further studies, namely SC81458 and SC83288.

The work presented here aims to characterize the *in vitro* activity of the SC-lead compounds. First, it revealed them as potent inhibitors of *P. falciparum* blood stage parasites, acting preferentially on late stages. The lack of activity on the ring stages is reflected in their fast speed of action, yet not as fast as artemisinin, the fastest compound described so far, that acts on all blood stages. Importantly, the SC-lead compounds were unaffected by the most common resistance mechanisms to antimalarial drugs used in the clinic. Particularly, no cross-resistance mechanism between artemisinin and its derivatives and the SC-lead compounds was observed, and their antiplasmodial modes of action appeared to be distinct from each other.

The second part of this work focused on the mode of action of the SC-lead compounds and the mechanisms of resistance that the parasite could develop. Although the Ca^{2+} ATPase pump PfATP6 was disproved as a direct molecular target of the SC-lead compounds, it was demonstrated to be implicated in a resistance mechanism. The F972Y mutation and the overexpression of the A108T, A109T variant led to a drastic decrease in the SC-lead compounds responsiveness. The F972Y substitution correlated with an *in vitro* fitness cost for the parasite, which was linked to a lower intracellular calcium resting concentration compared to its parental line. The molecular details of the disturbed calcium homeostasis and its correlation with the resistance to the SC-lead compounds remain to be unraveled.

Overall, the findings of this work demonstrate the promising *in vitro* potency of the SC-lead compounds, particularly SC83288, and highly support its further development into (pre)clinical trials.

Zusammenfassung

Trotz der enormen Fortschritte in den letzten zwei Jahrzehnten im Kampf gegen Malaria bleibt sie eine der wichtigsten Infektionskrankheiten weltweit, die hauptsächlich bei Kleinkindern jährlich zu etwa 500.000 Todesfällen führt. Das Auftreten und die Ausbreitung der Resistenz von Plasmodium-Parasiten gegenüber allen sich derzeit auf dem Markt befindlichen Medikamenten ist eine große Bedrohung für die Kontrolle und Ausrottung der Malaria und betont außerdem die Notwendigkeit neue Malariamittel mit unterschiedlichen Wirkmechanismen zu finden. Zuvor präsentierte das medizinische Chemieteam des Biotechnologieunternehmens 4SC, München, eine Reihe vielversprechender Antimalaria-Wirkstoffe, die um ein Amicarbalid-Rückgrat optimiert wurden. Aus diesen Wirkstoffen wurden zwei Leitverbindungen, SC81458 und SC83288, für weitere Studien ausgewählt.

Die vorliegende Arbeit über die *in vitro*-Aktivität der SC- Leitverbindungen offenbarte sie als potente Inhibitoren von *P. falciparum*-Blutstadienparasiten, die vorzugsweise auf späte Stadien wirken. Der Mangel an Aktivität auf Ringstadien spiegelt sich in ihrer schnellen Reaktionsgeschwindigkeit wider, welche jedoch nicht so schnell ist wie die von Artemisinin, der bisher schnellsten Verbindung, die auf alle Blutstadien wirkt. Ein wichtiger Faktor ist außerdem, dass die SC-Leitverbindungen nicht von den Resistenzmechanismen der am häufigsten in der Klinik verwendeten Malariamedikamente beeinflusst wurden. Insbesondere wurde kein Kreuzresistenzmechanismus zwischen Artemisinin und seinen Derivaten und den SC- Leitverbindungen beobachtet, und ihre antiplasmodialen Wirkmechanismen schienen sich voneinander zu unterscheiden.

Der zweite Teil dieser Arbeit konzentrierte sich auf die Wirkmechanismen der SC- Leitverbindungen und die Resistenzmechanismen der Parasiten gegen diese Verbindungen. Obwohl die Ca^{2+} ATPase-Pumpe PfATP6 als direktes molekulares Target von SC- Leitverbindungen ausgeschlossen wurde, konnte ihre Beteiligung an einem Resistenzmechanismus gezeigt werden. Die F972Y-Mutation und die Überexpression der A108T, A109T-Variante führten zu einer drastischen Abnahme der Reaktionsfähigkeit der SC-Leitverbindungen. Die F972Y-Substitution korreliert mit *in vitro*-Fitnesskosten für den Parasiten, einhergehend mit einer niedrigeren intrazellulären Calciumruhekonzentration im Vergleich zur parentalen Parasitenlinie. Die molekularen Details der gestörten Calciumhomöostase und ihre Korrelation mit der Resistenz gegenüber den SC-Leitverbindungen müssen noch geklärt werden.

Zusammengefasst, zeigen die Ergebnisse dieser Arbeit die vielversprechende *in vitro*-Wirksamkeit der SC- Leitverbindungen, insbesondere von SC83288, und unterstützen ihre Weiterentwicklung für (prä) klinische Studien.

Abbreviations

°C	Degree Celsius
µ	Micro
A	Adenine or Alanine
aa	Amino acids
ACT	Artemisinin-based combination therapy
ADMET	Absorption, distribution, metabolism, excretion and toxicity
ADP	Adenosine diphosphate
Amp	Ampicillin
AMP	Adenosine monophosphate
AmpR	Ampicillin resistance
APS	Ammonium persulphate
ATP	Adenosine triphosphate
ATP4	ATPase 4
ATP6	ATPase 6
bp	Base pair
bp	Base pairs
BSA	Bovine serum albumin
C	Cytosine or Cysteine
Ca	Calcium
$CaCl_2$	Calcium chloride
Cas	CRISPR associated
cDNA	Complementary DNA
CIP	Calf intestinal alkaline phosphatase
CPA	Cyclopiazonic acid

CQ	Chloroquine
CQR	Chloroquine resistance
CQS	Chloroquine sensitive
CRISPR	Interspaced short palindromic repeats
CRT	Chloroquine resistance transporter
C-terminus	Carboxy-terminus
Cyt b1	cytochrome bc1 mitochondrial complex
Da	Dalton
DAG	Diacylglycerol
dd	Double distilled
DHA	Dihydroartemisinin
DHFR	Dihydrofolate reductase
DMSO	Dimethyl sulfoxide
DNA	Desoxyribonucleic acid
DNase	Deoxyribonuclease
dNTP	Desoxyribonucleoside triphosphate
DSB	Double-strand break
DSBR	Double-strand break repair
dsDNA	Double stranded DNA
DV	Digestive vacuole
E.coli	*Escherichia coli*
ECL	Enhanced chemiluminescence
EDTA	Ethylenediaminotetraacetate
EJ	End joining
EMP1	Erythrocyte membrane protein 1

ER	Endoplasmic reticulum
et al.	Et alia (and others)
EtBr	Ethidium Bromide
F	Phenylalanine
for	Forward
g	Gram
gDNA	Genomic DNA
GFP	Green fluorescent protein
GTS	Global Technical Strategy for Malaria 2016-2030
h	Hour or human
H_2O	Water
HA	Hemagglutinin
HEPES	N-(2-Hydroxylethyl)piparacin-N´-(2-ethylsulphonacid
HR	Homology region
IC_{50}	Half of maximal inhibitory concentration
IC_{90}	90% inhibitory concentration
IFA	Indirect fluorescence assay
IP_3	Inositol-1, 4, 5-triphosphate
iRBC	Infected red blood cell
K13	Kelch 13 protein
K_2HPO_4	Dipotassium hydrogen phosphate
kb	Kilobase pair
KCl	Potassium chloride
kDA	Kilodalton
KH_2PO_4	Potassium dihydrogen phosphate

KOH	Potassium hydroxide
kV	Kilovolts
l	Liter
LB	Luria Bertani
LDH	Lactate dehydrogenase
m	Milli- or meter
M	Molar
MDR	Multi-drug resistance
MDR1	Multidrug resistance protein 1
MDR2	Multidrug resistance protein 2
$MgCl_2$	Magnesium chloride
min	Minute
ml	Milliliter
MMEJ	Microhomology-end joining
MMV	Medicine for Malaria Venture
mRNA	Messenger RNA
n	Nano
Na	Sodium
NaCl	Sodium chloride
NaOH	Sodium hydroxide
NCBI	National Center for Biotechnology Information
NEB	New England Biolabs
NHEJ	Non-homologous end joining
NLS	Nuclear localization signal
nm	Nanometer

NPPs	New permeation pathways
O_2	Oxygen
OD	Optical density
ON	Overnight
P.	*Plasmodium*
p.i.	Post-invasion
PAGE	Polyacrylamide gel electrophoresis
PAM	Protospacer adjacent motif
Pb	*Plasmodium berghei*
PBS	Phosphate buffered saline
PBST	Phosphate buffered saline supplemented with Tween-20
PC	Principal component
PCA	Principal component analysis
PCR	Polymerase chain reaction
PDB	Protein Data Bank
Pf	*Plasmodium falciparum*
PFA	Paraformaldehyde
pH	Potential hydrogenii
PIP_2	Phosphatidylinositol-4, 5-bisphosphate
PMCA	Plasma membrane ATPase
pmol	Picomole
POD	Peroxidase
PPi	Pyrophosphate
PTMs	Post-translational modifications
PV	Parasitophorous vacuole

PVM	Parasitophorous vacuolar membrane
QN	Quinine
RBC	Red blood cell
rev	Reverse
RNA	Ribonucleic acid
RNase	Ribonuclease
rpm	Revolution per minute
RPMI	Roswell Park Memorial Institute
RT	Room temperature or reverse transcriptase
SAP	Shrimp alkaline phosphatase
SAR	Structure-activity relationship
SB	Super broth
SDS	Sodium dodecyl sulfate
sec	Second
SEM	Standard error of the mean
SERCA	Sarcoendoplasmic reticular Ca^{2+} -ATPase
sgRNA	Single-guide RNA
SNP	Single nucleotide polymorphism
SOB	Super optimal broth
SOC	Super optimal broth with catabolite repression
SP	Sulfadoxine-pyrimethamine combination
SSA	Single strand annealing
T	Thymine or threonine
T4	Bacteriophage T4
TAE	Tris/acetic acid/EDTA

Taq	*Thermus aquati*cus
TB	Tris-Borate
TCA	Trichloroacetic acid
TE	Tris-EDTA
TEA	Tetraethylamonium
TEMED	Tetramethylethylenediamine
TM	Transmembrane domain
Tris	Tris (hydroxymethyl)- aminomethane
U	Unit
USA	United States of America
UTR	Untranslated region
UV	Ultra violet
V	Volt
v/v	Volume to volume
w/v	Weight to volume
WHO	World Health Organization
x	Times
Y	Tyrosine
ZFN	Zinc-finger nuclease

1. Introduction

1.1. Malaria – a major human infectious disease

1.1.1. Origin and history

Malaria is one of the most important human pathogen borne diseases, along with tuberculosis and AIDS [1]. It occupies a unique place in human history and malaria´s long reign is attested by various ancient writings and artifacts [2]. Indeed, malaria can be traced back to ancient Mesopotamia and Egypt (3200 BC) [3], and can be followed through the Antiquity from the Indian Vedic period (1500 to 800 BC) as the "king of diseases", to the earlier Greek times as Homer mentions malaria in his famous *Iliad* (around 750 BC), as well as Aristophanes in *The Wasps* (around 420 BC), Aristotle (384-322 BC), Sophocles (496-406 BC) or even Plato (428-347 BC) [4]. Scholars were therefore clearly aware of the characteristic poor health, fever and enlarged spleens observed in population living in swamps areas [5]. These typical symptoms of the so-called Roman fever actually inspired the name *mal´aria*, literally "bad air" [2].

The cause for malaria disease, i.e. the *Plasmodium* eukaryotic parasite located in human erythrocytes, was discovered in 1880 by the French army doctor (Charles Louis) Alphonse Laveran. He noticed crescent-shape bodies in the blood of a febrile soldier, nearly transparent to the exception of one small pigmented dot [2]. Laveran´s following work allowed him to further distinguish and characterize four distinct forms that would later prove to be different stages of the parasite erythrocytic life cycle [6] (see Section 1.2.1), and was later awarded with the Nobel Prize in Physiology or Medicine in 1907. Shortly after, in 1897, the British Surgeon-Major Ronald Ross demonstrated the transmission of avian malaria through the *Anopheles* mosquito [7]. He was similarly awarded the Nobel Prize in 1902 for discovering the mosquito stage of malaria. The latest Nobel Prizes associated with malaria were granted to the Swiss chemist Paul Müller in 1948, for discovering the potent insecticidal properties of dichloro-diphenyl-trichloroethane (DTT) against *Anopheles* mosquitos and its subsequent contribution to malaria control; and to the pharmaceutical chemist Tu Youyou in 2015, for the discovery of artemisinin and dihydroartemisinin [8,9] and their significant breakthrough for the treatment of malaria over the 20th century.

1.1.2. Clinical manifestations

Malaria infection results in a wide spectrum of outcomes, from the absence of symptoms, to mild or severe symptoms that may lead to the death of the patient. Malaria can be categorized according to the severity of these outcomes, i.e. as uncomplicated or severe.

Uncomplicated malaria can be defined as the absence of symptoms characteristic of severe malaria. As the symptoms of uncomplicated malaria are unspecific (Table 1.1), it might be difficult to distinguish from other febrile illnesses. If uncomplicated malaria is promptly and appropriately diagnosed and treated, the prognosis is favorable, and the infection rarely results in fatality. However, if a *Plasmodium falciparum* infection remains untreated, it might develop into severe malaria (Table 1.1), usually lethal if not treated.

Table 1.1: Principal symptoms of malaria, uncomplicated or severe [10]**.**

Uncomplicated malaria	**Severe malaria**
Fever, chills and perspiration	Cerebral malaria
Headache	Severe anemia
Fatigue	Acidosis and hypoglycemia
Muscle and joint aches	Respiratory distress
Abdominal discomfort	Pulmonary oedema
Vomiting	Acute kidney injury
	Jaundice

The broad range of clinical manifestations of malaria is primary due to the difference in the level of immunity between infected individuals. Immunity is generally correlated with the geographical transmission pattern, so that naïve infected individuals will develop symptoms whereas clinical immunity to malaria can be acquired in areas of stable transmission.

1.1.3. Global impact and eradication strategy

Malaria was once prevalent in most of the inhabited world, as 90% of the population was estimated to live in malaria-affected regions before 1900 [11]. By the mid-20th century, malaria was eliminated from North America, Europe and Russia, and ceased to be a major health issue in most of the world [10]. Endemic areas however remain, principally in Sub-Saharan Africa where malaria is still one of the largest factors in premature death [1,2]. To a lesser extent, malaria remains a prominent concern in South America and parts of South Asia [1]. Malaria gives rise to over 200 million cases annually, causing approximately 500 000 deaths per year [1]. Malaria particularly affects pregnant women and young children, and more than 70% of malaria deaths occur in children under five years old [1]. Despite these figures, tremendous progresses have been achieved in the battle for malaria eradication. According to the latest estimates by the World Health Organization (WHO), global malaria case incidence was reduced by 41% and malaria-related mortality rates by 62% between

2000 and 2016 [1] (Figure 1.1). This general trend has been sustained over the last few years, as a global decrease in malaria incidence of 18% was observed between 2010 and 2016 and the mortality rates dropped by 29% among all age groups, in particular by 35% among children under the age of five [1].

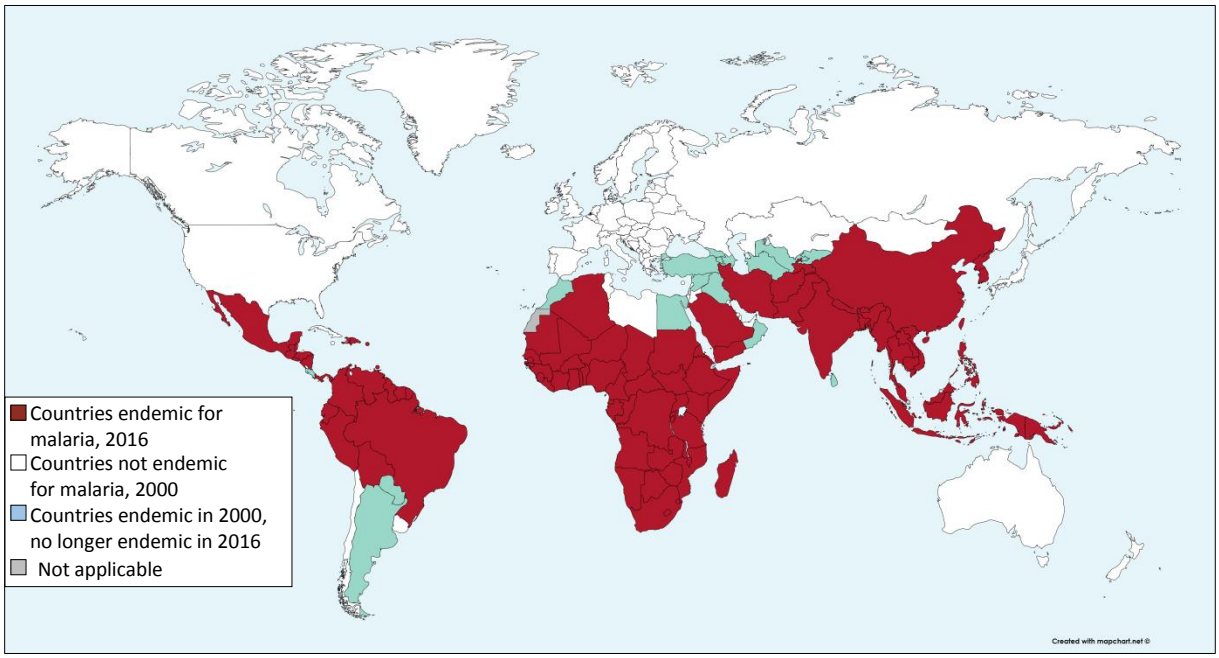

Figure 1.1: Countries endemic for malaria in 2000 and 2016. The number of indigenous cases was used as an indicator of whether a country is considered endemic for malaria. Countries with three consecutive years of zero indigenous cases are considered to have eliminated malaria. Cases were reported to the WHO by national malaria control programs (NMCPs). Since 2000, seventeen countries and territories, i.e. Argentina, Armenia, Azerbaijan, Costa Rica, Georgia, Iraq, Kyrgyzstan, Morocco, Oman, Paraguay, Sri Lanka, Syrian Arab Republic, Tajikistan, Turkey, Turkmenistan, United Arab Emirates and Uzbekistan, have been declared no longer endemic in 2016. This map was created using the online MapChart tool (https://mapchart.net/).Adapted from [12].

Aiming to accelerate the progresses in reducing the global malaria burden and highlighting the need for universal access to malaria prevention, diagnosis and treatment, the WHO developed the Global Technical Strategy for Malaria 2016-2030 (GTS) [13]. The GTS is based on two supporting elements, i.e. innovation and research, and strengthening of the enabling environment [13]. It sets the ambitious target of reducing malaria incidence and mortality by at least 90% from the levels in 2015 by the year 2030, and at least 35 countries where transmission occurred in 2015 should be malaria-free by the same deadline [13].

1.2. *Plasmodium falciparum´*s biology

The genus *Plasmodium* includes nearly 200 species able to infect various hosts, from mammals to birds and reptiles [14]. Five species are known to develop in a human host, *P. falciparum*, *P. vivax*, *P. ovale*, *P. malariae* and *P. knowlesi*. Recent studies reported that the *P. vivax*-diagnosed human infection cases observed in the Atlantic Forest region of Rio de Janeiro state were actually caused by *P. simium*, a species previously thought to infect exclusively primates [15].

1.2.1. Life cycle of *Plasmodium falciparum*

The *Plasmodium* life cycle is a complex process. It involves both a cold-blooded insect vector, the female *Anopheles* mosquito where it replicates sexually and a warm-blooded vertebrate host where asexual replication occurs [16] (Figure 1.2).The life cycle of the five established human pathogenic *Plasmodium* species are similar, with only minor variations, and can be exemplified by the life cycle of *P. falciparum*.

Female *Anopheles* mosquitoes ingest sexually differentiated gametocytes when feeding on an infected host. Inside the mosquito midgut, male gametocytes undergo DNA replication rounds and exflagellation to release eight motile microgametes from an erythrocyte. At the same time, the female gametocytes egress from the erythrocytes and develop into macrogametes. Fertilization occurs, and the resulting diploid zygote further differentiates into a motile ookinete, settling between the midgut and the basal lamina. It further develops into an oocyst, inside which the parasite replicates through sporogony, producing thousands of haploid sporozoites. The oocyst ruptures and the freed sporozoites migrate through hemolymph and actively invade the salivary glands of the mosquito. These infective sporozoites are injected into the human host by mosquito bite during its next blood meal [16,17]. Once released into the skin, the sporozoites become actively motile and quickly enter the blood stream and are passively transported to the liver, where they actively invade hepatocytes. The liver stage is a phase of intense asexual replication, resulting in the formation of hundreds of merozoites [16,17]. Even though clinically silent, this phase represents the bottleneck of the infection [18]. In contrast to *P. falciparum*, *P. ovale* and *P. vivax* can form dormant liver stages, the hypnozoites. The latent nature of this stage is responsible for the reactivation of the parasite´s life cycle and the frequent relapses of the disease, even years after the initial infection [17]. The merozoites are released into the blood stream and rapidly invade red blood cells (RBC) and initiate their intraerythrocytic development.

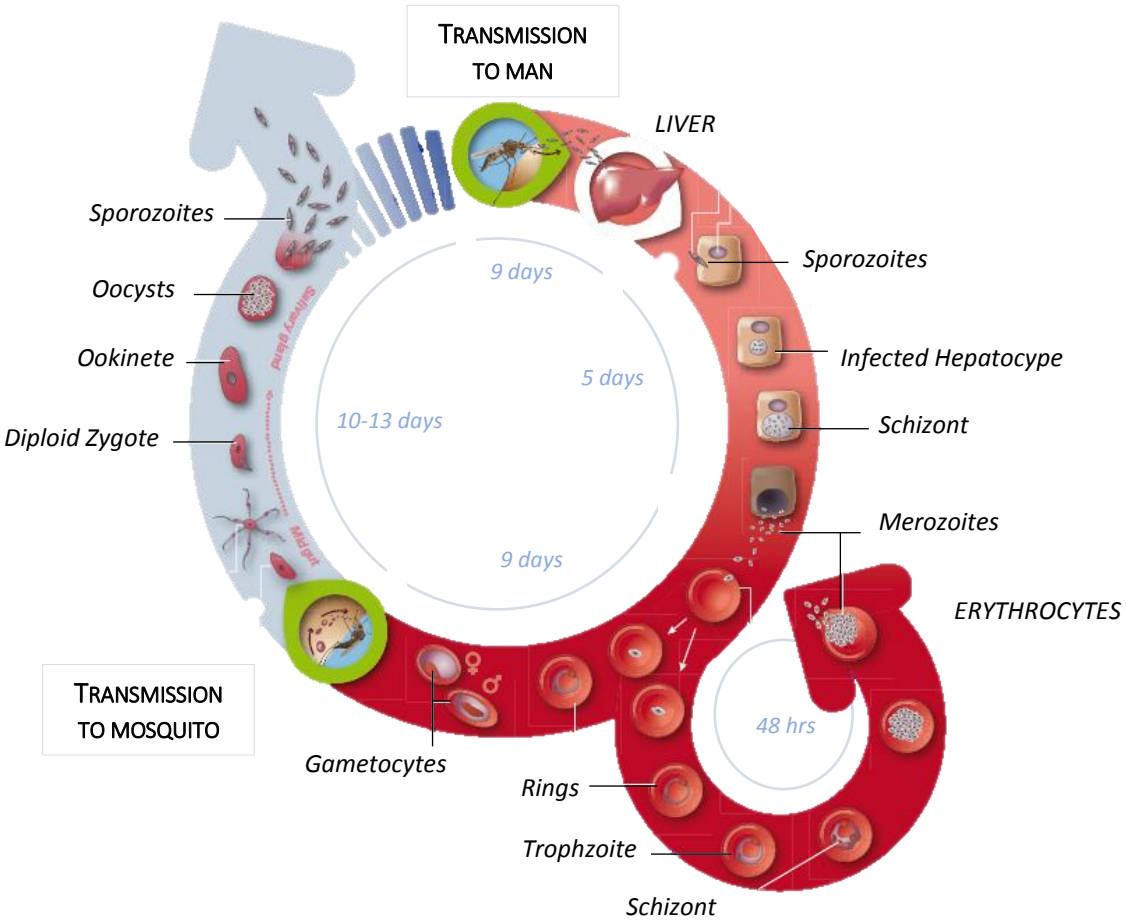

Figure 1.2: Life cycle of *Plasmodium falciparum* in the human body and the *Anopheles* mosquito. Adapted from https://www.mmv.org/

This intraerythrocytic cycle, responsible for the clinical symptoms associated with malaria, lasts around 48 hours in *P. falciparum*, *P. ovale* and *P. vivax*, with small variations according to the different strains, 72 hours in *P. malariae* and 24 hours in *P. knowlesi*. The parasite develops inside a parasitophorous vacuole and undergoes yet another asexual replication round, characterized by three morphologically distinct successive stages, which can be observed under light microscopy after Giemsa staining (Figure 1.3) [19]:

(1) The ring stages, observed between 6 to 22 hours post-invasion (p.i.).
(2) The trophozoite stages, observed between 22 to 38 hours p.i. The parasite is highly metabolically active during this stage, synthetizing macromolecules, degrading hemozoin and synthetizing the hemozoin pigment.

(3) The schizont stages, observed between 38 to 48 hours p.i., are polynucleated and reflect the differentiation into future merozoites. Merozoites can be observed at 48 hours p.i., just before invasion.

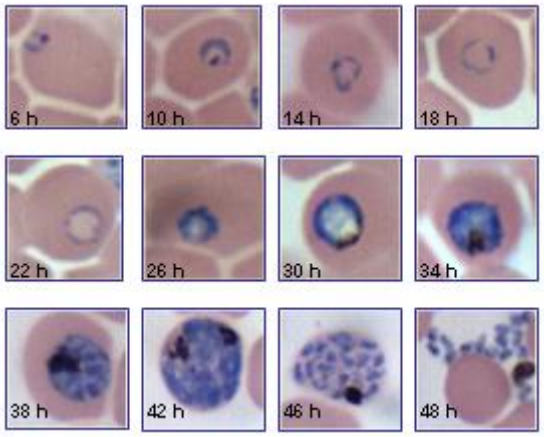

Figure 1.3: Intraerythrocytic blood stages of *Plasmodium falciparum* in culture. *P. falciparum* intraerythrocytic development stages every 4 hours post-invasion, on thin blood smears stained with Giemsa. Adapted from [19].

After rupture of the host erythrocyte, each mature schizont releases 10 to 30 infectious merozoites, able to rapidly reinvade erythrocytes and start a new cycle. The infected erythrocyte rupture combined with the release of its contained cells debris, parasite´s antigens and hemozoin crystals into the host circulation activates the immune system, inducing the typical fever peaks associated with malaria [20].

During the asexual intraerythrocytic cycle, a small population of the parasites commit to sexual development. Gametocytes develop in erythrocytes through five morphological stages, and the mature crescent-shaped stages [16] are taken up by the female *Anopheles* mosquito during a blood meal, allowing the beginning of a new cycle.

1.2.2. Calcium homeostasis in *P. falciparum*: the role of PfATP6

1.2.2.1. Calcium homeostasis in *Plasmodium*

Ca^{2+} is a ubiquitous intracellular secondary messenger in eukaryotes, where the basic signaling principles are conserved. A resting cell actively pumps Ca^{2+} into the extracellular space and into internal stores in order to maintain a low cytosolic calcium concentration, whereas the efflux of Ca^{2+} into the cytosol triggers signaling cascades involved in numerous cellular processes [21]. The prompt removal of Ca^{2+} from the cytosol back to its basal level, by pumps and exchangers, ends the signals and prevents toxic effects caused by an

elevated intracellular calcium concentration. The flexibility of Ca^{2+} signaling, in terms of amplitude, speed and spatio-temporality, accounts for its universality [22]. The wide repertoire of proteins involved in downstream calcium signaling significantly varies among eukaryotic organisms, consistent with lineage-specific adaptations. Yeast, plant and animal cells are commonly used as model organisms for the investigation of Ca^{2+} signaling and related proteins. Because of the evolutionary divergence, Ca^{2+} signaling in *Plasmodium* combines both unique and conserved features compared to these characteristic to other eukaryotes. A detailed molecular understanding of Ca^{2+} homeostasis mechanisms and of how Ca^{2+} is integrated in broader second messenger signaling networks over the *Plasmodium* life cycle remains a challenge [21], as many canonical Ca^{2+} regulators, transporters and channels characterized in models organisms have not yet been identified in *Plasmodium* genomes.

Nonetheless the necessity for *Plasmodium* to maintain a tight control of its Ca^{2+} intracellular concentration over its life cycle is established [21]. Calcium signaling is indeed virtually associated with every stages of the malaria parasite life cycle, from merozoite egress [23–25] and invasion [26–28], maturation of intraerythrocytic asexual stages [23,29–31], gametogenesis [32,33] and exflagellation [34], ookinete motility and oocyst formation [35,36], to sporozoite motility, invasion and liver stage development [37–39].

From the very low intracellular Ca^{2+} concentrations in the erythrocyte host (around 50 nM) to the high extracellular ones such as found in the blood plasma (around 1.8 mM), *Plasmodium* parasites have to face a wide range of Ca^{2+} surroundings, as well as to maintain a relatively high intracytosolic concentration varying from 100 nM to around 500 nM [40,41]. The endoplasmic reticulum (ER) is the main Ca^{2+} storage site in the parasite [41], and the mitochondrion was also proposed as a dynamic Ca^{2+} store [42] even though no clear orthologs of the mitochondrial Ca^{2+} uniporter have been identified in the *Plasmodium* genomes. Other organelles, such as acidocalcisomes [43] or the digestive vacuole [41] have been likewise suggested as calcium stores, although the understanding of their physiological relevance in Ca^{2+} signaling remains to be unraveled. Only a few *Plasmodium* proteins involved in Ca^{2+} homeostasis have been identified so far. Eukaryotic cells usually rely on ATPase pumps to transport Ca^{2+} into the extracellular space via plasma membrane ATPases (PMCAs) or into intracellular stores via the sarcoendoplasmic reticular Ca^{2+} ATPases (SERCAs). So far, no obvious orthologs of PMCAs or voltage-dependent Ca^{2+} channels have been identified in the *Plasmodium* genomes [44]. A divalent Ca^{2+}/H^{+} antiporter could be identified in both *P. berghei* (PbCAX) and *P. falciparum* (PfCHA), and was suggested to be involved *in vitro* in the Ca^{2+} efflux system from the mitochondrion [42]. A SERCA-type Ca^{2+}

ATPase, PfATP6, has been identified in *P. falciparum* and its Ca^{2+}-dependent activity has been characterized [21,45,46].

1.2.2.2. PfATP6: the *P. falciparum* SERCA

PfATP6 is the only identified SERCA-pump ortholog in *P. falciparum* [47]. The *pfatp6* gene (PF3D7_0106300) is located on chromosome 1, and is 4.3 Kb long (3684 bp in the coding sequence), composed of 3 exons and 2 introns (see Appendix I). PfATP6, a protein of 139.4 KDa (see Appendix I), localizes in the ER and is responsible for the transport of Ca^{2+} ions from the cytosol into the ER of the parasite.

PfATP6 conserves the key features of its well characterized rabbit ortholog SERCA1a (Figure 1.4). Indeed, PfATP6 displays the typical ten (putative) transmembrane domains, the two Ca^{2+}-binding sites in the fourth and sixth transmembrane helices, and the characteristic catalytic domain in the cytosol. The catalytic domain presents the phosphorylation domain (P domain), the nucleotide-binding domain (N domain) where ATP is bound and the actuator domain (A domain) that transmits the conformational changes to the transmembrane domains [45,48].

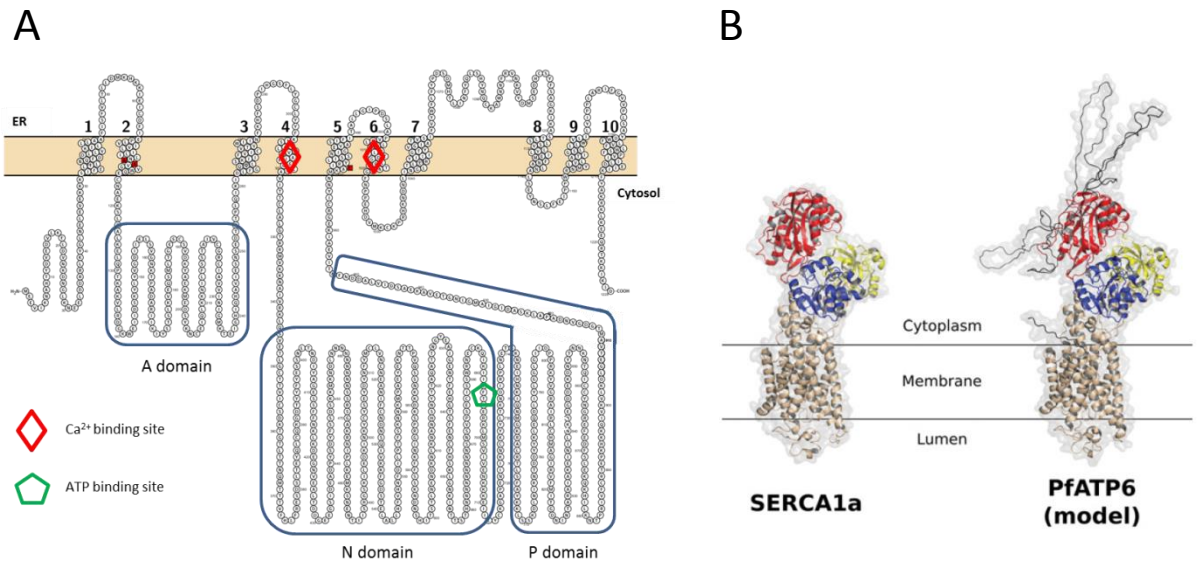

Figure 1.4: Predicted topological model of PfATP6. (**A**) Reconstruction of PfATP6 using the open-source visualization tool Protter [49], based on the predictive model described by Krishna et al. [50]. (**B**) Comparison of the structures of the mammalian SERCA1a (left) and PfATP6 (right). The A (actuator) domain is represented in yellow, the N (nucleotide-binding) domain in red and the P (phosphorylation) domain in blue. Amino acid sequences specific to PfATP6 are depicted as black loops with random coil, as no corresponding template structures were available for homology modeling. Obtained from [45].

These features allow PfATP6 to be classified as a P-type ATPase, along with the SERCA pumps. Amino acid sequence analysis reveals an overall identity of 39% between SERCA1a and PfATP6, increased to 53% when the N domain sequences are excluded [45] (Figure 1.4 B). The main divergence is therefore localized in the N domain, where PfATP6 displays 200 additional amino acid residues compared to SERCA1a, predicted to form non-globular structures due to the abnormal quantity of poly-asparagine motifs (Figure 1.4 and Appendix I) compared to other eukaryotes [45].

PfATP6 can be inhibited by the classical SERCA inhibitors, such as thapsigargin (Figure 1.5 A) or cyclopiazonic acid (CPA) (Figure 1.5 B) [51]. The inhibition of PfATP6 blocks the ability of the parasite to pump Ca^{2+} into the ER, depleting this calcium store. This depletion in turn secondarily activates plasma membrane calcium channels and allows an influx of calcium, overall raising the cytosolic Ca^{2+} concentration [52].

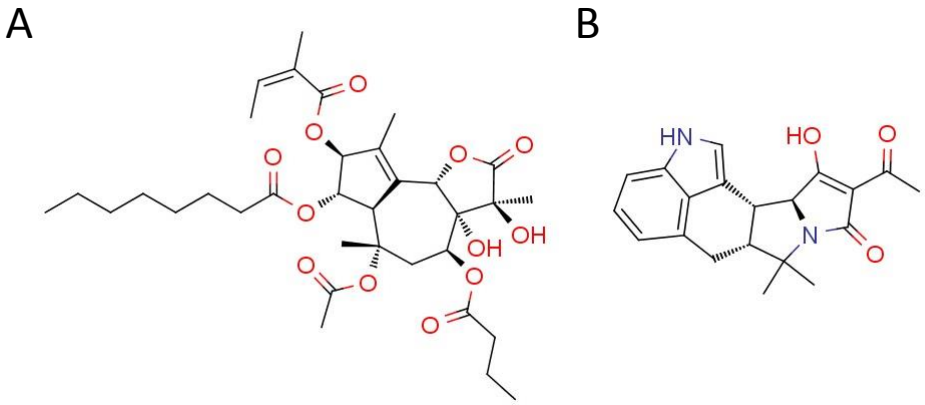

Thapsigargin Cyclopiazonic acid (CPA)

Figure 1.5: Chemical structures of SERCA1a and PfATP6 inhibitors. (**A**) Thapsigargin. (**B**) Cyclopiazonic acid.

Thapsigargin and CPA sensitivities and binding sites have been proven to be different in the mammalian SERCA and PfATP6 [53,54]. CPA is a more potent inhibitor of PfATP6 than SERCA1a, and the inverse can be observed for thapsigargin, marking CPA as a more appropriate tool to study PfATP6 inhibition in *P. falciparum*.

1.2.2.3. The PfATP6 - artemisinin controversy

Based on the structural similarities between thapsigargin and the potent antimalarial drug artemisinin, both sesquiterpene lactones, PfATP6 was proposed as the molecular target of artemisinin. This was supported by a study from the early 2000's, suggesting a specific inhibition by artemisinin of heterologously expressed PfATP6 in *Xenopus laevis* oocyte

membranes [55]. The same study also reported an antagonistic interaction between thapsigargin and artemisinin and a similar localization in the parasite [55]. These observations were supported by various *in silico* homology modeling and PfATP6 docking studies, claiming the ability of artemisinin to bind to PfATP6 through hydrophobic interactions [52,56,57]. However other studies similarly based on docking simulations found opposite results [58,59]. The original study was furthermore heavily criticized, particularly concerning the methodology, i.e. the lack of reliability of the heterologous expression system. The controversy continued in the malaria community until the early 2010's, when recent studies, both in *Saccharomyces cerevisiae* and *Xenopus laevis* oocytes, disproved the hypothesis of artemisinin or derivatives directly inhibiting PfATP6 [46,60].

Similarly, as PfATP6 was proposed as a molecular target, a long expected molecular marker to monitor the emergence of artemisinin resistance was assumed to have been found [61]. However, no clear association between PfATP6 polymorphisms and artemisinins reduced susceptibility could be established, as reports, both *in vitro* and on field isolates, presented contradictory results [62–68]. More will be discussed about the latest findings on artemisinin mode of action and resistance (see Sections 1.3.1.4. and 1.3.2.).

Although PfATP6 is now ruled out as a direct target of artemisinin, or as a component of resistance, it remains an attractive potential therapeutic target [45,69]. Not only the fruitless attempts to generate *pfatp6* knock-out *P. falciparum* lines, probably marking PfATP6 as an essential protein [70], but also the relative homology to the SERCA1a, to which several characterized inhibitors have a clinical potential [71,72], support this statement. CPA, with its higher affinity to PfATP6 then to SERCA1a [53,54], can for instance be considered a reasonable starting point for a medicinal chemistry program, in order to further optimize its antiplasmodial properties and increase its specificity toward PfATP6.

1.2.3. Editing *P. falciparum*´s genome

Since the establishment of the *in vitro* culture system in 1979 [73], tremendous progress has been achieved in the pursuit of transforming *P. falciparum* into a laboratory organism that can be genetically studied. Key developments include the establishment of transfection techniques in 1995 [74] and the sequencing of the full *P. falciparum* genome in 2002 [75,76]. Nevertheless, until the establishment of the CRISPR/Cas9 approach [77] in *P. falciparum* in 2014 [78], genetic engineering methods have been limited, due to a lack of tools and inefficient transfection and integration [79]. Gene disruption used to require up to three months of continuous culture, with a limited success rate [79].

Nowadays, genome editing in *P. falciparum* is mainly achieved using either the CRISPR/Cas9 (Figure 1.6 A) or the zinc-finger (Figure 1.6 B) technologies. Both approaches take advantage of DNA double-strand break repair (DSBR). DNA double-strand breaks (DSB) are virtually the most detrimental event a cell can encounter. A single DSB event leads to a general genome instability and can lead to cell death [80], particularly dramatic in single-cell haploid organisms, such as the blood-stages of *P. falciparum*. In eukaryotic cells, two types of responses can be involved in DSBR: either the homologous recombination (HR), considered error-free, or the more error-prone end-joining (EJ) pathway. The high fidelity of HR relies on the use of a homology sequence of DNA as a template to repair the break, whether it is a sister chromatid or a donor plasmid. The EJ repair pathway, which can be further separated into the classical non-homologous end joining (NHEJ) and the alternative microhomology-mediated end joining (MMEJ), does not use a homologous template but repairs the break by simply ligating broken DNA ends together (NHEJ) or by annealing the exposed homology sequences (MMEJ), increasing probabilities of insertions or deletions [80]. None of the genes involved in NHEJ have been identified in *P. falciparum*, strongly suggesting a lack of this particular DNA repair mechanism [80]. Although MMEJ events have been detected, they remain rare and the repairing system is considered inefficient [81,82]. These observations make genome editing based on DSB and HR repair an obvious and suitable choice in *P. falciparum*.

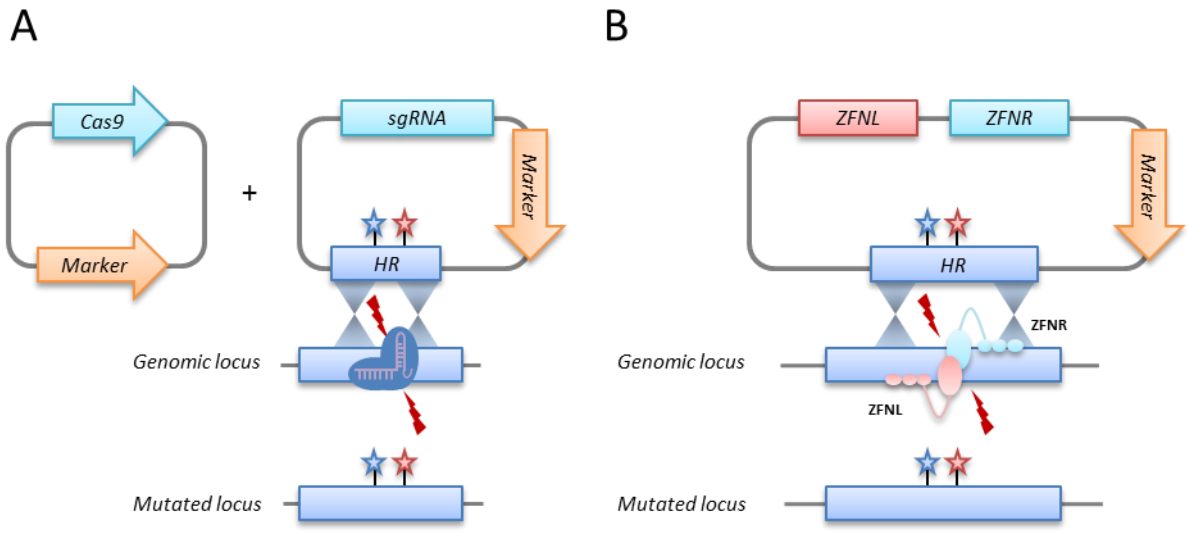

Figure 1.6 : Site specific genome modification strategies in *P. falciparum*. (A) Components of the CRISPR/Cas9 system, as described in [78] and used in this study: the Cas9 endonuclease, directed to the desired location by RNA-DNA pairing by the single guide RNA (sgRNA). **(B)** Basis of the ZFNs editing, where the heterodimerization of the specifically engineered pair of ZFNs (ZFNL and ZFNR) each fused to half of nuclease domain of the FokI restriction enzyme leads to a functional nuclease. Adapted from [79].

DSB can be generated by specifically engineered DNA endonucleases, designed to target investigator-defined DNA sequences. The CRISPR/Cas9 genome editing approach is based on a prokaryotic viral defense system, where short RNA sequences are used to target and degrade foreign nucleic acids [77]. This system can be adapted by fusing a specific genomic sequence displaying a unique protospacer-adjacent motif (PAM) with an RNA Cas9-binding domain. This single-guide RNA (sgRNA) allows a site-directed DSB by the RNA-guided Cas9 endonuclease (Figure 1.6 A). Alternatively, the zinc-finger nucleases (ZFNs) can be used to introduce specific DSB. ZFNs act as heterodimers, left (ZFNL) and right (ZFNR), where each monomer is formed of a specifically engineered DNA-binding domain, also known as the zinc finger protein region, fused to the nuclease domain of the FokI endonuclease [83] (Figure 1.6 B). In both methodologies, the genome is repaired by HR using a provided DNA template bearing the desired genetic modification(s) (Figure 1.6).

Both the ZFNs and the CRISPR/Cas9 technologies allow permanently mutating, replacing, disrupting and tagging genes without altering the endogenous genomic locus with the introduction of a selection marker as it was previously done. They can then not only be used for introducing point mutations, but also to introduce sequences involved in gene down-regulation systems, or in localization signaling.

1.3. Antimalarial chemotherapies and drug resistance

1.3.1. Antimalarial drugs and their mode of action

Despite constant efforts to develop a potent malaria vaccine and promising preliminary results of field testing [84,85], prevention and treatment of malaria still mainly rely on chemoprophylaxis and chemotherapy. The complex life cycle of *Plasmodium*, as previously illustrated by *P. falciparum*, offers multiple sites of action. An ideal drug would act on the asexual intraerythrocytic stages to treat the apparent symptoms, as well as on the gametocytes stages to limit further transmission, and on the liver stages, particularly on the hypnozoites generated by a *P. vivax* infection, to prevent recrudescence. Such a compound is not available yet, and drugs with different modes of action can be combined to act together on these distinct critical sites of the life cycle.

Four main classes of antimalarial drugs are currently in use: quinoline analogs (arylaminoalcohols, 4-aminoquinolines and 8-aminoquinolines), artemisinins, antifolates, and an inhibitor of the respiratory chain.

1.3.1.1. Quinolines

Quinoline antimalarials are the oldest compounds used for malaria treatment since the discovery and isolation of quinine (QN), an arylaminoalcohol obtained from the bark of the cinchona tree during the first part of the 19th century. Quinine, and its stereoisomer quinidine, were however not only difficult and onerous to naturally obtain but furthermore have later been associated with severe side effects [86–88].

Efforts were placed to produce synthetic quinine and resulted in the development of chloroquine (CQ), a 4-aminoquinoline. CQ was the most widely used quinoline for the treatment of *P. falciparum* malaria worldwide, due to its high potency, safety, and low production costs. The emergence of CQ-resistant *P. falciparum* strains in South-East Asia in the late 1960's [89], and the further spread to malaria endemic regions in Africa [90,91] led to the removal of CQ as a first-line treatment, to nowadays only be recommended for the treatment of uncomplicated non *P. falciparum* malaria in regions non affected with CQ-resistance.

Further quinoline analogs have been synthetized to overcome resistance in *P. falciparum*, such as, to cite only a few, amodiaquine, lumefrantrine, primaquine, tafenoquine or mefloquine. For every generation of derivative, chemical properties were optimized to improve pharmacological and pharmacokinetic properties, as well as reducing side-effects. Primaquine, an 8-aminoquinoline, is currently the only WHO-recommended drug for the treatment of relapsing infections induced by *P. vivax* hypnozoites [92], despite its short half-life [93] and its association with hemolytic anemia in patient with glucose-6-phosphate-dehydrogenase (G6PD) deficiency [94]. As the only available drug against young *Plasmodium* gametocyte stages, primaquine is also used for prophylaxis and to reduce transmission [92]. Tafenoquine, a primaquine analog with an extended half-life and similar efficacy, is currently under evaluation by the Medicine for Malaria Venture (MMV) for the treatment of *P. falciparum* and *P. vivax* [95,96].

Arylaminoalcohols and 4-aminoquinolines are known to exert their primary activity by preventing the hemozoin crystallization in the parasite digestive vacuole (DV), a heme detoxification process essential to the parasite survival [97,98]. Quinolines are weak bases and, when not protonated, are therefore able to diffuse through biological membranes. The acidic pH in the digestive vacuole (pH 5 – 5.2) promotes quinoline protonation, leading to a rapid accumulation [99]. Once entrapped in the DV, quinolines effectively inhibit hemozoin formation by forming a stable complex with the Fe^{3+} ion present in the heme ferriprotoporphyrin. The accumulation of the resulting free heme units in the DV is toxic and eventually lethal to the parasite [100].

The mode of action of the 8-aminoquinolines is not yet known, and primaquine has been shown to act differently than the other quinolines and does not inhibit hemozoin formation [101].

1.3.1.2. Antifolates

Antifolate drugs and their analogs interfere with folate synthesis, an essential pathway for *Plasmodium* DNA synthesis [102,103]. They target different enzymes of the folate synthesis pathway, particularly the dihydropteroate synthase (DHPS) and the dihydrofolate reductase (DHFR). Combining drugs, such as sulfadoxine, a competitive inhibitor of DHPS, and pyrimethamine, a competitive inhibitor of DHFR, results in a synergistic interference in the synthesis of tetrahydrofolate, a metabolite essential for the production of dTTPs and some amino acids such as methionine and glycine [102]. An additional antifolate, proguanil, inhibits DHFR through the formation of its active metabolite cycloguanil [104].

Although the sulfadoxine-pyrimethamine combination (SP) was adopted to resolve the widespread resistance to chloroquine, the resistance to SP paradoxically developed rapidly after its introduction in South-East Asia [105,106] and Africa [107,108]. Consequently, antifolate drugs are currently only used in combinations, for instance proguanil with atovaquone (see Section 1.3.1.3.) under the brand name Malarone® for a prophylactic purpose, or with artemisinins (see Section 1.3.1.4.) as the regimen of choice for intermittent preventive treatment in infants and pregnant women [92,109,110].

1.3.1.3. Inhibitor of the respiratory chain

Atovaquone, an antimalarial drug of the paphthoquinone class, inhibits the respiratory chain in the *Plasmodium* mitochondrion. Atovaquone targets the cytochrome bc1 mitochondrial complex (PfCyt b1) and consequently disrupts the electron transport chain [111] without affecting the mitochondria of the human host [108]. The resulting collapse of the mitochondrial membrane potential leads to the inhibition of the pyrimidine biosynthesis, essential for the parasite [112]. The cytochrome bc1 mitochondrial complex is however subjected to high-frequency mutations, and resistance developed rapidly after the introduction of atovaquone as a monotherapy [108,113]. Atovaquone is therefore exclusively used partnered with proguanil, a synergistic combination [114], in an effort to delay atovaquone resistance.

1.3.1.4. Artemisinins and Artemisinin-based Combination Therapies

Since the emergence of resistance to almost all used antimalarial drugs (Table 1.2), artemisinin and its derivatives have formed the backbone of malaria control since the early 2000´s [92]. Artemisinin is a natural sesquiterpene trioxane lactone isolated from the leaves of the Chinese sweet wormwood plant *Artemisia annua*. To avoid the isolation step and increase artemisinin's poor solubility, efforts led to the synthesis of the semi-synthetic derivative dihydroartemisinin (DHA), which itself served as a template for the synthesis of artesunate, artemether and arteether [115]. Artemisinin and its derivatives, or artemisinins, display a rapid onset of activity against all stages of intraerythrocytic *Plasmodium*, including early gametocytes [116,117], and hence are appropriate for the treatment of both uncomplicated and severe malaria [92].

The antimalarial activity of artemisinins is associated with their endoperoxide bridge. The hemolytic Fe^{2+} ion is thought to catalyze the reduction of this endoperoxide bound [118], generating activated artemisinins free radicals. Once activated, the artemisinins radicals rapidly react with exposed nucleophilic groups in proteins, particularly enzyme active sites or unsaturated lipids. These alkylations [119–121] result in irreversible damages in the parasite [55,122]. The wide and unspecific effect of activated artemisinins is therefore difficult to associate with one particular target, and various organelles such as the mitochondrion [123], the endoplasmic reticulum [55,62,124] or the digestive vacuole [124–127] have been proposed as sites of damage.

Regarding the development of resistance, artemisinins are advantaged by their extremely short half-lives of 1 to 3 hours [117]. Nonetheless, early artemisinins monotherapies in Cambodia already led to the emergence of *P. falciparum* strains with delayed or possibly reduced responsiveness to artemisinins [128]. This early resistance phenomenon is now threatening to spread across all of South-East Asia [129].

To reduce the risk of developing resistance, artemisinin derivatives are partnered with other long-acting drugs that target different metabolic pathways, in the so-called artemisinin based combination therapies (ACT). The artemisinin derivative rapidly reduces the parasite burden and is protected against the emergence of resistance. Indeed, the surviving parasites potentially bearing mutations conferring resistance to artemisinins are further eliminated by the long-lasting partner drug [130]. The latest is however not protected against resistance development during the phase where the artemisinin derivative is already cleared and the concentration of the partner drug is slowly decreasing [131].

Several ACT regimens have been recommended by the WHO as a first-line treatment for *P. falciparum* malaria, such as Coartem® (artemether-lumefantrine), Coarsucam® (artesunate-

amodiaquine), Pyramax® (pyronaridine-artesunate), Ariplus® (artesunate-sulfadoxine-pyrimethamine), Artekin® (dihydroartemisinin-piperaquine) or Mefliam Plus® (artesunate-mefloquine) [92].

1.3.2. Drug resistance mechanisms

Resistance to antimalarial drugs is defined by the WHO as “the ability of a parasite strain to survive and/or multiply despite the administration and absorption of a drug given in doses equal to, or higher than those usually recommended, but within the limits of tolerance of the subject” [132]. This clinical definition proves itself to be sometimes difficult to measure in the field, as well as to translate in laboratory-adjusted *in vitro* assays [133]. Antimalarial resistance is therefore not strictly defined, and many aspects can change the perception of resistance.

The development of drug resistance can be divided into two separate events: emergence by *de novo* mutations, and spread via drug selection pressure. *P. falciparum* parasites have developed resistance, to various extents, to all antimalarial drugs used so far (Table 1.2 and [133]). Historically, resistance almost always emerged from South-East Asia, in particular from Cambodia [134,135].

Table 1.2: Dates of introduction and first reports of resistance to antimalarial drugs.

Antimalarial drug	Introduced	First reported resistance	Difference (years)
Quinine	1632	1910	278
Chloroquine	1945	1957	12
Proguanil	1948	1949	1
Sulfadoxine-Pyrimethamine	1967	1967	0
Mefloquine	1977	1982	5
Atovaquone	1996	1996	0

Adapted from [108].

Drug resistance is likely to arise in instances of widespread exposure of the parasites to antimalarial drugs, as it was the case when the overuse of CQ created an optimal environment for the emergence and persistence of CQ-resistant parasites in the 1950´s. The use of subtherapeutic and/or uncontrolled antimalarial doses led to the residual presence of the drug in the subject´s circulation, creating favorable circumstances for the selection of fully

or partially resistant parasites [133]. Such lessons must imperatively be considered in the present on-going fight against drug resistance.

The majority of used antimalarial drugs target specific metabolic pathways in the intraerythrocytic cycle of the parasite. Their efficacy is however compromised by the development of resistant *Plasmodium* strains, through *de novo* mutations. These mutations can interfere with the drug´s mode of action in diverse ways, usually by (i) reducing the access of the active compounds to their site of action, through altered transport of the drug, enzymatic inactivation or decreased conversion of the drug into its active compound, (ii) altering their molecular target and decreasing its affinity for the drug, or (iii) increasing the amount of a metabolite antagonizing the drug´s action [136].

The characterized mechanisms of resistance in *P. falciparum* follow these general principles. For instance, resistance to pyrimethamine and sulfadoxine is mediated through mutations in their respective enzymatic target causing a decrease in affinity. Single nucleotide polymorphisms (SNP) in the *pfdhfr* gene leading to the S108N, N51I, C59R and I164L mutations have been identified in field isolated parasites with decreased pyrimethamine susceptibility [137–139], and were further confirmed to structurally modify PfDHFR and impair pyrimethamine binding [140]. Similarly, resistance to sulfadoxine was found to be correlated with polymorphisms in the *pfdhps* gene, leading to the mutations S436A/F, A437G, K540E, A581G, A613S/T [141–143]. *In vivo* combination of mutations in *pfdhfr* and *pfdhps* were associated with the sulfadoxine-pyrimethamine treatment failure, particularly in Africa [108].

Resistance to CQ is mediated through altered drug transport and reduction of the drug at its action site. CQ resistance has mainly been associated with mutations of the chloroquine resistance transporter (PfCRT), located in the membrane of the parasite´s DV. The polymorphisms leading to the K76T mutation in PfCRT has been shown to be the main determinant factor for CQ resistance [144–146], although other mutations are thought to balance the level of susceptibility. The positive charge on the original lysine residue at position 76 is assumed to prevent the binding of CQ to the active site of the transporter. The substitution into a neutral threonine residue therefore allows CQ to bind to PfCRT and be transported out of the DV, reducing the amount of CQ available to interfere with hemozoin crystallization [147,148].

The identification of artemisinins resistance markers has been a controversial topic over the last decades [119,120]. As mentioned above, PfATP6 has been extensively discussed as a component of artemisinins resistance. However, the correlation between artemisinins decreased susceptibility and polymorphisms in PfATP6 is being disputed, as some studies

confirmed this association [50,62–64], when others failed to [65,66,68,149]. Recently, multiple mutations in the propeller domain of the Kelch 13 protein (PfK13), beginning at amino acid residue 442, were associated with reduced susceptibility to artemisinins and extended clearance times [150–159]. These mutations show strong differences in their geographical distribution, consistent with multiple *de novo* mutational events. For instance, the C580Y mutation is prevalent at 50% in the Cambodia-Vietman-Laos region, whereas the F446I mutation is found to be dominant in samples from Thailand-Myanmar-China, with 20% of prevalence, and C580Y is only minimally found [116]. PfK13 mutations are now spread across South-East-Asia, and have reached India and some Central-Africa countries (Ethiopia, Mali, Senegal and Comoros) (Figure 1.7). It has been speculated that artemisinins inhibit the phosphorylation of phosphatidylinositol by the phosphatidylinositol 3-kinase (PfPI3K) in *P. falciparum*, overall decreasing the phosphatidylinositol 3-phosphate (PI3P) production and impairing lipid synthesis [160]. PfK13 is thought to polyubiquitinate PfPI3K, marking it for proteolytic degradation. When mutated, PfK13 fails to efficiently target PfPI3K to the proteasome, leading to its accumulation and to artemisinins resistance [161].

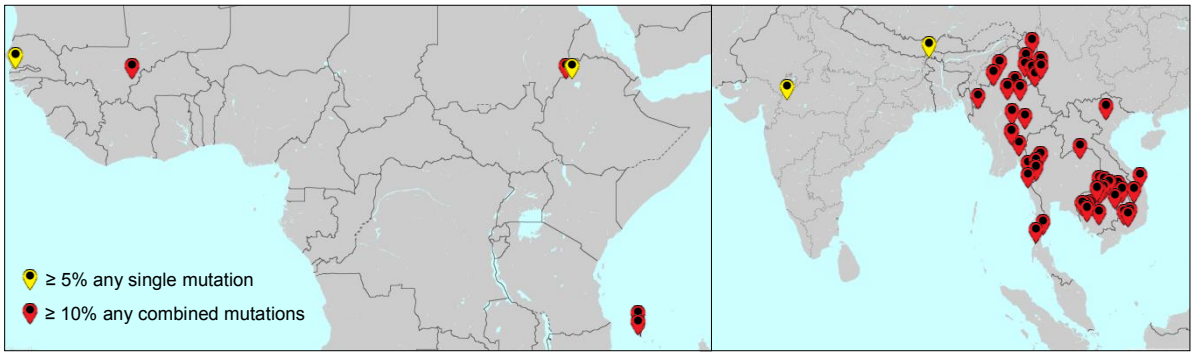

Figure 1.7: Current distribution of the mutations in PfKelch13. Prevalence in percent (%) of all the non-synonymous mutations within the propeller region of the PfK13 proteins alone or in combination, in Central Africa (left) and South-East Asia (right). Data obtain from the WorldWide Antimalarial Resistance Network (WWARN) online platform (http://www.wwarn.org/).

The multi-drug resistance receptor 1 (PfMDR1) has been found to be associated with resistance to various antimalarial drugs. PfMDR1 is an ATP-binding cassette transporter localized to the membrane of the parasite´s DV, and can modulate the response to a wide range of structurally diverse drugs, including artemisinins and their partner drugs. PfMDR1 is suggested to import antimalarial drugs into the DV [162], reducing the amount of drug at its action site, and SNPs in *pfmdr1* can modulate its affinity for a specific substrate [163]. Multiple SNPs and copy number variation in *pfmdr1* have been associated to both *in vivo* and *in vitro* decreased susceptibility to drugs as various as QN, CQ, mefloquine, halofantrine, lumefantrine, artemisnin, artesunate, dihydroartemisinin, as well as to some ACT´s [164].

1.3.3. Future perspectives for antimalarial drugs

It remains difficult to predict whether artemisinins resistance will spread as critically as resistance to CQ did decades ago. Nonetheless, this underlying threat, coupled with the creation of public-private partnerships such as the MMV and with financial support from philanthropic organizations such as the Wellcome Trust or the Bill & Melinda Gates Foundation, revived the field of antimalarial discovery.

Various strategies can be followed towards development of novel antimalarial agents (Figure 1.8), and either alone or combined, all the strategies endorsed promising drug candidates over the last decades.

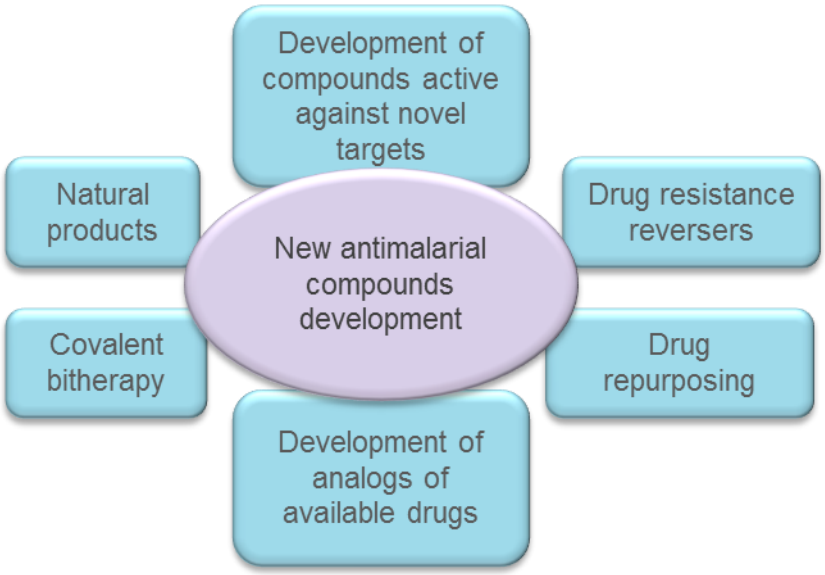

Figure 1.8: Various approaches for the development of new antimalarial agents. Adapted from [165].

The chemical optimization of existing and established antimalarial drugs, whether to improve pharmacological properties or to overcome resistance, has proven to be an effective approach, as illustrated by the development of the 4- and 8- aminoquinolines derived from quinine (see Section 1.3.1.1.). This development axis is still intensively exploited, and ferroquine, a ferrocene-containing analog of CQ, is currently under clinical evaluation as an antimalarial candidate [166,167]. Ferroquine has been shown to be active against CQ, amodiaquine and mefloquine resistant strains, due to its enhanced lipophilicity and hence increased ability to accumulate into the DV [168]. Similarly, the ozonide compounds have been derived from artemisinin, and display a trioxolane heterocycle in place of the trioxane present in artemisinins. Ozonides showed an improved efficacy against strains with reduced artemisinins susceptibility [169], and some are already marketed, such as OZ277, used in combination with piperaquine in India, under the brand name Synriam®. The representative

of the next generation of ozonides, OZ439 (Artefenomel), shows an increased bioavailability due to a higher susceptibility to heme degradation, and therefore a longer half-life [170]. OZ439 is currently evaluated in Phase II human clinical trials both as monotherapy or in combination with ferroquine [115, 116, MMV Artefenomel information sheet].

Exploiting compounds already proven to be active against other diseases is another widely used approach. Approved-drug repurposing is highly advantageous, as it allows cutting down the research timeline and costs of drug development. This strategy was for instance previously employed when tetracycline and macrolide antibiotics were adopted for prophylaxis and treatment of malaria [173,174]. More recently, the imidazolopiperazines, a family of folate inhibitors originally developed as antifungal and antihelminthic agents, are repurposed as antimalarials, to answer the growing resistance to the DHPS and DHFR inhibitors. Such a compound, KAF156, showing high potency against blood, gametocyte and liver stages of *P. falciparum* [175,176], is currently in phase I trial in malaria patients in Africa [MMV KAF156 information sheet].

Combining two pharmacophores with known antiplasmodial activity is a way to overcome resistance, by covalently linking two chemical moieties that act via different modes of action. This strategy can be illustrated by the development of SAR116242 (trioxaquine), a synthetic hybride between artemisinin and CQ pharmacophores, highly potent against sexual and asexual blood stages of both CQ-sensitive and resistant *P. falciparum* [177,178]. SAR116242 is currently under preclinical assessment at Sanofi-Aventis.

Finally, natural products have been a pillar for drug development over human history, and are constantly used as a source of molecular templates for developing new therapeutic agents. The recent progresses in developing highly efficient high-throughput screening technologies over the last decades made the exploitation of natural product libraries particularly effective. If natural products are rarely pharmacologically and pharmacokinetically adapted to be used as drug themselves, they however provide valuable hints and starting points for the development of new drugs. The emergence of a new antimalarial class, the spiroindolones is the results of such a screen of a natural compound library by Novartis [179]. One of the spiroindolone derivatives, KAE609 (cipargamin, formerly known as NITD609), highly potent against both *P. falciparum* and *P. vivax* in clinical isolates [179,180], is currently in Phase II of human clinical trials [165]. KAE609 was shown to interfere with the Na^+ transporter PfATP4, fatally disrupting sodium homeostasis in the parasite [179]. PfATP4 emerges as potential molecular target for rational drug design, further confirmed by the development of the clinical candidate (+)-SJ733 or the pyrazoleamide PA21A092, also inhibiting PfATP4 [181,182]. (+)-SJ733 is waiting for the recruitment of volunteers to enter the

first-in-human study [MMV (+)-SJ733 information sheet]. Identifying new molecular targets, such as PfATP4, and designing new chemical entities to interact with them is within the frame of the most scientifically sound approaches. The tremendous progress in deciphering the *Plasmodium* genomes and proteomes provided a solid basis to support such a rational design strategy.

1.4. Development of the drug candidate SC83288 for the treatment of severe malaria

The urgent need for novel antimalarial compounds, exploiting distinct molecular modes of action to the currently available antimalarial drugs was previously emphasized. In the field of drug development, diverse strategies can be followed, usually involving high-throughput screening at various steps of the entire development process. A drug candidate can be developed according to a rational design strategy, ligand- or structure-based, or following a wider phenotypic approach, i.e. “whole-cell”-based. The former relies on the identification of a therapeutic molecular target, and a precise structural knowledge of its active site to design potent inhibitors, whereas the latter aims on identifying compounds with a toxic effect on *Plasmodium* species (or any targeted organism), with lesser consideration for their mode of action. Several rounds of iterative structure-activity relationship analysis usually allow a selected compound, or hit-compound, to be further optimized into a pharmacologically and pharmacokinetically improved lead-compound [183]. Both approaches have already yielded promising results by identifying new classes of antimalarial compounds such as the spiroindolones [180], by phenotypic blood stage screen, or the ozonides by rational design [184,185].

As many prominent companies and institutions are dedicating tremendous resources into antimalarial libraries high-throughput screening, such as the Genomic Institute of the Novartis Institute for Biomedical Research (NIBR), GlaxoSmithKline (GSK) or the St. Jude Children´s Research Hospital (SJCRH) [183], other research and screens are conducted at a smaller scale. Accordingly, the original strategy of the biotechnological company 4SC AG, Munich, Germany, was to identify new inhibitors of the *P. falciparum* lactate dehydrogenase (PfLDH) by *in silico* screening [186]. A first *in silico* screen through docking of a virtual library of small organic molecules into the binding pocket of PfLDH allowed the identification of a series of molecules with high scoring, further tested in a whole cell-based assay. The benzamidine derivative amicarbalide (Figure 1.9) was identified as a potent *P. falciparum* growth inhibitor. Amicarbalide was formerly used as a veterinary antiprotozoal drug

[187,188], before underlining safety issues forced regulatory agencies to remove it from the market. Despite its promising antiplasmodial activity, amicarbalide displayed only a marginal activity as a PfLDH inhibitor [186]. Nonetheless, amicarbalide became the starting point of medicinal chemistry program for the development of potent and pharmacologically optimized antimalarial drugs.

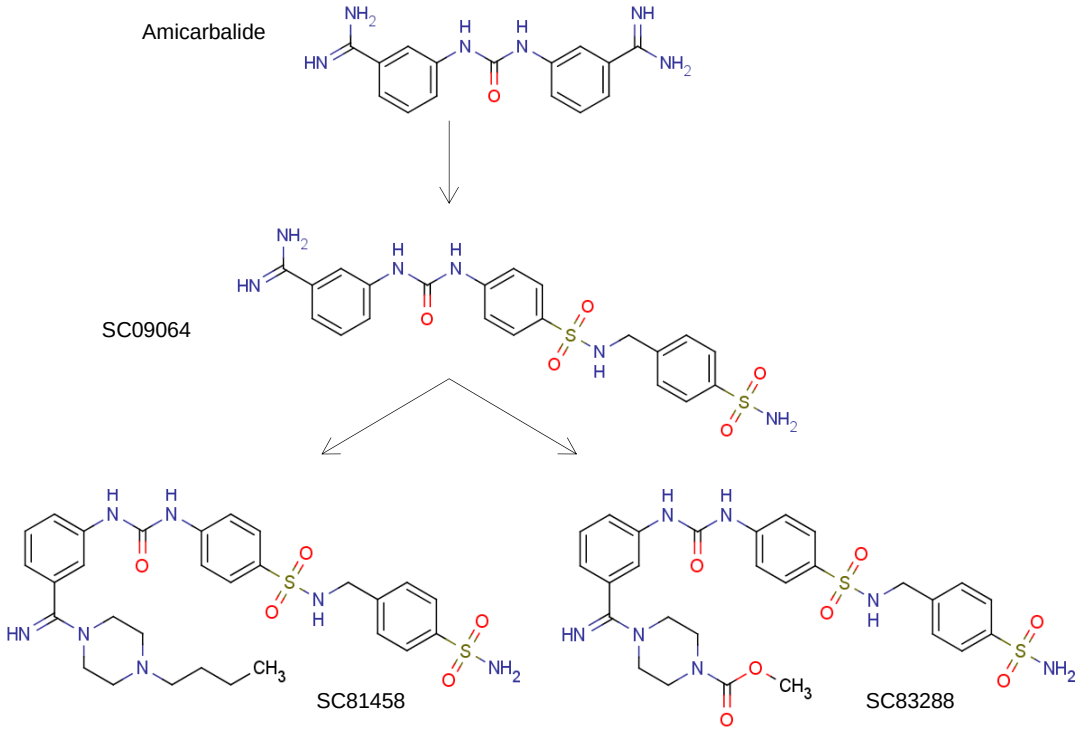

Figure 1.9: Chemical structures of the hit- and lead-compounds. Adapted from [189].

Out of this process a lead-compound, SC09064 (Figure 1.9) emerged, where the east-side amidino group was substituted by a bulky 4´-sulfonamidomethyl benzene para-sulfonamido group [186,189]. The further optimization of the west side of the molecule led to the two lead-compounds, SC81458 and SC83288 (Figure 1.9), after the functionalization of the amidine group with a piperazine ring, providing improved pharmacological properties [189]. SC83288, the second lead-compound, is considered a clinical development candidate for the treatment of severe malaria [189].

Preliminary studies linked PfATP6 with a decrease in responsiveness to the SC-lead compounds [189], building one of the founding pillars of the work presented here.

1.5. Aim of the study

Understanding the mode of action of a therapeutic molecule and identifying the components involved in resistance is not mandatory for a compound to be released on the market. However, gathering precise molecular insights on these aspects might be crucial as they may help to predict and control the molecule´s interactions with both its environment and with other drugs, once introduced in the field.

This doctoral study contributes to the evaluation and further development of the SC-lead compounds, particularly the clinical development candidate SC83288, as antimalarial compounds. The aim of this work is two-fold. On the one hand it focuses on the characterization of the antiplasmodial activity of the SC-lead compounds. It provides a detailed characterization of the *in vitro* activity profile against cultured blood-stages *P. falciparum* parasites, as well as preliminary insight into their mode of action. On the other hand, this work confirms and details the role of the Ca^{2+} ATPase pump PfATP6 in the resistance of *P. falciparum* to SC83288, particularly in regard with calcium homeostasis.

2. Materials and methods

2.1. Materials

2.1.1. Equipment

Equipment	Company
Analytical scales	Sartorius, Göttingen, Germany
ApE	http://biologylabs.utah.edu/jorgensen/wayned/ape/
Autoclave	Tuttnauer Systec 2540, Wettenberg, Germany
BD FACS Canto	BD Bioscences, Heidelberg, Germany
Bioedit	http://www.mbio.ncsu.edu/BioEdit/bioedi
Biofuge fresco	Heraeus Instruments, Hanau, Germany
Biofuge pico	Heraeus Instruments, Hanau, Germany
BioRad gel Dryer 583	BioRad, München, Germany
Blot Scanner C-DiGit	Li-cor, Bad Homburg, Germany
Camera S6X11	Rainbow CCTV, Ivrine, CA, USA
ClustalW2	http://www.ebi.ac.uk/Tools/msa/clustalw2/
Confocal Leica TCS SP5	Leica Microsystems CMS GmbH, Jena, Germany
Electroporator Gene Pulser® II	Biorad, München, Germany
FIJI image analysis	http://fiji.sc/Fiji
FlowingSoftware2.5.1	Cell Imaging Core, Turku Centre for Biotechnology, Finland
Freezer -20°C LGex3410 MedLine	Liebherr, Biberach, Germany
Freezer -80°C HERAfreeze	Thermo Fisher Scientific, Dreieich, Germany
Fridge LKexv 3910 MedLine	Liebherr, Biberach, Germany
Fujifilm Bas cassette 2040	Fujifilm, Düsseldorf, Germany
Fujifilm FLA-7000	Fujifilm, Düsseldorf, Germany

Gas burner gasprofi 1 micro	WLD-TEC
Heat block, NoeBlock Mono I	NeoLab, Heidelberg, Germany
Hybridizazion incubator Techne HB-1D	Bibby Scientific, Staffordshire, UK
Icemachine	Ziegra, Isernhagen, Germany
Incubator Heraeus B12/UB12	Thermo Fisher Scientific, Dreieich, Germany
J2-MC	Beckman, Krefeld, Germany
Kodak Digital Science 1D	Kodak, New York, USA
L-60 Ultracentrifuge	Beckman, Krefeld, Germany
Light optical microscope Axiolab.A1	Zeiss, Jena, Germany
LightCycler® 2.0 Instrument	Roche, Mannheim, Germany
Liquid nitrogen tank	Air Liquide, Ludwigshafen, Germany
Magnetic sorter VarioMACS	Miltenyi Biotec, Bergisch Gladbach, Germany
Magnetic stirrer	Heidolph, Schwabach, Germany
Magnetic stirrers	IKA, Staufen, Germany
Megafuge 1.0 R	Heraeus Instruments, Hanau, Germany
Megafuge 2.0 R	Heraeus Instruments, Hanau, Germany
Microwave oven	AEG, Nürnberg, Germany
MiliQ water system Purist ultrapure	Rephile, Germany
MS Excel 2010	Microsoft Corporation, CA USA
MS Powerpoint	Microsoft Corporation, CA USA
MS Word 2010	Microsoft Corporation, CA USA
MVE Cryosystem 6000	Thermo Fisher Scientific, Dreieich, Germany
LS 6000	Taylor-Wharton, Husum, Germany

Particle counter Z1	Beckman Coulter, Krefled, Germany
pDRAW32 software	AcaClone software
pH-meter pH 7110	WTW, Weilheim, Germany
Pipetman Gilson P10; P20; P200; P1000	Abimed, Langenfeld, Germany
Pipetus Forty/Standard	Hirschmann Labortechnik, Eberstadt, Germany
PlasmoDB	http://plasmodb.org/plasmo/
Plate reader FLUOstar OPTIMA	BMG Labtech, Ortenberg, Germany
Power Pac 300, Power Pac 200	Biorad, München, Germany
EPS 1001, EPS 3501	Amersham (GE Healthcare), München, Germany
Printer hp LaserJet 1300	Hewlett Packard, Heidelberg, Germany
Protein Data Bank	http://www.rcsb.org/pdb/home/home.do
PyroMark Q96 ID	QUIAGEN, Hilden, Germany
RC5BPlus	Sorvall, Langenselbold, Germany
Rotors JA20.2, JA20.1	Beckman instruments, Palo Alto, CA, USA
Rotors SS-34; GS-3 , SM24	DuPont Instruments, Bad Homburg, Germany
RS Series	Taylor-Wharton, Husum, Germany
Semi-dry transfer cell Trans blot SD	BioRad, München, Germany
Serial Cloner 2.6	http://serialbasics.free.fr/Serial_Cloner.html
Shaker KS 501 digital	IKA, Staufen, Germany
SigmaPlot 12.0	Systat Software Inc.
Sonicator Sonoplus HD 2070	Bandelin, Berlin, Germany
Spectrophotometer UVIKON 923	Kontron Instruments, München, Germany
Sterile work bench Herasafe	Heraeus Instruments, Hanau, Germany
Stop watch	Roth, Karlsruhe, Germany

Thermocycler Labcycler	SAensoquest, Göttingen, Germany
UV table TFX-35M	Vilber Lourmat, Eberhardzell, Germany
Vacuum workstation PyroMarkt Q96	QUIAGEN, Hilden, Germany
Vortex Genie 2	Roth, Karlsruhe, Germany
Water bath Julabo 7A	Julabo, Seelbach, Germany
Zeiss Image Examiner	Zeiss, Jena

2.1.2. Disposables

Diposable	**Company**
96-well plates, black, clear	Greiner Bio-One, Frickenhausen, Germany
Aluminium foil	Roth, Karlsruhe, Germany
Cell culture plates	Greiner Bio-One, Kremsmünster, Germany
Cellstar tubes	Greiner bio one, Frickenhausen, Germany
Coverslides	Roth, Karlsruhe, Germany
Cryovials	Nalgene®, Wiesbaden, Germany
Cuvettes	Sarstedt, Nümbrecht, Germany
Electroporation cuvettes Gene Pulser	Biorad, München, Germany
Eppendorf tubes	Sarstedt, Nümbrecht, Germany
Filter systems 500 ml	Corning, Kaiserslautern, Germany
Filters Millex GS (0.2 µm)	Merck Millipore, Darmstadt, Germany
Gloves TouchNTuff	Ansell, München, Germany
Immersion oil	Zeiss, Jena, Germany
LightCycler capillaries	Roche, Mannheim, Germany
MACS CS column	Miltenyi Biotec, Bergisch Gladbach, Germany

Object slides	Marienfeld, Lauda-Königshofen, Germany
Parafilm	Bemis, Londonerry, UK
PCR softtubes 0.25 ml	Biozym Scientific GmbH
Petri dishes (10 ml diameter)	Greiner Bio-one, Frickenhausen, Germany
Petri-dishes (25 ml diameter)	Greiner Bio-one, Frickenhausen, Germany
Pipette tips	Corning incorporation, Bodenheim, Germany
Plastic pipettes (1 ml; 2 ml; 5 ml; 10 ml: 25 ml)	Corning incorporation, Bodenheim, Germany
PVDF membrane	Biorad, München, Germany
PyroMark Q96 Plate low	QUIAGEN, Hilden, Germany
Sterile filtration devices	Corning incorporation, Bodenheim, Germany
Thermo well PCR	Corning incorporation, Bodenheim, Germany
Transfer pipettes	Sarstedt, Nümbrecht, Germany

2.1.3. Chemicals

The chemicals used in this study were obtained from the firms Roth, Merck, Sigma, Serva, Thermo and Applichem and were ordered directly or through the Heidelberg Medical Facility, unless mentioned otherwise.

The SC-compounds, namely SC81458 and SC83288 were provided by the 4SC AG, München, Germany.

2.1.4. Biological material

Enzymes and protein markers

Compound	Company
6 x DNA loading buffer	Thermo Fisher Scientific, Dreieich, Germany
EuroTaq polymerase	BioCat GmbH, Heidelberg, Germany
GeneRuler 1 kb ladder plus	Thermo Fisher Scientific, Dreieich, Germany
PageRuler	Thermo Fisher Scientific, Dreieich, Germany
Phusion Polymerase	Fermentas, Germany
Restriction enzymes	New England Biolabs, Frankfurt am Main, Germany
Shrimp Alkaline phosphatase	New England Biolabs, Frankfurt am Main, Germany
T4 ligase	Thermo Fisher Scientific, Dreieich, Germany

Kits

Kit	Company
BM chemiluminescence blotting substrate POD	Roche, Mannheim, Germany
CloneJET PCR Cloning Kit	Thermo Fisher Scientific, Dreieich, Germany
DNeasy Blood&Tissue kit	Qiagen, Hilden, Germany
Gel Extraction/PCR purification kit	Qiagen, Hilden, Germany
High Pure Plasmid Isolation kit	Roche, Mannheim, Germany
In-Fusion® HD Cloning kit	Clontech Laboratories, USA
LightCycler FastStart DNA Master SYBR Green I	Roche, Mannheim, Germany
Plasmid MaxiPrep kit	Qiagen, Hilden, Germany
PyroMark Gold Q96 Reagents kit	Qiagen, Hilden, Germany
SuperScript® III First-Strand Synthesis	Thermo Fisher Scientific, Dreieich, Germany

Supermix	
Calcium Calibration Buffer Kit #1	Thermo Fisher Scientific, Dreieich, Germany

Fluorescent dyes

Fluorescent dye	**Company**
Fluo4-AM	Thermo Fisher Scientific, Dreieich, Germany
FuraRed-AM	Thermo Fisher Scientific, Dreieich, Germany
Hoechst 33342	Thermo Fisher Scientific, Dreieich, Germany
CFDA SE Cell Tracer	Thermo Fisher Scientific, Dreieich, Germany
MitoTracker Orange CM-H_2TMRos	Thermo Fisher Scientific, Dreieich, Germany
DRAQ5	Biostatus, Leicestershire, United Kingdom

Antibodies

Antibody	**Source**	**Company**
Anti-HA tag monoclonal	Mouse	Roche, Mannheim, Germany
Anti-mouse-POD monoclonal	Donkey	Jackson ImmunoResearch, Suffolk, UK
Anti-α-tubulin monoclonal	Mouse	Sigma Aldrich, München, Germany

Parasites strains

Strain	**Origine**
P. falciparum 3D7	The Netherlands
P. falciparum 3D7 PfATP6 ^{F972Y}	Generated by Maëlle Duffey during this study, Heidelberg, Germany
P. falciparum Dd2	Indochina [190]
P. falciparum Dd2 pHBIRH-ATP6(A108T, A109T)-HA	Generated by Maëlle Duffey during this study, Heidelberg, Germany
P. falciparum Dd2 pHBIRH-ATP6(WT)-HA	Generated by Maëlle Duffey during this study, Heidelberg, Germany

P. falciparum HB3	Honduras [191]
P. falciparum NF54	The Netherlands [192]
P. falciparum NF54 PfK13 ^{C580Y}	Provided by Prof. Lopez-Rubio, Montpellier, France [78]

E. coli strains

Strain	**Origine**
E. coli PMC 103	Provided by Prof. Cowman [193]
E. coli XL-1-Blue	Thermo Fisher Scientific, Dreieich, Germany
E. coli XL10 Gold	Agilent Technologies, Böblingen, Germany

Plasmids

All the plasmids used in this study are described in Appendix II.

Plasmid	**Origin**
pARL-0105800-HA	Generated by Maëlle Duffey during this study, Heidelberg, Germany
pARL-0105900-HA	Generated by Maëlle Duffey during this study, Heidelberg, Germany
pARL-0106000-HA	Generated by Maëlle Duffey during this study, Heidelberg, Germany
pARL-0106100-HA	Generated by Maëlle Duffey during this study, Heidelberg, Germany
pARL-0106200-HA	Generated by Maëlle Duffey during this study, Heidelberg, Germany
pHBIRH-ATP6-(A108T, A109T)-HA	Generated by Maëlle Duffey during this study, Heidelberg, Germany
pHBIRH-ATP6-(WT)-HA	Generated by Maëlle Duffey during this study, Heidelberg, Germany
pL6-HRA-guide6	Generated by Maëlle Duffey during this study, Heidelberg, Germany

pL6-HRAsi-guide6	Generated by Maëlle Duffey during this study, Heidelberg, Germany
pL6-HRB-guide7	Generated by Maëlle Duffey during this study, Heidelberg, Germany
pUF1-Cas9	Provided by Prof. Lopez-Rubio, Montpellier, France [78]

Oligonucleotides

The oligonucleotides used in this study were purchased from Thermo Fisher Scientific or Eurofins.

- Oligonucleotide primers used for colony PCR and sequencing

Number	**Name**	**Sequence**
1	pJET-for	CGACTCACTATAGGGAGAGCGGC
2	pJET-rev	AAGAACATCGATTTTCCATGGCAG
3	pL6-guide-for	GTAACCAAAATGCATAATTTTTCC
4	pL6-guide-rev	TAGGAAATAATAAAAAAGCACC
5	pL6-HA-ribo-for-5´	ATTTAACTATATACTATGGAATAC
6	pL6-HA-ribo-rev-3´	ACCAATAGATAAAATTTGTAGAG
7	pARL-for	CTATAATATCCGTTAATAATAAATACACGCAGTC
8	pARL-rev	CACAACATACACATTTTTACAG
9	pHBIRH-for	ACAAACCTACATATACATAC
10	pHBIRH-rev	TTTGTAATTTATGGGATAGC

- Oligonucleotide primers used for qPCR

Number	Name	Sequence
11	Pf3D7_0105800-for	CGGAAGATTTTGAGAACAAC
12	Pf3D7_0105800-rev	AATTTAATTCCCCTTTGCTC
13	Pf3D7_0105900-for	CATATGAACAATTGGAGGCTC

14	Pf3D7_0105900-rev	CAATAATAAATTCCGTGTCGAATC
15	Pf3D7_010600-rev	CGATATCCTTTTTCTCATTAGGTAC
16	Pf3D7_010600-for	GAGCAGGTACCAAAGGTATTG
17	Pf3D7_0106100-for	GTGCTTAGCCGCTTTTTCAG
18	Pf3D7_0106100-rev	GAAGCAAAATTAGGTGGAACAC
19	Pf3D7_0106200-for	TGACAACCCAAATGAAGCTATC
20	Pf3D7_0106200-rev	CCTGAGCATCTAAAAAGTACTTC
21	cDNA-ATP6 2-rev	GTCAAAGAATCAGATTCTCTAAAC
22	cDNA-ATP6 3-for	GATGGATTACCAGCAACTGC
23	cDNA- aTub-for	CAGTTGGAGGTGGAACAGG
24	cDNA- aTub-rev	ATGGCCAACAGCAAAAATTC

- Oligonucleotides primers for cloning in the pARL and pHBIRH vectors

In blue, enzyme restriction sites.

Number	Name	Sequence
25	800-XhoI-for	CCGCTCGAGATGGCTACAAATAGTAATAATAACAACAG
26	800-AvrII-rev	ATCGCCTAGGATTATTTTTAGGTCGTCTAAAAAATAGGAC
27	900-XhoI-for	CCGCTCGAGATGCTGAAAGGATTTAAGCATATTTTAAAC
28	900-AvrII-rev	ATCGCCTAGGTGTGCAGAGCGTGTGATC
29	000-XhoI-for	CCGCTCGAGATGCGATCCAAATATTACAAGGAAG
30	000-AvrII-rev	ATCGCCTAGGGGAGGAGAAGGCAAAGTGG
31	100-XhoI-for	CCGCTCGAGATGAGTGAAATTCCCATGTG
32	100-AvrII-rev	ATCGCCTAGGTATTTTAAAGGACACCGAAACGTAG
33	200-XhoI-for	CCGCTCGAGATGGAAAATATAAATAGAGTAAATAAATATGACAAC

34	200-AvrII-rev	ATCGCCTAGGTATATATTTATAACATGTTAACATGTCAACG TAC
35	ScATPase6-SpeI-for	CCGACTAGTCACCATGGAAG
36	ScATPase6-SacI-rev	ATCGGAGCTCTTAAACACCATGA
37	ScATPase6-mut1/2-for	CTTAATTTTGAACACTACTGTTGGTG
38	ScATPase6-mut1/2-rev	CACCAACAGTAGTGTTCAA AATTAA G

- Oligonucleotides primers used for cloning of the CRISPR/Cas9 system

In blue, enzyme restriction sites; in orange, homology regions for the InFusion cloning; in red, desired mutations; in green, shield mutations.

Number	Name	Sequence
39	ATPase6-HRA(-79)-SpeI-for	GGACTAGTTTTCGTTGAACTTATTATATC
40	ATPase6-HRA-855-BssHII-rev	TTGGCGCGCGAATTGGATCTGAGAAATGT
41	ATPase6-HRB-2269-SpeI-for	GGACTAGTGCATTAAGAACACTTAGCTTTG
42	ATPase6-HRB-3409-BssHII-rev	TTGGCGCGCGTTATTCCATGCTTTACATTGGT
43	ATPase6-620-1080-for (2)	TTAAATACTACCGTAGGCGTGTGGCAAG
44	ATPase6- 620-1080-rev (2)	CTTGCCACACGCCTACGGTAGTATTTAA
45	ATPase6-shield(guide7)-for	GAAAGCATATATCCGATATTTAATTAG
46	ATPase6-shield(guide7)-rev	CTAATTAAATATCGGATATATGCTTTC
47	ATP6 HRA sil-for	TAATATTAAATGCCGCTGTAGGTG
48	ATP6 HRA sil-rev	CACCTACAGCGGCATTTAATATTA
49	ATPase6-guide 6-for	TAAGTATATAATATTTTAATATTAAATGCTGCC GTGTTTTAGAGCTAGAA
50	ATPase6-guide 6-rev	TTCTAGCTCTAAAACACGGCAGCATTTAATAT

		TAAAATATTATATACTTA
51	ATPase6-guide 7-for	TAAGTATATAATATTTATTACTACTAATTAGATA AGTTTTAGAGCTAGAA
52	ATPase6-guide 7-rev	TTCTAGCTCTAAAACTTATCTAATTAGTAGTAA TAAATATTATATACTTA

- Oligonucleotide primers used for the fitness assay and pyrosequencing

Number	Name	Sequence
53	PfATP6- for (Fit/PCR)	CTATGGGTATTAATGGAACGGAGG
54	PfATP6- rev2 (Fit/Biotin)	CGTCAGTAACCAAATTTACCCAC
55	PfATP6- for (Fit)	GATGTATATATAATAATATGAAAGC

2.1.5. Buffers, media and solutions

Buffer/Media/Solution	**Composition**
Albumax II	5% (w/v) Albumax II In RPMI 25 mM HEPES L-Glutamine (Gibco), filter sterilize
Ampicillin stock, 1000 x	100 mg/ml in ddH2O
Annealing buffer (pyrosequencing)	20 mM Tris 2 mM magnesium acetate Set pH to 7.6 with HCl and autoclave
Binding buffer (pyrosequencing)	10 mM Tris 2 M NaCl 1 mM EDTA Set pH to 7.6 with HCl and autoclave

	Add 0.1% Tween 20
Blocking solution	5% (w/v) skimmed milk in PBS
Cell culture media	
Non-transfectants	10% human serum
	0.2 µg/ml Gentamycin
	0.2 mM Hypoxanthine
	In RPMI 25 mM HEPES L-Glutamine (Gibco)
Transfectants	5% human
	5% Albumax II
	0.2 µg/ml Gentamycin
	0.2 mM Hypoxanthine
	In RPMI 25 mM HEPES L-Glutamine (Gibco)
Coomassie destaining solution	20% methanol
	7% acetic acid
Coomassie staining solution	50% methanol
	10% acetic acid
	0.5% Coomassie Blue R-250
Cytomix	120 mM KCl
	0.15 mM CaCl2
	10 mM K2HPO4/KH2PO4, pH 7.6
	25 mM HEPES/2 mM EGTA, pH 7.6
	5 mM MgCl2 in ddH2O
	Adjust to pH 7.6 with KOH
	Filter sterilize
Denaturation solution (pyrosequencing)	0.2 M NaOH

DNA loading buffer (6x)	60% glycerol
	60 mM EDTA
	0.25% Bromophenol Blue
Fixation solution	1x PBS
	4% paraformaldehyde
	0.0075% gluteraldehyde
Freezing solution	6.2 M glycerol
	0.14 M Na-lactate
	0.5 mM KCl
	Add ddH2O, adjust to pH 7.2 with 0.5 M NaHCO3, ph)
	Filter sterilize
IC_{50} lysis buffer	20 mM Tris base
	Adjust to pH 7.4 with concentrated HCl
	5 mM EDTA
	0.008% (w/v) Saponin
	0.08% (w/v) Triton X-100
	Mix, vacuum filter, store at RT
LB	1% (w/v) tryptone
	0.5% (w/v) yeast extract
	0.5% (w/v) NaCl
	Autoclave
LB agar	10 g tryptone/peptone
	5 g yeast extract
	5 g NaCl
	15 g agar

	In 1 l ddH2O, autoclave
LB broth	10 g tryptone/peptone
	5 g yeast extract
	5 g NaCl
	In 1 l ddH2O, autoclave
Lysis Buffer I	0.07% (w/v) saponin in PBS
	Protease inhibitors
	0.5 % (v/v) phosphatase cocktail inhibitors (Sigma)
Lysis Buffer II	1x PBS
	8 M urea
	100 mM NaCl
	25 mM Tris, pH 8
	Protease inhibitors
	0.5 % (v/v) phosphatase cocktail inhibitors (Sigma)
MACS buffer	2 mM EDTA
	1 x PBS
	Autoclave
	Add 0.5% (w/v) BSA prior to use
NZY^+ Broth	1% (w/v) NZ amine (casein hydrolysate)
	0.5% (w/v) yeast extract
	0.5% (w/v) NaCl
	Set pH to 7.5 with NaOH and autoclave
	Add the following filter-sterilized supplements prior to use:

	12.5 mM MgCl2
	12.5 mM MgSO4
	0.4% (w/v) glucose
Permeabilization solution	1x PBS
	0.1% Triton-100
Protease inhibitors (PI)	0.002% (w/v) leupeptin
	0.005% (w/v) aprotinin
	100 µM PMSF
Protein loading buffer (2x)	3% (w/v) SDS
	250 mM Tris pH 6.8
	20% glycerol
	0.1% Bromophenol blue
Protein lysis buffer	0.07% (w/v) saponin in PBS
	Protease inhibitors
Ringer solution	10 mM HEPES
	122.5 mM NaCl
	5.4 mM KCl
	1.2 mM CaCl2
	0.8 mM MgCl2
	1 mM NaH2PO4
	11 mM glucose
	Adjust to pH 7.4 with NaOH
	Sterilize by filtration
RNA running buffer (20x)	41.86 g MOPS
	6.8 g NaOAc

	3.8 g EDTA
	In 500 ml ddH2O
RNase solution	1x PBS
	0.3 mg/ml RNase A
SDS-PAGE running buffer	25 mM Tris
	250 mM glycine
	0.1% (w/v) SDS
SDS-PAGE transfer buffer	39 mM Tris
	48 mM glycine
	0.038% (w/v) SDS
SOB medium	20 g tryptone/peptone
	5 g yeast extract
	0.5 g NaCl
	5 g MgSO4 x 7 H2O
	In 1 l ddH2, autoclave
SOC medium	SOB + 20 mM D-Glucose, sterile
	Store at -20°C
Sorbitol solution	5% (w/v) D-sorbitol in ddH2O
	Filter sterilize
Stripping buffer	1x PBS
	2% SDS
	100 mM β-mercaptoethanol
Super Broth (SB)	35 g tryptone/peptone
	30 g yeast extract
	5 g NaCl

	In 1 l ddH2O, autoclave
SYBRGreen I Solution	1x PBS
	1:2 000 SYBRGreen I
TAE buffer, 1 x	4 mM Tris-acetate
	1 mM EDTA, pH 8
TB Buffer	10 mM PIPES
	15 mM CaCl2
	250 mM KCl
	Set pH to 6.7 with KOH
	Add 55 mM MnCl2
	Sterilize by filtration
TE Buffer	10 mM Tris/HCl, pH 8
	1 mM EDTA
	In ddH2O
	Filter sterilize
Thawing solution I	12% NaCl in ddH2O
	Filter sterilize
Thawing solution II	1.6% NaCl in ddH2O
	Filter sterilize
Thawing solution III	0.9% NaCl
	0.2% glucose
	In ddH2O
	Filter sterilize
Wash buffer (pyrosequencing)	10 mM Tris
	Set pH to 7.6 with HCl and autoclave

WR99210	20 µM in RPMI 25 mM HEPES L-Glutamine
WR99210 stock	10 mM in 20% DMSO (v/v)

2.2. Methods

2.2.1. Cell culture of *Plasmodium falciparum* parasites

2.2.1.1. *In vitro* culture conditions

Intraerythrocitic stages of *P. falciparum* were maintained in continuous blood culture according to standard protocols [73]. Cultures were maintained in an incubator with a fixed atmosphere of 5% O_2, 3% CO_2, 92% N_2 and 95% humidity at 37°C. Routine cultures were established at a hematocrit of 3% - 4% in final volumes of 14 ml or 35 ml in a 10 cm or 25 cm diameter petri dish, respectively. The parasitemia varied between 0.5% - 5% according to the need. The detailed composition of culture media is stated in Section 2.1.5. Parental strains were cultured in non-transfectant medium, containing 10% human serum. Transfected strains were cultured in transfectant medium, in which half of the serum was replaced by Albumax. Hematocrit and parasitemia were adjusted for individual experiments according to the respective protocol. Cultures were surveyed regularly on Giemsa-stained thin blood smears. According to the need, the medium was exchanged to avoid accumulation of toxic parasite metabolites or cultures were diluted with fresh erythrocytes to decrease parasitemia.

2.2.1.2. Morphological monitoring of parasites and determination of parasitemia

Parasite cultures were examined on Giemsa-stained thin blood smears, allowing the determination of developmental stages, morphological alterations and parasitemia. Thin blood smears were prepared from 50 µl of concentrated erythrocytes on clean microscope slides and subsequently air dried; fixed in 100% methanol for 30 seconds, air dried and stained in a 10% Giemsa solution for 10 to 30 minutes. After staining, slides were washed under running water and air dried. Smears were analyzed with a light microscope using an oil immersion 100 x objective. The numbers of both infected and total erythrocytes were counted on ten consecutive fields (approximately a total of 1000 cells) and the parasitemia was calculated according to the formula:

$$Parasitemia\ [\%] = \frac{Number\ of\ infected\ erythrocytes}{Number\ of\ erythrocytes} \times 100$$

2.2.1.3. Parasites synchronization with sorbitol

Synchronization of cultures to the ring stage was performed using the sorbitol method [194]. Sorbitol destroys trophozoite and schizont-stage parasites, which possess the tubovesicular network, by osmotic shock. Ring-stage parasites are still lacking this induced transport system and therefore survive sorbitol treatment. Whenever a synchronized trophozoite culture was required for an experiment, synchronization was performed approximately 16 to 18 hours prior the experiment. Briefly, pelleted infected erythrocytes (0.5 to 1.5 ml) were resuspended in a prewarmed 5% sorbitol solution (8 to 10 ml) and incubated in a closed falcon tube at 37°C for 5 minutes (e.g. water bath or incubator). After incubation, cells were centrifuged (2100 rpm, 2 min, RT) and the supernatant sorbitol solution was removed. Cells were resuspended in culture medium, adjusted to the desired hematocrit and returned to culture.

2.2.1.4. Cryopreservation and thawing of the parasites

P. falciparum ring-stage parasites are suitable for cryopreservation in a designated freezing solution (for composition see Section 2.1.5.). Since the percentage of ring-stage parasites will affect the revival speed after thawing, a culture containing at least 5% of rings is suggested for freezing. The culture was pelleted, and the supernatant completely discarded. The remaining pellet was mixed with approximately 1/3 volume of freezing solution (e.g. 500 µl cell pellet + 150 µl freezing solution) and incubated for 5 minutes at room temperature. Subsequently, another 4/3 volume of freezing solution was added (e.g. 600 µl) and the solution was thoroughly mixed. The cell solution was transferred to specific cryovials (approximately 500 µl per vial) and frozen at -80°C. Short-term storage was maintained in a -80°C freezer, while cryovials were transferred to a liquid nitrogen tank for long-term storage.

For thawing the parasites cultures, frozen cryovials were shortly warmed up in a 37°C water bath until the cell solution turned liquid. Then, 20 µl of Thawing Solution I was added dropwise and the resulting solution transferred to a fresh 15 ml falcon tube. Slowly, 9 ml of Thawing Solution II were added dropwise under steady rotation of the falcon tube. The solution was centrifuged (1900 rpm, 2 min, RT) and the supernatant discarded. The pellet was slowly resuspended in 7 ml of Thawing Solution III, which was added dropwise. The solution was centrifuged (1900 rpm, 2 min, RT), the supernatant removed, and the pellet resuspended in a few milliliters of culture medium. The cell solution was then transferred to a petri dish and fresh erythrocytes and fresh culture medium were added. All solutions were prewarmed at 37°C before starting the thawing procedure.

2.2.1.5. Magnetic purification of the parasites

P. falciparum trophozoite and schizont stages were purified using the MACS system. The MACS CS column was washed twice with MACS buffer and inserted into the VarioMACS separator. The cultured was resuspended and applied to the top of the column. The flow was adjusted to 1 drop every 3 seconds. The column was washed with MACS buffer until the flow-through was clear. The column was removed from the separator and the enriched late stages iRBC were eluted in 10 ml of MACS buffer. The cells were centrifuged (2100 rpm, 2 min, RT) and the pellet was resuspended in the appropriate buffer according to the experiment the cells were going to be used for.

2.2.1.6. Plasmid DNA transfection of parasites

Preparation of parasites:

The transfection of *P. falciparum* was performed by electroporation of 3 to 5 % ring stage parasite culture. Parasites were synchronized a few days before transfection. Prior to transfection the parasite culture was resuspended, centrifuged (1900 rpm, 2 min, RT) and the supernatant was removed.

Preparation of DNA:

After isolation of the transfection plasmids using the Plasmid Maxi Kit (Qiagen), the concentration and quality was estimated by spectrophotometry and agarose gel electrophoresis. A volume equal to 75 µg of DNA was used for transfection. The DNA was precipitated by addition of a 1:10 volume of sodium acetate (3M, pH 4.5 – 4.8) and 2.5 volumes of ethanol 99%. Short vortexing and incubation at -20°C for at least 30 minutes resulted in the visible condensation of DNA. After centrifugation at 13000 rpm at 4°C for 30 minutes, the pellet was desalted with 0.5 ml of ethanol 70%. Finally, after further centrifugation (13000 rpm, 10 min, 4°C), the pellet was air-dried and resuspended in 30 µl of sterile TE-Buffer and stored at -20°c until transfection. Prior to transfection, the DNA was supplemented with 370 µl of sterile cytomix solution.

Electroporation of infected red blood cells:

A fresh culture dish containing 14 ml transfection medium and 0.5 ml of fresh erythrocytes was prepared in advance shortly before the transfection procedure. 200 µl of 3 to 5 % ring-stage infected erythrocytes were combined with 400 µl of DNA/cytomix mixture, immediately transferred to an electroporation cuvette and electroporated in the gene pulser (Biorad) with 0.31 kV and 0.950 µF at the highest capacity settings. Quickly afterward the sample was pipetted into the prepared culture plate and incubated at 37°C for 4 to 6 hours before changing the medium and replacing it by fresh transfection medium.

Selection procedure:

One day after transfection the medium was exchanged and the positive selection marker(s) were added. Starting from the third day post-transfection, the transfection medium and the selection markers were exchanged daily for one week, during which the parasites disappeared from the blood smears. This was followed by a 3 to 5 weeks of selection period when fresh medium and markers were provided thrice a week until the parasites appeared again on the blood smears. 100 µl of fresh erythrocytes were added once per week.

	Stock	*Final*
DSM1:	10 mM	1.5 µM
WR 99210	20 µM	5 nM
Blasticidin	10 mg/ml	varying from 2.5 to 15 µg/ml

2.2.1.7. Cloning parasites by limiting dilution

Clonal parasite populations were retrieved by limiting dilution of a culture in 96-well plate, with an initial inoculum of 0.25 to 0.5 parasites per well. Individual clones in single wells were detected by visual and microscopic approach after 2 to 5 weeks in culture.

The starting parasitemia of the *P. falciparum* culture in 14 ml of medium at 3% hematocrit was carefully determined as a prerequisite for successful dilution of the parasites. Taking in account that 1 ml of a suspension at 50% hematocrit is considered to contain roughly 5.10^9 erythrocytes, the total number of parasites in this starting culture was calculated from the parasitemia.

From this information, a starting solution with 10^6 parasites per milliliter was prepared and subsequently diluted to obtain a working solution with 10 parasites per milliliter, using 1:10 dilution steps in a final volume of 10 ml. From this dilution, two final working solutions of 5 and 2.5 parasites per milliliter were prepared in a final volume of 15 ml or 10 ml of medium, using 1:2 dilution steps (Figure 2.1). 200 µl uninfected fresh erythrocytes (2% hematocrit) were added to those two solutions. The samples were repeatedly inverted to ensure proper mixing. 100 µl of these suspensions were seeded into 96-well plates (V-shape bottom), leading to 0.5 or 0.25 parasite per well respectively and incubated under the appropriate culture conditions.

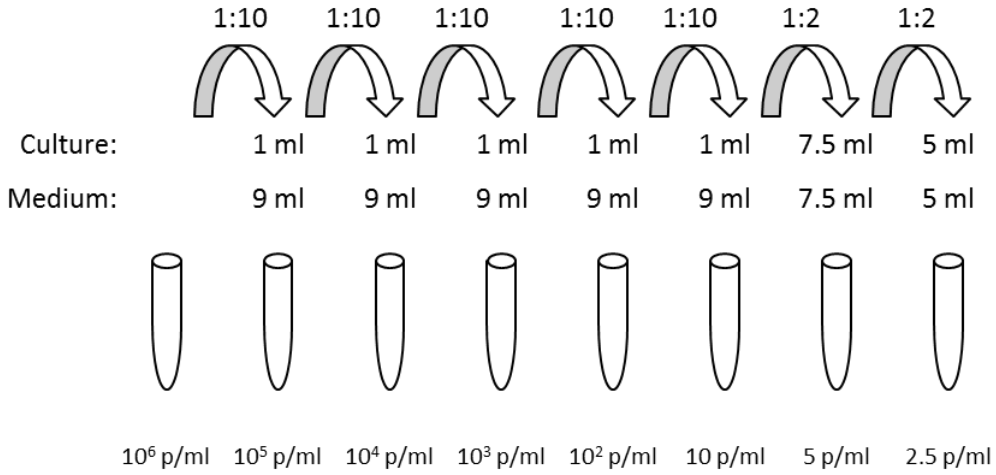

Figure 2.1: Stepwise dilution process. A starting solution with 10^6 parasites per ml is first prepared and sequentially diluted by a factor 10 to obtain a working solution with 10 parasites per ml in a final volume of 10 ml. Two final working solutions of 5 and 2.5 parasites per ml are then prepared by sequential dilution by a factor 2, in a final volume of 15 ml or 10 ml of medium, respectively.

Medium without selection marker was exchanged every second to fourth day until parasite appearance or for 2 to 5 weeks, and the haematocrit was increased by 1% each week. A dark color of the blood and a cloudy medium was usually indicative of parasitized wells, an observation further confirmed by microscopic analysis. Subsequently, the contents of parasitized wells were transferred to small culture plates to increase parasite numbers for freeze-downs and further investigations.

2.2.2. Microbiological methods

2.2.2.1. Preparation of electro-competent PMC 103 *E. coli* bacteria

To prepare electro-competent PMC 103 *E. coli* cells, 10 ml of Super Broth (SB) medium were inoculated with a single bacteria colony and incubated at 37°C under shaking conditions (230 rpm) overnight. The next day, 600 ml of SB medium were inoculated with a 1:100 dilution of this starter culture (i.e. 6 ml in a total volume of 600 ml) and incubated at 37°C for 3.5 hours under shaking conditions (230 rpm). The culture was then centrifuged at 4000 rpm for 10 minutes at 4°C. All the consecutive steps were carried out on ice with pre-chilled solution. The pellet was resuspended in equal volume of sterile water and centrifuged at 4000 rpm for 15 minutes at 4°C. This washing step was repeated twice. The pellet was then resuspended in equal volume of 10% glycerol water and centrifuged at 4000 rpm for 15 minutes at 4°C. The supernatant was discarded; the pellet was resuspended in 1.2 ml of 10% glycerol water

and aliquoted in Eppendorf tubes and snap frozen with ethanol and dry-ice. The bacteria were stored at -80°C until further use.

2.2.2.2. Preparation of chemo-competent XL-1-Blue *E. coli* bacteria

To prepare chemo-competent XL-1-Blue *E. coli* cells, 250 ml of SOB medium were inoculated with 10 to 12 colonies and incubated at 37°C under shaking conditions (230 rpm) up to an optical density (OD_{600}) of 0.6. The culture was allowed to rest on ice for 10 minutes before a centrifugation at 4000 rpm for 20 minutes at 4°C. All the consecutive steps were carried out on ice with pre-chilled solution. The pellet was resuspended in 80 ml of TB buffer, incubated on ice for 10 minutes and centrifuged at 4000 rpm for 10 minutes at 4°C. The supernatant was discarded, the pellet was resuspended in 20 ml of TB buffer and 1.4 ml of DMSO was added under slight agitation. The cells were then aliquoted in Eppendorf tubes, snap frozen with ethanol and dry-ice and stored at -80°C until further use.

2.2.2.3. Transformation of electro-competent PMC 103 *E. coli* bacteria

Plasmid DNA was introduced into electro-competent PMC 103 *E. coli* bacteria by electroporation. For this purpose, 50 µl of bacterial cells were thawed on ice and supplemented with 100 µl of 10% glycerol water. 10 µl of DNA were carefully added and the mixture was transferred into an electroporation cuvette. The electroporation was then performed at 2500 volts. 1 ml of prewarmed Super Optimal Broth with Catabolic repression (SOC) medium was directly added and the mixture was transferred to a 15 ml falcon tube and incubated for 1 h at 37°C under shaking conditions (230 rpm). Finally, the bacterial suspension was pelleted or directly plated onto selective LB agar plates and incubated overnight at 30°C.

2.2.2.4. Transformation of chemo-competent XL1-Blue cells

Plasmid DNA was introduced into chemo-competent XL-10-Gold Ultracompetent cells (Agilent Technologies) by heat shock. For this purpose, 50 µl of bacterial cells were thawed on ice. 10 µl of DNA were carefully added. After incubation on ice for 30 minutes, the cells were incubated for 45 seconds at 42°C, followed by 2 minutes cooling down on ice. The transformed bacteria were then supplemented with 900 µl of SOC medium, transferred to a 15 ml falcon tube and incubated for 1 h at 37°C under shaking conditions (230 rpm). Finally, the bacterial suspension was directly plated onto selective LB agar plates and incubated overnight at 37°C.

2.2.2.5. Transformation of chemo-competent XL10-Gold Ultracompetent Cells

Plasmid DNA was introduced into chemo-competent XL-10-Gold Ultracompetent cells (Agilent Technologies) by heat shock. For this purpose, 40 µl of bacterial cells were thawed on ice and supplemented with 1.6 µl of β-mercaptoethanol. The cells mixture was incubated on ice for 10 minutes. 10 µl of DNA were carefully added. After incubation on ice for 30 minutes, the cells were incubated for 30 seconds at 42°C, followed by 2 minutes cooling down on ice. The transformed bacteria were then supplemented with 900 µl of NZY^+ broth medium, transferred to a 15 ml falcon tube and incubated for 1 h at 37°C under shaking conditions (230 rpm). Finally, the bacterial suspension was directly plated onto selective LB agar plates and incubated overnight at 37°C.

2.2.2.6. Isolation of plasmid DNA from bacteria (Miniprep)

A single colony was inoculated into 10 ml of LB medium (supplemented with the appropriate antibiotic, i.e. 100 µg/ml of ampicillin) and grown overnight at 37°C with shaking at 230 rpm. Small scale plasmid DNA isolation was achieved using High Pure Plasmid Isolation kit (Roche), which is based on alkaline lysis and specific adsorption of released DNA onto glass fiber columns. According to the standard protocol the overnight bacteria culture was centrifuged at 3800 rpm for 5 minutes at room temperature, and the pellet was treated with suspension and lysis buffers and incubated for 5 minutes at room temperature. After addition of chilled DNA binding buffer and incubation for 5 minutes on ice, the suspension was centrifuged at 13000 rpm for 10 minutes at 4°C. The supernatant was transferred onto the column and centrifuged at 13000 rpm for 1 minute at room temperature. After two washing steps, the DNA was eluted with 50 µl of elution buffer and stored at -20°C.

2.2.2.7. Isolation of plasmid DNA from bacteria (Maxiprep)

A single colony was inoculated in 3 ml of LB medium (supplemented with the appropriate antibiotic, i.e. 100 µg/ml of ampicillin) and grown for 6 to 8 hour at 37°C with shaking at 230 rpm. This starter culture was diluted 1:1000 in LB medium containing the appropriate antibiotic (i.e. 400 µl in 400 ml of LB medium) and grown overnight at 37°C under 230 rpm shaking. Large scale plasmid DNA isolation was performed using the Plasmid Maxi Kit (Qiagen) according to the manufacturer´s protocol. Briefly, cells from the overnight bacteria suspension were harvested by centrifugation (4000 rpm, 15 min, 4°C) and sequentially mixed and incubated with resuspension, lysis and neutralization buffers. Precipitation of genomic DNA, proteins and cell debris was carried out on ice. The supernatant containing the plasmid

DNA was separated from the debris by centrifugation (10800 rpm, 30 min, 4°C) and loaded onto and equilibrated tip. After several washing steps, DNA was eluted, precipitated with isopropanol and centrifuged (10800 rpm, 30 min, 4°C), and wash with ethanol 70%. The DNA pellet was air-dried, resuspended in an appropriated amount of water and stored at -20°C.

2.2.3. Molecular Biology

2.2.3.1. Genomic DNA isolation from *P. falciparum* parasites

To isolate *P. falciparum* from erythrocytes, 14 ml of a trophozoite and schizont- rich culture (at least 5% parasitemia) were resuspended and transferred into a 15 ml falcon tube and centrifuged 2 minutes at 1900 rpm. The pellet was washed in PBS and centrifuged again under the same conditions. The pellet was resuspended in 10 ml of freshly prepared 0.1% Saponin in PBS, inverted several times and incubated on ice for 2 minutes. The lysate was centrifuged at 3800 rpm for 8 minutes at 4°C, and the supernatant was discarded. The pellet was washed with 10 ml of PBS and centrifuged in the same setting, and resuspended in 200 µl of PBS and transferred in a 1.5 ml Eppendorf tube.

The isolation of genomic DNA was carried out via DNeasy kit (Qiagen). Briefly, the parasites were lysed with 200 µl AL buffer and 20 µl of proteinase K, vortexed and incubated at 56°C for 10 minutes. 200 µl of ethanol (99%) were added and the mixture was thoroughly vortexed. The mixture was then transferred to a Mini Spin column and centrifuged at 8000 rpm for 1 minute. The flow-through was discarded and 500 µl of AW1 buffer were added, followed by a centrifugation at 8000 rpm for 1 minute. Again, the flow-through was discarded and 500 µl of AW2 buffer were added, followed by a centrifugation at 13000 rpm for 3 minutes. The column was then transferred to a fresh 1.5 ml Eppendorf tube, and 30 µl of water buffer were loaded to the membrane and incubated 1 minute at room temperature, followed by a centrifugation at 8000 rpm for 1 minute. The genomic DNA was stored at -20°C.

2.2.3.2. RNA isolation from *P. falciparum* parasites

To isolate *P. falciparum* from erythrocytes, 5 plates of 25 cm diameter of a trophozoite and schizont- rich culture (35 ml, 3 to 5% parasitemia, 3 to 4% hematocrit) were resuspended and transferred into a 50 ml falcon tubes and centrifuged 2 minutes at 2000 rpm without breaks at 800 rpm, at 4°C. The supernatants were discarded, and the pellets were resuspended in the same volume of freshly prepared 0.2% Saponin in PBS. The tubes were

inverted several times and incubated on ice for 3 minutes. PBS was added up to 25 ml and the tubes were centrifuged for 8 minutes at 3800 rpm at 4°C. The supernatants were discarded, and the pellets were transferred in one 50 ml falcon tube and subsequently washed with PBS and centrifuged for 8 minutes at 3800 rpm at 4°C.

To extract the RNA from the parasites, 1 to 2 ml of Trizol® were added to the pellet, mixed thoroughly by vortexing, and directly frozen at -80°C for at least 2 hours. The mixture was then thawed at 37°C and transferred in 1.5 ml Eppendorf tubes. 200 µl of chloroform per milliliter of Trizol® were added, the mixture was hand-shaken vigorously for 30 seconds and centrifuged at 10500 rpm for 30 minutes at 4°C. The upper aqueous phase containing mostly RNA was transferred to a fresh 1.5 ml Eppendorf tube. 500 µl of isopropanol per milliliter of Trizol® were added to the aqueous phase, the mixture was incubated at -20°C for at least 30 minutes and subsequently centrifuged at 10500 rpm for 10 minutes at 4°C. The pellet was washed with ethanol 70% and centrifuged at 10500 rpm for 10 minutes at 4°C. The RNA pellet was then air-dried at room temperature to eliminate any trace of ethanol, and dissolved in a certain amount of Ribonuclease-free water, depending of the size of the RNA pellet, in a range of 20 µl to 100 µl. The concentration was measured by spectrophotometry and the RNA was stored at -80°C. The integrity of the RNA was assessed on a denaturing agarose gel (0.7% agarose).

2.2.3.3. DNase treatment of the isolated RNA

The freshly isolated RNA was rendered DNA-free using the The Ambion ®DNA-free kit (Invitrogen). Briefly, 5 µg of RNA were mixed with 1.5 µl of 10X DNase I Buffer and 1 µL rDNase I, adjusted to a total volume of 15 µl with nuclease-free water. The mixture was gently shaken by hand and incubated at 37°C for 30 minutes. 1.5 µl of DNase Inactivation Reagent was added before a subsequent incubation period of 5 minute at room temperature. The mixture was centrifuged at 10000 rpm for 2 minutes at 4°C and the supernatant was transferred in a fresh Eppendorf tube and stored at -80°C if not used directly for cDNA synthesis.

2.2.3.4. Reverse transcription

The cDNA was synthesized with SuperScript® III First-Strand Synthesis Supermix (Invitrogen). Briefly, 5 µg of DNase-treated RNA were mixed with 1 µl of oligo$(dT)_{20}$ 50 µM and 1 µl of annealing buffer, adjusted to a total volume of 10 µl with nuclease-free water, incubated for denaturation at 65°C for 5 minutes and placed on ice for 2 minutes. 10 µl of 2X First-Strand Reaction Mix and 2 µl of the SuperScrip III/RNaseOUT Enzyme Mix were then added to the RNA mixture, incubated 50 minutes at 42°C. The reaction was heat-inactivated

at 85°C for 5 minutes before being allowed to chill on ice for 1 minute. The concentration was measured by spectrophotometry and adjusted to 50 ng/ml. The cDNA was stored at -20°C.

2.2.3.5. Polymerase chain reaction (PCR)

Specific DNA sequences can be amplified *in vitro* using PCR, involving a temperature dependent DNA polymerase, a template DNA sequence and forward and reverse primers that bind specifically to the DNA template.The amplification of the DNA fragments used for cloning was performed using the Phusion polymerase. The reactions were set as follows:

Buffer 5x	:	4 µl	10 µl
dNTPs 2 mM	:	2 µl	5 µl
Forward primer 5 µM	:	0.5 µl	0.5 µl
Forward primer 5 µM	:	0.5 µl	0.5 µl
DNA template	:	1 µl	1 µl
Phusion	:	0.2 µl	0.5 µl
H_2O	:	11.8 µl	32 µl
Total volume	:	20 µl	50 µl

The thermocycler was programmed as followed:

Initial denaturation	:	95 °C	10 min	
Denaturation	:	95 °C	45 sec	} 35 cycles
Annealing	:	X °C	45 sec	
Elongation	:	68 °C	X sec	
Termination	:	68 °C	10 min	
Maintaining	:	4 °C	∞	

The amplification of the DNA fragments for colony screening was performed using the Taq polymerase. The reactions were set as follows:

Buffer 5x	:	2.5 µl
dNTPs 2 mM	:	2.5 µl
$MgCl_2$ 50 mM	:	1.25 µl
Forward primer 5 µM	:	0.25 µl
Forward primer 5 µM	:	0.25 µl
Taq	:	0.25 µl
H_2O	:	18 µl
Total volume	:	25 µl

The primer pair was chosen to start amplifying in the plasmid and not in the ligated DNA fragment.

The thermocycler was programmed as followed:

Initial denaturation	:	90 °C	5 min	
Denaturation	:	90 °C	45 sec	} 30 cycles
Annealing	:	X °C	45 sec	
Elongation	:	68 °C	X sec	
Termination	:	68 °C	10 min	
Maintaining	:	4 °C	∞	

2.2.3.6. Quantitative real-time PCR (qRT-PCR)

Quantitative real-time PCR was performed using the LightCycler® 2.0 Instrument detection system and the LightCycler® FastStart DNA Master SYBR Green I kit. The samples were prepared in technical triplicates in the following manner:

LightCycler FastStart Reaction Mix SYBR Green 10x	:	1 µl
$MgCl_2$ 25 mM	:	0.8 µl

Forward primer 0.5 µM	:	0.25 µl
Forward primer 0.5 µM	:	0.25 µl
cDNA	:	2 µl (100 ng)
H_2O	:	5.7 µl
Total volume	:	20 µl

The thermocycler was programmed as followed:

Denaturation	:	95 °C	1 sec	
Annealing	:	50 °C	10 sec	} 50 cycles
Elongation	:	68 °C	10 sec	

Data were analyzed with LightCycler® Software 4.1.

2.2.3.7. Agarose gel electrophoresis and nucleic acids

Agarose is widely used for the separation of DNA and RNA molecules according to their size and charge. The resolution of the nucleic acid bands is dependent on the concentration of the agarose gel. The most common concentration used for DNA electrophoresis varies from 0.8% (for large 4 to 10 kb fragments) to 2% (for small 0.1 to 1 kb fragments).

DNA electrophoresis was performed by weighing an appropriate amount of agarose mixed with TAE buffer. The mixture was boiled in a microwave until complete dissolution of the agarose. The gel was subsequently cooled down to 55°C, supplemented with EtBr (1:10 000 dilution) and poured in a gel cast. 6 x DNA loading buffer was added to the DNA samples for a final concentration of 1x, and samples were then loaded onto the gel. A 1 kb Plus DNA Ladder™ was run alongside the samples as a size marker. Electrophoresis was carried out for 30 to 90 minutes at a constant voltage of 90 to a40 volts depending of the need. Samples were photographed under UV illumination using a DC120 Zoom Digital camera (Kodak).

As RNA shows a tendency to form secondary structures, formaldehyde was used for RNA electrophoresis to maintain the denaturated form of RNA. The gel was prepared by dissolving 0.28 grams of agarose (leading to a 0.7% gel) in 2 ml of 20 x RNA gel running buffer and 30 ml of water. The mixture was boiled in the microwave until complete dissolution of the agarose, then allowed to cool down to 55°C. 8 ml of formaldehyde and 0.5 µl of EtBR

were then added and the mixture was poured into a gel cast. Electrophoresis was carried out for 60 to 90 minutes at a constant voltage of 60 volts in RNA gel running buffer. The gel was then photographed under UV illumination using a DC120 Zoom Digital camera (Kodak).

2.2.3.8. Agarose gel extraction and PCR product purification

The purification of specific DNA fragment from agarose gel or the cleanup of digested DNA fragments from the digestion mixture was performed using the Qiagen gel extraction kit. Briefly, the specific agarose gel fragments were cut and solubilized in QG buffer (1:3 w/v ratio) at 50°C until complete dissolution. In the presence of isopropanol and high salt concentration, the DNA was separated and bound to a QIAquick™ membrane inside the column, while the contaminants flowed through. After washing with PE buffer, the DNA was eluted with an appropriated amount of water. For digested DNA fragments, the digestion mixture first mixed with PB buffer (1:3 ratio) and applied to the column without the first solubilization step at 50°C. The purified fragments were stored at -20°C.

2.2.3.9. Photometric determination of DNA/RNA concentration

Nucleic acid concentration was measured by spectrophotometry using the UVIKON 923 photometer (Kontron instruments). The absorbance (OD) at 260 nm was analyzed for DNA and RNA, where and OD_{260} of 1 equals 50 µg/ml dsDNA, 30 µg/ml ssDNA and 40 µg/ml ssRNA.

Dilutions were included using the following formula:

OD_{260} x 50 (dsDNA) x dilution factor /1000 = X µg/µl

OD_{260} x 30 (ssDNA) x dilution factor /1000 = X µg/µl

OD_{260} x 40 (ssRNA) x dilution factor /1000 = X µg/µl

2.2.3.10. Restriction digestion of DNA

DNA can be enzymatically cleaved by restriction endonucleases, which recognize short, often palindromic sequences and catalyze a break in the backbone of DNA by hydrolysis.

The DNA digestion reactions of plasmids and PCR products were set up as follows:

Digestion of vectors or inserts for cloning		
NEB buffer	:	10 µl
DNA	:	30 µg
Enzymes	:	1 µl of each
H_2O	:	X µl
Total volume	:	100 µl

Control digestion		
NEB buffer	:	1 µl
DNA	:	1 µg
Enzymes	:	0.4 µl of each
H_2O	:	X µl
Total volume	:	10 µl

The control digestions were incubated for 90 min and the digestions of vectors and inserts for cloning for a minimum of 2 hours at the temperature for each enzyme recommended by NEB.

2.2.3.11. Dephosphorylation of DNA with alkaline phosphatase

Shrimp alkaline phosphatase (SAP) from *Pandalus borealis* catalyses the dephosphorylation of 5´phosphates from DNA, thus preventing the religation of plasmid vectors. Appropriate ligation is only possible with the insert which still has intact phosphate groups. SAP is completely and irreversibly inactivated by heat. All the vectors used for cloning were dephosphorylated prior to their use on ligation reactions. After restriction digestion, 1 µl of SAP enzyme (Promega) was added to the digestion mix as well as 1 µl of the 10X SAP Buffer, incubated at 37°C for 30 minutes and heat-inactivated for 15 minutes at 65°C. The vector was then purified using the QIAGEN PCR Purification kit and eluted in 30 µl of water.

2.2.3.12. Ligation of digested DNA fragments

T4 DNA ligation

The vectors and DNA fragments ligated using the T4 DNA ligase were previously digested with the adapted restriction enzymes and purified using the QIAquick gel extraction kit. The ligation reaction was set in the following manner:

Vector	:	1 µg
Insert	:	3 -7 µg
T4 DNA ligase buffer 10X	:	1 µl

T4 DNA ligase	:	1 µl
H_2O	:	X µl
Total volume	:	10 µl

The reaction mixture was usually incubated at room temperature during 30 minutes to 1 hour before transformation. If the transformation was performed on the following day, the reaction was incubated over-night at 16°C.

In Fusion

The InFusion cloning technology was used to introduce the guide sequences into the pL6 plasmids. The pL6 plasmid of interest was first digested with the enzyme BtgZI at 60°C for 3 hours, dephosphorylated and purified with the QIAquick gel extraction kit. The primers containing the both guide sequences and the sequences for homology recombination were adjusted at 100 µM in water and 5 µl of each primer (forward and reverse) were mixed together with 1.1 µl of NEB buffer #2. The mixture was heated for 5 minutes at 94°C, allowed to cool down to 25°C in a step-wise manner and was kept on ice or frozen until use for the ligation reaction.
The reaction ligation was set as follows:

Vector	:	0.5 µl (≈ 200 ng)
Hybridized primers (1:10 dilution)	:	3.5 µl
Fusion enzyme mix	:	1 µl
Total volume	:	5 µl

The reaction mixture was incubated 15 minutes at 50°C and was kept on ice until its transformation into XL-10 Gold cells.

Ligation into pJET1.2/blunt

As an intermediate cloning step, some of the inserts used for this work were cloned into the pJET1.2/blunt plasmid. In this situation, the CloneJET PCR Cloning Kit (Fermentas) was used. The reaction was set in the following manner:

Reaction buffer 2X	:	5 µl
DNA bunting enzyme	:	0.5 µl
Insert	:	3.5 µl (≈ 100 ng)
Total volume	:	5 µl

The reaction mixture was incubated at 70°C for 5 minutes and chilled on ice. The following reagents were subsequently added:

pJET1.2/blunt cloning vector	:	0.5 µl
T4 DNA ligase	:	0.5 µl
Total volume	:	6 µl

The ligation mixture was incubated at room temperature for 30 minutes and used directly to transform *E. coli* PMC 103 electrocompetent or XL-1-Blue chemocompetent cells.

2.2.3.13. DNA sequencing

DNA samples were sent to GATC (Konstanz) for sequencing. The Sanger dideoxynucleotide method [195] was used. The sent samples were prepared as follows:

Plasmids	:	30 µl, 30 – 100 ng/µl
PCR products	:	30 µl, 10 – 50 ng/µl
Primers	:	10 µl, 10 pmol/µl

The GATC viewer software and the online platform ClustalW2 from EMBL were used to analyze the obtained sequences.

2.2.3.14. Pyrosequencing

The pyrosequencing technique is based on the quantification of a light-generating reaction, which depends on the amount of nucleotide that is incorporated at a specific base pair position. Consequently, this approach allows the determination of allele proportions in DNA mixtures. Briefly, the immobilized single stranded template DNA is hybridized with a sequencing primer binding in a directly adjacent manner to the polymorphic base pair.

Further, the enzymes DNA polymerase, ATP sulfurylase, luciferase and apyrase are added with the substrates adenosine 5'-Phosphosulfate (APS) as well as with luciferin. In a initial sequencing step, one of the four deoxynucleotide triphosphates (dNTPs) is added to the mixture. If the dNTP is complementary to the template, the DNA polymerase incorporates it into the newly synthesized strand, which releases pyrophosphate molecules (PPi) in a stoichiometric fashion. The ATP-sulfurylase then converts PPi into ATP in presence of APS. This freshly synthesized ATP subsequently fuels the luciferase-mediated conversion of luciferin into oxyluciferin, which in turn generates a visible light reaction proportional to the amount of previously generated ATP. This light reaction can be quantified and used to calculate the proportions of the two alleles in the mixture.

A portion of the *pfatp6* sequence was amplified by PCR using the biotinylated primers (primers [53]-for and [54]-rev). 37 µl of the resulting PCR product were mixed with 3 µl of Streptavidin Sepharose HP (GE Healthcare) and 40 µl of binding buffer, to a final volume of 80 µl. The mixture was transferred to a 96 well-plate V-bottom and shaken for 10 minutes at 1400 rpm. The strand separation was performed using the PyroMark Q96 vacuum workstation. Briefly, the filter probes were washed with 180 ml of water before being lowered into the 96 well-plate containing the samples to capture the beads. The beads were washed with 70% ethanol by flushing the filter probes for 5 seconds, denatured with the denaturation solution for 5 seconds and finally washed with wash buffer for 10 seconds. The filter probes were drained by raising the tool at 90° for 5 seconds and the beads were subsequently released into a PyroMark Q96 Plate Low containing 0.4 µM of the sequencing primer (primer [55]-for) in 40 µl of annealing buffer. The samples were heated at 80°C for 2 minutes and allowed to cool down to RT. The reagent cartridge was filled with the recommended volumes of PyroMark Gold Q96 Reagents provided by the software, according to the number of samples to analyze. The PyroMark Q96 Plate Low was placed on the heating block of the PyroMark Q96 ID and the cartridge on the dispensing unit. The set up and the run analysis were performed using the PyroMark Q96 Software v1.0.

2.2.4. Protein Biochemistry

2.2.4.1. Preparation of *P. falciparum* protein extract

P. falciparum cultures at a parasitemia in trophozoites of 3 to 5% were magnetically purified using the MACS system. After elution of the iRBC, the samples were centrifuged 2 minutes at 2100 rpm and the pellets were washed once with ice-cold PBS. The iRBCs were resuspended in approximately 1 ml of Protein Lysis Buffer, an appropriate volume for the amount of *P. falciparum* parasites obtained from such a culture, and subsequently incubated

on ice for 3 minutes. The samples were then centrifuged at 13 000 rpm for 1 minute at 4°C and the pellet of parasites was washed 2 times with ice-cold PBS and kept at -80°C or directly resuspended in an appropriate volume of Protein Loading Buffer. The samples were then sonicated (20% output) twice for 5 seconds, allowing a 30 seconds break on ice in between the two sonications. After centrifugation for 15 minutes at 4°C at 13 000 rpm, the supernatant was transferred in a fresh Eppendorf tube and kept at -20°C.

2.2.4.2. SDS-PAGE electrophoresis

Protein samples were analyzed by SDS-PAGE electrophoresis. Before being loaded on the SDS-PAGE gel, the samples were heated at 70°C for 5 minutes. The PageRuler Plus Prestained (Ambion) was used as a protein ladder. The gels were run at 40 mA and 150 V during approximately 90 min in SDS-PAGE running buffer.

SDS-PAGE gels were prepared as follows:

Resolving gel

		8%	10%	12%
H_2O	:	4.68 ml	3.96 ml	3.35 ml
1.5 M Tris pH 8.6	:	2.50 ml	2.50 ml	2.50 ml
10% SDS	:	100 µl	100 µl	100 µl
30% Acrylamid	:	2.66 ml	3.33 ml	4.00 ml
10% APS	:	100 µl	100 µl	100 µl
TEMED	:	6 µl	6 µl	6 µl
Total volume	:	10 ml	10 ml	10 ml

Stacking gel

H_2O	:	3.46 ml
1 M Tris pH 6.8	:	630 µl
10% SDS	:	50 µl
30% Acrylamid	:	830 µl
10% APS (fresh)	:	50 µl
TEMED	:	5 µl
Total volume	:	5.025 ml

2.2.4.3. Visualization of proteins by Coomassie staining

To visualize the proteins in the whole extract after the SDS-PAGE electrophoresis, the gels were soaked in Coomassie Solution for 30 minutes under constant shaking and then washed with Coomassie Destaining Solution until the protein bands could be clearly distinguished.

2.2.4.4. Western blotting

The SDS-PAGE gels were transferred to an Immun-Blot® PVDF membrane (Bio-Rad) using a Trans-blot SD semi-dry transfer cell. The membrane was activated with methanol for 30 seconds. Afterwards, 3 Whatman papers were soaked in transfer buffer and placed on the

device, followed by the membrane placed on top, the SDS-PAGE gel and finally 3 more soaked Whatman papers. The transfer was run for 1 hour at 230 mA and 30 V. The membrane was blocked over 1 hour with 5% (w/v) milk in PBS, and incubated overnight at 4°C with the first antibody diluted in 3% (w/v) BSA in. The following day, three washes of 15 minutes with PBST (0.1% (v/v) of Tween in PBS) were performed. The membrane was blocked again with 5% (w/v) milk in PBS for 1 hour. The incubation of the second antibody (diluted as well in 3% (w/v) BSA in PBS) was carried out for 30 minutes. Before development, the membrane was washed three times more during 15 minutes with PBST. The developing solution (BM chemiluminescence blotting substrate POD, Roche) was freshly prepared (2 ml of solution A + 20 µl of solution B) and the membrane was incubated with the solution for 5 minutes. The signal was captured with a blot scanner (C-DiGit from Li-Cor).
The dilutions of the antibodies that were used for western blot are the following:

Anti-α-tubulin monoclonal	:	1:1000
Anti-HA tag monoclonal	:	1:1000
Anti-mouse-POD monoclonal	:	1:10000

2.2.4.5. Western blot striping

In order to strip of the antibodies out of the western blot membrane, they were incubated for 30 minutes with stripping buffer and then washed 3 times during 15 minutes with PBST (0.1% (v/v) of Tween in PBS).

2.2.4.6. [^{35}S]-methionine incorporation assay during protein synthesis

A [^{35}S]-methionine incorporation assay was performed to investigate the possible effect of SC83288 on protein synthesis. The assay was performed at the Zentrum für Molekular Biologie (ZMBH) in Heidelberg, in Prof. Christine Clayton´s lab, together with Dr. Chaitali Chakraborty. Briefly, samples of approximately 3x10^6 iRBC were resuspended in 500 µl of prewarmed labeling medium (DMEM without methionine, ThermoFisher Scientific) and treated with various concentrations of SC83288 for 1 hour at 37°C. 1 µl of of 10 µCi/µl [^{35}S]-methionine stock solution (Hartmann Analytic) was added and the samples were further incubated for 30 minutes at 37°C. After 2 washes with PBS, the samples were resuspended in 10 µl of 2x Laemmli lysis buffer, and incubated 5 minutes at 95°C, before being loaded on a 10% SDS_PAGE gel for 2 hours. The gel was fixed for 30 minutes at room temperature in an aqueous solution containing 7.5% of acetic acid and 10% of methanol. It was

subsequently stained with Coomassie Blue for 1 hour and allowed to destain overnight before being imaged. The gel was then dried for 1 hour at 80°C, exposed over 2 days in a cassette and developed using a Fujifilm FLA-7000 detector.

2.2.5. Growth inhibition assay and determination of IC_{50} values

The anti-malarial activity of a compound is generally assessed by measuring the growth inhibition of *P. falciparum* blood-stage parasites under drug treatment, and is expressed as 50% inhibitory concentration (IC_{50} value). IC_{50} values indicate the concentration needed to inhibit the parasite´s multiplication by 50% over a chosen period of time. Growth inhibition assays were performed according to standard protocol based on the detection of parasitic DNA by fluorescent SYBRgreen staining [196]. Briefly, a synchronous culture of ring-stage *P. falciparum* blood-stage parasites was incubated for 72 hours in presence of decreasing drug concentrations in a black 96-well microtiter plate. The final conditions of the tests were 100 µl volume per well, 0.5% parasitemia, 2% final hematocrit and 72 hours incubation time at 37°C.

On the day of the assay a ring-stage culture, previously synchronized by sorbitol treatment, was established at 0.5% parasitemia and 4% hematocrit. A solution of niRBC at 4% hematocrit was used as a negative control.

Drug solutions were prepared as working solutions (6x) in culture medium by diluting freshly thawed stock solution to 6x starting concentration (i.e. highest drug concentration to be tested). Per drugs, 60 µl of working solution was prepared. The starting concentration was chosen to allow the IC_{50} concentration to fall around the midpoint of a threefold serial dilution. This concentration was calculated based on IC_{50} values found in the literature or was tested in preceding growth-inhibition assays. The range of drug concentrations should cover parasite viability from 0 – 100% with sufficient data points all over this range in order to assure correct IC_{50} value calculation by the SigmaPlot Software.

Growth inhibition assays were performed on black 96-well plates according to the following plate scheme (Figure 2.2). Firstly, 50 µl of culture medium was filled in each well. For preparation of serial drug dilutions, 25 µl of drug working solution (6x) was added in the first well and thoroughly mixed. A 10-points 1:3 serial dilution was obtained by transferring 25 µl from one row to the next row containing 50 µl of culture medium. The 25 µl drug solution from the final row was discarded. One line was reserved for non-infected erythrocytes (negative control) and another one for infected erythrocytes (positive control). Subsequently, 50 µl of prepared parasites culture was added to each well and 50 µl of niRBC solution were added to respective wells. Plates were covered with clear lids and incubated for 72 hours in the

usual incubator. After incubation period, plates were wrapped in aluminum foil and frozen at -80°C until use in order to obtain complete lysis of erythrocytes, usually overnight.

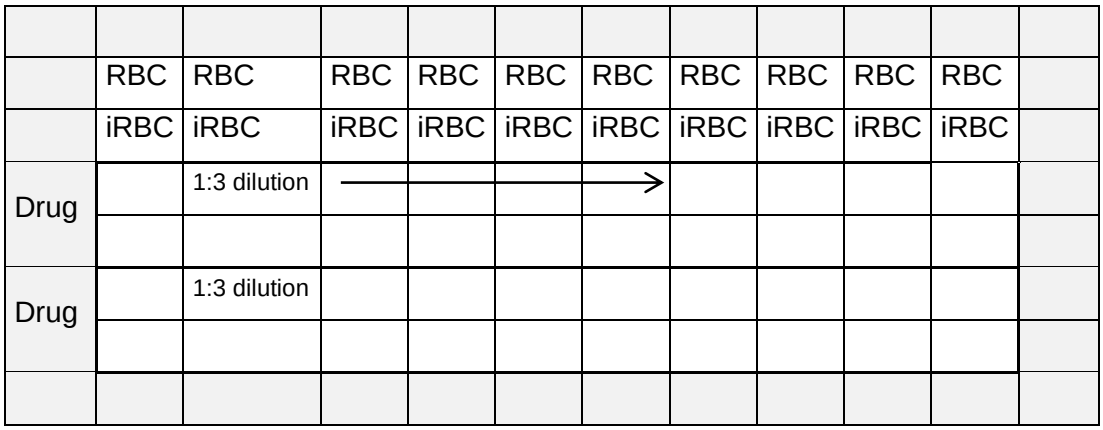

Figure 2.2: Plate scheme of growth inhibition assay. Abbreviations: RBC, non-infected red blood cells; iRBC, infected red blood cells.

Parasite multiplication was assessed by fluorescent SYBRgreen staining of the parasites of parasitic DNA. Measured fluorescence intensity stems from SYBRgreen binding to double stranded DNA and is associated to DNA replication by multiplying parasites

On the day of the measurement, plates were thawed for at least 1 hour at room temperature. The plates were filled with 100 µl/well of a 1x SYBRGreen solution in Lysis Buffer, briefly shaken and incubated at room temperature for 1 hour protected from direct light exposure. Fluorescence was measured in a fluorescence plate reader (ext/em: 485/520 nm, gain 1380, 10 flashes/well, top optic).

IC_{50} values were calculated as followed. The fluorescence intensity of non-infected erythrocytes represents the background fluorescence of the cell solution; thus the calculated mean fluorescence intensity of non-infected erythrocytes was deducted from all infected erythrocytes measurements. The fluorescence intensity of untreated infected erythrocytes represents 100% parasite survival. Thus, the survival of treated infected erythrocytes was calculated based on the calculated mean fluorescence intensity of infected erythrocytes and expressed as percentage. These values, together with the respective drug concentrations, were plotted in form of a dose-response curve in SigmaPlot (x-axis = drug concentration [M], y-axis = parasite survival [%]). The IC_{50} values were calculated by SigmaPlot according to the Hill function (four parameters).

2.2.6. *In vitro* speed of action or "killing speed" experiments

Three independent methods were used to determine the *in vitro* speed of action of the drugs used in this study.

2.2.6.1. Relative speed of action assay

In order to obtain information on the speed of action of antimalarial drugs in a relatively fast manner, the approach developed by Le Manach et al. [197] was applied. Briefly, the growth of asynchronized parasites in the presence of antimalarial compounds was assessed using SYBRGreen staining, as described above, and expressed as IC_{50} values. For each compound, three incubation times were employed 72 (standard assay time), 48 and 24 hours. Unless mentioned otherwise, the experimental conditions were similar to the ones used during the growth inhibition assay previously described. The IC_{50} ratios, normalized to the 72 hours assay were subsequently used to classify the compound as fast- or slow-acting. Here artemisinin and quinine were used as fast-acting reference, and atovaquone as slow-acting reference.

2.2.6.2. Recrudescence assay

The so called “killing speed” experiment, based on the original protocol established by Sanz et al. [198], is founded on determination of parasite viability in response to drug treatment by assessing re-growth of treated parasites over time. The *in vitro* speed of action of SC81458, SC83288, artemisinin and atovaquone were assessed following this approach. Treatment was performed with concentrations corresponding to 10x IC_{50} value of each drug, previously established as described in Sanz et al [198].

Briefly, an asynchronous culture of *P. falciparum* Dd2 blood-stage parasites, with a predominant ring-stage population was treated with a concentration corresponding to 10×IC_{50} for a total duration of 7 days (168 h). Every 24 hours, a defined sample of parasites was taken from the treated culture, washed with drug-free medium and transferred to a 96-well plate, where 12-steps dilution was performed, 1:3 series in order to obtain a limiting dilution (i.e. one single parasite per well). Parasites were cultured for a total duration of 28 days to allow viable parasites to grow to higher parasitemia, further detected by SYBRgreen. The number of the last dilution step containing growing parasites was used to back-calculate the number of viable parasites present in the initial aliquot. Results are presented in graphical form as numbers of viable parasites over time of drug treatment. These results allow to obtain various parameters concerning the speed of action of the tested compounds, such as a potential lag phase (i.e. time needed to reach the maximal killing rate), the parasite reduction ratio (PRR) over one parasitic life cycle of 48 hours and the parasite clearance time (PCT) (i.e. time needed to kill 99.9% parasites).

On the day of the assay, an asynchronous culture was established at 0.5% parasitemia and 2% hematocrit, corresponding to 10^6 iRBC per ml, and distributed in small culture flasks (10 ml per flask per drug treatment). An aliquot of 1 ml of the initial culture was kept separately in

order to establish the first serial dilution of untreated parasite (0 hour). Drug solutions for the complete experiment were prepared as 100× working solutions in culture medium by diluting a freshly thawed stock solution, aliquoted for each day and stored at -20 °C. Culture medium and drug were renewed daily over the entire treatment period.

Drug treatment was started on day 0 by adding 100× working solution (10 µl per 1 ml of culture) into prepared culture flasks that were subsequently maintained under usual conditions in the incubator. At different time points (8, 24, 48, 72, 96, 120, 144 and 168 hours), aliquots of treated parasites à 500 µl were taken from the treated culture. Before preparing the serial dilutions, treated parasites were thoroughly washed 3 times with fresh culture medium to wash out the drug. After the last washing step, it was important to restore the original volumes and thereby the original hematocrit (i.e. number of cells per µl).

Serial dilutions (12 steps, 1:3 dilutions) of untreated or treated parasites were prepared in triplicates on 96-well plates (F-bottom). Therefore, a solution of non-infected red blood cells (niRBC) at 2% hematocrit was prepared. The plates were prepared as follows. The outer rows were omitted from use due to extensive evaporation and were filled with 200 µl of sterile water. Wells 2 to12 of the serial dilution (in triplicates) were filled with 100 µl of the prepared niRBC solution, leaving the first well empty for the treated parasite culture. These ones were then filled with the washed parasites (150 µl per well). A 1:3 serial dilution was obtained by transferring 50 µl each from one row to the next row containing 100 µl niRBC solution. One additional column of wells was filled with 100 µl niRBC solution as negative control for SYBR® green detection. At the end, another 50 µl of prewarmed culture medium was added to each well (final conditions: 150 µl volume, 1.33% hematocrit). Plates were maintained under usual conditions in the incubator for a total duration of 28 days. Medium was replaced twice a week (100 µl), once a week with addition of fresh erythrocytes (100 µl niRBC solution of 0.66% hematocrit). Detection of viable parasites was performed using SYBRGreen according to Smilkstein et al. [196], as previously described in section 2.2.5.

Calculation of viable parasites, parasite reduction ratio and parasite clearance time:

All parameters were calculated as described in the original protocol established by Sanz et al. [198]. The number of viable parasites was back-calculated by using the formula $X^{(n-1)}$, where X stands for the dilution factor (i.e. 3) and n the number of wells detected positive for viable parasites i.e., the number of the last dilution step containing growing parasites. When no well showed any parasite recovery (n=0), the number of viable parasites was estimated as zero. The numbers of viable parasites after drug treatment are presented in graphical form as “viable parasites +1” in logarithmic scale. This presentation was adopted from the original protocol [198] since only values greater than zero can be plotted on a logarithmic scale. A possible stagnation of parasite numbers during the first hours of treatment is

considered as lag phase, displaying a characteristic plateau. The parasite reduction ratio (PRR) was calculated as the decrease of viable parasite numbers over 48 h in the phase of maximal killing, therefore by excluding the period of lag phase. The parasite clearance time was determined using a linear regression of the time-response curve. The linear regression was calculated from time-point 0 h until the first time-point at which parasites were cleared (parasite number = 0) and included the possible lag phase.

2.2.6.3. Dual-color flow cytometry assay

Another faster method to measure the speed of action of antimalarial compounds, based on the approach described by Linares et al. [199] was used. This method uses the quantification of new infections to determine the parasite viability.

Briefly, an asynchronous culture of *P. falciparum* Dd2 blood-stage parasites, with a predominant ring-stage population was treated with a concentration corresponding to 10×IC_{50} for a total duration of up to 72 hours.

On the day of the assay, an asynchronous culture was established at 0.5% parasitemia and 4% hematocrit, and distributed at 50 µl per well in a 96-well V-shape bottom plate in triplicates. Drug treatment started on day 0 by adding 50 µl per well of 20×IC_{50} drug solution, resulting to a treatment corresponding to 10x the IC_{50}. The drugs were freshly renewed every 24 hours. At different time points (8, 14, 24, 48 and 72 hours), the parasites were washed-out the drug and resuspended in 100 µl of medium. 70 µl were then transferred into a fresh 96-well V-shape bottom plate, containing 130 µl of CFDA-stained non-infected erythrocytes at 2% hematocrit, resulting into a 1/3 dilution. After 48 hours of subsequent incubation at 37°C, the parasites were washed in PBS, and the DNA content was stained using Draq5 (1:500 dilution in PBS) for 20 minutes at room temperature. The samples were washed once with PBS and fixed in PBS 0.05% glutaraldehyde for 20 minutes at room temperature. The fixed samples were kept in PBS at 4°C until flow cytometry analysis.

Flow cytometry using a BD FACS Canto collecting fluorescence in the FITC and the PerCP-Cy5 channels allowed defining the proportion of the doubly stained parasites, corresponding to the new infections. The total infections were calculated as followed:

$$Total\ infections = \frac{3}{2}\ RBC^{CFDA/Draq5}$$

The parasite viability was then expressed as a percentage of the untreated parasites.

2.2.7. *In vitro* drug combination assays

The fixed-ration isobologram method, established by Fivelman et al. [200] was used to investigate the *in vitro* interaction between two compounds. This approach relies on

determining the IC_{50} values of each individual drug on its own and the IC_{50} values of a mixture of both drugs at fixed concentration ratios. The shift of a drug´s IC_{50} value in combination with a second compound compared to the one determined for the drug on its own is indicative of the nature of the drug-drug interaction. Furthermore, arithmetical analysis allows obtaining the mean sum of fractional 50% inhibitory concentration (mean $\sum FIC_{50}$), i.e. the unit of measurement. Both graphical, in the form of isobolograms and arithmetical analysis were used to establish the nature of the interaction between the two studied compounds.

Assay

The experimental set-up is similar to the growth inhibition assay (see 2.2.5). Briefly, a synchronous culture of ring-stage *P. falciparum* blood-stage parasites was incubated for 72 hours in the presence of decreasing drug concentrations in a 96-well black microtiter plate. The final conditions of the tests were 100 µl volume per well, 0.5% parasitemia, 2% final hematocrit and 72 hours incubation time at 37°C.

On the day of the assay a ring-stage culture, previously synchronized by sorbitol treatment, was established at 0.5% parasiteamia and 4% hematocrit. A solution of niRBC at 4% hematocrit was used as a negative control. Drugs were applied alone (A or B) and in combination at fixed concentration ratios (A:B) and analyzed in treefold serial dilutions. Drug mixtures were prepared from 2x working solution of each drug in the following fixed concentration ratios (v/v): ratio A:B = 4:1, 3:2, 2.5:2.5, 2:3, 1:4, directly in the 96-well plate. IC_{50} values of drugs A and B alone were determined on the same plate to ensure accurate calculation of drug interaction.

The assays were performed according to the plate scheme showed below. The outer rows were omitted from used due to extensive evaporation and were filled with 200 µl of sterile water. Firstly, 50 µl of culture medium was filled in each well, leaving the first well empty for the drug solutions. For preparation of serial drug dilutions, 75 µl of 2x working solution (individual or as mix of drug A and drug B) was added in the first well and thoroughly mixed. A 10-points 1:3 serial dilution was obtained by transferring 25 µl from one row to the next row containing 50 µl of culture medium. The 25 µl drug solution from the final row was discarded. One line was reserved for non-infected erythrocytes (negative control) and another one for infected erythrocytes (positive control). Subsequently, 50 µl of prepared parasites culture was added to each well and 50 µl of niRBC solution were added to respective wells. Plates were covered with clear lids and incubated for 72 hours in the usual incubator. After incubation period, plates were wrapped in aluminum foil and frozen at -80°C until use in order to obtain complete lysis of erythrocytes, usually overnight. Parasite growth was assessed using SYBRGreen as described above.

Arithmetical analysis

The fractional IC_{50} (FIC_{50}) of each drug in a given concentration ratio was calculated according to the following definitions:

FIC_{50}(A) = IC_{50} in combination / IC_{50} of A alone

FIC_{50}(B) = IC_{50} in combination / IC_{50} of B alone

The sum of FIC_{50}(A) and FIC_{50}(B) ($\sum FIC_{50}$) was established for each combination and the mean value of the four $\sum FIC_{50}$s was calculated. A mean $\sum FIC_{50} \leq 0.7$ was assumed to represent a synergistic interaction and a mean $\sum FIC_{50} \geq 1.3$ an antagonistic interaction between the tested drugs. Any value in between (0.7 – 1.3) was considered as an indifferent interaction.

Graphical analysis was performed on isobolograms, obtained by plotting pairs of FIC_{50} values of drug A and drug B for each combination. The isobologram Figure 2.3 illustrates the characteristic isoboles for different drug-drug interaction. A straight line represents an indifferent interaction, i.e. a simple additive effect, a concave curve towards the origin of the axes indicates a synergy and a convex curve towards the opposite suggests antagonism.

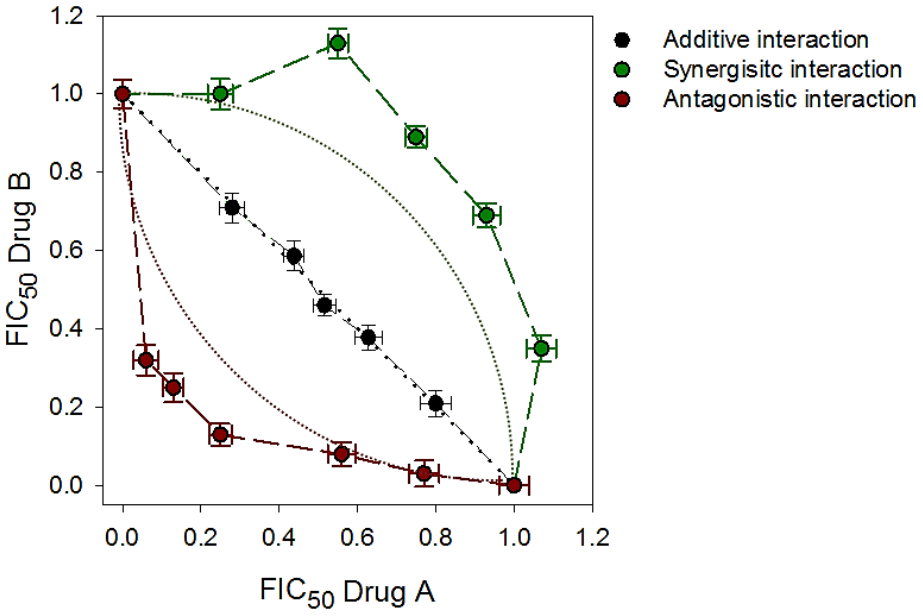

Figure 2.3: Theoretical example of isobologram illustrating the characteristic curves, or isoboles, for various types of *in vitro* drug-drug interactions. A straight diagonal line denotes an indifferent interaction (black), i.e. a simple additive effect, a concave curve towards the origin of the axes indicates a synergy (green) and a convex curve towards the opposite suggests antagonism (red).

2.2.8. Ring Survival assay (RSA)

The *in vitro* ring survival assay (RSA) rate was assessed as previously described by Mbengue et al. [161]. Briefly, tightly synchronized parasites were obtained by a double sorbitol treatment, 12 hours apart. Early ring parasites (0 to 3 hours p.i.) at a parasitemia of 0.5 to 1% were exposed to various drugs at a concentration of 700 nM, or to PBS for 6 hours. The parasites were subsequently washed four times with plain medium and returned in culture for 66 hours. The parasites were then harvested, washed once with PBS, resuspended in fixation solution and incubated either for 2 hours at room temperature or overnight at 4°C. The samples were then washed once with PBS, resuspended in 400 µl of PBS and kept at 4°C until further determination of the parasitemia by flow cytometry analysis. Parasites survival rates (%RSA) were expressed as a percentage by comparing the parasitemia between the drug-treated and the untreated control as followed:

$$RSA\ score\ (\%) = \frac{P_{drug-treated}\ (\%)}{P_{PBS-treated}\ (\%)} \times 100$$

2.2.9. Fitness assay

The relative fitness of parasites was determined in a growth competition assay. For this purpose, *P. falciparum* 3D7 parasite lines, with isogenic background and differing *pfatp6* alleles were carefully counted, mixed 1:1 and seeded at an initial parasitemia of 3% of trophozoite stage, in triplicate. The parasitemia was maintained between 0.5 and 6% to assure optimal growing conditions of the cultures. The mixed parasites were kept in culture for 20 cycles, i.e. 40 days. In order to determine the ratio of both strains in the mixture overtime, saponin-lysed parasite pellets of the mixed cultures were collected every 4 days and the genomic DNA was extracted from the pellets using the DNeasy Tissue Kit (Qiagen). The DNA was then used as a template for specific amplification and further ratiometric analysis by pyrosequencing (see Section 2.2.3.14).

2.2.10. Progression of *P. falciparum* through the life cycle

In order to follow the parasites through their life cycle, cultures were tightly synchronized by a double sorbitol treatment, 12 hours apart. The parasites were then treated as late trophozoites/early schizonts with 50 U/ml of heparin to block further invasion. The growth of the parasites was monitored by Giemsa staining under light microscopy, and the heparin was washed-out at late schizont stage (42 to 48 hours p.i.). The point of invasion was considered 4 hours after the washing steps. At around 10 hours post-invasion, the parasites were set in

culture at a parasitemia of 1%, and eventually exposed to drugs. Samples were collected every 2 to 4 hours from this point, until 52 hours post-invasion, washed once with PBS, resuspended in fixation solution and incubated either for 2 hours at room temperature or overnight at 4°C. The samples were then washed once with PBS, resuspended in 400 µl of PBS and kept at 4°C until further analysis.

2.2.11. Flow cytometry analysis

DNA content analysis was performed by flow cytometry on SYBRGreen-stained parasites either to follow their evolution through the life cycle or to measure the precise parasitemia, using a BD FACS Canto. The staining procedure was performed as described by Ganter et al. [201]. Briefly, the fixed collected parasites were first transferred in a 96-well microtiter plate (V-shape bottom) and washed with 200 µl of PBS per well, by centrifugation for 2 minutes at 2 100 rpm. The parasites were then permeabilized for 8 minutes at room temperature in 200 µl per well of permeabilization solution, before being washed two times with 200 µl of PBS as previously. The samples were subsequently subjected to a light RNase treatment, by incubation for 30 minutes at 37°C in 200 µl per well of RNase solution. The treated parasites were then washed two times as previously, and their DNA content was stained with SYBRGreen I by incubating them in 200 µl per well of SYBRGreen I solution for 20 minutes at room temperature protected from direct light. After two PBS-washes, the parasites were transferred in tubes adapted for flow cytometry measurements. Fluorescence was collected in the green channel (FITC-H) of the FACS Canto. A minimum of 2 000 iRBCs were counted per measurement and plotted in the form of dot-plots using the software FlowingSoftware2.5.1. A region of interest excluding background fluorescence was determined and information such as the mean and gated events was collected for this selected area.

2.2.12. Microscopy techniques

2.2.12.1. Live Fluorescence microscopy

Live Calcium measurement

Trophozoite-stage *P. falciparum* HB3 parasites were incubated with 10 µM of Fluo-4-AM in Ringer solution with Pluoronic F-127 (0,1% v/v) and 40 µM of probenecid and 0.1% of Pluoroninc acid for 40 minutes at 37°C, as previously described [202]. Dye-loaded parasites were washed two times before settling onto poly-L-lysine coated glass slides. Confocal laser scanning fluorescence microscopy was performed using a confocal Leica TCS SP5 (Leica

Microsystems CMS GmbH). Fluo-4-AM was excited at 488 nm (argon laser, 0.03 %) and the emitted fluorescence was collected from 505-520 nm. Single images were obtained using a 63 x objective, with a 5-fold software zoom, 1024x1024 pixels, every 2 seconds over a time span of 120 seconds. The Ca^{2+} ATPase inhibitor CPA, the Na^{+}/K^{+} ATPase inhibitor oubain, SC81458 and SC83288 were added to a final concentration of 10 µM at 45 seconds. The calcium signal was further analyzed using Fiji, and the mean fluorescence signals were compared using one-way ANOVA in SigmaPlot 13 (Systat Software Inc.).

Calcium resting concentration measurement

The ratiometric dye FuraRed shows a significant spectral shift with changes of free calcium Ca^{2+}. Live cell confocal scanning imaging can be performed using excitation wavelengths of 458 and 488 nm. The fluorescence emission is measured using a 570 nm long pass filter. Calibration of the FuraRed fluorescence was achieved using the Calcium Calibration Buffer Kit (ThermoFisher Scientific). Cells were permeabilized with 10 µM of the Ca^{2+} ionophore ionomycin, adjusted to varying free Ca^{2+} concentration and imaged. The fluorescent signal was also evaluated in the intact parasites, to obtain the calcium resting concentration.

Trophozoite-stage *P. falciparum* 3D7 parasites were incubated with 9 µM of FuraRed-AM in Ringer solution with Pluoronic F-127 (0,1% v/v) and 40 µM of probenecid and 0.1% of Pluoroninc acid for 45 minutes at 37°C, as previously described [202]. Dye-loaded parasites were washed two times before settling onto poly-L-lysine 8 well chamber (ibidi). Confocal laser scanning fluorescence microscopy was performed using a confocal Leica TCS SP5 (Leica Microsystems CMS GmbH). Single images were obtained using a 63x objective, 1024x1024 pixels. Single cell fluorescent images were further analyzed using Fiji and regions of interest were defined to measure the mean fluorescent intensity. A region of interest was also defined in non-infected erythrocytes to allow for background subtraction. The mean fluorescence ratio ($R_{458/488\ nm}$) was then calculated. A calcium calibration curve was constructed as described in Rohrbach et al. [202] using a least square fit to a Hill function. The Hill coefficient was fixed to unity reflecting the 1:1 stoichiometry of the FuraRed binding to Ca^{2+} ions. A Grubbs test was performed to identify outliers (at the p = 0.01 level). These outliers were omitted for further analysis. The $R_{458/488\ nm}$ ratio measured in resting parasites were then converted to the corresponding resting free [Ca^{2+}] using the inverse Hill equation. The mean calcium resting concentrations between the wild-type and mutant parasites were compared using one-way ANOVA in SigmaPlot 13 (Systat Software Inc.).

2.2.12.2. Immunofluorescence analysis (IFA)

In preparation for IFA, young trophozoite stage infected erythrocytes were purified using the MACS column. The samples were fixed in fixation solution for 30 minutes at room temperature. The cells were washed 3 times with PBS by centrifugation at 2 100 rpm for 1 minute, permeabilized in permeabilization solution for 15 minutes and washed 3 times as described above. A 3% (w/v) BSA in PBS solution was used for the blocking as well as to dilute the antibodies. The samples were blocked for 2 hours at room temperature and further incubated with the first antibody for 90 minutes. The samples were washed 3 times and incubated with the secondary antibody, and if necessary along with 5 µM of Hoechst 33342 for 45 min. The samples were then washed again 3 times and kept over-night in PBS at 4°C until they were analyzed using the confocal microscope Leica TCS SP5, equipped with an objective providing 63-fold magnification. Hoechst was excited at 364 nm and emission detected using a 385-470 filter, whereas 2nd antibody conjugated with Alexa 488 was excited using the 488 nm Argon laser and the emission was captured through a 505~550 filter.

Anti-HA tag monoclonal	:	1:1000
Anti-mouse Alexa Fluor 488	:	1:1000

2.2.13. Untargeted metabolomics analysis sample preparation

Metabolites from the *P. falciparum* wild-type 3D7 or PfATP6 ^{F972Y} strains, in absence or presence of SC83288 were extracted for further quantitative analysis by mass spectrometry. Briefly, 6 culture plates of 35 ml at a parasitemia in trophozoites stages (10 to 12 hours p.i.) of 5% were treated with a concentration of SC83288 corresponding to 5xIC_{50} (i.e. 40 nM), or with the respective amount of DMSO as negative control, for 12 hours. Parasites were then magnetically purified using the MACS system. In order to avoid a long detainment of the parasites in the magnetic column, the culture plates were purified three by three, and the eluted iRBC were kept in medium at 37°C upon regular addition of glucose. Once pooled together, the iRBC were centrifuged for 2 minutes at 2 100 rpm and washed once in 10 ml of pre-warmed PBS. The parasites were allowed to recover from the magnetic purification in 5 ml of RPMI at 37°C for 1 hour, with regular glucose addition. The metabolism was subsequently quenched by exchanging the medium with 2 ml of ice-cold RPMI and kept on ice. For each sample, 3.10^7 parasites were transferred into a fresh eppendorf tube, centrifuged at 2 100 rpm for 2 minutes at 4°C and washed one more time with ice-cold PBS.

The complete supernatant was removed, and the pellet was quickly resuspended in 150 µl of extraction buffer (Chloroform/Methanol/H2O at a 1:3:1 ratio, approximately 15:1 ration of extraction buffer to pellet size). The samples were incubated in a vortex for 1 hour at 4°C, and centrifuged for 10 minutes at 13 000 rpm at 4°C. 100 µl of each sample was transferred into a fresh eppendorf tube, sealed and kept at -80°C until further analysis. The remaining 20 µl of each sample were pooled together and centrifuged for 10 minutes at 13 000 rpm at 4°C. The supernatant was transferred into a fresh eppendorf tube, sealed and kept at -80°C until further analysis. The samples were shipped to Glasgow Polyomics Center (College of Medical, Veterinary & Life Sciences, University of Glasgow, Research group of Prof. Michael Barrett) for quantitative mass spectrometry analysis.

2.2.14. Data and statistical analysis

All the data analysis and display were performed using SigmaPlot 13.0.

3. Results

3.1. Characterization of the *in vitro* antiplasmodial activity of SC81458 and SC83288

3.1.1. Susceptibility of *P. falciparum* to SC81458 and SC83288

To assess the *in vitro* parasite susceptibility to both the SC-lead compounds, the half maximal growth inhibitory concentrations (IC_{50}) and the maximal concentrations to inhibit the growth of the parasites by 90 and 99% (IC_{90} and IC_{99}, respectively) were determined for the Dd2 strain of *P. falciparum*. Both compounds exhibited inhibitory concentrations in the low nanomolar range (Table 3.1) and steep dose-response curves [189].

Table 3.1: Relevant activity parameters of SC81458, SC83288, artemisinin and atovaquone.

	SC81458	SC83288	Artemisinin	Atovaquone
IC_{50}, IC_{90}, IC_{99} (nM)	8, 18, 50	3, 8, 20	2, 6, 50	0.6, 0.9, 2
in vitro $PCT_{99.9\%}$ (h) [(1)]	37 ± 4	51 ± 6	21 ± 3	87 ± 7
in vitro logPRR	3.4 ± 0.4	3.0 ± 0.5	4.5 ± 0.5	2.1 ± 0.4
in vitro lag phase (h)	< 5	< 5	0	< 24
in vitro $PCT_{90\%}$ (h) [(2)]	n.d.	17 ± 3	11 ± 0.8	< 80

Mean ± SEM of at least 4 independent determinations; [(1)] values obtained using a recrudescence assay described by Sanz et al. [198], [(2)] values obtained using the method described by Linares et al. [199]. IC, inhibitory concentration; PCT, parasite clearance time; PRR, parasite reduction ratio; n.d., non-determined. Adapted from Pegoraro et al. [189].

Previous work showed that if SC81458 and SC83288 displayed their highest antiparasitic activity against trophozoite stages, a slightly lower activity was observed against schizont-stages and only a moderate one on ring-stages [189].

SC81458 and SC83288 were also found to be active against a range of other *P. falciparum* lab strains, including multi-drug resistant strains other than Dd2, consistently displaying IC_{50} values lower than 20 nM *in vitro* [189].

3.1.2. SC81458 and SC83288 *in vitro* speed of action in *P. falciparum*

The efficiency of antimalarial compounds to decrease the parasite load in the blood and cure patients is partially mediated through their speed of action. In order to evaluate how quickly the SC-lead compounds were able to kill the parasites *in vitro*, various methods were used.

First, an approach based on parasites recrudescence was employed [198]. The principle is based on the determination of the parasites viability following drug exposure at a 10-fold IC_{50} concentration for various periods of time. Parasite viability was assessed by monitoring the re-growth of exposed parasites over time. This method enabled the extraction of different information regarding the speed of action, such as the potential lag phase in the action of the compound, the parasite reduction ratio (PRR), i.e. the decrease of viable parasites over one life cycle of 48 hours, and the parasite clearance time ($PCT_{99.9\%}$), corresponding to the time needed to kill 99.9% of the parasites. Those parameters are summed up in Table 3.1 [189]. For comparison purpose, two marketed antimalarial drugs were also evaluated, namely artemisinin and atovaquone, as fast- and slow-acting reference drugs, respectively (Figure 3.1 and [189]).

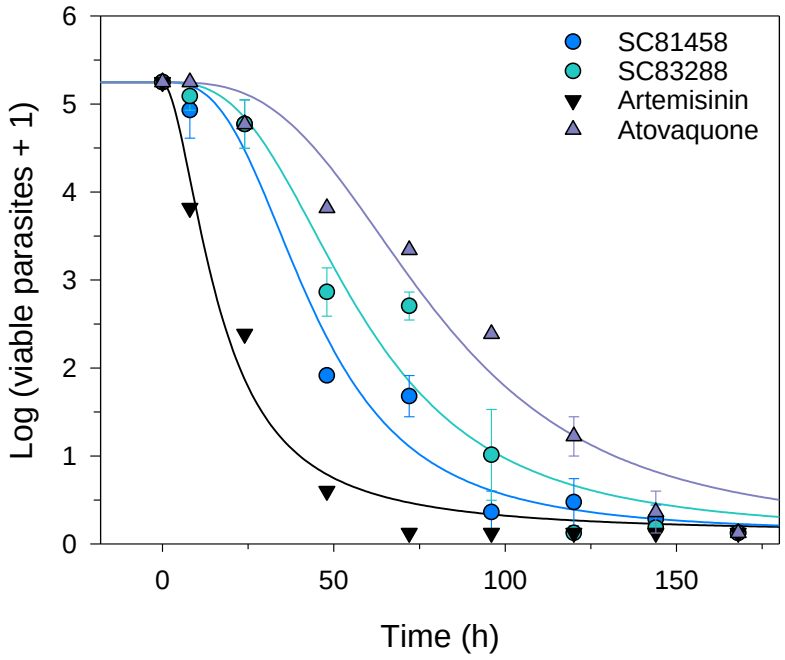

Figure 3.1: *In vitro* speed of action profiles of SC81458 and SC83288 in comparison to licensed antimalarial drugs. Number of Dd2 *P. falciparum* parasites in response to drug treatment at concentrations corresponding to 10 times the IC_{50} of SC81458 (80 nM), SC83288 (30 nM), artemisinin (20 nM) and atovaquone (10 nM). According to the original protocol, results are presented in logarithmic form (log10) as "viable parasites +1" (34). Mean ± SEM of at least 3 independent experiments. Adapted from Pegoraro et al. [189]**.**

SC81458 and SC83288 were able to clear 99.9% of the initial parasite population ($PCT_{99.9\%}$) within 37 ± 4 hours and 51 ± 6 hours, respectively, corresponding to a PRR of 3.4 ± 0.4 and 3.0 ± 0.5 log phases over 48h (Table 3.1, Figure 3.1 and [189]). This assay classified the SC-lead compounds as fast acting compounds, with a short lag phase of less than 5 hours, acting significantly faster than atovaquone ($PCT_{99.9\%}$ = 89 ± 7 hours, PRR = 2.1 ± 0.4, lag phase of more than 24 hours), although still not as fast as artemisinin ($PCT_{99.9\%}$ = 21 ± 3 hours, PRR = 4.5 ± 0.5, no lag phase) (Table 3.1, Figure 3.1 and [189]).

To further confirm the SC-lead compounds as fast-acting, the approach developed by Le Manach et al. [197] was applied. The IC_{50} values of asynchronous *P. falciparum* cultures over 24, 48 and 72 hours were determined, and the IC_{50} ratios, normalized to the 72 hours value, were calculated. It is worth mentioning that this approach allows only a rough classification of the antimalarial compounds, as fast- or slow-acting, but does not compare the speed of action of one compound to the other. This assay validated SC81458 and SC83288 as fast-acting compounds. Indeed, the relative IC_{50} ratios were independent of exposure time for both SC81458 (0.96 ± 0.08, 1.21 ± 0.16 and 1.00 ± 0.08, respectively for 24, 48 and 72 hours of incubation, One-way ANOVA Holm-Sidak test, $p > 0.05$, n.s.) and SC83288 (1.28 ± 0.08, 1.24 ± 0.05 and 1.00 ± 0.06, respectively for 24, 48 and 72 hours of incubation, One-way ANOVA Holm-Sidak test, $p > 0.05$, n.s.) (Figure 3.2), indicating a fast mode of action. Similarly, exposure time did not affect the IC_{50} ratios of artemisinin (0.98 ± 0.07, 0.88 ± 0.01 and 1.00 ± 0.01, respectively for 24, 48 and 72 hours of incubation, One-way ANOVA Holm-Sidak test, $p > 0.05$, n.s.) and quinine (1.19 ± 0.06, 1.24 ± 0.06 and 1.00 ± 0.06, respectively for 24, 48 and 72 hours of incubation, One-way ANOVA Holm-Sidak test, $p > 0.05$, n.s.). In comparison, the IC_{50} ratios of atovaquone were significantly different (3.44 ± 0.11, 1.35 ± 0.05 and 1.00 ± 0.04, respectively for 24, 48 and 72 hours of incubation, One-way ANOVA Holm-Sidak test, $p < 0.001$, ***), consistent with atovaquone being a slow acting antimalarial drug (Figure 3.2).

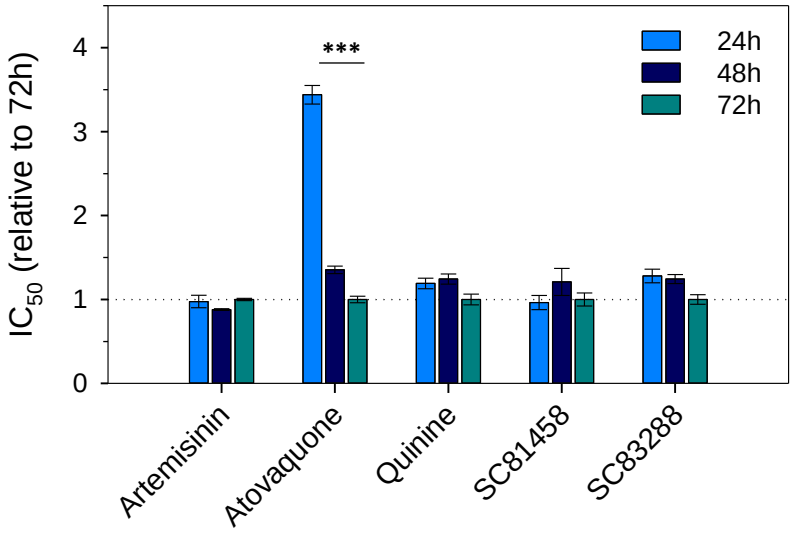

Figure 3.2: IC_{50}-based relative speed of action profiles of SC81458, SC83288, artemisinin, quinine and atovaquone. The assay was performed as described previously [197], on unsynchronized cultures of *P. falciparum* Dd2. Mean ± SEM of at least 4 independent determinations.

Finally, a third approach was used to evaluate the speed of action of SC83288, alone as well as in combination with artesunate or atovaquone, in the prospect of a potential combination therapy. The method described by Linares et al. [199] quantifies the new infections to back-calculate the parasite viability, using a two-color flow cytometry analysis. As it does not rely on parasite re-growth, this assay is considerably shorter than the recrudescence assay, and limits the risk of contamination compromising the experiments. The results of this assay were consistent with the previous ones, marking SC83288 as a potent antimalarial compound, with a 90% parasite clearance time ($PCT_{90\%}$) of 17 ± 3 hours. In comparison, the measured $PCT_{90\%}$ of artesunate and atovaquone were 11 ± 0.8 hours and > 80 hours, respectively (Figure 3.3 and Table 3.1). Combining artesunate and SC83288 did not lead to a significant difference in the $PCT_{90\%}$ compared with artesunate alone (9 ± 0.5 hours, Student's t-test, $p > 0.05$, n.s.) (Figure 3.3). Similarly, combining SC83288 with atovaquone did not significantly alter the $PCT_{90\%}$ of SC83288 alone (17 ± 6 hours Student's t-test, $p > 0.05$, n.s.) (Figure 3.3).

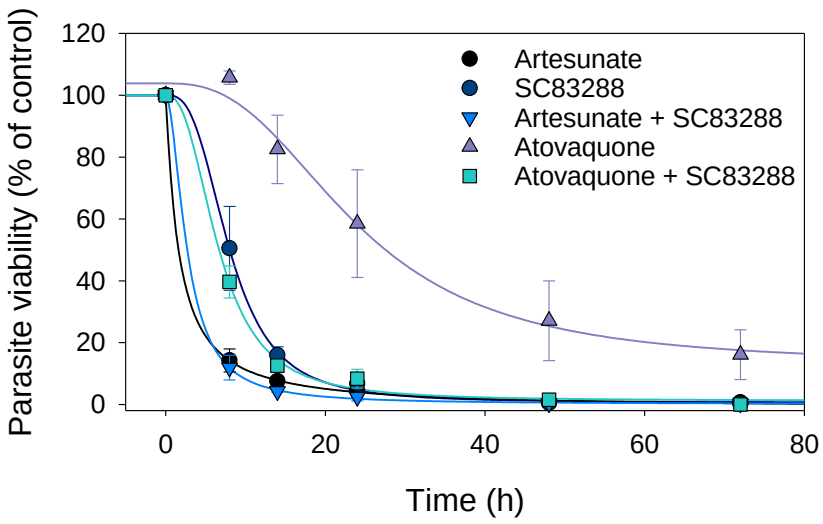

Figure 3.3: Killing rate profiles for artesunate, atovaquone, SC83288 and combinations of artesunate+SC83288 and atovaquone+SC83288. The assay was performed as described previously [199] on unsynchronized cultures of *P. falciparum* Dd2. Viability profiles of parasites treated with concentrations corresponding to 10x the IC_{50} values of artesunate, atovaquone, SC83288 alone or in combinations. The number of viable infected erythrocytes was normalized using the number of untreated parasites. Mean ± SEM of 4 independent experiments.

3.1.3. Progression of *P. falciparum* over its life cycle upon SC83288 treatment

Giemsa (Figure 3.4 A) and Hoechst (Figure 3.4 B) stained smears of Dd2 *P. falciparum* parasites over their 48 hours life cycle revealed that early treatment, i.e. before 24 hours p.i., with a concentration corresponding to 10x the IC_{50} value of SC83288 appeared to cause an arrest of the parasite at the early trophozoite stage, possibly inhibiting the necessary DNA replication to further progress in the cycle.

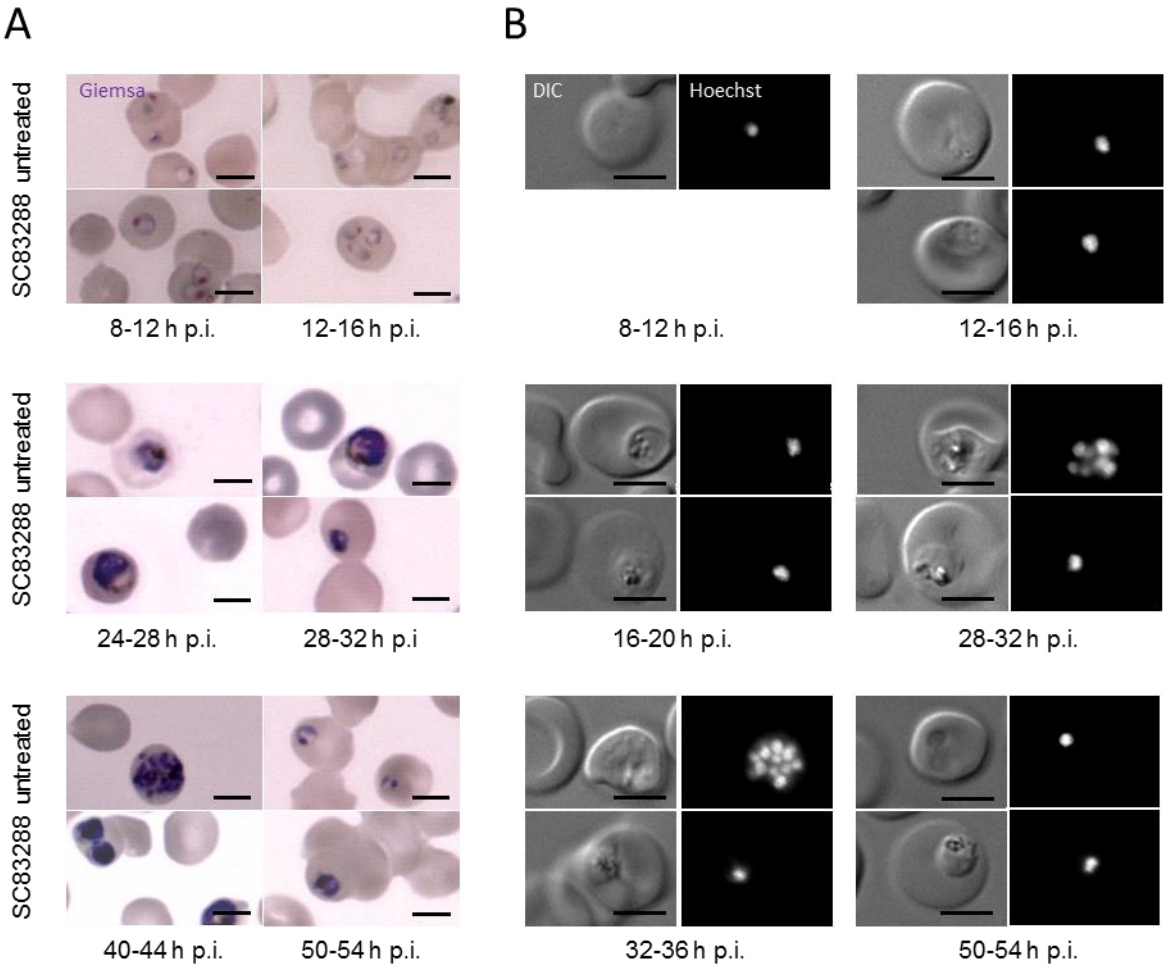

Figure 3.4: Progression of Dd2 *P. falciparum* parasites over their life cycle in presence or absence of SC83288. Parasites were treated with a concentration of SC83288 corresponding to 10x the IC_{50} value (30 nM) as early ring-stages (6 to 12 hours p.i.). **(A)** Thin blood smears were performed every 4 hours, shortly fixed in methanol, stained with Giemsa and further analyzed by light microscopy. **(B)** Parasites were harvested every 4 hours and analyzed by fluorescent microscopy after fixation and staining with the Hoechst DNA marker. Representative images of at least 3 independent experiments. Scale bar 5 µm.

These qualitative observations were corroborated using flow cytometry, where the DNA content of the parasites was stained with SYBRGreen. This quantitative analysis confirmed the absence of DNA replication in the parasites when treated early in their life-cycle (up to 24 hours p.i.) (Figure 3.5).

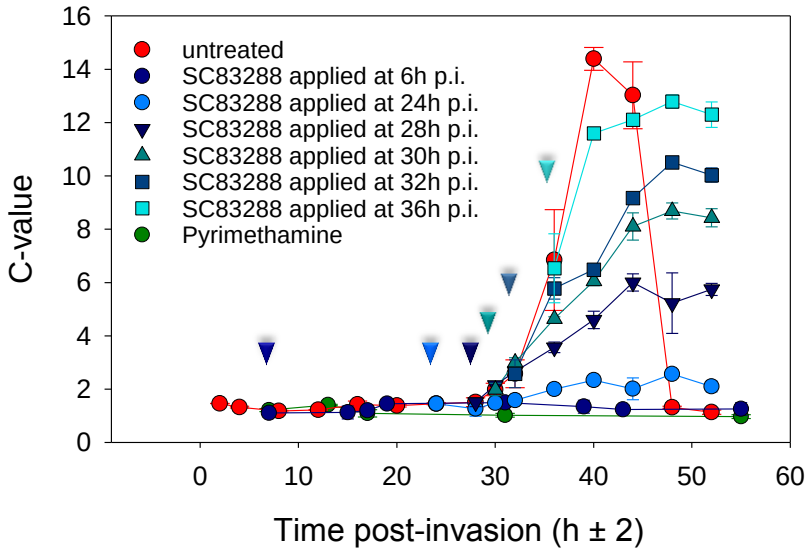

Figure 3.5: SC83288 fully inhibits DNA replication of Dd2 *P. falciparum* only when applied on early stages. Parasites were treated with a concentration of SC83288 corresponding to 10x the IC_{50} value (30 nM), or with 200 µM pyrimethamine, starting at different time points of their life cycle (arrowheads of respective colors) and harvested every 4 hours, up to 52 hours p.i. After fixation, permeabilization and light RNase A treatment, the parasites were stained with SYBRGreen and submitted to flow cytometry analysis. The C-value was obtained by normalization to the signal corresponding to the single infection by ring stages at 2 hours p.i. Mean ± SEM of at least 3 independent experiments.

However, when treated later (after 24 hours p.i.), the parasites still underwent DNA replication, even though not to the full extent, and their DNA content never dropped back as it should if the parasites were invading new erythrocytes and starting a new cycle as rings (Figure 3.5).

The interference of SC83288 with the DNA replication process was further confirmed by a quantitative metabolomics analysis. 3D7 *P. falciparum* parasites were treated with a concentration of SC83288 corresponding to 5x IC_{50} (i.e. 40 nM) as young trophozoites (10 to 12 hours p.i.) for 12 hours. These conditions were pre-determined to achieve a killing of half of the parasite´s population. 15 of the 32 detected metabolites involved in nucleotide metabolism showed a clear, yet non-significant on a Student´s T-test, increase when the parasites were treated with SC83288 compared to the untreated control (Figure 3.6 A). The distinct profiles of the nucleotide metabolites under the treated and untreated conditions were validated by the principal component analysis (PCA), with Eigenvectors almost diametrically opposed (Figure 3.6 B).

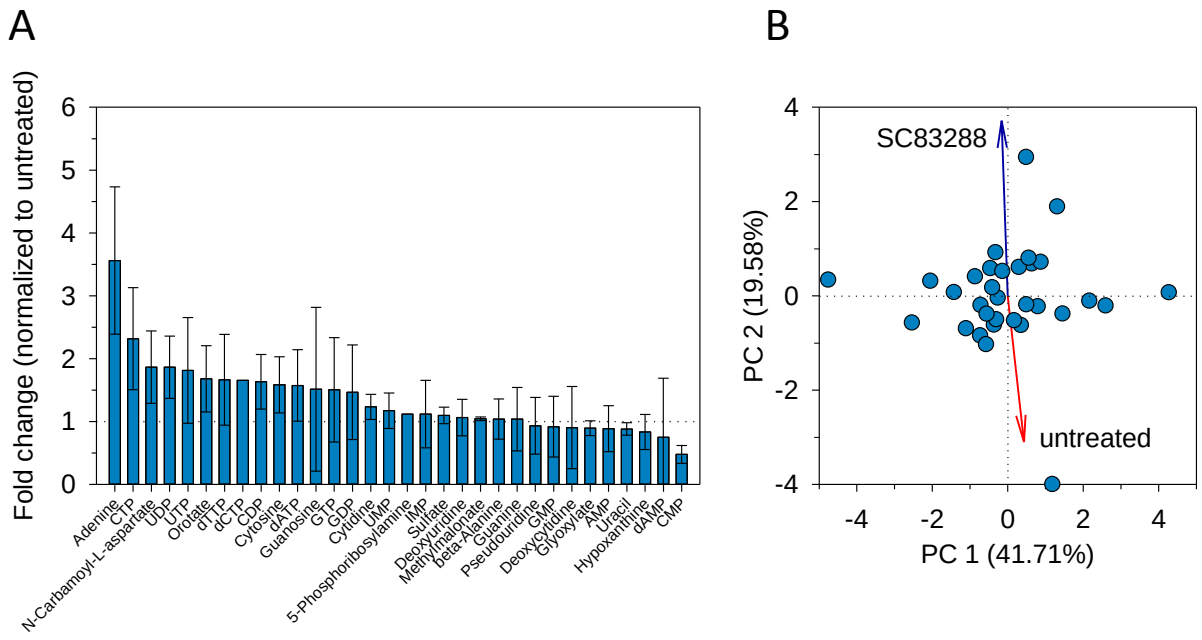

Figure 3.6: Nucleotide metabolism profile of *P. falciparum* 3D7 parasites untreated or treated with 5x IC_{50} of SC83288. (A) Relative concentration fold change of various metabolites involved in nucleotide metabolism when treated with SC83288, normalized to the untreated parasites. Mean ± SEM of at 4 independent experiments. **(B)** Principal component analysis (PCA) of the metabolites involved in nucleotide metabolism when untreated and treated with SC83288. The biplot of the first two principal components is shown (PC 1 and PC 2) and the percentage of the total variance explained by each principal component is displayed in parenthesis. The Eigenvectors are represented as arrows (red, untreated; blue, SC83288-treated), and their amplitude was multiplicated by 5 for visualization purposes.

3.1.4. Profiling the SC-lead compounds against artemisinins

Although artemisinin and its derivatives are established treatments against malaria [203], their mode of action is still a highly controversial subject [119,120]. Over the last decades, PfATP6 was discussed as a potential target of artemisinin [55,204], or to be involved in a resistance mechanism [61]. However, these hypotheses are now questioned [46,60] and resistance seems to rather be associated with mutation in the kelch13 protein in *P. falciparum* [205].

Since similar observations and hypotheses were issued concerning SC81458 and SC83288 with regard to PfATP6 [189], we investigated the possibility of a similar mode of action, and therefore and interaction between the SC-lead compounds and artemisinin.

3.1.4.1. The SC-lead compounds do not interact with artemisinin

The interaction profiles were established on *P. falciparum* Dd2 using a fixed-ratio isobologram approach [200]. This method is based on determining the IC_{50} values of two

individual drugs alone and the IC_{50} values of the two drugs in combination at different concentration ratios. In principle, the shift of a drug´s IC_{50} value assessed in combination compared to the one determined for this drug alone is indicative of the nature of the interaction between the two drugs. It is commonly accepted that a mean sum of fractional 50% inhibitory concentrations (mean ΣFIC_{50}) lower than 0.5 corresponds to a synergistic interaction, and higher than 1.5 to an antagonistic one [206]. A mean ΣFIC_{50} between these two cut-off values represents an indifferent interaction between the two investigated drugs. The arithmetical analysis revealed mean ΣFIC_{50} values of 0.99 ± 0.09 and 0.97 ± 0.06, respectively for SC81458 and SC83288, suggesting an indifferent interaction between artemisinin and the SC-lead compounds. The graphical analysis, obtained by plotting the pairs of fractional IC_{50} (FIC_{50}) values of artemisinin and SC81458 or SC83288 for each combination, agreed with the arithmetical observation, following almost perfectly the diagonal trend line (fit to a linear curve with R^2 = 0.944 and 0.972, respectively for SC81458 and SC83288), thereby corroborating the conclusion that both drugs do not interact with each other (Figure 3.7).

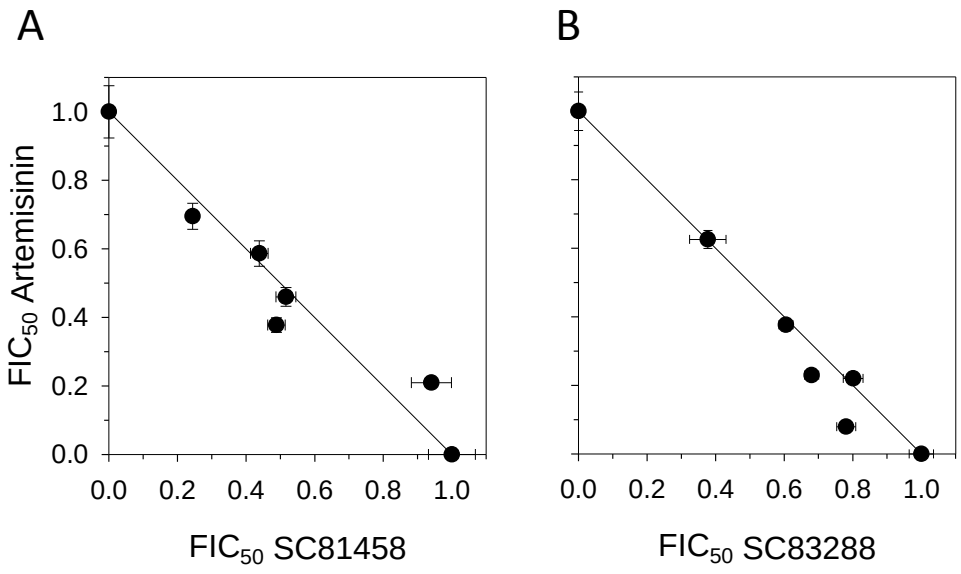

Figure 3.7: Indifferent interaction between artemisinin and the SC-lead compounds. Isobolograms showing the interaction between artemisinin and SC81458 **(A)** or SC83288 **(B)** in *P. falciparum* Dd2 parasites. The diagonal line represents an indifferent interaction of the two drugs. Mean ± SEM of 7 independent experiments.

3.1.4.2. The SC-lead compounds show no cross-resistance with artemisinins

The matter of cross-resistance between artemisinin and the SC-lead compounds was assessed using two independent approaches. First, the susceptibility to SC81458 and SC83288 of artemisinin-resistant parasites was evaluated, using the *P. falciparum* NF54

strain bearing an artificially introduced mutation in the kelch protein 13 ($K13^{C580Y}$), an established marker of artemisinin resistance [161]. A significant difference in the artemisinin responsiveness in the wild-type NF54 line and the $PfK13^{C580Y}$ lines was observed, with IC_{50} values of 20 ± 0.6 nM and 3.5 ± 1.3 nM, respectively (Student's t-test, $p < 0.001$, ***). In comparison none were observed concerning the sensitivity to SC81458 (3.4 ± 0.6 nM and 5.3 ± 0.7 nM, respectively, Student's t-test, $p > 0.05$, n.s.) or SC83288 (5.1 ± 0.7 nM and 4.9 ± 0.8 nM, respectively, Student's t-test, $p > 0.05$, n.s.) (Table 3.2).

Conversely, the susceptibility to artemisinin of *P. falciparum* lines resistant to the SC-lead compounds was evaluated. The Dd2 *P. falciparum* parasites, selected *in vitro* with the SC-lead compounds, described in details in Section 3.2 (Table 3.3 and [189], namely Dd2 ^{SC81458} and Dd2 ^{SC83288}) and the 3D7 *P. falciparum* genetically engineered to be resistant to the SC-lead compounds, described in Section 3.2.3.1 (Table 3.4 and Figure 3.15, namely 3D7 PfATP6 ^{F972Y}), were used to this purpose. Dd2 ^{SC81458}, Dd2 ^{SC83288} and their parental Dd2 strain revealed comparable IC_{50} values to artemisinin (3.8 ± 1.0 nM, 4.9 ± 0.5 nM, and 3.3 ± 0.3 nM, respectively, Student's t-test, $p > 0.05$, n.s.) (Table 3.2). Similarly, the IC_{50} values to artemisinin of 3D7 ATP6 ^{F972Y} and its parental line 3D7 showed no significant difference (18 ± 0.9 nM and 11 ± 1.0 nM, respectively, Student's t-test, $p > 0.05$, n.s.) (Table 3.2).

Table 3.2: Susceptibility, expressed as IC_{50} values, of the NF54 WT and NF54 $PfK13^{C580Y}$, Dd2 WT, Dd2 ^{SC81458}, Dd2 ^{SC83288}, 3D7 WT and 3D7 ATP6 ^{F972Y} *P. falciparum* lines to SC81548, SC83288 and artemisinin.

Line	IC_{50} (nM)		
	SC81458	**SC83288**	**Artemisinin**
NF54 WT	3.4 ± 0.6	5.1 ± 0.7	20 ± 0.6
NF54 PfK13 ^{C580Y}	5.3 ± 0.7	4.9 ± 0.8	35 ± 1.3 *
Dd2 WT	8.1 ± 0.5	3.1 ± 0.2	3.3 ± 0.3
Dd2 ^{SC81458}	1200 ± 900 *	1000 ± 100 *	3.8 ± 1.0
Dd2 ^{SC83288}	6200 ± 700 *	1000 ± 200 *	4.9 ± 0.5
3D7 WT	5.6 ± 0.6	8.2 ± 2.0	11 ± 1.0
3D7 ATP6 ^{F972Y}	3600 ± 300 *	5000 ± 300 *	18 ± 0.9

Mean ± SEM of 6 to 13 independent determinations. *, $p < 0.001$ as compared with the parental strain.

A ring survival assay (RSA) was further performed to take into account the activity of artemisinin against the ring stages of *P. falciparum* [161]. As expected, the NF54 PfK13 ^{C580Y} line showed a significant difference in its RSA score to dihydroartemisinin (DHA) compared

to its parental line (RSA score of 11.5 ± 1.51 % and 24.1 ± 1.87 %, respectively, Student's t-test, $p < 0.001$, ***). In comparison, various SC-resistant parasite lines displayed low and comparable RSA scores with respect to their parental lines (RSA scores of 9.94 ± 2.66 %, 12.0 ± 0.99 % and 7.65 ± 0.31%, for the wild-type Dd2, Dd2^{SC81458} and Dd2^{SC83288}, respectively, One-way ANOVA Holm-Sidak test, $p > 0.05$, n.s.; RSA scores of 11.6 ± 3.41 %, 13.8 ± 2.12 %, for the wild-type 3D7 and 3D7 PfATP6 ^{F972Y}, respectively, One-way ANOVA Holm-Sidak test, $p > 0.05$, n.s.) (Figure 3.8). The data from these two independent assays strongly suggest against any kind of cross-resistance effects between artemisinins and the SC-lead compounds.

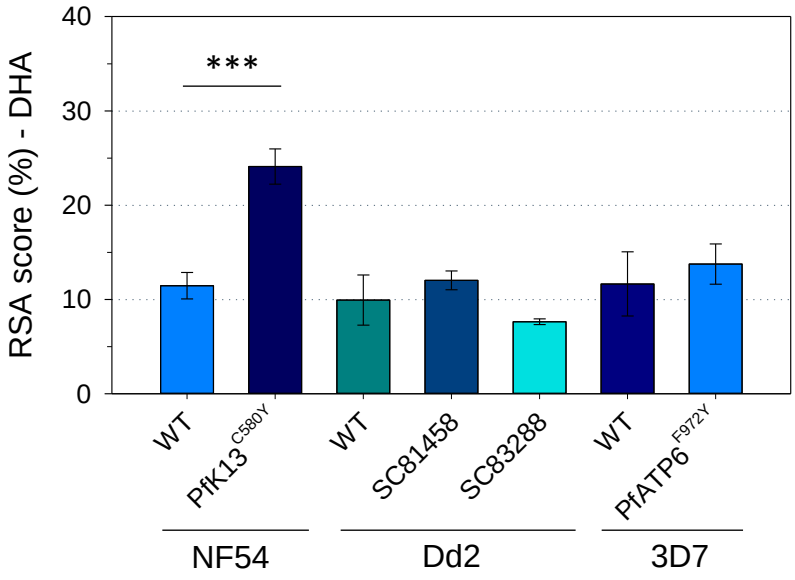

Figure 3.8: Ring survival rate to dihydroartemisinin (DHA). RSA scores of different *P. falciparum* strains: NF54, wild-type (WT) or bearing the PfK13 ^{C580Y} mutation; Dd2, wild-type (WT) or the *in vitro*-generated parasites resistant to 1 µM of either SC81458 or SC83288; 3D7, wild-type (WT) or bearing the PfATP6 ^{F972Y} mutation, to DHA. Mean ± SEM of 3 to 6 independent determinations; ***, $p < 0.001$.

Considering the similar parasite clearance time of the artesunate + SC83288 combination, compared to artesunate alone (Figure 3.3), the indifferent interaction and the lack of cross-resistance firmly point toward distinct modes of action and resistance between the SC-lead compounds and artemisinins.

3.2. Investigation of the role of PfTAP6 and calcium homeostasis with respect to the SC-lead compounds mode of action and resistance mechanism

Preceding the work presented here, and in order to obtain insights into the mode of action of the SC-lead compounds and into the mechanisms by which the parasites could develop resistance, *P. falciparum* Dd2 parasites were selected under gradual increase of SC81458 or SC83288 concentration (from 50 nM up to 1 µM), during a period of approximately 240 days [189]. All selected lines, namely Dd2 ^{SC81458} and Dd2 ^{SC83288}, showed a cross-resistance to the two SC-lead compounds, suggesting a shared mode of action and/or similar mechanism of resistance from the parasite [189]. Importantly, resistance to the SC-lead compounds did not decrease the susceptibility to various licensed antimalarial drugs (Table 3.3 and [189]).

Table 3.3: Susceptibility, expressed as IC_{50} values, of the *in vitro* developed SC-lead compounds resistant Dd2 *P. falciparum* lines to various licensed drugs.

Drug	IC_{50} (nM)		
	Dd2^{SC81458}	**Dd2^{SC83288}**	**Dd2 WT**
Chloroquine	150 ± 12	120 ± 25	135 ± 21
Quinine	160 ± 10	94 ± 9.0	100 ± 10
Quinidine	26 ± 1.0	9 ± 0.4	15 ± 1.0
Mefloquine	18 ± 1.0	6 ± 0.4	4 ± 0.1
Pyrimethamine	31000 ± 2000	22000 ± 2000	22000 ± 2000
Amodiaquine	8 ± 3.0	5 ± 1.0	7 ± 1.0
Artemisinin	4 ± 1.0	5 ± 0.5	3 ± 0.3
Atovaquone	3 ± 0.1	0.8 ± 0.1	0.6 ± 0.1

Mean ± SEM of 5 independent determinations. Adapted from Pegoraro et al. [189]**.**

All selected clones were submitted to ultra-deep sequencing analysis to identify genomic differences between the sensitive and the SC-lead compounds resistance parasites. A copy number variation (CNV) in chromosome 1, as well as several single nucleotide polymorphisms (SNPs) were consistently detected in the selected clones [189]. These SNPs led to mutations in the genes encoding the multi-drug resistance transporter 2 (PfMDR2, Pf3D7_1447900), a putative ATP-dependent RNA helicase DBP9 (Pf3D7_1241800), and the Ca^{2+} transporting PfATP6 (Pf3D7_0106300). The *pfatp6* locus and its upstream flanking region on chromosome 1 were duplicated in the Dd2 ^{SC83288} lines, and SNPs in the amplified *pfatp6* sequence were identified, leading to the substitution of the two consecutive alanine residues at positions 108 and 109 into threonines within the second transmembrane domain of PfATP6 (Figure 3.9) [189]. Five others identified genes were also present in this amplified locus, three of those annotated to encode conserved *Plasmodium* proteins of unknown

function (Pf3D7_0105800, Pf3D7_0106000 and Pf3D7_0106200), a putative DNA binding protein (Pf3D7_0105900), and a putative V-type proton ATPase subunit C (Pf3D7_0106100) (http://PlasmoDB.org). Additionally, another polymorphism was identified in the Dd2 ^{SC81458} lines, leading to the substitution of a phenylalanine residue at position 972 into tyrosine within the fifth transmembrane domain of PfATP6 (Figure 3.9) [189]. The presence of both point mutations and gene amplification was striking and led us to investigate the role of PfATP6 in the development of resistance to SC81458 and SC83288, as well as their mode of action(s).

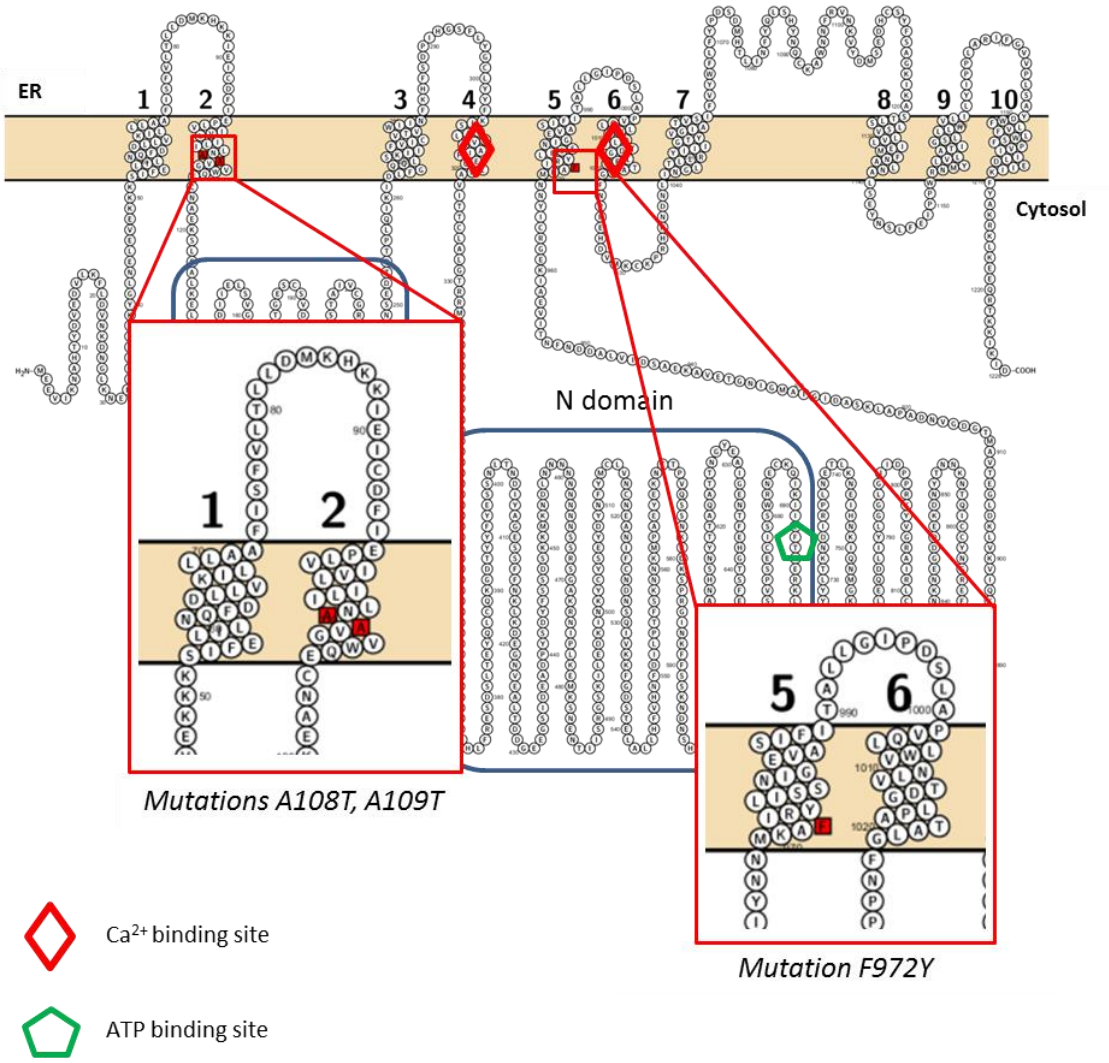

Figure 3.9: Predicted topological model of PfATP6. Reconstruction using the open-source visualization tool Protter [49], based on the model described in [50]. This model highlights the mutations in the amino acid sequence caused by the single nucleotide polymorphisms identified in the *in vitro* developed SC-lead compounds resistant Dd2 *P. falciparum* clones: the double mutation A108T, A109T in the second transmembrane domain found in the Dd2^{SC83288} line, and the F972Y mutation in the fifth transmembrane domain found in the DD2^{SC81458} line.

3.2.1. PfATP6 is not a direct molecular target of the SC-lead compounds

To investigate PfATP6 as a potential biological target, dynamic changes in cytoplasmic free Ca^{2+} levels were monitored using the Ca^{2+} sensitive fluorochrome Fluo-4-AM in a live cell confocal setup. The cell-permeable, established and reversible inhibitor of PfATP6 cyclopiazonic acid (CPA) [207] was used as a positive control, and the Na^{+}/K^{+} ATPase inhibitor ouabain as a negative control.

Under those conditions, treatment of the *P. falciparum* HB3 parasites with 10 µM of SC81458 or SC83288 resulted in no significant increase in cytoplasmic free Ca^{2+} (mean F_{75}/F_0 ratio 0.98 ± 0.10 and 0.99 ± 0.09, respectively), as opposed to the response induced by 10 µM of CPA (mean F_{75}/F_0 ratio 1.55 ± 0.15). The Na^{+}/K^{+} ATPase inhibitor ouabain (10 µM) had no effect on the cytoplasmic Ca^{2+} concentration in the parasite (mean F_{75}/F_0 ratio 0.99 ± 0. 04) (Figure 3.10).

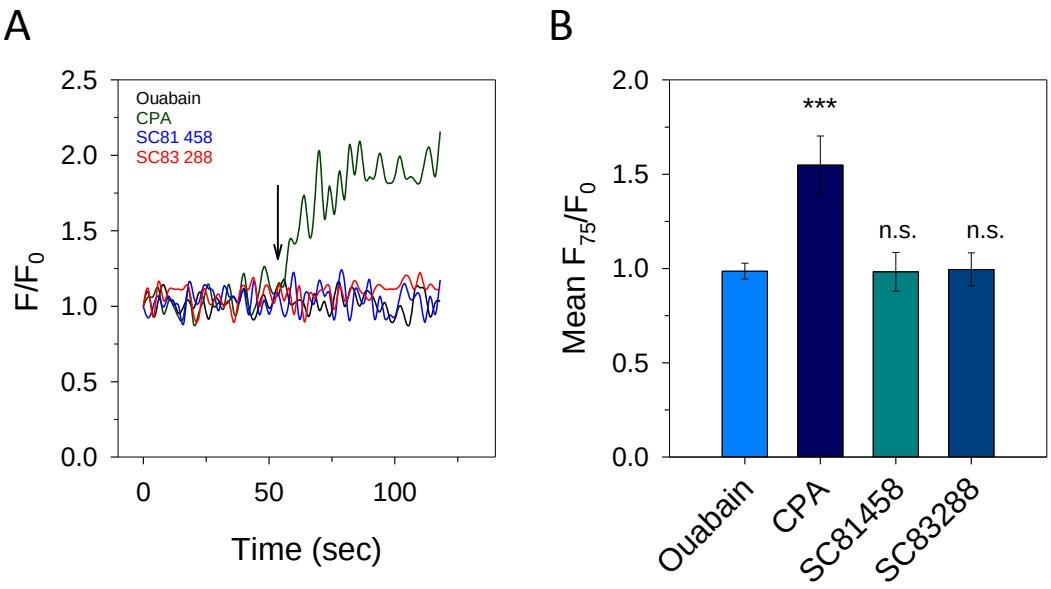

Figure 3.10: SC81458 and SC83388 induced cytoplasmic Ca^{2+} responses in *P. falciparum*. Trophozoite stages of HB3 *P. falciparum* strain were stained with Fluo-4-AM (10 µM) and transient cytoplasmic Ca^{2+} levels were recorded in response to SC81458 (10 µM), SC83288 (10 µM), ouabain (10 µM), and CPA (10 µM), using a confocal live cell setup. **(A)** Representative Ca^{2+} traces in the parasite's cytoplasm. The mean fluorescence intensity (F) was normalized to the fluorescence intensity at time point zero (F_0). **(B)** Mean fluorescence intensity at time point 75 seconds (F_{75}) normalized to the fluorescence intensity at time point zero (F_0). Mean ± SEM of at least 4 independent experiments with at least four determinations in each replicate. One-way ANOVA, $p < 0.001$, ***. Adapted from Pegoraro et al. [189].

To confirm the live calcium observations, a different approach was used. SC81458 and SC83288 were sent to our collaborators at St George's University of London (Prof. Sanjeev

Krishna´s group), to investigate PfATP6 as a direct target in a different experimental system. The compounds were tested in K667 *Saccharomyces cerevisiae*, lacking the endogenous vacuolar Ca^{2+} exchanger Vcx1, calcineurin regulatory subunit B cnb1 and the vacuolar calcium pump Pmc1 [70,208]. Only the heterologous expression of PfATP6 allows these yeasts to tolerate high calcium levels. Dose-response assays (experiments performed by Hatoon Abdullah Niyazi) showed no direct inhibition of PfATP6 by the SC-lead compounds (Figure 3.11). Indeed, concentrations of up to 10^{-2} M of SC83288 (Figure 3.11 B) or SC81458 (Figure 3.11 C), did not interfere with *S. cerevisiae* growth, as opposed to a concentration higher than 10^{-5} M of CPA (Figure 3.11 A).

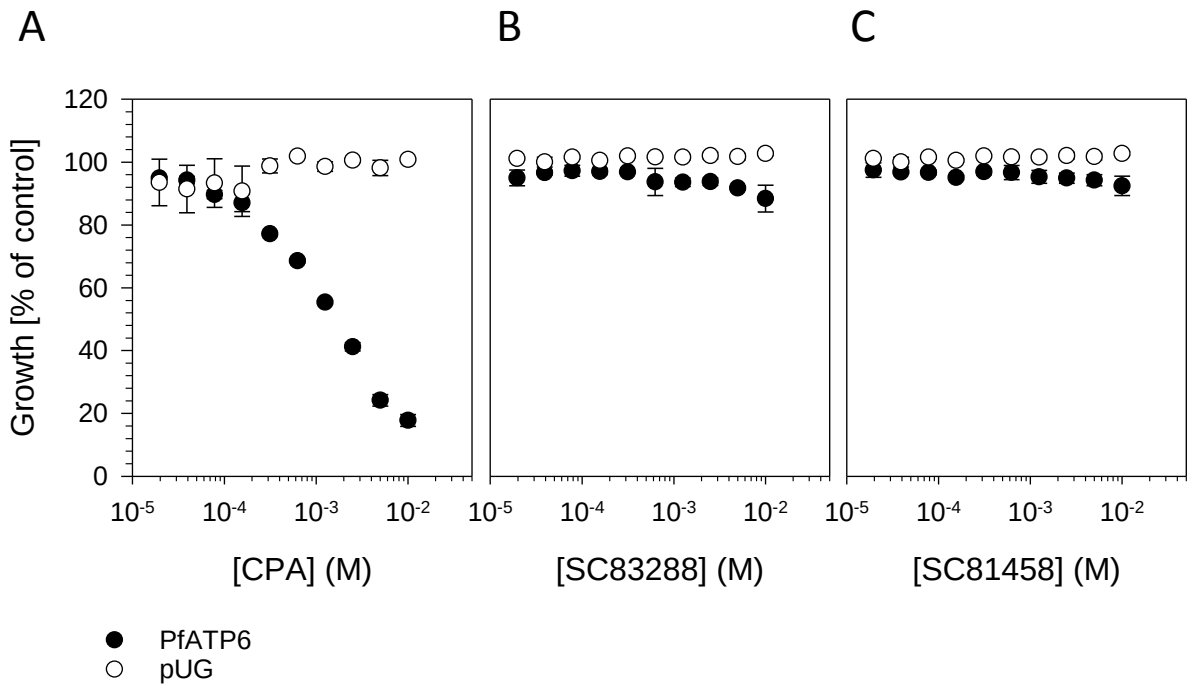

Figure 3.11: Effect of CPA, SC83288 and SC81458 on high calcium concentration tolerance on knock-out *S. cerevisiae*. Dose-response assays using the *S. cerevisiae* knock-out of the endogenous vacuolar Ca^{2+} exchanger Vcx1, calcineurin regulatory subunit B cnb1 and the vacuolar calcium pump Pmc1, to CPA **(A)**, SC83288 **(B)** and SC81458 **(C)** when transfected with PfATP6 or a control empty plasmid pUG. Mean ± SEM of 3 independent experiments, performed by Hatoon Abdullah Niyazi (St George's University of London, UK).

These observations are not consistent with SC81458 and SC83288 directly targeting PfATP6, but rather tend to suggest an involvement of PfATP6 in a mechanism of resistance to those compounds.

3.2.2. Use of the CRISPR/Cas9 system for genetically engineering PfATP6

Even though it was ruled out as a direct target for SC81458 or SC83288, PfATP6 was kept under investigation for a possible role in the resistance mechanisms to those compounds. In order to properly correlate the identified SNPs in PfATP6 in the Dd2 ^{SC81458} and Dd2 ^{SC83288} lines with SC-lead compounds resistance, the CRISPR-Cas9 system was used to introduce these mutations into the *P. falciparum* genome in a marker-free fashion [78] (Figure 3.12).

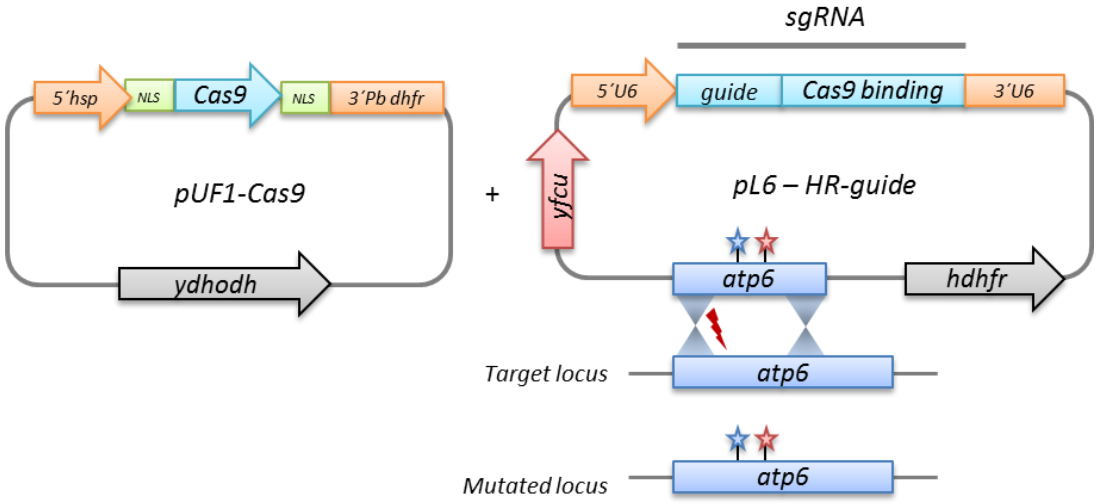

Figure 3.12: General CRISPR-Cas9 strategy used to mutate PfATP6. The vector pUF1-Cas9 (left) encodes the Cas9 endonuclease (light blue) flanked by nuclear localization signals (NLS, green). Its expression is regulated by the promoter region of the heat shock protein 86 (5' hsp, orange) and the 3'UTR region of the *P. berghei* dhfr (3' Pb dhfr, orange). The selection marker of the plasmid is the yeast dihydroorotate dehydrogenase gene (ydhodh, grey). The pL6 plasmid (right) contains the single-guide RNA (sgRNA)-expression cassette. The expression of the sgRNA is regulated by the promoter of the *P. falciparum* U6 snRNA polymerase III (5' U6, orange) and the 3'UTR region (orange). The homology region (dark blue) contains the desired mutation(s) (blue star) as well as the necessary shield mutation(s) (red star). The selection marker of the plasmid is the human dihydrofolate reductase gene (hdhfr, grey) and the negative selection marker is the bifunctional yeast cytosine deaminase and uridyl phosphoribosyl transferase (yfcu). Both plasmids are transfected together in *P. falciparum* parasites by electroporation.

After several trials, the parasites transfected with the plasmid containing the mutations coding for the A108T, A109T substitutions never showed recombination events (Figure 3.13).

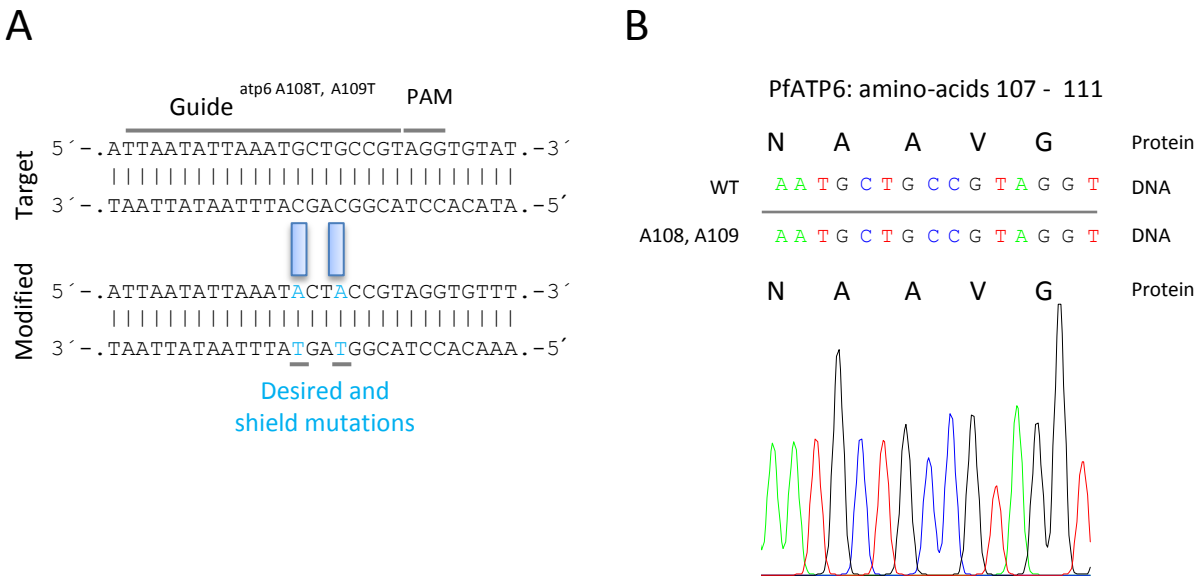

Figure 3.13: Attempted generation of the PfATP6 A108T, A109T mutant using the CRISPR/Cas9 system. (A) Target sequence recognized by sgRNA^{atp6}:Cas9 highlighting the 20-nucleotide guide sequence and the PAM motif (top). Modified locus showing the desired mutations (blue) to generate the A108T, A109T replacement. In this case, both the desired mutations play also the role of shield mutations, as they directly overlap with the sgRNA guide (bottom). **(B)** Chromatogram showing the sequence analysis of the resulting transfectants. The DNA sequence and consequently the amino acid sequence remained unchanged. Representative of 6 independent transfection rounds.

A single control transfection with a plasmid encoding for synonymous mutations led to a successful recombination, demonstrating a proper activity of the designed RNA guide (Figure 3.14). This observation suggests that the double mutation is probably not viable on its own, and the parasites must rely on other compensatory mutations to survive.

This approach was however successful for introducing the mutation leading to the substitution of the phenylalanine at position 972 into tyrosine in the endogenous locus of *pfatp6* (Figure 3.15). Two pure clones, namely #E4 and #H12, were obtained by limiting dilution and used for characterization and further experiments.

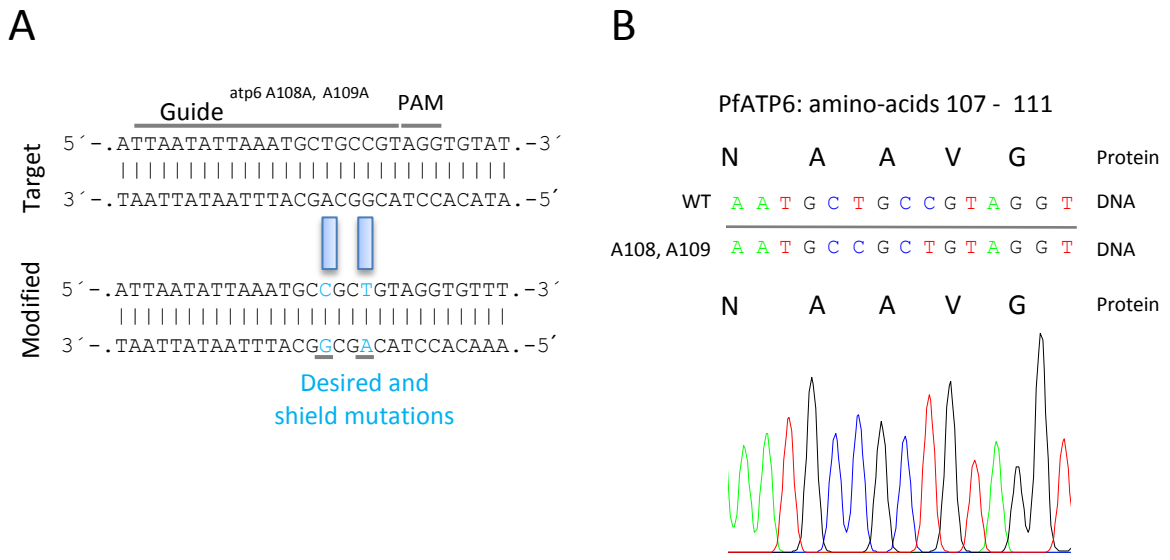

Figure 3.14: Generation of the PfATP6 A108A, A109A mutant using the CRISPR/Cas9 system and sgRNA guide efficiency confirmation. (A) Target sequence recognized by sgRNA^{atp6}:Cas9 highlighting the 20-nucleotide guide sequence and the PAM motif (top). Modified locus showing the desired silent-mutations (blue) to generate the A108A, A109A replacement. In this case, both the desired mutations play also the role of shield mutations, as they directly overlap with the sgRNA guide (bottom). **(B)** Chromatogram showing the sequence analysis of the resulting transfectants. The presence of the silent mutations demonstrated a successful recombination event, testifying for the sgRNA efficiency.

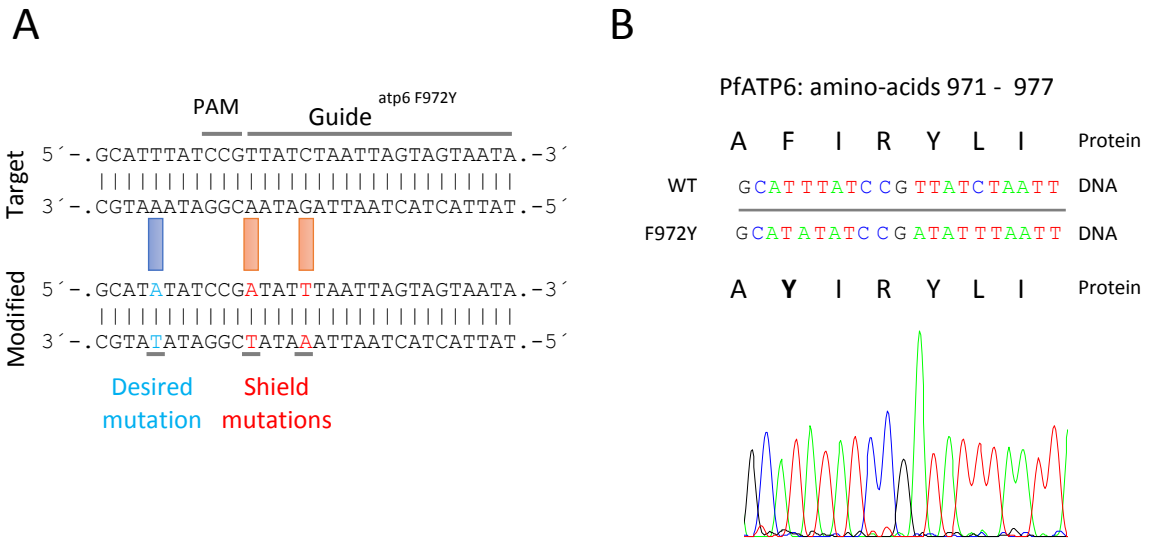

Figure 3.15: Generation of the PfATP6 F972Y mutant using the CRISPR/Cas9 system. (A) Target sequence recognized by sgRNA^{atp6}:Cas9 highlighting the 20-nucleotide guide sequence and the PAM motif (top). Modified locus showing the desired silent-mutations (blue) to generate the F972Y replacement and the necessary shield mutations (red) (bottom). **(B)** Chromatogram showing the sequence analysis of the resulting transfectants. The presence of the desired and silent mutations demonstrated a successful recombination event. The designed amino acid change is highlighted in bold.

3.2.3. Characterization of the 3D7 PfATP6 ^{F972Y} mutant line

3.2.3.1. *P. falciparum* 3D7 PfATP6 ^{F972Y} susceptibility to SC81458 and SC83288

To assess the effect of the F972Y mutation in PfATP6 on the susceptibility of the parasite to the SC-lead compounds, the IC_{50} value was determined for both SC81458 and SC83288. The sensitivity to chloroquine was evaluated in parallel as a control.

Table 3.4: Susceptibility, expressed as IC_{50} values, of the 3D7 WT and 3D7$^{PfATP6\ F972Y}$ to SC81548, SC83288 and chloroquine.

Line	IC_{50} (nM)		
	SC81458	SC83288	Chloroquine
3D7^{WT}	5.6 ± 0.6	8.2 ± 2.0	8.6 ± 0.4
3D7 ATP6^{F972Y}	3600 ± 300	5000 ± 300	7.9 ± 0.5

The values obtained for the #E4 and #H12 pure clones were combined. Mean ± SEM of 3 to 6 independent determinations.

The presence of the F972Y mutation led to a drastic effect, i.e. an increase of approximately three orders of magnitude on the IC_{50} values for SC83288 (8.2 ± 2.0 nM and 5.0 ± 0.3 µM, for the wild-type and the mutant, respectively, Student‘s t-test, $p < 0.001$, ***) (Figure 3.16 A and C, Table 3.4), and SC81458 (5.6 ± 0.6 nM and 3.6 ± 0.3 µM, for the wild-type and the mutant, respectively, Student‘s t-test, $p < 0.001$, ***) (Figure 3.16 B and C, Table 3.4). The susceptibility to chloroquine was not affected by the introduction of the F972Y mutation (IC_{50} values of 86 ± 0.4 nM and 79 ± 0.4 nM, for the wild-type and the mutant, respectively, Student‘s t-test, $p > 0.05$, n.s.).

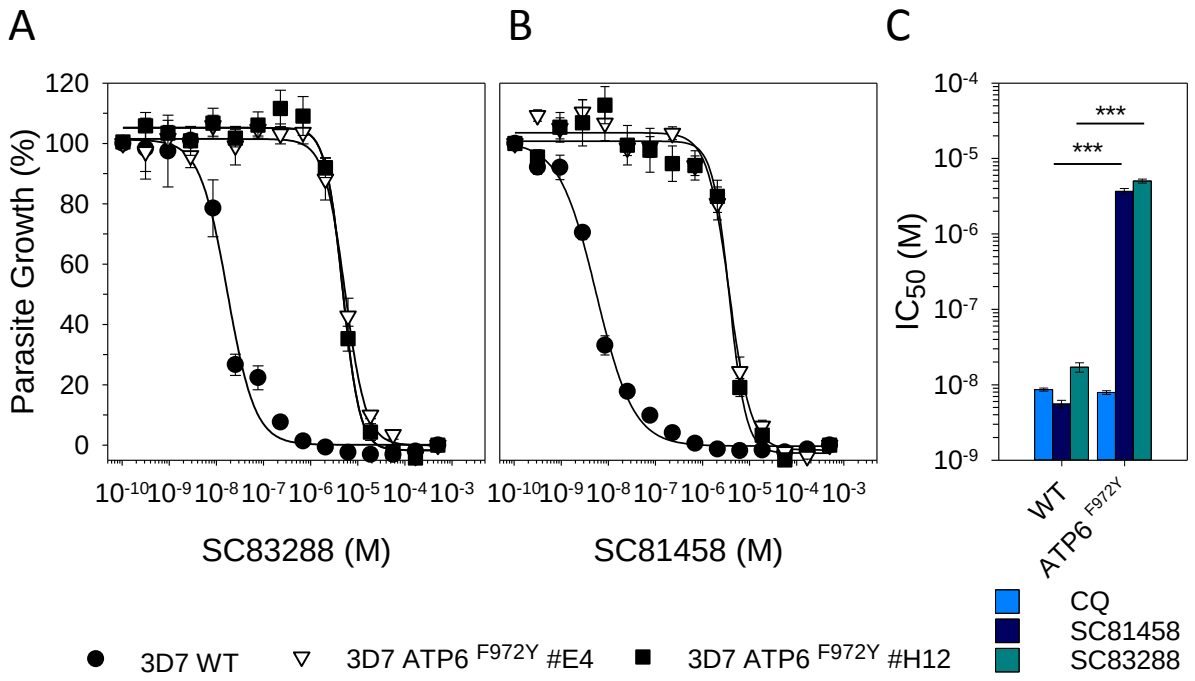

Figure 3.16: Susceptibility of the 3D7 wild-type and 3D7 PfATP6 ^{F972Y} *P. falciparum* parasites to SC81548, SC83288 and chloroquine. (A and **B)** Growth inhibition assay by SC83288 **(A)** or SC81458 **(B)** for the wild-type (WT) and both 3D7 PfATP6 ^{F972Y} clones (#E4 and #H12). **(C)** IC_{50} values obtained from the growth inhibition assays, by combining the results obtained by the two mutant clones for SC81458, SC83288 and chloroquine (CQ) as a control. Mean ± SEM of 3 to 6 independent determinations, One-way ANOVA, $p < 0.001$, ***.

Additionally, the ring sensitivity of the mutant parasites to the SC-lead compounds was evaluated by performing a ring survival assay (RSA), as previously described [161]. No significant difference was observed in the ring-stage susceptibility of the wild-type or mutant parasites to SC81458 (RSA score of 94.5 ± 11.9 %, 109 ± 6.54 % and 109 ± 6.11 %, respectively for the wild-type and the two mutant clones, One-way ANOVA, $p > 0.05$, n.s.) (Figure 3.17 A) or SC83288 (RSA score of 90.5 ± 1.16 %, 111 ± 19.4 % and 94.3 ± 3.84 %, respectively for the wild-type and the two mutant clones, One-way ANOVA, $p > 0.05$, n.s.) (Figure 3.17 B).

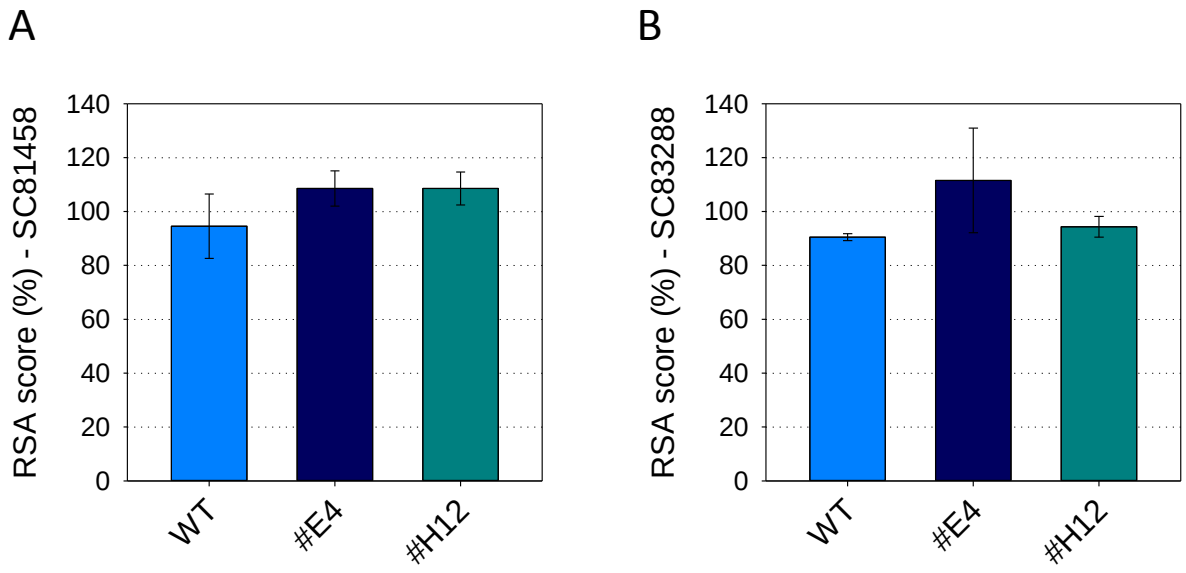

Figure 3.17: Ring survival rate of 3D7 wild-type and 3D7 PfATP6 ^{F972Y} *P. falciparum* parasites. RSA score of wild-type (WT) and both 3D7 PfATP6 ^{F972Y} clones (#E4 and #H12) in response to a 6 hours pulse treatment of 700 nM of SC81458 **(A)** and SC83288 **(B)**. Mean ± SEM of 3 to 6 independent determinations.

Finally, wild-type or mutant parasites were treated with a concentration of SC83288 corresponding to 10x the IC_{50} value on the wild-type (i.e. 80 nM) as ring stages, and their DNA content was followed by flow cytometry over their life cycle. While the SC83288-treated wild-type *P. falciparum* parasites did not show DNA replication, the mutants, treated with or without SC83288, behaved similarly to the non-treated wild-type line, undergoing schizogony as suggested by the increase of their DNA content over time, and by the sudden drop around 48 hours post-invasion corresponding to the beginning of a new cycle as ring stages (Figure 3.18).

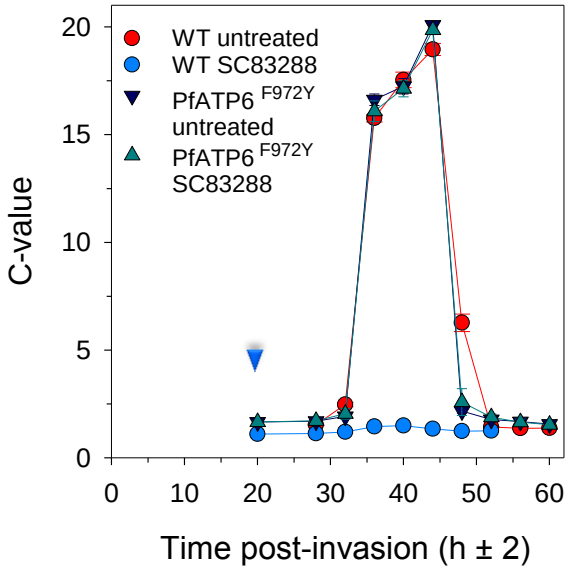

Figure 3.18: Progression of 3D7 wild-type and 3D7 PfATP6 ^{F972Y} *P. falciparum* parasites over their life cycle in presence of absence of SC83288. Parasites were treated with a concentration of SC83288 corresponding to 10x the IC_{50} value (80 nM) as ring-stages (approximately 20 hours p.i., arrowhead) and harvested every 4 hours, up to 60 hours p.i. After fixation, permeabilization and light RNase A treatment, the parasites were stained with SYBRGreen and submitted to flow cytometry analysis. The C-value was obtained by normalization to the signal corresponding to the single infection by ring stages at 20 hours p.i. Mean ± SD of technical duplicates of one experiment.

3.2.3.2. The PfATP6 ^{F972Y} mutation gives rise to a fitness cost related to calcium homeostasis

To measure the extent to which the PfATP6 ^{F972Y} mutation influenced the relative growth rate of asexual blood stage parasites and serving as a partial proxy for assessing fitness costs, an *in vitro* co-culture competition assay was performed, as previously described [209,210]. Briefly, the wild-type 3D7 line was mixed with the 3D7 ATP6 ^{F972Y} clones at a 1:1 ratio and the proportions of the individual *pfap6* alleles were quantified by pyrosequencing every 2 cycles (i.e. every 4 days), over a period of 20 cycles. Results were fit to a linear function of the relative proportion of the wild-type or the mutated *pfatp6* alleles over time (y = (55.5 ± 4) + (1.6 ± 0.4) * x, with an R^2 = 0.675; y = (43.7 ± 4) - (1.5 ± 0.4) * x, with an R^2 = 0.658 for the wild-type and the mutated *pfatp6* alleles respectively) (Figure 3.19). The PfATP6 ^{F972Y} mutations led to a growth deficiency compared to the wild-type line, which was predicted to completely take over the mutant line in approximately 29 cycles.

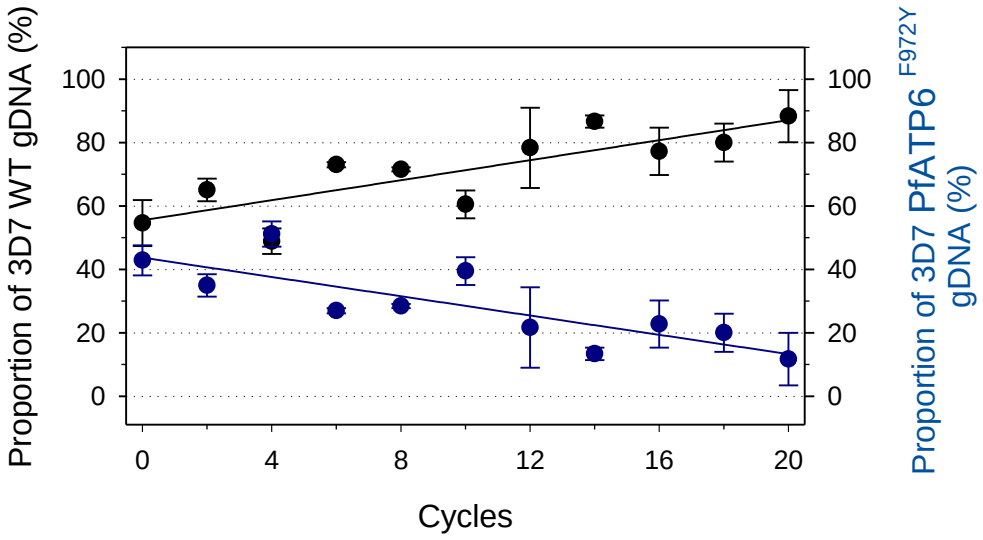

Figure 3.19: Effect of the PfATP6 ^{F972Y} mutation on the parasite fitness. Mixed cultures at a 1:1 ratio between 3D7 wild-type (WT) and 3D7 PfATP6 ^{F972Y} were cultured over 20 cycles. The allelic proportions of *pfatp6* were measured by pyrosequecning every 2 cycles. The proportion of 3D7 WT in the cultures overtime is represented in black (left y-axis) and the proportion of the 3D7 PfATP6 ^{F972Y} allele in dark blue (right y-axis). Results were fit to a linear function of the relative proportion of the wild-type or the mutated *pfatp6* alleles over time. Mean ± SEM of 3 independent determinations.

Considering the role of PfATP6 in the parasite calcium homeostasis, it was tempting to speculate on a possible alteration of the calcium resting concentration in the mutant parasites.

In order to quantitatively measure the cytosolic calcium resting concentration in the wild-type and PfATP6 ^{F972Y} 3D7 *P. falciparum* parasites, the ratiometric dye Fura-Red-AM was used

[202]. The Ca^{2+} fluorophore Fura-Red can be excited using an argon laser at 458 and 488 nm. Unlike most other Ca^{2+} indicators, Fura-Red fluorescence decreases upon binding to free Ca^{2+}, and the fluorescence ratio ($F_{458/488}$ nm) increases with rising free Ca^{2+} concentrations. Parasites were stained with Fura-Red-AM and stable fluorescence intensities (F_{458} nm and F_{488} nm) were recorded in the cell cytoplasm (Figure 3.20).

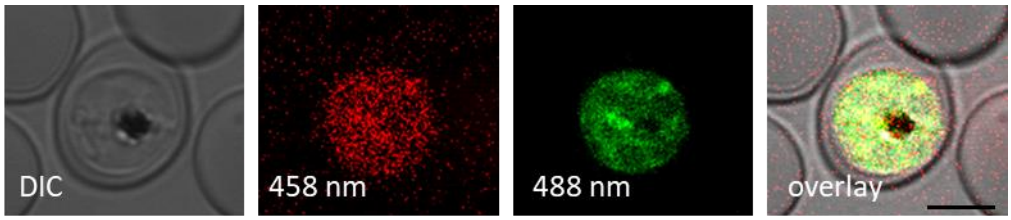

Figure 3.20: Confocal live cell Fura-Red-AM imaging of *P. falciparum* infected erythrocytes. Representative trophozoite stage 3D7 *P. falciparum* infected erythrocyte stained Fura-Red-AM, excited at 458 nm (0.15% laser intensity) and 488 nm (0.04% laser intensity). Scale bar 5 µm.

First, this method was validated on Dd2 *P. falciparum* parasites. A calibration curve was established using free Ca^{2+} concentrations ranging from 0.6 nM to 1.2 mM (Figure 3.21 A), and was used to quantify the free calcium resting concentration in the cytosol of untreated parasites, or in presence of 30 µM of CPA (Figure 3.21 B and Table 3.5). The measurement of 97 cells allowed determining a calcium resting concentration in untreated Dd2 *P. falciparum* of 308 ± 82 nM, consistent with the value of 352 ± 42 nM previously reported [202]. As expected, short treatment with CPA led to a significant increase in the cytosolic free calcium concentration, to 840 ± 83 nM (for 43 cells measured) (Rank Sum test, $p < 0.001$, ***) (Figure 3.21 B).

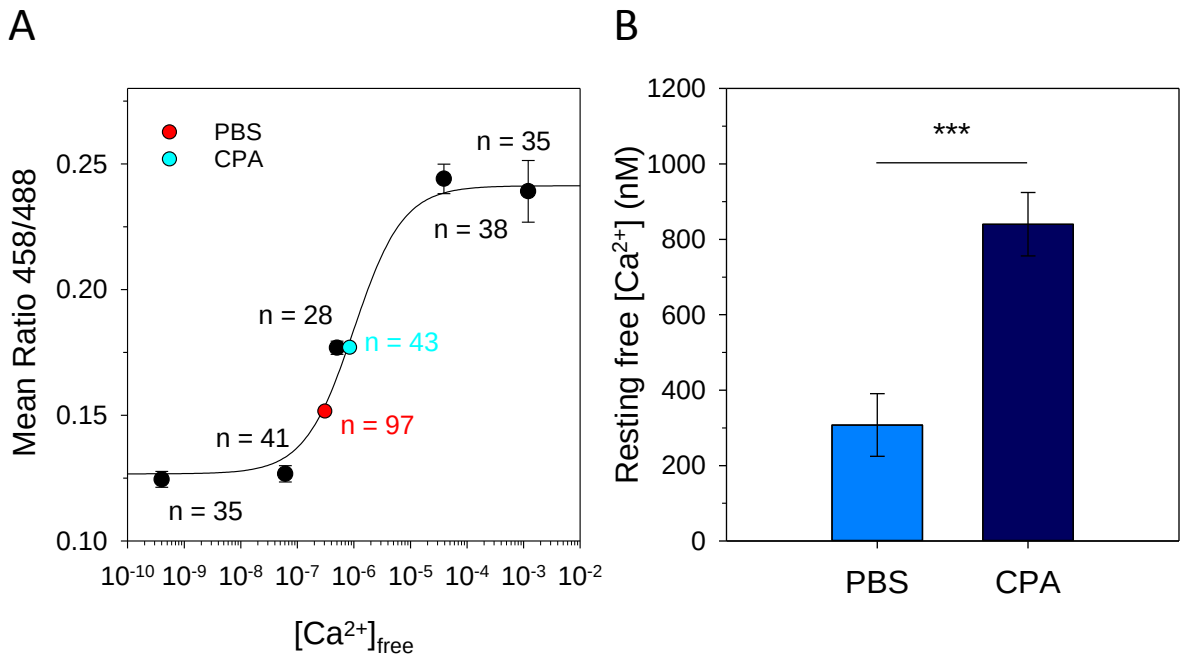

Figure 3.21: Calibration of Fura-Red-AM fluorescence and determination of apparent resting free Ca^{2+} concentration in the *P. falciparum* Dd2 cytoplasm. (A) Ca^{2+} equilibration curve for the steady-state Fura-Red-AM fluorescence ratio (458/488 nm) from the cytoplasm of Dd2 *P. falciparum* parasites at the young-trophozoite stage. Cells were permeabilized with the Ca^{2+} ionophore ionomycin and adjusted to the indicated free-Ca^{2+} concentrations. N corresponds to the total number of measured cells. **(B)** Mean apparent cytoplasmic resting Ca^{2+} ($[Ca^{2+}]$) concentrations in absence or presence of the PfATP6 inhibitor CPA. Mean ± SEM of respectively 97 and 43 independent determinations. Rank Sum test, $p < 0.001$, ***.

These preliminary experiments confirmed the use of FuraRed as a reliable method to measure cytosolic calcium concentration in a quantitative manner.

This approach was then used on the *P. falciparum* 3D7 wild-type and PfATP6 ^{F972Y} parasites, in presence or absence of SC83288. Preliminary experiments were first conducted to determine the appropriate SC83288 concentration and time of treatment that would affect the parasite viability on the long term, i.e. one cycle, but not within the experimental measuring time. From both the recrudescence and the direct speed of action assays, we knew that a concentration corresponding to 10 times the IC_{50} value was already sufficient to obtain a $PCT_{99.9\%}$ of approximately 50 hours. To ensure a similar effect even after a short treatment time, a concentration corresponding to 50 times the IC_{50} concentration (i.e. 400 nM in the 3D7 strain) for 1 hour was used. Such a treatment resulted in the death of the SC83288-sensitive parasites on the next day, as demonstrated by the absence of ring stages (Figure 3.22 A), without affecting the PfATP6 ^{F972Y} line (Figure 3.22 B).

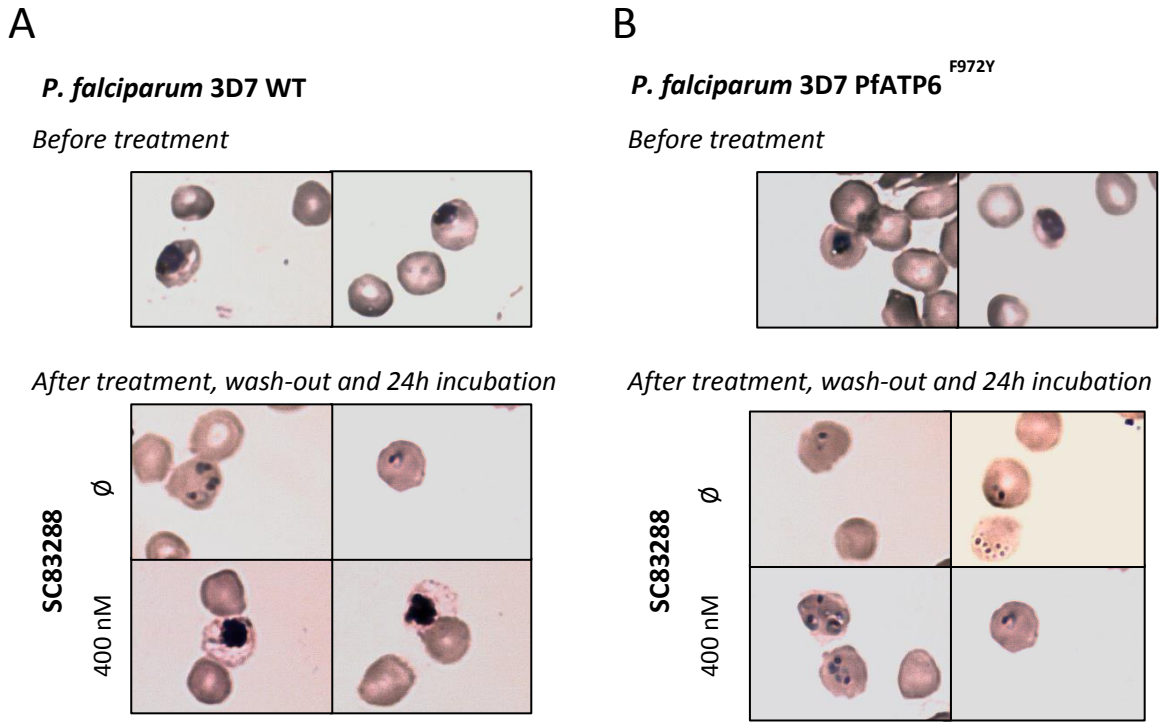

Figure 3.22: Morphological appearance of *P. falciparum* 3D7 wild-type and PfATP6 ^{F972Y} mutant after a SC83288 pulse treatment. *P. falciparum* 3D7 wild-type (WT) **(A)** or PfATP6^{F972Y} mutant **(B)** parasites were treated with 50x IC_{50} concentration of SC83288 (400 nM) for 1 hour before removal of the compound. Parasites were further incubated for 24 hours and Giemsa-stained smears were produced. WT parasites appeared as arrested trophozoites, whereas the PfATP6 ^{F972Y} mutants progressed into a new life cycle as ring stages.

However, after 1 hour of treatment, both the wild-type and the PfATP6 ^{F972Y} mutant were alive, with intact membranes, as confirmed by cFDA-SE (Figure 3.23 A and B) and MitoTracker (Figure 3.23 C and D) staining, and were metabolically active, as shown by ATP level measurements (Figure 3.24).

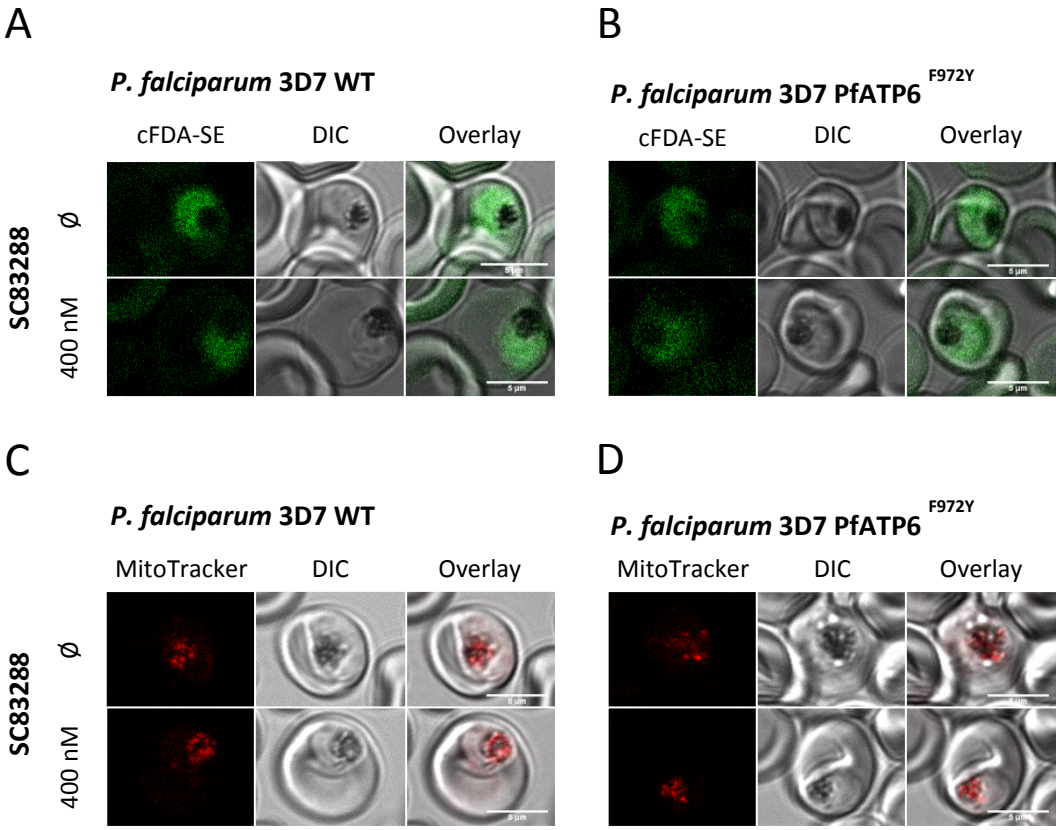

Figure 3.23: Integrity of *P. falciparum* 3D7 wild-type and PfATP6 ^{F972Y} mutant after a SC83288 pulse treatment. *P. falciparum* 3D7 wild-type (WT) **(A** and **C)** and PfATP6 ^{F972Y} mutant **(B** and **D)** parasites were treated with 50x IC_{50} concentration of SC83288 (400 nM) for 1 hour. Parasites were fixed and permeabilized and further stained either with cFDA (10 µM) **(A** and **B)** for membrane integrity or with Mitotracker (80 nM) **(C** and **D)** fluorescent dyes for 1 hour before imaging. No differences in staining pattern or intensity are noteworthy between the WT and the PfATP6 ^{F972Y} mutant. Scale bar 5 µm.

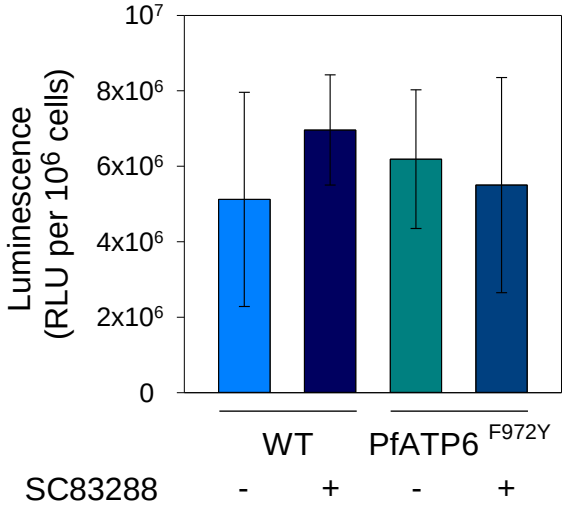

Figure 3.24: Variation in ATP levels in *P. falciparum* 3D7 wild-type and PfATP6 ^{F972Y} mutant after a SC83288 pulse treatment. *P. falciparum* 3D7 wild-type (WT) or PfATP6 ^{F972Y} mutant parasites were treated with 50x IC_{50} concentration of SC83288 (400 nM) for 1 hour. Parasites were magnetically enriched for trophozoite stages and their ATP content was determined using a luminescence-based approach (ATP Bioluminescence Assay Kit CLS II, Roche). Mean ± SD of technical duplicates.

A treatment with a concentration corresponding to 50x IC_{50} of SC83288 for 1 hour was then considered appropriate for cytosolic calcium measurement. In a similar manner as for the Dd2 strain, a calibration curve was established using free Ca^{2+} concentrations ranging from 0.6 nM to 1.2 mM in 3D7 *P. falciparum* parasites (Figure 3.25 A). A significantly lower free cytosolic calcium concentration was observed in the PfATP6 ^{F972Y} line compared to the wild-type (299 ± 35 nM versus 550 ± 31 nM, for the PfATP6 ^{F972Y} and the wild-type respectively, measured on 310 and 361 cells, Rank Sum test, p <0.001, ***) (Figure 3.25 B and Table 3.5). If the wild-type parasites displayed no difference in their calcium level when treated with SC83288 (441 ± 37 nM, measured on 310 cells, Rank Sum test, p > 0.05, n.s.), the PfATP6 ^{F972Y} mutants showed a significant increase in their calcium concentration upon SC83288 treatment (610 ± 27 nM, measured on 369 cells, Rank Sum test, p < 0.001, ***) (Figure 3.25 B and Table 3.5), reaching back the basal level.

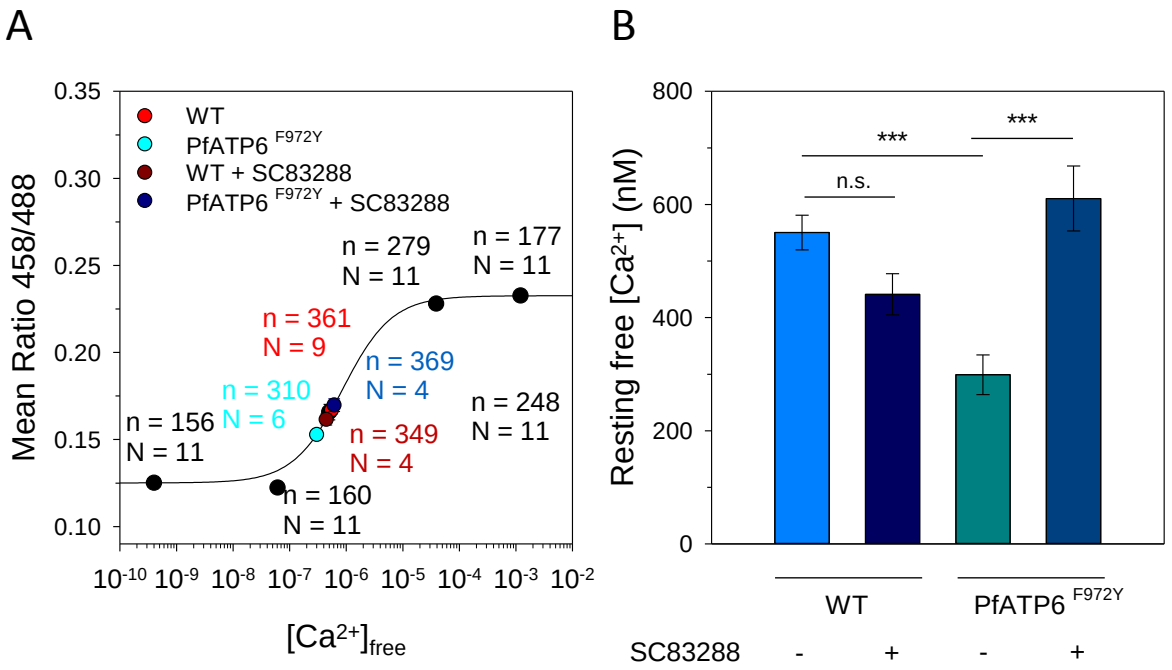

Figure 3.25: Calibration of Fura-Red-AM fluorescence and determination of apparent resting free Ca^{2+} concentration in the *P. falciparum* 3D7 wild-type and PfATP6 ^{F972Y} mutant cytoplasm. (A) Ca^{2+} equilibration curve for the steady-state Fura-Red-AM fluorescence ratio (458/488 nm) from the cytoplasm of 3D7 *P. falciparum* parasites at the young-trophozoite stage. Cells were permeabilized with the Ca^{2+} ionophore ionomycin and adjusted to the indicated free-Ca^{2+} concentrations. N corresponds to the number of independent experiments, and n to the total number of measured cells. **(B)** Mean apparent cytoplasmic resting Ca^{2+} ($[Ca^{2+}]$) concentrations in untreated or SC83288-treated parasites. Mean ± SEM of respectively 361, 310, 349 and 369 independent determinations. Rank Sum test, p < 0.001, ***.

Finally, all lines, untreated or pre-treated with SC83288, showed the expected significant increase in their cytosolic free calcium concentration in response to brief CPA exposure (Figure 3.25 and Table 3.5).

Table 3.5: Measured free cytosolic calcium concentration ($[Ca^{2+}]_{free}$] in *P. falciparum* Dd2, 3D7 wild-type and PfATP6 ^{F972Y} mutant.

Strain/Line	$[Ca^{2+}]_{free}$ (nM)			
	Untreated	SC83288 (400 nM)	CPA (30 µM)	SC83288 + CPA
3D7 WT	550 ± 31 (361)	441 ± 37 (310)	1311 ± 219 (113)	1279 ± 215 (101)
3D7 PfATP6 ^{F972Y}	299 ± 35 (349)	610 ± 27 (369)	901 ± 151 (98)	1863 ± 316 (83)
Dd2 WT	308 ± 82 (97)	-	840 ± 83 (43)	-

Mean ± SEM of (n) measured cells.

The lower cytoplasmic Ca^{2+} concentration in the PfATP6 ^{F972Y} mutant suggests a higher ATPase activity of the mutated PfATP6 compared to its wild-type variant. This hypothesis further awaits confirmation in the *S. cerevisiae* complementation model.

3.2.4. Overexpression of the PfATP6 T108, T109 variant in *P. falciparum* is altering the susceptibility to SC83288

Episomal transfection was used to overexpress the wild-type variant of PfATP6 (ATP6 WT) (Figure 3.26 A) in the Dd2 *P. falciparum* parasite, and the PfATP6 A108T, A109T variant (ATP6 A108T, A109T) (Figure 3.26 B) as an alternative to CRISPR-Cas9 genome editing. The respective coding sequences of PfATP6 were C-terminally fused to a hemagglutinin (HA) tag, and episomaly expressed under the control of the PFC0005w promoter [211].

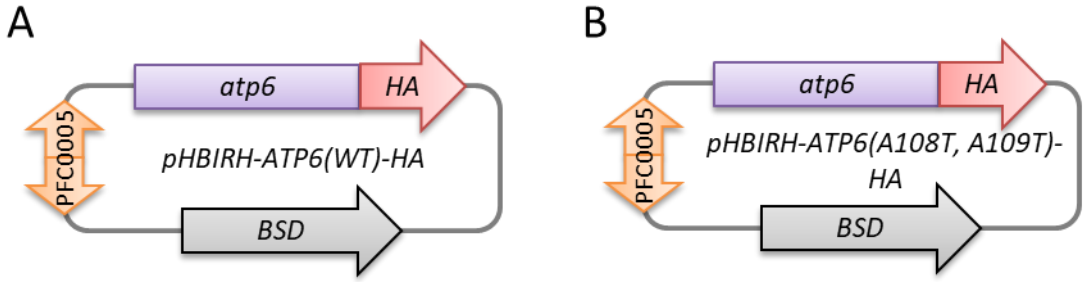

Figure 3.26: PfATP6 variants overexpression strategy. The plasmid pHBIRH encodes the *S. cerevisiae* codon-optimized *pfatp6* sequence (purple), wild-type **(A)** or bearing the mutations coding for the A108T, A109T **(B)**, fused with a hemagglutinin tag (HA, red) on the C-terminal end. The selection marker of the plasmid is the blasticidin-S-deaminase gene (BSD, grey). Their expression is regulated by a bi-directional *P. falciparum* promoter (intron of PFC0005w). Both plasmids are transfected in Dd2 *P. falciparum* parasites by electroporation.

After transfection by electroporation, the parasites were selected with concentrations of 2.5 µg/ml (mild selection) or 15 µg/ml (high selection) of blasticidin. The overexpression of PfATP6 was confirmed both on the transcript level by RT-qPCT (relative transcript levels to wild-type 1.01 ± 0.003, 3.51 ± 0.20 and 1.60 ± 0.19 for *P. falciparum* Dd2 wild-type (WT) or transfected with the pHBIRH-ATP(WT)-HA or pHBIRH-ATP6(A108T, A109T)-HA plasmids, respectively) (Figure 3.27 A) and on the protein level by western blot analysis, by detecting the C-terminal HA-tag (Figure 3.27 B).

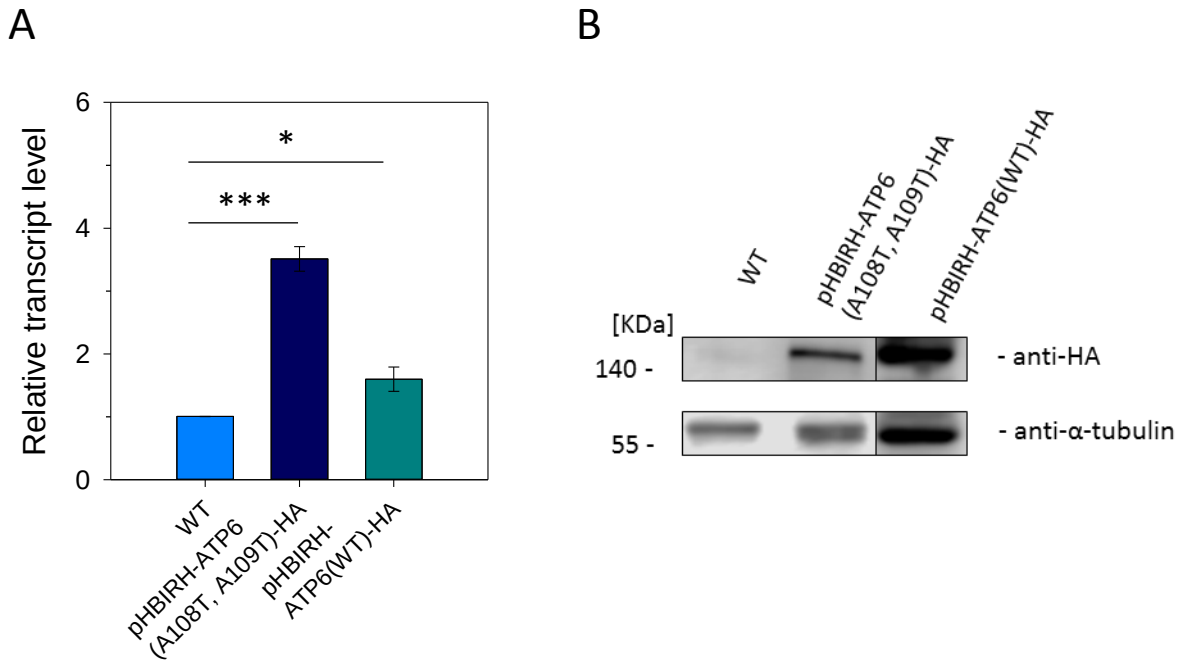

Figure 3.27: Episomal overexpression of PfATP6 variants in Dd2 *P. falciparum* parasites. (A) Transcript levels of *pfatp6*. Levels of *pfatp6* transcripts measured by RT-qPCR in wild-type (WT) parasites or transfected with the pHBIRH-ATP6(A108T, A109T)-HA or pHBIRH-ATP(WT)-HA plasmids. Mean ± SEM of 3 independent determinations (3 independent mRNA isolations on late-stage parasites), normalized to the wild-type (WT). Tubulin was used as a housekeeping gene for calibration. **(B)** Western blot analysis of the Dd2 wild-type and Dd2 ATP6-overexpressing parasites. Lysates corresponding to the Dd2 parasites wild-type (WT, lane 1), or transfected with the pHBIRH-ATP6(A108T, A109T)-HA (lane 2) or pHBIRH-ATP6(WT)-HA (lane 3) plasmids. The signal at 140 KDa corresponds to the PfATP6 variant, and the one at 55 KDa to the α-tubulin, used as a loading control.

The Dd2 pHBIRH-ATP6(A108T, A109T)-HA parasites showed a decrease in their susceptibility to SC83288, displaying a four-fold increase in their IC_{50} value compared to the wild-type parasites (3.1 ± 0.2 nM and 12.5 ± 1.0 nM, respectively for parental and the overexpressing parasite lines, Student´s t-test, $p < 0.001$, ***) (Figure 3.28 A and Table 3.6). The overexpression of the wild-type PfATP6 did not lead to such an increase (3.1 ± 0.2 nM and 3.2 ± 0.2 nM, respectively for the parental and the overexpressing parasite lines, Student´s t-test, $p > 0.05$, n.s.) (Figure 3.28 B and Table 3.6).

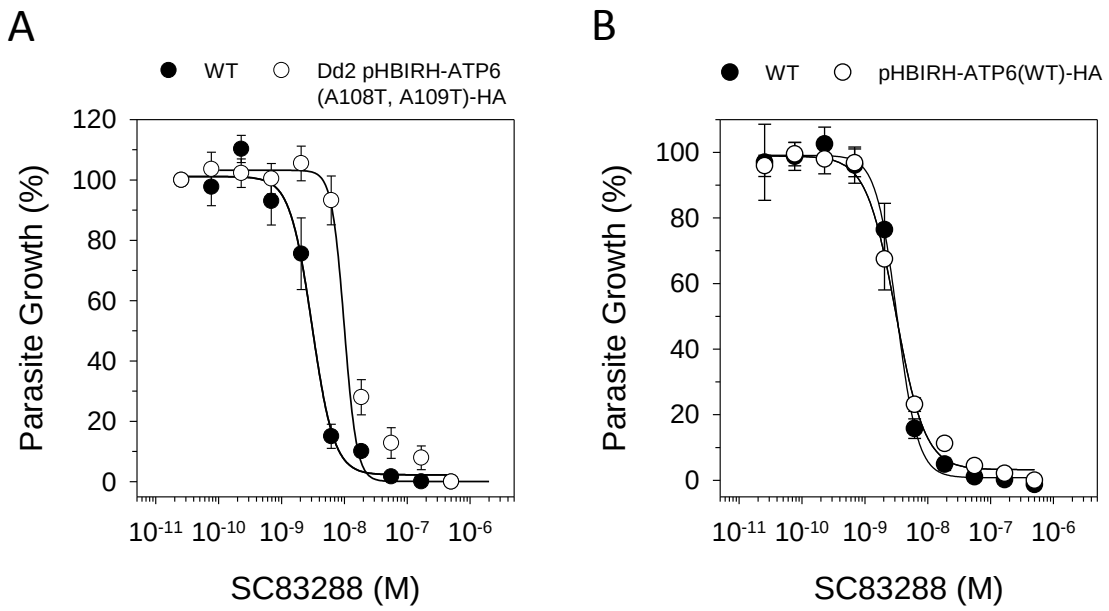

Figure 3.28: Susceptibility of the Dd2 wild-type and PfATP6-overexpressing Dd2 *P. falciparum* parasites to SC83288. Growth inhibition assay by SC83288 for the wild-type (WT) and Dd2 *P. falciparum* parasites overexpressing the T108, T109 variant of PfATP6 **(A)** or the wild-type variant **(B)**. Mean ± SEM of 11 to 13 independent determinations.

The susceptibility to chloroquine was not affected by overexpression of PfATP6 (IC_{50} values of 96 ± 2.0 nM, 110 ± 1.0 nM and 99.0 ± 0.5 nM, for the wild-type and the mutants, respectively, Student's t-test, $p > 0.05$, n.s.) (Table 3.6).

Table 3.6: Susceptibility, expressed as IC_{50} values, of the Dd2 WT, Dd2 pHBIRH-ATP6(WT)-HA and Dd2 pHBIRH-ATP6(A108T,A109T)-HA parasites to SC83288 and chloroquine.

Line	IC_{50} (nM)	
	SC83288	Chloroquine
Dd2 WT	3.1 ± 0.2	96 ± 2.0
Dd2 pHBIRH-ATP6(WT)-HA	3.2 ± 0.2	110 ± 1.0
Dd2 pHBIRH-ATP6(A108T,A109T)-HA	12.5 ± 1.0	99 ± 0.5

Mean ± SEM of 11 to 13 independent determinations.

3.2.5. The *pfatp6* amplified locus in Dd2^{SC83288} *P. falciparum* does not carry genes coding for proteins involved in the resistance mechanism to the SC-lead compounds

The parasites selected for SC83288 resistance consistently showed an amplification on chromosome 1. Even though the duplications were of different nature, the four sequenced clones duplicated the same six genes [189]. Three of those are annotated to encode for conserved Plasmodium proteins of unknown function (Pf3D7_0105800, Pf3D7_0106000 and Pf3D7_0106200), one for a putative DNA binding protein (Pf3D7_0105900), another one for a putative V-type proton ATPase subunit C (Pf3D7_0106100), and the last one for PfATP6 (Pf3D7_0106300). The increase in transcript levels of these six genes in the SC83288 selected clones was assessed by qPCR (Figure 3.29 and Table 3.7).

A

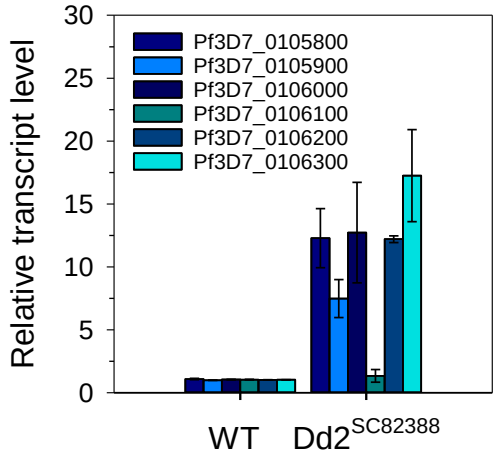

B

Gene	Relative transcript level	
	Dd2 WT	Dd2^{SC83288}
Pf3D7_0105800	1.09 ± 0.06	12.3 ± 2.3
Pf3D7_0105900	1.00 ± 0.01	7.49 ± 1.5
Pf3D7_0106000	1.05 ± 0.02	12.7 ± 3.9
Pf3D7_0106100	1.05 ± 0.02	1.35 ± 0.5
Pf3D7_0106200	1.03 ± 0.01	12.2 ± 0.3
Pf3D7_0106300	1.04 ± 0.01	17.3 ± 3.7

Figure 3.29: Transcript levels of the genes in the amplified DNA locus identified in the SC83288-resistant *in vitro* generated Dd2 *P. falciparum* as graphical (A) or numerical (B) form. Levels of Pf3D7_0105800, Pf3D7_0105900, Pf3D7_0106000, Pf3D7_0106100, Pf3D7_0106200 and Pf3D7_0106300 transcripts, measured by RT-qPCR in *P. falciparum* Dd2^{SC83288}. Mean ± SEM of 4 independent determinations (3 independent mRNA isolations on late-stage parasites), normalized to the parental Dd2 line (WT). Tubulin was used as a housekeeping gene for calibration.

The coding sequences of Pf3D7_0105800, Pf3D7_0105900, Pf3D7_0106000, Pf3D7_0106100 and Pf3D7_0106200 were amplified from a wild-type *P. falciparum* Dd2 strain, and cloned in the pARL vector for overexpression and fused with an HA-tag, each protein encoded by these genes being investigated as potential target or their involvement in a resistance mechanism. After confirmation of the overexpression of the proteins by Western blot (Figure 3.30 A), the susceptibility to SC81458 and SC83288 was assessed (Figure 3.30

B). No significant difference in their SC-lead compounds responsiveness was observed upon the episomal overexpression of the various proteins (F-test, p > 0.05, n.s.).

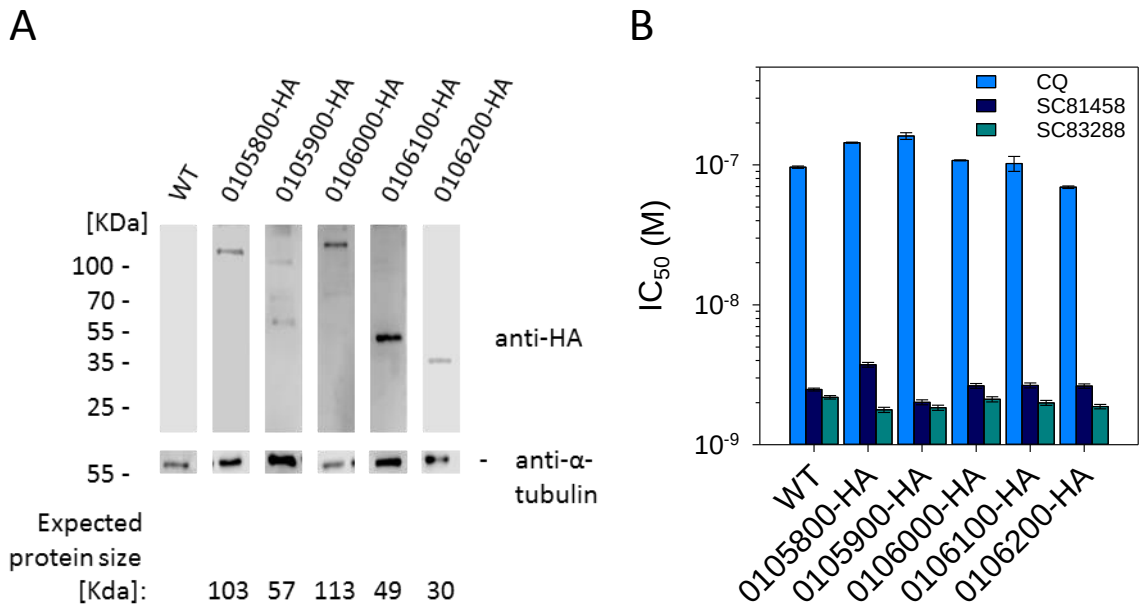

Figure 3.30: The overexpression of the amplified genes did not affect the responsiveness to the SC-lead compounds. (A) Overexpression confirmation by western blot analysis of the Dd2 wild-type and Dd2 pARL-gene-HA *P. falciparum* parasites. Lysates corresponding to the Dd2 parasites wild-type (WT, lane 1), Dd2 pARL-0105800-HA (lane 2, ≈ 103 KDa), Dd2 pARL-0105900-HA (lane 3, ≈ 57 KDa), Dd2 pARL-0106000-HA (lane 4, ≈ 113 KDa), Dd2 pARL-0106100-HA (lane 5, ≈ 49 KDa), Dd2 pARL-0106200-HA (lane 6, ≈ 30 KDa). The signal at 55 KDa corresponds to the α-tubulin, used as a loading control. **(B)** Susceptibility of the Dd2 wild-type and Dd2 pARL-*gene*-HA *P. falciparum* parasites to SC81548, SC83288 and chloroquine. IC_{50} values obtained from the growth inhibition assays by SC83288, SC81458 or chloroquine (CQ) for the wild-type (WT) and the parasites overexpressing the Pf3D7_0105800, Pf3D7_0105900, Pf3D7_0106000, Pf3D7_0106100 and Pf3D7_0106200 genes. Mean ± SEM of 6 independent determinations, F-test, p > 0.05, n.s.

The susceptibility to chloroquine was not affected by overexpression of any of these genes (Figure 3.30 B) (F-test, p > 0.05, n.s.).

4. Discussion

4.1. Characterization of SC83288 *in vitro* antiplasmodial activity as a candidate for clinical development

Despite the substantial progress regarding the decrease of case incidence over the last two decades, malaria continues to impose a heavy burden upon mankind. Not only the death toll remains concerning, but the loss of development potential for malaria-endemic countries and the impact on their economic growth and health-care systems are to be taken into account [212]. Fortunately, the past decade has seen a renaissance on the research and development for antimalarial medicine, with a particular focus on finding new chemotypes. As a result, the antimalarial drug portfolio rapidly transformed, and now contains more than a dozen of new chemical entities in (pre)clinical development. Nonetheless, however optimistic this pipeline appears, there is still a dire need for new antimalarial chemical agents, particularly regarding the alarming development of resistance to marketed therapies.

Here the *in vitro* antiplasmodial activity of two lead compounds arising from a medicinal chemistry program [189] was characterized, specifically the second lead compound SC83288, considered as a clinical development candidate for the treatment of severe malaria.

Both SC81458 and SC83288 displayed advantageous parasitological properties, according to the MMV´s Target Compound Profiles [213], such as their steep growth inhibition curves [189] and low nanomolar IC_{50}, IC_{90} and IC_{99} values. They fall in the range of both the old and current gold standards, i.e. respectively quinine and chloroquine (with *in vitro* IC_{50} values in the moderate nanomolar range, depending of the sensitive lab strains) and artemisinin. Even though a low *in vitro* IC_{50} value does not directly translate into a low *in vivo* effective dose, it is already a first discriminative step towards the selection of a compound for preclinical development.

A previous study reported a stage specificity of SC81458 and SC83288 on asexual blood stages [189]. In a 6 hours exposure assay, the SC-lead compounds showed their higher activity against trophozoites stages, with IC_{50} values in the moderate nanomolar range. A slightly lower activity was observed in schizonts, with two-fold increased IC_{50} values compared to trophozoite stages, and the activity on ring stages was limited, with IC_{50} values in the micromolar range [189]. These observations were confirmed by following the morphology and the DNA content of the parasites when treated with SC83288 over their life cycle. Ring stage parasites did not appear to be affected by SC83288, and were able to

develop into morphologically healthy young trophozoites. These ones were however not able to progress further into schizogony, underlining the potent action of SC83288 against *P. falciparum* trophozoite stages. When SC83288 was applied on young trophozoites (i.e. about 24 hours p.i.), the parasites were still able to enter schizogony, but to a limited extend as they appeared to be able to undergo only one round of DNA replication. This delayed antiplasmodial effect reflects the 5 hours lag-phase of the SC-lead compounds observed during the recrudescence assay. Similarly, the later in their life cycle the parasites were exposed to SC83288, the more DNA replication cycles they were able to undertake before arresting. Indeed, whether partially or fully formed, the SC83288-treated schizonts did not appear to be able to burst and release merozoites, suggesting a toxic activity of SC83288 even on late *P. falciparum* stages.

While the SC-lead compounds are primarily active against asexual blood stages, they also have been shown to target early stage gametocytes (stages I to III), showing IC_{50} values in the moderate nanomolar range. They were however proven to be devoid of activity against late stage gametocytes (stages IV and V), suggesting no potential for the blocking of the parasite´s transmission [189]. The SC-lead compounds could therefore only be considered as chemotherapeutic agents, and not in a prophylactic prospect. Such a goal could however be achieved by combining SC83288 with a gametocidal activity, such as the 8-aminoquinoline primaquine [92].

A quality feature emphasized by the MMV for an antimalarial compound is the PRR after a single dose, i.e. the speed of action of a molecule [213]. The speed of action takes a particular importance in the context of severe malaria, where the rapid clearance of sequestered parasites from the patient´s microvasculature can make the difference between survival and death. Furthermore, fast-acting antimalarial drugs are now favored for their ability to reduce the risk of resistant parasites arising within the patient. Here, the speed of action profile of SC832288 was characterized using three different approaches: a recrudescence assay [198], a relative speed assay [197] and a re-invasion assay [199]. The recrudescence assay revealed a profile for the SC-lead compounds closer to the fast-acting artemisinin than to the slow-acting atovaquone, although they showed a slightly longer clearance time and a lower PRR than artemisinin. Nonetheless a logPRR ≥ 3, obtained for both SC81458 and SC83288, is considered a favorable property of an antimalarial drug candidate [214]. The results of the somewhat controversial recrudescence assay [198,199] were confirmed by relative speed and re-invasion assays, consistently marking SC81458 and SC83288 as fast-acting antimalarial compounds. These *in vitro* observations were confirmed

in vivo by our collaborators, in a humanized SCID/NSG mouse model system, where a similar logPRR was measured and an intraperitoneal injection of a minimum dose of 2.5 mg/kg of SC83288 was sufficient to reduce the parasite load by more than 99.9% in 48 hours [189].

The *in vitro* or in *vivo* pharmacokinetic parameters are obviously not the only crucial aspects to be considered when developing an antimalarial compound. As for any exogenous molecule, the beneficial versus detrimental effects have to be carefully weighed. For instance, the two standards of care for severe malaria, artesunate and quinine, are associated with various side-effects, such as injection-site pathology [86] and cinchonism [87,88] in the case of intravenous quinine treatment, or a delayed hemolysis after artesunate treatment [215–217]. Preliminary results of the SC83288 safety and toxicological studies on mice and dogs, in the frame of the Non-Clinical Assessment for First-in-Human Study, are promising in this regard (unpublished data). Profiling the side-effects on human early-on during the drug development process would be ideal; unfortunately, possible adverse effects are usually reported during the phase IV of clinical trials and during the post-marketing surveillance studies. Developing compounds with independent mode(s) of action from the drugs with known side-effects might decrease this risk. In line with this, this study revealed no interaction between artemisinin and SC81458 or SC83288, suggesting distinct modes of action. This observation was supported by both the graphical and arithmetical analysis of an isobolomic assay, with an isobologram following a linear trend, and a mean sum of fractional 50% inhibitory concentration ($\sum FIC_{50}$) falling into the commonly admitted range of an indifferent interaction [206]. Such an assay may however overlook possible similar modes of action, particularly if the two tested compounds are either competitive inhibitors or mutually exclusive non-competitive inhibitors. A competition of both compounds for the same binding site, independently of an interference with the binding site of the endogenous substrate, would not be noticed during an isobolomic assay. However, in the case of artemisinin and SC81458 or SC83288, such a competition is considered highly unlikely. Both the chemical and structural differences between the SC-lead compounds and artemisinin (Figure 4.1), and the wide range of proposed modes of action and molecular targets proposed for artemisinin [116] strongly argue against this possibility.

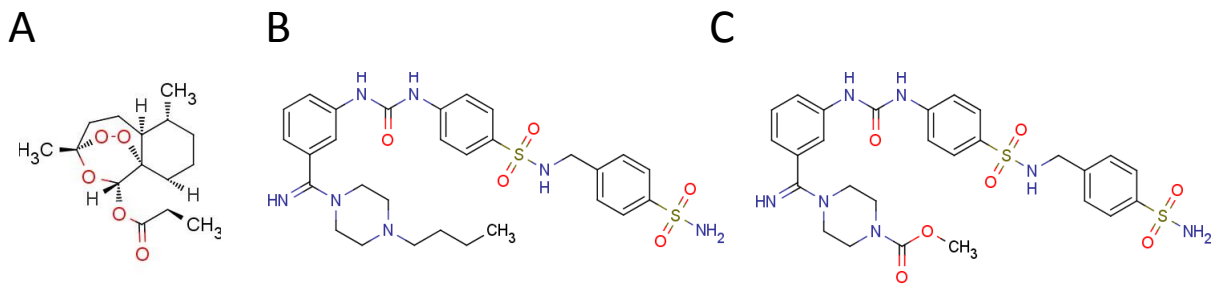

Figure 4.1: Chemical structures of artemisinin (A), and the SC-lead compounds SC81458 (B) and SC83288 (C) for comparison purpose.

The distinct mode of action of the SC-lead compounds and artemisinin and its derivatives was further confirmed when combining SC83288 with artesunate, which did not alter the artesunate clearance time in the re-invasion assay.

Drug resistance is another critical aspect of the MMV´s antimalarial candidate profiles [213]. Resistance to all past and current marketed antimalarial drugs has been identified to various degrees [218]. Therefore, novel drugs need to be able to overcome these existing resistance mechanisms. Along this line, resistance to either SC81458 or SC83288 did not affect the susceptibility of *P. falciparum* to other antimalarial drugs, including artemisinins, chloroquine, mefloquine and the folate antagonists. It is important to mention that the case of sensitivity to artemisinin required both a growth inhibition assay, as well as a ring survival assay. The RSA takes into account the antiplasmodial activity of artemisinins against the early blood stages [116,161], that can easily be overlooked in the standardized 72 hours growth inhibition assay. In both these assays, the SC-lead compound resistant parasite strains proved to be fully sensitive to artemisinins. Conversely, the activity of SC81458 and SC83288 against various *P. falciparum* lab strains was previously established, including parasites strains resistant to quinoline, quinoline-like and antifolate antimalarials [189]. This analysis was further extended in this study to include the *in vitro* engineered *P. falciparum* that carry the C580Y mutation in the kelch 13 protein associated with reduced artemisinin responsiveness. These experiments profiling the SC-lead compounds against artemisinins suggest that both SC8148 and SC83288 were able to break established resistance in *P. falciparum* and maintain their full activity independently of the parasite´s resistance status.

In light of these preclinical observations, and in the context of a dire need for artemisinins alternatives in areas where artemisinin-resistance is becoming a growing concern, the SC-lead compounds, in particular SC83288, might be considered as apotential alternative chemotherapeutic option for severe malaria. However, such a conclusion is a bit premature and still awaits the results of clinical studies demonstrating the safety and efficacy of SC83288 in humans.

4.2. PfTAP6 is a component of resistance to SC83288

Novel antimalarial compounds identified by whole cell-based assays, such as SC81458 and SC83288, inherently have poorly defined modes of action. While understanding the mode of action or the mechanisms of resistance of new potential antimalarial drugs is not critical for their development, it can for instance become a paramount concern in case of failure during clinical trials. In this instance, knowledge of the mode of action and possibly of the molecular target(s) may help guide further development of the compounds. Similarly, understanding the mechanisms underlying the resistance to the compounds, some of those possibly involving their molecular targets, could on the one hand allow tracking the selection and spread of resistance by monitoring patients for the emergence of drug-resistant parasites and on the other hand help the design of more potent antimalarials.

Previously, proteins involved in drug resistance could be identified by mating drug-sensitive and drug-resistant parasites and mapping the sensitivity in their recombinant progeny. Although this approach successfully allowed identifying PfCRT as a principal actor of CQ resistance [219], it remains an extremely intensive and time consuming process, and nowadays made obsolete due to the rapidity of whole genome sequencing. Over the last decades, this method has been replaced with the *in vitro* selection of resistant parasites. The selected resultant clones can then be submitted to either genome scanning or whole genome sequencing to identify mutations, i.e. SNPs, copy number variations and small insertions or deletions, conferring resistance [220]. This method successfully identified nonsynonymous SNPs resulting in resistance in genes coding for the molecular targets of various marketed antimalarial drugs, particularly in the drug-binding pockets of PfDHFR [138], PfDHPS [221] and PfCyt b1 [222,223]. It is however crucial to bear in mind that the detected change in the genomes of the resistant parasites directly reveals only the mechanisms of resistance. Some of these acquired genetic changes, as illustrated by the role or PfCRT in resistance to CQ [144–148], or of PfMDR1 in the resistance to QN, CQ and halofantrine [164], are not involved in the mode of action of the drugs, but rather in biological processes to reduce the

concentration of the compounds at their site of action. The role of the selected proteins of interest must therefore be further confirmed as targets or components of resistance by other molecular, chemical and/or modeling approaches. Recently, PfATP4 was confirmed as the molecular target of the promising new antimalarial class spiroindolones [181,224], after its identification in such a comparative genomic approach [179]. Similar successes in directly identifying the molecular target of antimalarial compounds can further be illustrated by the benzoxaborole AN3661 targeting the pre-mRNA processing factor (PfCPSF3) [225] or the aminopyridine MMV390048 as an inhibitor of the phosphatidylinositol 4-kinase PfI4K [226].

In the case of SC83288, the identification of the molecular target is not as straightforward. Comparative genomics of the SC-lead compounds selected Dd2 *P. falciparum* parasites with their parental line identified the Ca^{2+} ATPase pump PfATP6 as a protein of interest regarding their mode of action [189]. The finding of both nonsynonymous SNPs and duplications of the *pfatp6* gene locus led us to consider PfATP6 as a direct molecular target of the SC-lead compounds. The cell permeable Ca^{2+} indicator Fluo-4-AM used in a live confocal laser-scanning microscopy set-up allows to directly follow the fluctuation in the intracytosolic calcium concentration. However, the *P. falciparum* strain loaded with Fluo-4-AM has to be carefully considered for this assay, as certain polymorphisms in the multi-drug resistance protein 1 (PfMDR1) modulate its affinity to Fluo-4-AM, leading to an accumulation of the dye in the parasite's DV [162]. Such strains, i.e. Dd2, K1 and FCB, cannot reliably be used to quantitively measure intracytosolic Ca^{2+} variations. The HB3 strain however, shows a uniform distribution of Fluo-4-AM between the parasite's cytosol and it's DV, and was therefore used for this assay. Under these experimental conditions, no relative increase in the intracellular calcium level was observed upon addition of the SC-lead compounds, as it is clearly observed when the parasites are treated with established PfATP6 inhibitors such as thapsigargin or CPA [202]. The absence of direct PfATP6 inhibition by the SC-lead compounds was further confirmed using a yeast complementation assay. Yeast complementation studies are simple approaches to assess the *in vitro* inhibition potential of chemical compounds on proteins otherwise difficult to express in heterologous systems. This generally implies replacing a yeast's gene with the *Plasmodium* homologous gene either by allelic exchange or by episomal overexpression [220]. The *S. cerevisiae* model recently developed by Pulcini et al. is knocked-out of various genes encoding proteins essential to Ca^{2+} homeostasis. The yeasts are therefore not able to grow when stressed with high ambient calcium concentrations. As growth rescue relies on episomal overexpression of PfATP6, the yeasts growth directly correlates with PfATP6 inhibition and therefore represents and ideal system to study the effect of small molecules on PfATP6 activity [70]. The growth of these complemented *S. cerevisiae* was however proven to be unaffected by the addition of

either SC81458 or SC83288, while CPA induced the expected concentration-dependent growth inhibition. Both these assays strongly argue against the rapid and direct inhibition of PfATP6 by the SC-lead compounds, excluding PfATP6 as a primary molecular target.

PfATP6 was nonetheless kept under investigation as a protein involved in a resistance mechanism, if not as a molecular target. Genome editing using the CRISPR/Cas9 approach [78] and episomal overexpression allowed the genomic variations observed in the Dd2 ^{SC81458} and Dd2 ^{SC83288} parasites to be introduced into either their parental line or the 3D7 wild-type parasites. The CRIPSR/Cas9-mediated genome editing was carried out in the 3D7 strain. Indeed, the design of the sgRNA was based on this strain's genome and all our transfections in the Dd2 strain were unsuccessful, suggesting off-target effects of the RNA guide in Dd2 that were not predicted from the 3D7 genome. The F972Y substitution in PfATP6, previously identified in the Dd2 ^{SC81458} line, was successfully introduced in 3D7 and led to an approximate 1000-fold decrease in the sensitivity to the SC-lead compounds. The overexpression of the T108, T109 PfATP6 variant, identified in the Dd2 ^{SC83288} line, similarly induced a decrease in the parasite's susceptibility to SC83288, moderate yet significantly marked. However, the overexpression of the wild-type PfATP6 was insufficient to affect the susceptibility of the parasites. It is worth to note that the multiple attempts to introduce the SNPs leading to the A108T, A109T substitutions on PfATP6 using the CRISPR/Cas9 system were unsuccessful. This further confirmed the vital role of PfATP6 in Ca^{2+} homeostasis, as this double substitution might alter the PfATP6 essential function in a detrimental fashion for the parasite. This damaging effect was not observed in the Dd2 ^{SC83288} line, as the SNPs were identified on the extra copy of *pfatp6*, leaving a residual regular activity of the non-mutated PfATP6. The hypothesized abnormal activity of the mutant PfATP6 might furthermore have been compensated by other mutations, either on *pfatp6* specifically or on other genomic loci, that might not have been consistently detected in the comparative genomic analysis. These hypotheses are further supported by the fact that the selection of parasites with high pHBIRH-ATP(WT)-HA plasmid copy number was straightforward, hence non-detrimental, whereas it was only possible to select parasites with low copy number of the pHBIRH-ATP6(A108T, A109T)-HA plasmid, suggesting a toxic effect of a too important overexpression of this variant relative to the wild-type one.

These various genomic modifications confirmed the correlation between PfATP6 and the resistance to the SC-lead compounds. To further understand the molecular details of the role of PfATP6 in a resistance mechanism to the SC-lead compounds, we used the genetically engineered 3D7 PfATP6 ^{F972Y} line generated using the CRISPR/Cas9 approach. Compared

to the Dd2 line overexpressing the T108, T109 PfATP6 variant, it had the advantage to be stable and did not require a constant selection.

Drug-resistance conferring mutations are generally associated with fitness costs, leading to the attrition of the mutant parasites upon drug pressure removal, allowing the reemergence of the fitter wild-type ones [227]. This general observation was confirmed in the case of the 3D7 PfATP6 ^{F972Y} mutants during an *in vitro* co-culture competition assay with its parental 3D7 wild-type strain. The proportions of the wild-type and mutated PfATP6 alleles were determined by pyrosequencing. Pyrosequencing is a fast technique based on sequencing-by-synthesis with real-time read-out and is highly suitable for sequencing short stretches of DNA [228]. Its high reliability, particularly for SNP genotyping [209,229], is based on a combination of four enzymes eventually leading to the quantitative detection of pyrophosphate (PPi) release during DNA synthesis [230]. The four deoxynucleotide triphosphates (dNTPs) are sequentially added to the reaction mixture containing the desired DNA locus previously amplified by PCR. Each nucleotide incorporation by the DNA polymerase is directly followed by the release of PPi in a quantity equimolar to the amount of incorporated nucleotides. The PPi is subsequently quantitatively converted into ATP by the ATP sulfurylase. The luciferase, driven by the generated ATP, catalyzes the conversion of luciferin into the visible light-producing oxyluciferin. The detected light signal is proportional to the amount of ATP. The last enzyme, the apyrase, continuously degrades ATP and the non-incorporated dNTPs from the reaction mixture, preventing signal overlaps and allowing a precise quantification of the proportion of each allele present in the amplified DNA locus. This approach clearly revealed a fitness cost of the 3D7 PfATP6 ^{F972Y} mutant, as its proportion gradually decreased over the 20 analyzed life cycles of the parasites, suggesting a growth deficiency compared to parental line. Extrapolation predicted the complete attrition of the mutants after approximately 29 cycles. It is difficult to estimate whether these *in vitro* observations could directly be translated to the field, as they were obtained in absence of drug pressure. Indeed, a prolonged drug exposure can provide the resistant parasite the opportunity to acquire additional mutations, either within the primary resistance factor or within secondary factors. The new mutations can potentially compensate for the initial fitness cost, and these new mutants can further compete with and eventually take over the wild-type ones, even in a drug-free environment [210].

Considering the crucial role of PfATP6 in Ca^{2+} homeostasis, a link between the observed fitness cost in the 3D7 PfATP6 ^{F972Y} mutants and abnormal intracellular Ca^{2+} levels was speculated. In order to measure the intracellular Ca^{2+} concentration in a quantitative manner, the Fura-Red-AM indicator was used. Fura-Red is a ratiometric dye widely used for absolute calcium quantification, and offers several advantages over other Ca^{2+}-sensitive

fluorochromes such as Fluo-4 [202]. Unlike Fluo-4, Fura-Red can be used for ratiometric measurement and therefore the intensity of the measured signal does not depend on dye loading efficiency and/or partitioning, which would not allow a direct absolute quantification of Ca^{2+} concentration [202]. After a calibration including both the ionophore ionomycin and the calcium chelator EGTA to control the free Ca^{2+} concentrations, it was possible to quantitatively determine the intracytosolic free Ca^{2+} concentrations in various parasites lines under different conditions. As previously measured in a relative manner, the treatment of 3D7 *P. falciparum* parasites with SC83288 did not lead to a notable change in their free Ca^{2+} concentrations, refuting again a direct inhibition of PfATP6 by SC83288. Interestingly, the 3D7 PfATP6^{F972Y} mutant showed a significantly lower cytosolic free Ca^{2+} concentration, almost diminished by half compared to the parental line. This would suggest a higher activity of PfATP6 ^{F972Y}, pumping Ca^{2+} into the ER more efficiently than the wild-type variant. Such a drastic change in the ATPase activity could be explained by the introduction of a tyrosine residue at the position 972 and/or its potential phosphorylation, although this remains to be properly demonstrated by mass spectrometric analysis. It is however difficult to affirm that the lower intracellular Ca^{2+} concentration in the mutant is exclusively caused by the abnormal activity of the PfATP6 ^{F972Y} variant. Preliminary metabolomics analysis of the mutant line revealed a not significant yet marked decrease in the concentration of several precursors of inositol-1,4,5-triphosphate (IP_3). In eukaryotic cells, and presumably in the *P. falciparum* wild type parasite, Ca^{2+} effluxes from the ER mainly through the opening of IP_3-gated Ca^{2+} channels. These channels are activated upon binding of the IP_3 produced by the dissociation of the phosphatidylinositol-4,5-bisphosphate (PIP_2) into IP_3 and diacylglycerol (DAG) catalyzed by the phosphoinositide phospholipase C (PLC) (Figure 4.2 A). In the 3D7 PfATP6^{F972Y} mutant, the possible decrease in IP_3 concentration compared to the parental strain may contribute to the low cytosolic Ca^{2+} concentration, as the reduced amount of IP_3 may not be sufficient to trigger the opening of enough IP_3-gated Ca^{2+} channels to allow a proper efflux of Ca^{2+} into the cytosol (Figure 4.2 B). This hypothesis is however to be taken with caution, as pharmacological approaches have suggested the presence of a IP_3 canonical pathway in *P. falciparum* [21], although it still remains unidentified in its genome. Moreover, it is impossible to exclude regulatory processes involving the release of Ca^{2+} from the other storage compartments, such the mitochondrion, the acidocalcisomes or the parasitophorous vacuole. The difficulty mainly relies in our present lack of a full understanding of the mechanisms of Ca^{2+} homeostasis in *P. falciparum* and the involved proteins [21].

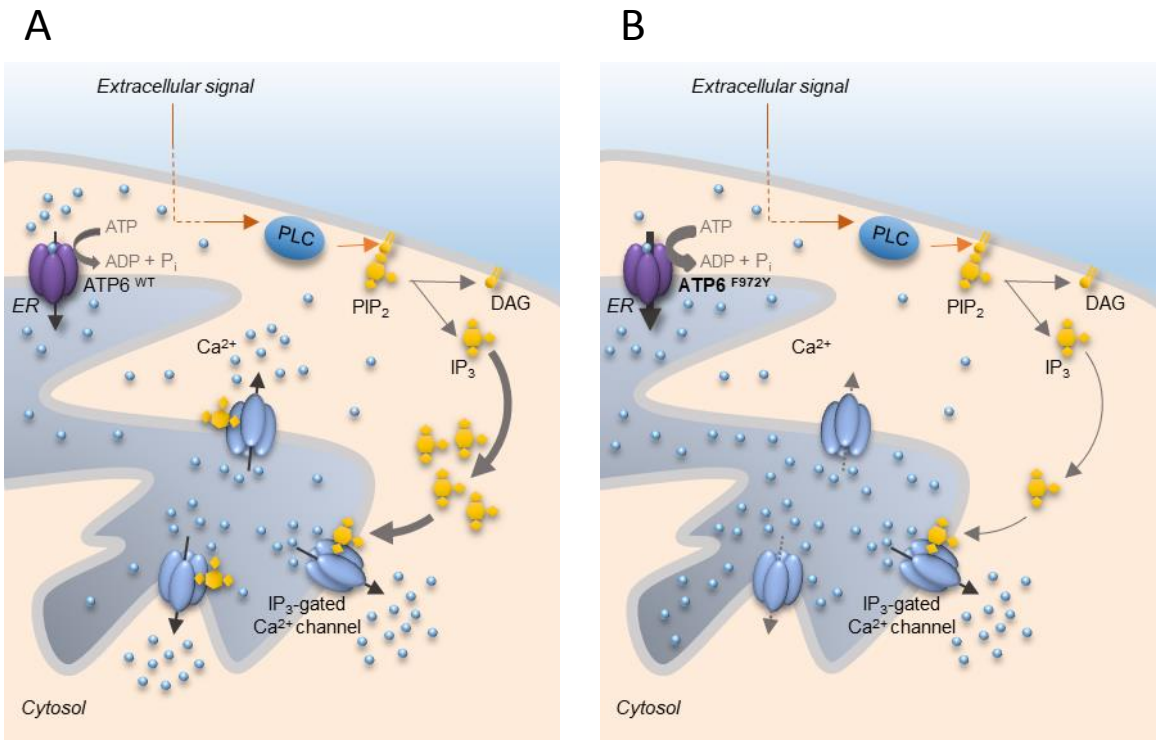

Figure 4.2: Hypothetical partial model of Ca^{2+} regulation in wild-type *P. falciparum* and the PfATP6 ^{F972Y} mutant. (**A**) In the wild type parasite, IP_3, along with DAG, is produced by the dissociation of PIP_2 catalyzed by PLC. The opening of the Ca^{2+} channels localized in the ER membrane is triggered by the binding of IP_3 allowing the efflux of Ca^{2+} from the ER into the cytosol. The PfATP6 actively pumps the cytosolic Ca^{2+} into the ER for storage. (**B**) In the PfATP6 ^{F972Y} mutant, the decreased amount of IP_3 does not allow the opening of enough ER Ca^{2+} channels for an efficient release of Ca^{2+} into the cytosol. This low intracytosolic Ca^{2+} concentration is accentuated by the higher activity of the mutant PfATP6 ^{F972Y}. ER, endoplasmic reticulum; PLC, phospholipase C; IP_3, inositol-1,4,5-triphosphate; PIP_2, phosphatidylinositol-4,5-bisphosphate; DAG, diacylglycerol.

The analysis of the PfATP6 ^{F972Y} variant in the *S. cerevisiae* complementation model will confirm the hypothesis of a higher ATPase activity (Figure 4.2 B) by placing PfATP6^{F972Y} out of its biological context and excluding other actors of Ca^{2+} homeostasis that could possibly act downstream or in parallel of PfATP6, and influence the Ca^{2+} resting concentration.

Surprisingly, the treatment of the 3D7 PfATP6 ^{F972Y} mutant with SC83288 restored the resting free Ca^{2+} concentration to its basal level, i.e. to a concentration similar as the one measured in the parental strain, even though the concentration of SC83288 used on the mutant parasites was shown not to affect the growth in the standard 72 hours growth inhibition assay. Here again, our lack of defined Ca^{2+} influx and efflux processes make it difficult to speculate on the molecular mechanisms taking place in the mutant in presence of SC83288, and deeper calcium signaling studies would be necessary.

All our observations confirmed the role of PfATP6 as a component of resistance. Whether it is a primary factor or a secondary one is a more complex issue and remains an unanswered question. Up to date, efforts to determine the precise localization of the SC-lead compounds in the parasites have been unsuccessful. Indeed, covalently tagging the SC-lead compounds with flurophores led to compounds with a drastically reduced antiplasmodial activity. Furthermore, click-chemistry experiments [231–233] were performed in vain, as the interaction between SC83288 and its molecular target appears to be non-covalent and a milder approach used to a localization purpose only led to highly unspecific signals. Consequently, this lack of knowledge both concerning the cellular localization of the SC-lead compounds and their direct molecular target does not allow to speculate on a potential role of the mutated PfATP6 pumping SC83288 into the ER where the damage for the parasite could be minimized. We rather favor a compensatory role of PfATP6 in the resistance to the SC-lead compounds, instead of being a primary factor related to the mode of action of the compounds. This hypothesis is further supported by the recurrence of PfATP6 in the investigation of the mechanisms to other antimalarial drugs, particularly artemisinins. The inconsistency of the appearance of PfATP6 in the artemisinins resistance studies [50,62–66,68,149] tends to confirm the role of PfATP6 as a secondary compensatory mechanism of resistance. Furthermore, PfATP6, despite its essentiality, has been shown to be prone to acquired spontaneous mutations in the field, therefore displaying an already important geographic diversity, even in a drug-free environment [234–236].

5. Conclusion and outlooks

SC83288, an amicarbalide-based compound issued from a medicinal chemistry optimization program, is a potent blood schizonticide. Its fast antiplasmodial activity has been demonstrated both *in vitro* using different blood culture-based approaches during this study and *in vivo* in a humanized mice model by our collaborators [189]. No cross-resistance to artemisinins, nor any similar mode of action were detected, marking SC83288 as a possible candidate for complementing artemsinins in geographic areas where artemisinin-resistance is becoming a growing concern, providing a positive and secure evaluation of SC83288 during human clinical trials.

This study further aimed to gain insight into the mode of action of SC83288, as well as on the mechanisms by which the *P. falciparum* parasite could develop resistance against it. The Ca^{2+} ATPase PfATP6 has been ruled out as a direct molecular target of SC83288, but was confirmed as a component of an assumed compensatory resistance mechanism. Even though a disruption of Ca^{2+} homeostasis in the PfATP6 ^{F972Y} mutant was clearly observed, the molecular details of resistance to SC83288 remain to be unraveled. Similarly, if the treatment of the PfATP6 ^{F972Y} mutant with SC83288 brought back the possibility of a more pleiotropic mode of action through disturbed calcium signaling, consistent with the toxic activity of SC83288 on both the trophozoite and schizonts stages, the mode of action of the SC-lead compounds remains far from understood.

The role of extracellular calcium in the antiplasmodial action of SC83288 could be further investigated using either higher, yet non-toxic, calcium concentrations, or known Ca^{2+} chelators, such as EGTA [237]. The SC83288 responsiveness in a standard growth inhibition assay could be measured under these conditions, to determine if the antiplasmodial action is dependent of extracellular calcium.

An untargeted metabolomics approach, as previously used to determine the mode of action of some antibiotics [238] or antiprotozoal drugs [239], has up to now not been successful to that regard. However, the treatment conditions as well as the exposure time could be adjusted to obtain more precise results. The progress in the quantitative mass spectrometry analysis field opened other doors of the “omics” approaches, such a proteomics as a mean of target identification [240]. Even if preliminary results did not mark SC83288 as a *de novo* protein synthesis inhibitor in *P. falciparum* (See Appendix III, Figure 9.1), a full proteomics analysis, particularly a comparison between the PfATP6 ^{F972Y} mutant and its parental line, could give helpful insights to determine a more precise mechanism of resistance.

Finally, the other two proteins identified with nonsynonymous SNPs in the $Dd2^{SC814158}$ and $Dd2^{SC83288}$ parasites could be further investigated. PfMDR2 (PF3D7_1447900) could also be contemplated as a component of a secondary resistance mechanism expelling SC83288 out of the parasite. This hypothesis of PfMDR2 acting as an export system is supported by its localization at the plasma membrane of the parasite [241,242] and its implication in heavy metal tolerance [243] and contribution to a decreased responsiveness to several antimalarial drugs such as atovaquone, chloroquine, quinine or mefloquine [241,244]. It should however be confirmed using genetic engineering and uptake assays with radiolabeled SC83288. The role of the putative ATP-dependent RNA helicase (PF3D7_1241800) is more difficult to predict and a confirmation of its role in resistance to SC83288, and possibly its mode of action, is deserved. RNA helicases have not yet been considered as druggable targets in *Plasmodium*, although they are considered suitable drug targets for antiviral and anticancer therapies and are suggested to have a crucial role in various protozoic, bacterial or fungal infections [245].

Independently of the identifications of a direct molecular target for the SC-lead compounds or of the components of their resistance mechanisms, SC83288 will hopefully prove to be successful in the clinical trials and contribute to the eradication of malaria.

6. References

[1] World Health Organization, World Malaria Report 2017, WHO Press. (2017).

[2] K.J. Arrow, C. Panosian, H. Gelband, Saving lives, buying time : economics of malaria drugs in an age of resistance, National Academies Press, 2004.

[3] R.L. Miller, S. Ikram, G.J. Armelagos, R. Walker, W.B. Harer, C.J. Shiff, D. Baggett, M. Carrigan, S.M. Maret, Diagnosis of Plasmodium falciparum infections in mummies using the rapid manual ParaSight-F test., Trans. R. Soc. Trop. Med. Hyg. 88 (n.d.) 31–2.

[4] I.W. Sherman, Malaria : parasite biology, pathogenesis, and protection, ASM Press, 1998.

[5] F.E. Cox, History of the discovery of the malaria parasites and their vectors, Parasit. Vectors. 3 (2010) 5.

[6] C.L.A. Laveran, Classics in infectious diseases: A newly discovered parasite in the blood of patients suffering from malaria. Parasitic etiology of attacks of malaria: Charles Louis Alphonse Laveran (1845-1922)., Rev. Infect. Dis. 4 (n.d.) 908–11.

[7] R. Ross, On some Peculiar Pigmented Cells Found in Two Mosquitos Fed on Malarial Blood., Br. Med. J. 2 (1897) 1786–8.

[8] Y. Tu, The discovery of artemisinin (qinghaosu) and gifts from Chinese medicine, Nat. Med. 17 (2011) 1217–1220.

[9] Qinghaosu Antimalaria CoordinatiTeg Research group, Chinese Medical Journal: a peer reviewed, open access journal, published semimonthly by the Chinese Medical Association, Chinese Med. J. . 92 (1978) 811–816.

[10] N.J. White, S. Pukrittayakamee, T.T. Hien, M.A. Faiz, O.A. Mokuolu, A.M. Dondorp, Malaria., Lancet. 383 (2014) 723–35.

[11] World Health Organization, Global malaria control and elimination – Report of a technical review, WHO Press. (2008).

[12] World Health Organization, World Malaria Report 2016, WHO Press. (2016).

[13] World Health Organization, Global Technical Strategy for Malaria 2016–2030, WHO Press. (2016).

[14] B.M. Greenwood, D.A. Fidock, D.E. Kyle, S.H.I. Kappe, P.L. Alonso, F.H. Collins, P.E. Duffy, Malaria: progress, perils, and prospects for eradication., J. Clin. Invest. 118 (2008) 1266–76.

[15] P. Brasil, M.G. Zalis, A. de Pina-Costa, A.M. Siqueira, C.B. Júnior, S. Silva, A.L.L. Areas, M. Pelajo-Machado, D.A.M. de Alvarenga, A.C.F. da Silva Santelli, H.G. Albuquerque, P. Cravo, F.V. Santos de Abreu, C.L. Peterka, G.M. Zanini, M.C. Suárez Mutis, A. Pissinatti, R. Lourenço-de-Oliveira, C.F.A. de Brito, M. de Fátima Ferreira-da-Cruz, R. Culleton, C.T. Daniel-Ribeiro, Outbreak of human malaria caused by Plasmodium simium in the Atlantic Forest in Rio de Janeiro: a molecular epidemiological investigation., Lancet. Glob. Heal. 5 (2017) e1038–e1046.

[16] T.F. de Koning-Ward, M.W.A. Dixon, L. Tilley, P.R. Gilson, Plasmodium species: master renovators of their host cells, Nat. Rev. Microbiol. 14 (2016) 494–507.

[17] M. Prudêncio, A. Rodriguez, M.M. Mota, The silent path to thousands of merozoites: the Plasmodium liver stage, Nat. Rev. Microbiol. 4 (2006) 849–856.

[18] F. Frischknecht, K. Matuschewski, *Plasmodium* Sporozoite Biology, Cold Spring Harb. Perspect. Med. 7 (2017) a025478.

[19] A. Radfar, D. Méndez, C. Moneriz, M. Linares, P. Marín-García, A. Puyet, A. Diez, J.M. Bautista, Synchronous culture of Plasmodium falciparum at high parasitemia levels, Nat. Protoc. 4 (2009) 1828–1844.

[20] M.S. Oakley, N. Gerald, T.F. McCutchan, L. Aravind, S. Kumar, Clinical and molecular aspects of malaria fever, Trends Parasitol. 27 (2011) 442–449.

[21] M. Brochet, O. Billker, Calcium signalling in malaria parasites, Mol. Microbiol. 100 (2016) 397–408.

[22] M.J. Berridge, P. Lipp, M.D. Bootman, The versatility and universality of calcium signalling., Nat. Rev. Mol. Cell Biol. 1 (2000) 11–21.

[23] S. Glushakova, V. Lizunov, P.S. Blank, K. Melikov, G. Humphrey, J. Zimmerberg, Cytoplasmic free Ca2+ is essential for multiple steps in malaria parasite egress from infected erythrocytes, Malar. J. 12 (2013) 41.

[24] S. Garg, S. Agarwal, S. Kumar, S. Shams Yazdani, C.E. Chitnis, S. Singh, Calcium-dependent permeabilization of erythrocytes by a perforin-like protein during egress of malaria parasites, Nat. Commun. 4 (2013) 1736.

[25] C. Withers-Martinez, M. Strath, F. Hackett, L.F. Haire, S.A. Howell, P.A. Walker, E. Christodoulou, C. Evangelos, G.G. Dodson, M.J. Blackman, The malaria parasite egress protease SUB1 is a calcium-dependent redox switch subtilisin., Nat. Commun. 5 (2014) 3726.

[26] G.E. Weiss, P.R. Gilson, T. Taechalertpaisarn, W.-H. Tham, N.W.M. de Jong, K.L. Harvey, F.J.I. Fowkes, P.N. Barlow, J.C. Rayner, G.J. Wright, A.F. Cowman, B.S. Crabb, Revealing the Sequence and Resulting Cellular Morphology of Receptor-Ligand Interactions during Plasmodium falciparum Invasion of Erythrocytes, PLOS Pathog. 11 (2015) e1004670.

[27] J.G. Johnson, N. Epstein, T. Shiroishi, L.H. Miller, Factors affecting the ability of isolated Plasmodium knowlesi merozoites to attach to and invade erythrocytes., Parasitology. 80 (1980) 539–50.

[28] Y. Matsumoto, G. Perry, L.W. Scheibel, M. Aikawa, Role of calmodulin in Plasmodium falciparum: implications for erythrocyte invasion by the merozoite., Eur. J. Cell Biol. 45 (1987) 36–43.

[29] M. Wasserman, C. Alarcón, P.M. Mendoza, Effects of Ca++ depletion on the asexual cell cycle of Plasmodium falciparum., Am. J. Trop. Med. Hyg. 31 (1982) 711–7.

[30] J. Adovelande, B. Bastide, J. Délèze, J. Schrével, Cytosolic free calcium in Plasmodium falciparum-infected erythrocytes and the effect of verapamil: a cytofluorimetric study., Exp. Parasitol. 76 (1993) 247–58.

[31] M. Enomoto, S. Kawazu, S. Kawai, W. Furuyama, T. Ikegami, J. Watanabe, K. Mikoshiba, Blockage of Spontaneous Ca2+ Oscillation Causes Cell Death in Intraerythrocitic Plasmodium falciparum, PLoS One. 7 (2012) e39499.

[32] O. Billker, S. Dechamps, R. Tewari, G. Wenig, B. Franke-Fayard, V. Brinkmann, Calcium and a calcium-dependent protein kinase regulate gamete formation and mosquito transmission in a malaria parasite., Cell. 117 (2004) 503–14.

[33] F. Kawamoto, H. Fujioka, R. Murakami, Syafruddin, M. Hagiwara, T. Ishikawa, H. Hidaka, The roles of Ca2+/calmodulin- and cGMP-dependent pathways in

gametogenesis of a rodent malaria parasite, Plasmodium berghei., Eur. J. Cell Biol. 60 (1993) 101–7.

[34] S. Sebastian, M. Brochet, M.O. Collins, F. Schwach, M.L. Jones, D. Goulding, J.C. Rayner, J.S. Choudhary, O. Billker, A Plasmodium Calcium-Dependent Protein Kinase Controls Zygote Development and Transmission by Translationally Activating Repressed mRNAs, Cell Host Microbe. 12 (2012) 9–19.

[35] M. Brochet, M.O. Collins, T.K. Smith, E. Thompson, S. Sebastian, K. Volkmann, F. Schwach, L. Chappell, A.R. Gomes, M. Berriman, J.C. Rayner, D.A. Baker, J. Choudhary, O. Billker, Phosphoinositide Metabolism Links cGMP-Dependent Protein Kinase G to Essential Ca2+ Signals at Key Decision Points in the Life Cycle of Malaria Parasites, PLoS Biol. 12 (2014) e1001806.

[36] T. Ishino, Y. Orito, Y. Chinzei, M. Yuda, A calcium-dependent protein kinase regulates Plasmodium ookinete access to the midgut epithelial cell., Mol. Microbiol. 59 (2006) 1175–84.

[37] A.F. Carey, M. Singer, D. Bargieri, S. Thiberge, F. Frischknecht, R. Ménard, R. Amino, Calcium dynamics of *P lasmodium berghei* sporozoite motility, Cell. Microbiol. 16 (2014) 768–783.

[38] N. Philip, A.P. Waters, Conditional Degradation of Plasmodium Calcineurin Reveals Functions in Parasite Colonization of both Host and Vector., Cell Host Microbe. 18 (2015) 122–31.

[39] Y. Doi, N. Shinzawa, S. Fukumoto, H. Okano, H. Kanuka, Calcium signal regulates temperature-dependent transformation of sporozoites in malaria parasite development, Exp. Parasitol. 128 (2011) 176–180.

[40] C.R. Garcia, A.R. Dluzewski, L.H. Catalani, R. Burting, J. Hoyland, W.T. Mason, Calcium homeostasis in intraerythrocytic malaria parasites., Eur. J. Cell Biol. 71 (1996) 409–13.

[41] P. Rohrbach, O. Friedrich, H. Plattner, R.H.A. Fink, M. Lanzer, J. Hentschel, Metabolism and Bioenergetics : Quantitative Calcium Measurements in Subcellular Compartments of Plasmodium falciparum -infected Erythrocytes Quantitative Calcium Measurements in Subcellular Compartments of Plasmodium falciparum -infected Erythrocytes *, (2005).

[42] A. Rotmann, C. Sanchez, A. Guiguemde, P. Rohrbach, A. Dave, N. Bakouh, G. Planelles, M. Lanzer, PfCHA is a mitochondrial divalent cation/H+ antiporter in Plasmodium falciparum., Mol. Microbiol. 76 (2010) 1591–606.

[43] R. Docampo, S.N.J. Moreno, Acidocalcisomes, Cell Calcium. 50 (2011) 113–119.

[44] D.L. Prole, C.W. Taylor, Identification of Intracellular and Plasma Membrane Calcium Channel Homologues in Pathogenic Parasites, PLoS One. 6 (2011) e26218.

[45] B. Arnou, C. Montigny, J.P. Morth, P. Nissen, C. Jaxel, J. V Møller, M. Maire, The Plasmodium falciparum Ca2+-ATPase PfATP6 insensitive to artemisinin , but a potential drug target, Biohem. Soc. Trans. 39 (2011) 823–831.

[46] D. Cardi, A. Pozza, B. Arnou, E. Marchal, J.D. Clausen, J.P. Andersen, S. Krishna, J. V Møller, M. le Maire, C. Jaxel, Purified E255L mutant SERCA1a and purified PfATP6 are sensitive to SERCA-type inhibitors but insensitive to artemisinins., J. Biol. Chem. 285 (2010) 26406–16.

[47] M. Kimura, Y. Yamaguchi, S. Takada, K. Tanabe, Cloning of a Ca(2+)-ATPase gene of Plasmodium falciparum and comparison with vertebrate Ca(2+)-ATPases., J. Cell

Sci. 104 (Pt 4) (1993) 1129–36.

[48] D. Cardi, A. Pozza, B. Arnou, E. Marchal, J.D. Clausen, J.P. Andersen, S. Krishna, J. V Møller, M. le Maire, C. Jaxel, Purified E255L mutant SERCA1a and purified PfATP6 are sensitive to SERCA-type inhibitors but insensitive to artemisinins., J. Biol. Chem. 285 (2010) 26406–16.

[49] U. Omasits, C.H. Ahrens, S. Müller, B. Wollscheid, Protter: interactive protein feature visualization and integration with experimental proteomic data., Bioinformatics. 30 (2014) 884–6.

[50] S. Krishna, S. Pulcini, F. Fatih, H. Staines, Artemisinins and the biological basis for the PfATP6/SERCA hypothesis, Trends Parasitol. 26 (2010) 517–523.

[51] F.P. Varotti, F.H. Beraldo, M.L. Gazarini, C.R.S. Garcia, Plasmodium falciparum malaria parasites display a THG-sensitive Ca2+ pool., Cell Calcium. 33 (2003) 137–44.

[52] M. Jung, H. Kim, K.Y. Nam, K.T. No, Three-dimensional structure of Plasmodium falciparum Ca2+ -ATPase(PfATP6) and docking of artemisinin derivatives to PfATP6., Bioorg. Med. Chem. Lett. 15 (2005) 2994–7.

[53] H. Plattner, I.M. Sehring, I.K. Mohamed, K. Miranda, W. De Souza, R. Billington, A. Genazzani, E.-M. Ladenburger, Calcium signaling in closely related protozoan groups (Alveolata): Non-parasitic ciliates (Paramecium, Tetrahymena) vs. parasitic Apicomplexa (Plasmodium, Toxoplasma), Cell Calcium. 51 (2012) 351–382.

[54] A. Kotšubei, M. Gorgel, J.P. Morth, P. Nissen, J.L. Andersen, Probing determinants of cyclopiazonic acid sensitivity of bacterial Ca2+-ATPases., FEBS J. 280 (2013) 5441–9.

[55] U. Eckstein-Ludwig, R.J. Webb, I.D.A. Van Goethem, J.M. East, A.G. Lee, M. Kimura, P.M. O'Neill, P.G. Bray, S.A. Ward, S. Krishna, Artemisinins target the SERCA of Plasmodium falciparum., Nature. 424 (2003) 957–61.

[56] P.K. Naik, M. Srivastava, P. Bajaj, S. Jain, A. Dubey, P. Ranjan, R. Kumar, H. Singh, The binding modes and binding affinities of artemisinin derivatives with Plasmodium falciparum Ca2+-ATPase (PfATP6), J. Mol. Model. 17 (2011) 333–357.

[57] A. Shandilya, S. Chacko, B. Jayaram, I. Ghosh, A plausible mechanism for the antimalarial activity of artemisinin: A computational approach., Sci. Rep. 3 (2013) 2513.

[58] F.B.-E. Garah, J.-L. Stigliani, F. Coslédan, B. Meunier, A. Robert, Docking studies of structurally diverse antimalarial drugs targeting PfATP6: no correlation between in silico binding affinity and in vitro antimalarial activity., ChemMedChem. 4 (2009) 1469–79.

[59] R. Lepore, S. Simeoni, D. Raimondo, A. Caroli, A. Tramontano, A. Via, Identification of the Schistosoma mansoni Molecular Target for the Antimalarial Drug Artemether, J. Chem. Inf. Model. 51 (2011) 3005–3016.

[60] S. David-Bosne, M.V. Clausen, H. Poulsen, J.V. Møller, P. Nissen, M. le Maire, Reappraising the effects of artemisinin on the ATPase activity of PfATP6 and SERCA1a E255L expressed in Xenopus laevis oocytes., Nat. Struct. Mol. Biol. 23 (2016) 1–2.

[61] L.W. Brasil, A.L.L. Areas, G.C. Melo, C.M.C. Oliveira, M.G.C. Alecrim, M.V.G. Lacerda, C. O'Brien, W.M.R. Oelemann, M.G. Zalis, Pfatp6 molecular profile of Plasmodium falciparum isolates in the western Brazilian Amazon., Malar. J. 11 (2012)

111.

[62] A.-C. Uhlemann, A. Cameron, U. Eckstein-Ludwig, J. Fischbarg, P. Iserovich, F.A. Zuniga, M. East, A. Lee, L. Brady, R.K. Haynes, S. Krishna, A single amino acid residue can determine the sensitivity of SERCAs to artemisinins, Nat. Struct. Mol. Biol. 12 (2005) 628–629.

[63] L. Bertaux, L.H. Quang, V. Sinou, N.X. Thanh, D. Parzy, New PfATP6 Mutations Found in Plasmodium falciparum Isolates from Vietnam, Antimicrob. Agents Chemother. 53 (2009) 4570–4571.

[64] D.R. Pillai, R. Lau, K. Khairnar, R. Lepore, A. Via, H.M. Staines, S. Krishna, Artemether resistance in vitro is linked to mutations in PfATP6 that also interact with mutations in PfMDR1 in travellers returning with Plasmodium falciparum infections., Malar. J. 11 (2012) 131.

[65] M. Imwong, A.M. Dondorp, F. Nosten, P. Yi, M. Mungthin, S. Hanchana, D. Das, A.P. Phyo, K.M. Lwin, S. Pukrittayakamee, S.J. Lee, S. Saisung, K. Koecharoen, C. Nguon, N.P.J. Day, D. Socheat, N.J. White, Exploring the Contribution of Candidate Genes to Artemisinin Resistance in Plasmodium falciparum, Antimicrob. Agents Chemother. 54 (2010) 2886–2892.

[66] M.R. Adhin, M. Labadie-Bracho, S.G. Vreden, Status of potential PfATP6 molecular markers for artemisinin resistance in Suriname, Malar. J. 11 (2012) 322.

[67] L. Cui, Z. Wang, H. Jiang, D. Parker, H. Wang, X.-Z. Su, L. Cui, Lack of Association of the S769N Mutation in Plasmodium falciparum SERCA (PfATP6) with Resistance to Artemisinins, Antimicrob. Agents Chemother. 56 (2012) 2546–2552.

[68] M. Miao, Z. Wang, Z. Yang, L. Yuan, D.M. Parker, C. Putaporntip, S. Jongwutiwes, P. Xangsayarath, T. Pongvongsa, H. Moji, T. Dinh Tuong, T. Abe, S. Nakazawa, M.P. Kyaw, G. Yan, J. Sirichaisinthop, J. Sattabongkot, J. Mu, X. Su, O. Kaneko, L. Cui, Genetic diversity and lack of artemisinin selection signature on the Plasmodium falciparum ATP6 in the Greater Mekong Subregion., PLoS One. 8 (2013) e59192.

[69] M. Bublitz, J.P. Morth, P. Nissen, P-type ATPases at a glance., J. Cell Sci. 124 (2011) 2515–9.

[70] S. Pulcini, H.M. Staines, J.K. Pittman, K. Slavic, C. Doerig, J. Halbert, R. Tewari, F. Shah, M.A. Avery, R.K. Haynes, S. Krishna, Expression in Yeast Links Field Polymorphisms in PfATP6 to in Vitro Artemisinin Resistance and Identifies New Inhibitor Classes, J. Infect. Dis. 208 (2013) 468–478.

[71] S.R. Denmeade, J.T. Isaacs, The SERCA pump as a therapeutic target: making a “smart bomb” for prostate cancer., Cancer Biol. Ther. 4 (2005) 14–22.

[72] L. Yatime, M.J. Buch-Pedersen, M. Musgaard, J.P. Morth, A.-M.L. Winther, B.P. Pedersen, C. Olesen, J.P. Andersen, B. Vilsen, B. Schiøtt, P-type ATPases as drug targets: Tools for medicine and science, Biochim. Biophys. Acta - Bioenerg. 1787 (2009) 207–220.

[73] W. Trager, J.B. Jensen, Human malaria parasites in continuous culture., Science. 193 (1976) 673–5.

[74] Y. Wu, C.D. Sifri, H.H. Lei, X.Z. Su, T.E. Wellems, Transfection of Plasmodium falciparum within human red blood cells., Proc. Natl. Acad. Sci. U. S. A. 92 (1995) 973–7.

[75] M.J. Gardner, N. Hall, E. Fung, O. White, M. Berriman, R.W. Hyman, J.M. Carlton, A. Pain, K.E. Nelson, S. Bowman, I.T. Paulsen, K. James, J.A. Eisen, K. Rutherford, S.L.

Salzberg, A. Craig, S. Kyes, M.-S. Chan, V. Nene, S.J. Shallom, B. Suh, J. Peterson, S. Angiuoli, M. Pertea, J. Allen, J. Selengut, D. Haft, M.W. Mather, A.B. Vaidya, D.M.A. Martin, A.H. Fairlamb, M.J. Fraunholz, D.S. Roos, S.A. Ralph, G.I. McFadden, L.M. Cummings, G.M. Subramanian, C. Mungall, J.C. Venter, D.J. Carucci, S.L. Hoffman, C. Newbold, R.W. Davis, C.M. Fraser, B. Barrell, Genome sequence of the human malaria parasite Plasmodium falciparum, Nature. 419 (2002) 498–511.

[76] T. Anderson, S. Nkhoma, A. Ecker, D. Fidock, How can we identify parasite genes that underlie antimalarial drug resistance?, Pharmacogenomics. 12 (2011) 59–85.

[77] R. Sapranauskas, G. Gasiunas, C. Fremaux, R. Barrangou, P. Horvath, V. Siksnys, The Streptococcus thermophilus CRISPR/Cas system provides immunity in Escherichia coli, Nucleic Acids Res. 39 (2011) 9275–9282.

[78] M. Ghorbal, M. Gorman, C.R. Macpherson, R.M. Martins, A. Scherf, J.-J. Lopez-Rubio, Genome editing in the human malaria parasite Plasmodium falciparum using the CRISPR-Cas9 system., Nat. Biotechnol. 32 (2014) 819–21.

[79] M.C. Lee, D.A. Fidock, CRISPR-mediated genome editing of Plasmodium falciparum malaria parasites., Genome Med. 6 (2014) 63.

[80] A.H. Lee, L.S. Symington, D.A. Fidock, DNA Repair Mechanisms and Their Biological Roles in the Malaria Parasite Plasmodium falciparum, Microbiol. Mol. Biol. Rev. 78 (2014) 469–486.

[81] M. Singer, F. Frischknecht, Time for Genome Editing: Next-Generation Attenuated Malaria Parasites, Trends Parasitol. 33 (2017) 202–213.

[82] M. Singer, J. Marshall, K. Heiss, G.R. Mair, D. Grimm, A.-K. Mueller, F. Frischknecht, Zinc finger nuclease-based double-strand breaks attenuate malaria parasites and reveal rare microhomology-mediated end joining, Genome Biol. 16 (2015) 249.

[83] F.D. Urnov, E.J. Rebar, M.C. Holmes, H.S. Zhang, P.D. Gregory, Genome editing with engineered zinc finger nucleases, Nat. Rev. Genet. 11 (2010) 636–646.

[84] RTS,S Clinical Trials Partnership, S.T. Agnandji, B. Lell, S.S. Soulanoudjingar, J.F. Fernandes, B.P. Abossolo, C. Conzelmann, B.G.N.O. Methogo, Y. Doucka, A. Flamen, B. Mordmüller, S. Issifou, P.G. Kremsner, J. Sacarlal, P. Aide, M. Lanaspa, J.J. Aponte, A. Nhamuave, D. Quelhas, Q. Bassat, S. Mandjate, E. Macete, P. Alonso, S. Abdulla, N. Salim, O. Juma, M. Shomari, K. Shubis, F. Machera, A.S. Hamad, R. Minja, A. Mtoro, A. Sykes, S. Ahmed, A.M. Urassa, A.M. Ali, G. Mwangoka, M. Tanner, H. Tinto, U. D'Alessandro, H. Sorgho, I. Valea, M.C. Tahita, W. Kaboré, S. Ouédraogo, Y. Sandrine, R.T. Guiguemdé, J.B. Ouédraogo, M.J. Hamel, S. Kariuki, C. Odero, M. Oneko, K. Otieno, N. Awino, J. Omoto, J. Williamson, V. Muturi-Kioi, K.F. Laserson, L. Slutsker, W. Otieno, L. Otieno, O. Nekoye, S. Gondi, A. Otieno, B. Ogutu, R. Wasuna, V. Owira, D. Jones, A.A. Onyango, P. Njuguna, R. Chilengi, P. Akoo, C. Kerubo, J. Gitaka, C. Maingi, T. Lang, A. Olotu, B. Tsofa, P. Bejon, N. Peshu, K. Marsh, S. Owusu-Agyei, K.P. Asante, K. Osei-Kwakye, O. Boahen, S. Ayamba, K. Kayan, R. Owusu-Ofori, D. Dosoo, I. Asante, G. Adjei, G. Adjei, D. Chandramohan, B. Greenwood, J. Lusingu, S. Gesase, A. Malabeja, O. Abdul, H. Kilavo, C. Mahende, E. Liheluka, M. Lemnge, T. Theander, C. Drakeley, D. Ansong, T. Agbenyega, S. Adjei, H.O. Boateng, T. Rettig, J. Bawa, J. Sylverken, D. Sambian, A. Agyekum, L. Owusu, F. Martinson, I. Hoffman, T. Mvalo, P. Kamthunzi, R. Nkomo, A. Msika, A. Jumbe, N. Chome, D. Nyakuipa, J. Chintedza, W.R. Ballou, M. Bruls, J. Cohen, Y. Guerra, E. Jongert, D. Lapierre, A. Leach, M. Lievens, O. Ofori-Anyinam, J. Vekemans, T. Carter, D. Leboulleux, C. Loucq, A. Radford, B. Savarese, D. Schellenberg, M. Sillman, P. Vansadia, First Results of Phase 3 Trial of RTS,S/AS01 Malaria Vaccine in African Children, N. Engl. J. Med. 365 (2011) 1863–1875.

[85] RTS,S Clinical Trials Partnership, S.T. Agnandji, B. Lell, J.F. Fernandes, B.P. Abossolo, B.G.N.O. Methogo, A.L. Kabwende, A.A. Adegnika, B. Mordmüller, S. Issifou, P.G. Kremsner, J. Sacarlal, P. Aide, M. Lanaspa, J.J. Aponte, S. Machevo, S. Acacio, H. Bulo, B. Sigauque, E. Macete, P. Alonso, S. Abdulla, N. Salim, R. Minja, M. Mpina, S. Ahmed, A.M. Ali, A.T. Mtoro, A.S. Hamad, P. Mutani, M. Tanner, H. Tinto, U. D'Alessandro, H. Sorgho, I. Valea, B. Bihoun, I. Guiraud, B. Kaboré, O. Sombié, R.T. Guiguemdé, J.B. Ouédraogo, M.J. Hamel, S. Kariuki, M. Oneko, C. Odero, K. Otieno, N. Awino, M. McMorrow, V. Muturi-Kioi, K.F. Laserson, L. Slutsker, W. Otieno, L. Otieno, N. Otsyula, S. Gondi, A. Otieno, V. Owira, E. Oguk, G. Odongo, J. Ben Woods, B. Ogutu, P. Njuguna, R. Chilengi, P. Akoo, C. Kerubo, C. Maingi, T. Lang, A. Olotu, P. Bejon, K. Marsh, G. Mwambingu, S. Owusu-Agyei, K.P. Asante, K. Osei-Kwakye, O. Boahen, D. Dosoo, I. Asante, G. Adjei, E. Kwara, D. Chandramohan, B. Greenwood, J. Lusingu, S. Gesase, A. Malabeja, O. Abdul, C. Mahende, E. Liheluka, L. Malle, M. Lemnge, T.G. Theander, C. Drakeley, D. Ansong, T. Agbenyega, S. Adjei, H.O. Boateng, T. Rettig, J. Bawa, J. Sylverken, D. Sambian, A. Sarfo, A. Agyekum, F. Martinson, I. Hoffman, T. Mvalo, P. Kamthunzi, R. Nkomo, T. Tembo, G. Tegha, M. Tsidya, J. Kilembe, C. Chawinga, W.R. Ballou, J. Cohen, Y. Guerra, E. Jongert, D. Lapierre, A. Leach, M. Lievens, O. Ofori-Anyinam, A. Olivier, J. Vekemans, T. Carter, D. Kaslow, D. Leboulleux, C. Loucq, A. Radford, B. Savarese, D. Schellenberg, M. Sillman, P. Vansadia, A Phase 3 Trial of RTS,S/AS01 Malaria Vaccine in African Infants, N. Engl. J. Med. 367 (2012) 2284–2295.

[86] S. Krishna, N. V Nagaraja, T. Planche, T. Agbenyega, G. Bedo-Addo, D. Ansong, A. Owusu-Ofori, A.L. Shroads, G. Henderson, A. Hutson, H. Derendorf, P.W. Stacpoole, Population pharmacokinetics of intramuscular quinine in children with severe malaria., Antimicrob. Agents Chemother. 45 (2001) 1803–9.

[87] A.M. Barrocas, T. Cymet, Cinchonism in a patient taking Quinine for leg cramps., Compr. Ther. 33 (2007) 162–3.

[88] L.R. Wolf, E.J. Otten, M.P. Spadafora, Cinchonism: two case reports and review of acute quinine toxicity and treatment., J. Emerg. Med. 10 (1992) 295–301.

[89] D.E. Eyles, C.C. Hoo, M. Warren, A.A. Sandosham, Plasmodium falciparum Resistant to Chloroquine in Cambodia., Am. J. Trop. Med. Hyg. 12 (1963) 840–3.

[90] S. Fogh, S. Jepsen, R.H. Mataya, R-III chloroquine-resistant Plasmodium falciparum malaria from northern Malawi., Trans. R. Soc. Trop. Med. Hyg. 78 (1984) 282.

[91] C.M. Kihamia, H.S. Gill, Chloroquine-resistant falciparum malaria in semi-immune African Tanzaniana., Lancet (London, England). 2 (1982) 43.

[92] World Health Organization, Guidelines for the Treatment of Malaria, WHO Press. (2015).

[93] E. Beutler, The hemolytic effect of primaquine and related compounds: a review., Blood. 14 (1959) 103–39.

[94] L.J. Bolchoz, R.A. Budinsky, D.C. McMillan, D.J. Jollow, Primaquine-induced hemolytic anemia: formation and hemotoxicity of the arylhydroxylamine metabolite 6-methoxy-8-hydroxylaminoquinoline., J. Pharmacol. Exp. Ther. 297 (2001) 509–15.

[95] D.S. Walsh, P. Wilairatana, D.B. Tang, D.G. Heppner, T.G. Brewer, S. Krudsood, U. Silachamroon, W. Phumratanaprapin, D. Siriyanonda, S. Looareesuwan, Randomized trial of 3-dose regimens of tafenoquine (WR238605) versus low-dose primaquine for preventing Plasmodium vivax malaria relapse., Clin. Infect. Dis. 39 (2004) 1095–103.

[96] G.D. Shanks, A.J. Oloo, G.M. Aleman, C. Ohrt, F.W. Klotz, D. Braitman, J. Horton, R. Brueckner, A New Primaquine Analogue, Tafenoquine (WR 238605), for Prophylaxis

against *Plasmodium falciparum* Malaria, Clin. Infect. Dis. 33 (2001) 1968–1974.

[97] T.J. Egan, D.C. Ross, P.A. Adams, Quinoline anti-malarial drugs inhibit spontaneous formation of beta-haematin (malaria pigment)., FEBS Lett. 352 (1994) 54–7.

[98] P.G. Bray, M. Mungthin, R.G. Ridley, S.A. Ward, Access to hematin: the basis of chloroquine resistance., Mol. Pharmacol. 54 (1998) 170–9.

[99] A. Yayon, Z.I. Cabantchik, H. Ginsburg, Identification of the acidic compartment of Plasmodium falciparum-infected human erythrocytes as the target of the antimalarial drug chloroquine., EMBO J. 3 (1984) 2695–700.

[100] J.M. Combrinck, T.E. Mabotha, K.K. Ncokazi, M.A. Ambele, D. Taylor, P.J. Smith, H.C. Hoppe, T.J. Egan, Insights into the role of heme in the mechanism of action of antimalarials., ACS Chem. Biol. 8 (2013) 133–7.

[101] S.R. Hawley, P.G. Bray, M. Mungthin, J.D. Atkinson, P.M. O'Neill, S.A. Ward, Relationship between antimalarial drug activity, accumulation, and inhibition of heme polymerization in Plasmodium falciparum in vitro., Antimicrob. Agents Chemother. 42 (1998) 682–6.

[102] C.H. Sibley, J.E. Hyde, P.F. Sims, C. V Plowe, J.G. Kublin, E.K. Mberu, A.F. Cowman, P.A. Winstanley, W.M. Watkins, A.M. Nzila, Pyrimethamine-sulfadoxine resistance in Plasmodium falciparum: what next?, Trends Parasitol. 17 (2001) 582–8.

[103] J.E. Salcedo-Sora, E. Ochong, S. Beveridge, D. Johnson, A. Nzila, G.A. Biagini, P.A. Stocks, P.M. O'Neill, S. Krishna, P.G. Bray, S.A. Ward, The molecular basis of folate salvage in Plasmodium falciparum: characterization of two folate transporters., J. Biol. Chem. 286 (2011) 44659–68.

[104] M.D. Edstein, J.R. Veenendaal, H. V Scott, K.H. Rieckmann, Steady-state kinetics of proguanil and its active metabolite, cycloguanil, in man., Chemotherapy. 34 (1988) 385–92.

[105] J.G. Kublin, F.K. Dzinjalamala, D.D. Kamwendo, E.M. Malkin, J.F. Cortese, L.M. Martino, R.A.G. Mukadam, S.J. Rogerson, A.G. Lescano, M.E. Molyneux, P.A. Winstanley, P. Chimpeni, T.E. Taylor, C.V. Plowe, Molecular Markers for Failure of Sulfadoxine-Pyrimethamine and Chlorproguanil-Dapsone Treatment of Plasmodium falciparum Malaria, J. Infect. Dis. 185 (2002) 380–388.

[106] A.M. Nzila, E.K. Mberu, J. Sulo, H. Dayo, P.A. Winstanley, C.H. Sibley, W.M. Watkins, Towards an understanding of the mechanism of pyrimethamine-sulfadoxine resistance in Plasmodium falciparum: genotyping of dihydrofolate reductase and dihydropteroate synthase of Kenyan parasites., Antimicrob. Agents Chemother. 44 (2000) 991–6.

[107] M. Warsame, A.M. Hassan, A. Barrette, A.M. Jibril, H.H. Elmi, A.M. Arale, H. El Mohammady, R.A. Nada, J.G.H. Amran, A. Muse, F.E. Yusuf, A.S. Omar, Treatment of uncomplicated malaria with artesunate plus sulfadoxine-pyrimethamine is failing in Somalia: evidence from therapeutic efficacy studies and Pfdhfr and Pfdhps mutant alleles., Trop. Med. Int. Health. 20 (2015) 510–7.

[108] C. Wongsrichanalai, A.L. Pickard, W.H. Wernsdorfer, S.R. Meshnick, Epidemiology of drug-resistant malaria., Lancet. Infect. Dis. 2 (2002) 209–18.

[109] P.J. Peters, M.C. Thigpen, M.E. Parise, R.D. Newman, Safety and toxicity of sulfadoxine/pyrimethamine: implications for malaria prevention in pregnancy using intermittent preventive treatment., Drug Saf. 30 (2007) 481–501.

[110] World Health Organization, Technical expert group meeting on preventive chemotherapy : report of the technical consultation on intermittent preventive

treatment in infants (IPTi), WHO Press. (2009).

[111] M. Fry, M. Pudney, Site of action of the antimalarial hydroxynaphthoquinone, 2-[trans-4-(4'-chlorophenyl) cyclohexyl]-3- hydroxy-1,4-naphthoquinone (566C80), Biochem. Pharmacol. 43 (1992) 1545–1553.

[112] H.J. Painter, J.M. Morrisey, M.W. Mather, A.B. Vaidya, Specific role of mitochondrial electron transport in blood-stage Plasmodium falciparum., Nature. 446 (2007) 88–91.

[113] S. Looareesuwan, C. Viravan, H.K. Webster, D.E. Kyle, D.B. Hutchinson, C.J. Canfield, Clinical studies of atovaquone, alone or in combination with other antimalarial drugs, for treatment of acute uncomplicated malaria in Thailand., Am. J. Trop. Med. Hyg. 54 (1996) 62–6.

[114] C.J. Canfield, M. Pudney, W.E. Gutteridge, Interactions of Atovaquone with Other Antimalarial Drugs against Plasmodium falciparum in Vitro, Exp. Parasitol. 80 (1995) 373–381.

[115] P.G. Bray, S.A. Ward, P.M. O'Neill, Quinolines and Artemisinin: Chemistry, Biology and History, in: Malar. Drugs, Dis. Post-Genomic Biol., Springer-Verlag, Berlin/Heidelberg, 2005: pp. 3–38.

[116] L. Tilley, J. Straimer, N.F. Gnädig, S.A. Ralph, D.A. Fidock, Artemisinin Action and Resistance in Plasmodium falciparum, Trends Parasitol. (2016).

[117] A. O. Achieng, M. Rawat, B. Ogutu, B. Guyah, J. Michael Ong'echa, D. J. Perkins, P. Kempaiah, Antimalarials: Molecular Drug Targets and Mechanism of Action, Curr. Top. Med. Chem. 17 (2017) 2114–2128.

[118] B. Meunier, A. Robert, Heme as Trigger and Target for Trioxane-Containing Antimalarial Drugs, Acc. Chem. Res. 43 (2010) 1444–1451.

[119] P.M. O'Neill, V.E. Barton, S.A. Ward, The molecular mechanism of action of artemisinin--the debate continues., Molecules. 15 (2010) 1705–21.

[120] S.R. Meshnick, Artemisinin: mechanisms of action, resistance and toxicity, Int. J. Parasitol. 32 (2002) 1655–1660.

[121] J. Li, B. Zhou, Biological Actions of Artemisinin: Insights from Medicinal Chemistry Studies, Molecules. 15 (2010) 1378–1397.

[122] A. Robert, F. Benoit-Vical, C. Claparols, B. Meunier, The antimalarial drug artemisinin alkylates heme in infected mice, Proc. Natl. Acad. Sci. 102 (2005) 13676–13680.

[123] J. Wang, L. Huang, J. Li, Q. Fan, Y. Long, Y. Li, B. Zhou, Artemisinin Directly Targets Malarial Mitochondria through Its Specific Mitochondrial Activation, PLoS One. 5 (2010) e9582.

[124] W.K. Milhous, M. Aikawa, Y. Maeno, T. Toyoshima, H. Fujioka, Y. Ito, A. Benakis, S.R. Meshnick, Morphologic Effects of Artemisinin in Plasmodium Falciparum, Am. J. Trop. Med. Hyg. 49 (1993) 485–491.

[125] A. V Pandey, B.L. Tekwani, R.L. Singh, V.S. Chauhan, Artemisinin, an endoperoxide antimalarial, disrupts the hemoglobin catabolism and heme detoxification systems in malarial parasite., J. Biol. Chem. 274 (1999) 19383–8.

[126] M. del Pilar Crespo, T.D. Avery, E. Hanssen, E. Fox, T. V. Robinson, P. Valente, D.K. Taylor, L. Tilley, Artemisinin and a Series of Novel Endoperoxide Antimalarials Exert Early Effects on Digestive Vacuole Morphology, Antimicrob. Agents Chemother. 52 (2008) 98–109.

[127] C.L. Hartwig, A.S. Rosenthal, J. D'Angelo, C.E. Griffin, G.H. Posner, R.A. Cooper, Accumulation of artemisinin trioxane derivatives within neutral lipids of Plasmodium falciparum malaria parasites is endoperoxide-dependent., Biochem. Pharmacol. 77 (2009) 322–36.

[128] A.M. Dondorp, F. Nosten, P. Yi, D. Das, A.P. Phyo, J. Tarning, K.M. Lwin, F. Ariey, W. Hanpithakpong, S.J. Lee, P. Ringwald, K. Silamut, M. Imwong, K. Chotivanich, P. Lim, T. Herdman, S.S. An, S. Yeung, P. Singhasivanon, N.P.J. Day, N. Lindegardh, D. Socheat, N.J. White, Artemisinin resistance in Plasmodium falciparum malaria., N. Engl. J. Med. 361 (2009) 455–67.

[129] E.A. Ashley, M. Dhorda, R.M. Fairhurst, C. Amaratunga, P. Lim, S. Suon, S. Sreng, J.M. Anderson, S. Mao, B. Sam, C. Sopha, C.M. Chuor, C. Nguon, S. Sovannaroth, S. Pukrittayakamee, P. Jittamala, K. Chotivanich, K. Chutasmit, C. Suchatsoonthorn, R. Runcharoen, T.T. Hien, N.T. Thuy-Nhien, N.V. Thanh, N.H. Phu, Y. Htut, K.-T. Han, K.H. Aye, O.A. Mokuolu, R.R. Olaosebikan, O.O. Folaranmi, M. Mayxay, M. Khanthavong, B. Hongvanthong, P.N. Newton, M.A. Onyamboko, C.I. Fanello, A.K. Tshefu, N. Mishra, N. Valecha, A.P. Phyo, F. Nosten, P. Yi, R. Tripura, S. Borrmann, M. Bashraheil, J. Peshu, M.A. Faiz, A. Ghose, M.A. Hossain, R. Samad, M.R. Rahman, M.M. Hasan, A. Islam, O. Miotto, R. Amato, B. MacInnis, J. Stalker, D.P. Kwiatkowski, Z. Bozdech, A. Jeeyapant, P.Y. Cheah, T. Sakulthaew, J. Chalk, B. Intharabut, K. Silamut, S.J. Lee, B. Vihokhern, C. Kunasol, M. Imwong, J. Tarning, W.J. Taylor, S. Yeung, C.J. Woodrow, J.A. Flegg, D. Das, J. Smith, M. Venkatesan, C. V Plowe, K. Stepniewska, P.J. Guerin, A.M. Dondorp, N.P. Day, N.J. White, Tracking Resistance to Artemisinin Collaboration (TRAC), Spread of artemisinin resistance in Plasmodium falciparum malaria., N. Engl. J. Med. 371 (2014) 411–23.

[130] N. White, Antimalarial drug resistance and combination chemotherapy, Philos. Trans. R. Soc. B Biol. Sci. 354 (1999) 739–749.

[131] I.M. Hastings, W.M. Watkins, N.J. White, The evolution of drug-resistant malaria: the role of drug elimination half-life., Philos. Trans. R. Soc. Lond. B. Biol. Sci. 357 (2002) 505–19.

[132] World Health Organization, Chemotherapy of malaria : report of a WHO scientific group, 1967.

[133] A.M. Thu, A.P. Phyo, J. Landier, D.M. Parker, F.H. Nosten, Combating multidrug-resistant *Plasmodium falciparum* malaria, FEBS J. 284 (2017) 2569–2578.

[134] D. Payne, Spread of chloroquine resistance in Plasmodium falciparum, Parasitol. Today. 3 (1987) 241–246.

[135] C. Roper, R. Pearce, S. Nair, B. Sharp, F. Nosten, T. Anderson, Intercontinental spread of pyrimethamine-resistant malaria., Science. 305 (2004) 1124.

[136] E.M. (Eric M. Scholar, W.B. Pratt, The antimicrobial drugs, Oxford University Press, 2000.

[137] A.F. Cowman, M.J. Morry, B.A. Biggs, G.A. Cross, S.J. Foote, Amino acid changes linked to pyrimethamine resistance in the dihydrofolate reductase-thymidylate synthase gene of Plasmodium falciparum., Proc. Natl. Acad. Sci. U. S. A. 85 (1988) 9109–13.

[138] D.S. Peterson, W.K. Milhous, T.E. Wellems, Molecular basis of differential resistance to cycloguanil and pyrimethamine in Plasmodium falciparum malaria., Proc. Natl. Acad. Sci. U. S. A. 87 (1990) 3018–22.

[139] S. Thaithong, S.W. Chan, S. Songsomboon, P. Wilairat, N. Seesod, T. Sueblinwong,

M. Goman, R. Ridley, G. Beale, Pyrimethamine resistant mutations in Plasmodium falciparum., Mol. Biochem. Parasitol. 52 (1992) 149–57.

[140] W. Sirawaraporn, T. Sathitkul, R. Sirawaraporn, Y. Yuthavong, D. V Santi, Antifolate-resistant mutants of Plasmodium falciparum dihydrofolate reductase., Proc. Natl. Acad. Sci. U. S. A. 94 (1997) 1124–9.

[141] D.R. Brooks, P. Wang, M. Read, W.M. Watkins, P.F. Sims, J.E. Hyde, Sequence variation of the hydroxymethyldihydropterin pyrophosphokinase: dihydropteroate synthase gene in lines of the human malaria parasite, Plasmodium falciparum, with differing resistance to sulfadoxine., Eur. J. Biochem. 224 (1994) 397–405.

[142] T. Triglia, A.F. Cowman, Primary structure and expression of the dihydropteroate synthetase gene of Plasmodium falciparum., Proc. Natl. Acad. Sci. U. S. A. 91 (1994) 7149–53.

[143] P. Wang, C.S. Lee, R. Bayoumi, A. Djimde, O. Doumbo, G. Swedberg, L.D. Dao, H. Mshinda, M. Tanner, W.M. Watkins, P.F. Sims, J.E. Hyde, Resistance to antifolates in Plasmodium falciparum monitored by sequence analysis of dihydropteroate synthetase and dihydrofolate reductase alleles in a large number of field samples of diverse origins., Mol. Biochem. Parasitol. 89 (1997) 161–77.

[144] A. Djimdé, O.K. Doumbo, J.F. Cortese, K. Kayentao, S. Doumbo, Y. Diourté, D. Coulibaly, A. Dicko, X. Su, T. Nomura, D.A. Fidock, T.E. Wellems, C. V. Plowe, A Molecular Marker for Chloroquine-Resistant Falciparum Malaria, N. Engl. J. Med. 344 (2001) 257–263.

[145] A.B.S. Sidhu, D. Verdier-Pinard, D.A. Fidock, Chloroquine Resistance in Plasmodium falciparum Malaria Parasites Conferred by pfcrt Mutations, Science (80-.). 298 (2002) 210–213.

[146] V. Lakshmanan, P.G. Bray, D. Verdier-Pinard, D.J. Johnson, P. Horrocks, R.A. Muhle, G.E. Alakpa, R.H. Hughes, S.A. Ward, D.J. Krogstad, A.B.S. Sidhu, D.A. Fidock, A critical role for PfCRT K76T in Plasmodium falciparum verapamil-reversible chloroquine resistance., EMBO J. 24 (2005) 2294–305.

[147] S.G. Valderramos, D.A. Fidock, Transporters involved in resistance to antimalarial drugs, Trends Pharmacol. Sci. 27 (2006) 594–601.

[148] C.P. Sanchez, W.D. Stein, M. Lanzer, Is PfCRT a channel or a carrier? Two competing models explaining chloroquine resistance in Plasmodium falciparum, Trends Parasitol. 23 (2007) 332–339.

[149] L. Cui, Z. Wang, H. Jiang, D. Parker, H. Wang, X.-Z. Su, L. Cui, Lack of association of the S769N mutation in Plasmodium falciparum SERCA (PfATP6) with resistance to artemisinins., Antimicrob. Agents Chemother. 56 (2012) 2546–52.

[150] B. Witkowski, C. Amaratunga, N. Khim, S. Sreng, P. Chim, S. Kim, P. Lim, S. Mao, C. Sopha, B. Sam, J.M. Anderson, S. Duong, C.M. Chuor, W.R.J. Taylor, S. Suon, O. Mercereau-Puijalon, R.M. Fairhurst, D. Menard, Novel phenotypic assays for the detection of artemisinin-resistant Plasmodium falciparum malaria in Cambodia: in-vitro and ex-vivo drug-response studies, Lancet Infect. Dis. 13 (2013) 1043–1049.

[151] S. Mok, E.A. Ashley, P.E. Ferreira, L. Zhu, Z. Lin, T. Yeo, K. Chotivanich, M. Imwong, S. Pukrittayakamee, M. Dhorda, C. Nguon, P. Lim, C. Amaratunga, S. Suon, T.T. Hien, Y. Htut, M.A. Faiz, M.A. Onyamboko, M. Mayxay, P.N. Newton, R. Tripura, C.J. Woodrow, O. Miotto, D.P. Kwiatkowski, F. Nosten, N.P.J. Day, P.R. Preiser, N.J. White, A.M. Dondorp, R.M. Fairhurst, Z. Bozdech, Drug resistance. Population transcriptomics of human malaria parasites reveals the mechanism of artemisinin

resistance., Science. 347 (2015) 431–5.

[152] S. Takala-Harrison, T.G. Clark, C.G. Jacob, M.P. Cummings, O. Miotto, A.M. Dondorp, M.M. Fukuda, F. Nosten, H. Noedl, M. Imwong, D. Bethell, Y. Se, C. Lon, S.D. Tyner, D.L. Saunders, D. Socheat, F. Ariey, A.P. Phyo, P. Starzengruber, H.-P. Fuehrer, P. Swoboda, K. Stepniewska, J. Flegg, C. Arze, G.C. Cerqueira, J.C. Silva, S.M. Ricklefs, S.F. Porcella, R.M. Stephens, M. Adams, L.J. Kenefic, S. Campino, S. Auburn, B. MacInnis, D.P. Kwiatkowski, X. -z. Su, N.J. White, P. Ringwald, C. V. Plowe, Genetic loci associated with delayed clearance of Plasmodium falciparum following artemisinin treatment in Southeast Asia, Proc. Natl. Acad. Sci. 110 (2013) 240–245.

[153] I.H. Cheeseman, B.A. Miller, S. Nair, S. Nkhoma, A. Tan, J.C. Tan, S. Al Saai, A.P. Phyo, C.L. Moo, K.M. Lwin, R. McGready, E. Ashley, M. Imwong, K. Stepniewska, P. Yi, A.M. Dondorp, M. Mayxay, P.N. Newton, N.J. White, F. Nosten, M.T. Ferdig, T.J.C. Anderson, A Major Genome Region Underlying Artemisinin Resistance in Malaria, Science (80-.). 336 (2012) 79–82.

[154] O. Miotto, J. Almagro-Garcia, M. Manske, B. MacInnis, S. Campino, K.A. Rockett, C. Amaratunga, P. Lim, S. Suon, S. Sreng, J.M. Anderson, S. Duong, C. Nguon, C.M. Chuor, D. Saunders, Y. Se, C. Lon, M.M. Fukuda, L. Amenga-Etego, A.V.O. Hodgson, V. Asoala, M. Imwong, S. Takala-Harrison, F. Nosten, X. Su, P. Ringwald, F. Ariey, C. Dolecek, T.T. Hien, M.F. Boni, C.Q. Thai, A. Amambua-Ngwa, D.J. Conway, A.A. Djimdé, O.K. Doumbo, I. Zongo, J.-B. Ouedraogo, D. Alcock, E. Drury, S. Auburn, O. Koch, M. Sanders, C. Hubbart, G. Maslen, V. Ruano-Rubio, D. Jyothi, A. Miles, J. O'Brien, C. Gamble, S.O. Oyola, J.C. Rayner, C.I. Newbold, M. Berriman, C.C.A. Spencer, G. McVean, N.P. Day, N.J. White, D. Bethell, A.M. Dondorp, C. V Plowe, R.M. Fairhurst, D.P. Kwiatkowski, Multiple populations of artemisinin-resistant Plasmodium falciparum in Cambodia, Nat. Genet. 45 (2013) 648–655.

[155] F. Ariey, B. Witkowski, C. Amaratunga, J. Beghain, A.-C. Langlois, N. Khim, S. Kim, V. Duru, C. Bouchier, L. Ma, P. Lim, R. Leang, S. Duong, S. Sreng, S. Suon, C.M. Chuor, D.M. Bout, S. Ménard, W.O. Rogers, B. Genton, T. Fandeur, O. Miotto, P. Ringwald, J. Le Bras, A. Berry, J.-C. Barale, R.M. Fairhurst, F. Benoit-Vical, O. Mercereau-Puijalon, D. Ménard, A molecular marker of artemisinin-resistant Plasmodium falciparum malaria., Nature. 505 (2014) 50–5.

[156] R. Isozumi, H. Uemura, I. Kimata, Y. Ichinose, J. Logedi, A.H. Omar, A. Kaneko, Novel Mutations in K13 Propeller Gene of Artemisinin-Resistant *Plasmodium falciparum*, Emerg. Infect. Dis. 21 (2015) 490–492.

[157] J. Straimer, N.F. Gnadig, B. Witkowski, C. Amaratunga, V. Duru, A.P. Ramadani, M. Dacheux, N. Khim, L. Zhang, S. Lam, P.D. Gregory, F.D. Urnov, O. Mercereau-Puijalon, F. Benoit-Vical, R.M. Fairhurst, D. Menard, D.A. Fidock, K13-propeller mutations confer artemisinin resistance in Plasmodium falciparum clinical isolates, Science (80-.). 347 (2015) 428–431.

[158] M.H. Nyunt, T. Hlaing, H.W. Oo, L.-L.K. Tin-Oo, H.P. Phway, B. Wang, N.N. Zaw, S.S. Han, T. Tun, K.K. San, M.P. Kyaw, E.-T. Han, Molecular Assessment of Artemisinin Resistance Markers, Polymorphisms in the K13 Propeller, and a Multidrug-Resistance Gene in the Eastern and Western Border Areas of Myanmar, Clin. Infect. Dis. 60 (2015) 1208–1215.

[159] D.R. Pillai, A. Alemu, S. Getie, A.G. Bayih, A.N. Mohon, G. Getnet, A Unique Plasmodium falciparum K13 Gene Mutation in Northwest Ethiopia, Am. J. Trop. Med. Hyg. 94 (2016) 132–135.

[160] A. Vaid, R. Ranjan, W.A. Smythe, H.C. Hoppe, P. Sharma, PfPI3K, a

phosphatidylinositol-3 kinase from Plasmodium falciparum, is exported to the host erythrocyte and is involved in hemoglobin trafficking., Blood. 115 (2010) 2500–7.

[161] A. Mbengue, S. Bhattacharjee, T. Pandharkar, H. Liu, G. Estiu, R. V Stahelin, S.S. Rizk, D.L. Njimoh, Y. Ryan, K. Chotivanich, C. Nguon, M. Ghorbal, J.-J. Lopez-Rubio, M. Pfrender, S. Emrich, N. Mohandas, A.M. Dondorp, O. Wiest, K. Haldar, A molecular mechanism of artemisinin resistance in Plasmodium falciparum malaria., Nature. 520 (2015) 683–7.

[162] P. Rohrbach, C.P. Sanchez, K. Hayton, O. Friedrich, J. Patel, A.B.S. Sidhu, M.T. Ferdig, D.A. Fidock, M. Lanzer, Genetic linkage of pfmdr1 with food vacuolar solute import in Plasmodium falciparum., EMBO J. 25 (2006) 3000–11.

[163] C.P. Sanchez, A. Rotmann, W.D. Stein, M. Lanzer, Polymorphisms within PfMDR1 alter the substrate specificity for anti-malarial drugs in *Plasmodium falciparum*, Mol. Microbiol. 70 (2008) 786–98.

[164] C.P. Sanchez, A. Dave, W.D. Stein, M. Lanzer, Transporters as mediators of drug resistance in Plasmodium falciparum, Int. J. Parasitol. 40 (2010) 1109–1118.

[165] M. Mishra, V.K. Mishra, V. Kashaw, A.K. Iyer, S.K. Kashaw, Comprehensive review on various strategies for antimalarial drug discovery., Eur. J. Med. Chem. 125 (2017) 1300–1320.

[166] J.S. McCarthy, T. Rückle, E. Djeriou, C. Cantalloube, D. Ter-Minassian, M. Baker, P. O'Rourke, P. Griffin, L. Marquart, R. Hooft van Huijsduijnen, J.J. Möhrle, A Phase II pilot trial to evaluate safety and efficacy of ferroquine against early Plasmodium falciparum in an induced blood-stage malaria infection study., Malar. J. 15 (2016) 469.

[167] J. Held, C. Supan, C.L.O. Salazar, H. Tinto, L.N. Bonkian, A. Nahum, B. Moulero, A. Sié, B. Coulibaly, S.B. Sirima, M. Siribie, N. Otsyula, L. Otieno, A.M. Abdallah, R. Kimutai, M. Bouyou-Akotet, M. Kombila, K. Koiwai, C. Cantalloube, C. Din-Bell, E. Djeriou, J. Waitumbi, B. Mordmüller, D. Ter-Minassian, B. Lell, P.G. Kremsner, Ferroquine and artesunate in African adults and children with Plasmodium falciparum malaria: a phase 2, multicentre, randomised, double-blind, dose-ranging, non-inferiority study, Lancet Infect. Dis. 15 (2015) 1409–1419.

[168] F. Dubar, S. Bohic, D. Dive, Y. Guérardel, P. Cloetens, J. Khalife, C. Biot, Deciphering the Resistance-Counteracting Functions of Ferroquine in *Plasmodium falciparum* -Infected Erythrocytes, ACS Med. Chem. Lett. 3 (2012) 480–483.

[169] T. Yang, S.C. Xie, P. Cao, C. Giannangelo, J. McCaw, D.J. Creek, S.A. Charman, N. Klonis, L. Tilley, Comparison of the Exposure Time Dependence of the Activities of Synthetic Ozonide Antimalarials and Dihydroartemisinin against K13 Wild-Type and Mutant Plasmodium falciparum Strains., Antimicrob. Agents Chemother. 60 (2016) 4501–10.

[170] S.A. Charman, S. Arbe-Barnes, I.C. Bathurst, R. Brun, M. Campbell, W.N. Charman, F.C.K. Chiu, J. Chollet, J.C. Craft, D.J. Creek, Y. Dong, H. Matile, M. Maurer, J. Morizzi, T. Nguyen, P. Papastogiannidis, C. Scheurer, D.M. Shackleford, K. Sriraghavan, L. Stingelin, Y. Tang, H. Urwyler, X. Wang, K.L. White, S. Wittlin, L. Zhou, J.L. Vennerstrom, Synthetic ozonide drug candidate OZ439 offers new hope for a single-dose cure of uncomplicated malaria., Proc. Natl. Acad. Sci. U. S. A. 108 (2011) 4400–5.

[171] A.P. Phyo, P. Jittamala, F.H. Nosten, S. Pukrittayakamee, M. Imwong, N.J. White, S. Duparc, F. Macintyre, M. Baker, J.J. Möhrle, Antimalarial activity of artefenomel (OZ439), a novel synthetic antimalarial endoperoxide, in patients with Plasmodium falciparum and Plasmodium vivax malaria: an open-label phase 2 trial., Lancet. Infect.

Dis. 16 (2016) 61–69.

[172] P.J. Rosenthal, Artefenomel: a promising new antimalarial drug., Lancet. Infect. Dis. 16 (2016) 6–8.

[173] T. Gaillard, J. Dormoi, M. Madamet, B. Pradines, Macrolides and associated antibiotics based on similar mechanism of action like lincosamides in malaria, Malar. J. 15 (2016) 85.

[174] T. Gaillard, M. Madamet, B. Pradines, Tetracyclines in malaria., Malar. J. 14 (2015) 445.

[175] A. Nzila, The past, present and future of antifolates in the treatment of Plasmodium falciparum infection, J. Antimicrob. Chemother. 57 (2006) 1043–1054.

[176] S. Meister, D.M. Plouffe, K.L. Kuhen, G.M.C. Bonamy, T. Wu, S.W. Barnes, S.E. Bopp, R. Borboa, A.T. Bright, J. Che, S. Cohen, N. V. Dharia, K. Gagaring, M. Gettayacamin, P. Gordon, T. Groessl, N. Kato, M.C.S. Lee, C.W. McNamara, D.A. Fidock, A. Nagle, T. -g. Nam, W. Richmond, J. Roland, M. Rottmann, B. Zhou, P. Froissard, R.J. Glynne, D. Mazier, J. Sattabongkot, P.G. Schultz, T. Tuntland, J.R. Walker, Y. Zhou, A. Chatterjee, T.T. Diagana, E.A. Winzeler, Imaging of Plasmodium Liver Stages to Drive Next-Generation Antimalarial Drug Discovery, Science (80-.). 334 (2011) 1372–1377.

[177] O. Dechy-Cabaret, F. Benoit-Vical, C. Loup, A. Robert, H. Gornitzka, A. Bonhoure, H. Vial, J.-F. Magnaval, J.-P. Séguéla, B. Meunier, Synthesis and Antimalarial Activity of Trioxaquine Derivatives, Chem. - A Eur. J. 10 (2004) 1625–1636.

[178] F. Benoit-Vical, J. Lelievre, A. Berry, C. Deymier, O. Dechy-Cabaret, J. Cazelles, C. Loup, A. Robert, J.-F. Magnaval, B. Meunier, Trioxaquines Are New Antimalarial Agents Active on All Erythrocytic Forms, Including Gametocytes, Antimicrob. Agents Chemother. 51 (2007) 1463–1472.

[179] M. Rottmann, C. McNamara, B.K.S. Yeung, M.C.S. Lee, B. Zou, B. Russell, P. Seitz, D.M. Plouffe, N. V Dharia, J. Tan, S.B. Cohen, K.R. Spencer, G.E. González-Páez, S.B. Lakshminarayana, A. Goh, R. Suwanarusk, T. Jegla, E.K. Schmitt, H.-P. Beck, R. Brun, F. Nosten, L. Renia, V. Dartois, T.H. Keller, D.A. Fidock, E.A. Winzeler, T.T. Diagana, Spiroindolones, a potent compound class for the treatment of malaria., Science (80-.). 329 (2010) 1175–80.

[180] B.K.S. Yeung, B. Zou, M. Rottmann, S.B. Lakshminarayana, S.H. Ang, S.Y. Leong, J. Tan, J. Wong, S. Keller-Maerki, C. Fischli, A. Goh, E.K. Schmitt, P. Krastel, E. Francotte, K. Kuhen, D. Plouffe, K. Henson, T. Wagner, E.A. Winzeler, F. Petersen, R. Brun, V. Dartois, T.T. Diagana, T.H. Keller, Spirotetrahydro beta-carbolines (spiroindolones): a new class of potent and orally efficacious compounds for the treatment of malaria., J. Med. Chem. 53 (2010) 5155–64.

[181] M.B. Jiménez-Díaz, D. Ebert, Y. Salinas, A. Pradhan, A.M. Lehane, M.-E. Myrand-Lapierre, K.G. O'Loughlin, D.M. Shackleford, M. Justino de Almeida, A.K. Carrillo, J.A. Clark, A.S.M. Dennis, J. Diep, X. Deng, S. Duffy, A.N. Endsley, G. Fedewa, W.A. Guiguemde, M.G. Gómez, G. Holbrook, J. Horst, C.C. Kim, J. Liu, M.C.S. Lee, A. Matheny, M.S. Martínez, G. Miller, A. Rodríguez-Alejandre, L. Sanz, M. Sigal, N.J. Spillman, P.D. Stein, Z. Wang, F. Zhu, D. Waterson, S. Knapp, A. Shelat, V.M. Avery, D.A. Fidock, F.-J. Gamo, S.A. Charman, J.C. Mirsalis, H. Ma, S. Ferrer, K. Kirk, I. Angulo-Barturen, D.E. Kyle, J.L. DeRisi, D.M. Floyd, R.K. Guy, (+)-SJ733, a clinical candidate for malaria that acts through ATP4 to induce rapid host-mediated clearance of Plasmodium., Proc. Natl. Acad. Sci. U. S. A. (2014).

[182] A.B. Vaidya, J.M. Morrisey, Z. Zhang, S. Das, T.M. Daly, T.D. Otto, N.J. Spillman, M.

Wyvratt, P. Siegl, J. Marfurt, G. Wirjanata, B.F. Sebayang, R.N. Price, A. Chatterjee, A. Nagle, M. Stasiak, S.A. Charman, I. Angulo-Barturen, S. Ferrer, M. Belén Jiménez-Díaz, M.S. Martínez, F.J. Gamo, V.M. Avery, A. Ruecker, M. Delves, K. Kirk, M. Berriman, S. Kortagere, J. Burrows, E. Fan, L.W. Bergman, Pyrazoleamide compounds are potent antimalarials that target Na(+) homeostasis in intraerythrocytic Plasmodium falciparum., Nat. Commun. 5 (2014) 5521.

[183] E.L. Flannery, A.K. Chatterjee, E.A. Winzeler, Antimalarial drug discovery - approaches and progress towards new medicines., Nat. Rev. Microbiol. 11 (2013) 849–62.

[184] J.L. Vennerstrom, S. Arbe-Barnes, R. Brun, S.A. Charman, F.C.K. Chiu, J. Chollet, Y. Dong, A. Dorn, D. Hunziker, H. Matile, K. McIntosh, M. Padmanilayam, J. Santo Tomas, C. Scheurer, B. Scorneaux, Y. Tang, H. Urwyler, S. Wittlin, W.N. Charman, Identification of an antimalarial synthetic trioxolane drug development candidate., Nature. 430 (2004) 900–4.

[185] S.A. Charman, S. Arbe-Barnes, I.C. Bathurst, R. Brun, M. Campbell, W.N. Charman, F.C.K. Chiu, J. Chollet, J.C. Craft, D.J. Creek, Y. Dong, H. Matile, M. Maurer, J. Morizzi, T. Nguyen, P. Papastogiannidis, C. Scheurer, D.M. Shackleford, K. Sriraghavan, L. Stingelin, Y. Tang, H. Urwyler, X. Wang, K.L. White, S. Wittlin, L. Zhou, J.L. Vennerstrom, Synthetic ozonide drug candidate OZ439 offers new hope for a single-dose cure of uncomplicated malaria., Proc. Natl. Acad. Sci. U. S. A. 108 (2011) 4400–5.

[186] J. Leban, S. Pegoraro, M. Dormeyer, M. Lanzer, A. Aschenbrenner, B. Kramer, Sulfonyl-phenyl-ureido benzamidines; a novel structural class of potent antimalarial agents., Bioorg. Med. Chem. Lett. 14 (2004) 1979–82.

[187] A.J. De Vos, P.R. Barrowman, J.A. Coetzer, T.S. Kellerman, Amicarbalide: a therapeutic agent for anaplasmosis., Onderstepoort J. Vet. Res. 45 (1978) 203–8.

[188] G.G.L. Beveridge., J.W. Thwaite, G. Shepherd, A field trial of amicarbalide -a new babesicide., Vet. Rec. 72 (1960) 383–386.

[189] S. Pegoraro, M. Duffey, T.D. Otto, Y. Wang, R. Rösemann, R. Baumgartner, S.K. Fehler, L. Lucantoni, V.M. Avery, A. Moreno-Sabater, D. Mazier, H.J. Vial, S. Strobl, C.P. Sanchez, M. Lanzer, A.M. Dondorp, E.A. Ashley, M.B. Jimenez-Diaz, S.A. Charman, H.J. Vial, J. Held, S. Jeyaraj, A. Kreidenweiss, F. Cosledan, P.S. Hameed, S. Ramachandran, A. Nilsen, B. Baragana, A.B. Vaidya, T. Rolling, T. Agbenyega, S. Krishna, P.G. Kremsner, J.P. Cramer, K. Rehman, F. Lotsch, P.G. Kremsner, M. Ramharter, J. Achan, J. Leban, J.N. Ashley, S.S. Berg, J.M. Lucas, A.J. De Vos, P.R. Barrowman, J.A. Coetzer, T.S. Kellerman, G.G.L. Beveridge, J.W. Thwaite, G. Shepherd, C. Reeh, J. Wundt, B. Clement, R.E. Desjardins, C.J. Canfield, J.D. Haynes, J.D. Chulay, L.M. Sanz, A.M. Stead, S. Baumeister, I. Angulo-Barturen, B.J. Ring, Y. Cao, W.J. Jusko, P. Linder, E. Jankowsky, J.P. Rubio, A.F. Cowman, M.G. Zalis, C.M. Wilson, Y. Zhang, D.F. Wirth, E. Rosenberg, M. van der Velden, S.R. Rijpma, F.G. Russel, R.W. Sauerwein, J.B. Koenderink, S. David-Bosne, J.N. Burrows, R.H. van Huijsduijnen, J.J. Mohrle, C. Oeuvray, T.N. Wells, A.C. Uhlemann, U. Eckstein-Ludwig, S. David-Bosne, A. Mbengue, L. Steimer, D. Klostermeier, W. Trager, J.B. Jensen, M. Smilkstein, N. Sriwilaijaroen, J.X. Kelly, P. Wilairat, M. Riscoe, N. Elabbadi, M.L. Ancelin, H.J. Vial, N. Ibrahim, N. Van Rooijen, A. Sanders, F. Tacchini-Cottier, M.A. Quail, T.D. Otto, M. Sanders, M. Berriman, C. Newbold, T.D. Otto, G.P. Dillon, W.S. Degrave, M. Berriman, B. Langmead, S.L. Salzberg, A. McKenna, H. Li, T. Carver, P. Rohrbach, L. Lucantoni, S. Duffy, S.H. Adjalley, D.A. Fidock, V.M. Avery, L. Lucantoni, D.A. Fidock, V.M. Avery, S. Duffy, S. Loganathan, J.P. Holleran, V.M. Avery, M. Turpeinen, J. Uusitalo, J. Jalonen, O. Pelkonen, M.W.

Karaman, H. Boxenbaum, SC83288 is a clinical development candidate for the treatment of severe malaria, Nat. Commun. 8 (2017) 14193.

[190] F. Guinet, J.A. Dvorak, H. Fujioka, D.B. Keister, O. Muratova, D.C. Kaslow, M. Aikawa, A.B. Vaidya, T.E. Wellems, A developmental defect in Plasmodium falciparum male gametogenesis., J. Cell Biol. 135 (1996) 269–78.

[191] V.K. Bhasin, W. Trager, Gametocyte-forming and non-gametocyte-forming clones of Plasmodium falciparum., Am. J. Trop. Med. Hyg. 33 (1984) 534–7.

[192] D. Walliker, I.A. Quakyi, T.E. Wellems, T.F. McCutchan, A. Szarfman, W.T. London, L.M. Corcoran, T.R. Burkot, R. Carter, Genetic analysis of the human malaria parasite Plasmodium falciparum., Science. 236 (1987) 1661–6.

[193] J.P. Doherty, R. Lindeman, R.J. Trent, M.W. Graham, D.M. Woodcock, Escherichia coli host strains SURE and SRB fail to preserve a palindrome cloned in lambda phage: improved alternate host strains., Gene. 124 (1993) 29–35.

[194] C. Lambros, J.P. Vanderberg, Synchronization of Plasmodium falciparum erythrocytic stages in culture., J. Parasitol. 65 (1979) 418–20.

[195] F. Sanger, S. Nicklen, A.R. Coulson, DNA sequencing with chain-terminating inhibitors., Proc. Natl. Acad. Sci. U. S. A. 74 (1977) 5463–7.

[196] M. Smilkstein, N. Sriwilaijaroen, J.X. Kelly, P. Wilairat, M. Riscoe, Simple and inexpensive fluorescence-based technique for high-throughput antimalarial drug screening., Antimicrob. Agents Chemother. 48 (2004) 1803–6.

[197] C. Le Manach, C. Scheurer, S. Sax, S. Schleiferböck, D. Cabrera, Y. Younis, T. Paquet, L. Street, P. Smith, X.C. Ding, D. Waterson, M.J. Witty, D. Leroy, K. Chibale, S. Wittlin, A. Dondorp, F. Nosten, P. Yi, D. Das, A. Phyo, J. Tarning, K. Lwin, F. Ariey, W. Hanpithakpong, S. Lee, P. Ringwald, K. Silamut, M. Imwong, K. Chotivanich, P. Lim, T. Herdman, S. An, S. Yeung, P. Singhasivanon, N. Day, N. Lindegardh, D. Socheat, N. White, A. Phyo, S. Nkhoma, K. Stepniewska, E. Ashley, S. Nair, R. McGready, C. ler Moo, S. Al-Saai, A. Dondorp, K. Lwin, P. Singhasivanon, N. Day, N. White, T. Anderson, F. Nosten, D. Fidock, F. Gamo, L. Sanz, J. Vidal, C. de Cozar, E. Alvarez, J. Lavandera, D. Vanderwall, D. Green, V. Kumar, S. Hasan, J. Brown, C. Peishoff, L. Cardon, J. Garcia-Bustos, D. Plouffe, A. Brinker, C. McNamara, K. Henson, N. Kato, K. Kuhen, A. Nagle, F. Adrian, J. Matzen, P. Anderson, T. Nam, N. Gray, A. Chatterjee, J. Janes, S. Yan, R. Trager, J. Caldwell, P. Schultz, Y. Zhou, E. Winzeler, W. Guiguemde, A. Shelat, D. Bouck, S. Duffy, G. Crowther, P. Davis, D. Smithson, M. Connelly, J. Clark, F. Zhu, M. Jiménez-Diaz, M. Martinez, E. Wilson, A. Tripathi, J. Gut, E. Sharlow, I. Bathurst, F. El Mazouni, J. Fowble, I. Forquer, P. McGinley, S. Castro, I. Angulo-Barturen, S. Ferrer, P. Rosenthal, J. DeRisi, D. Sullivan, J. Lazo, D. Roos, M. Riscoe, T. Wells, P. Alonso, W. Gutteridge, J. Burrows, D. Leroy, J. Lotharius, D. Waterson, M. Biamonte, J. Wanner, K. Le Roch, J. Burrows, R.H. van Huijsduijnen, J. Möhrle, C. Oeuvray, T. Wells, L. Sanz, B. Crespo, C. De-Cozar, X. Ding, J. Llergo, J. Burrows, J. Garcia-Bustos, F.-J. Gamo, Y. Younis, F. Douelle, T.-S. Feng, D.G. Cabrera, C. Le Manach, A. Nchinda, S. Duffy, K. White, D. Shackleford, J. Morizzi, J. Mannila, K. Katneni, R. Bhamidipati, K. Zabiulla, J. Joseph, S. Bashyam, D. Waterson, M. Witty, D. Hardick, S. Wittlin, V. Avery, S. Charman, K. Chibale, D.G. Cabrera, F. Douelle, T.-S. Feng, A. Nchinda, Y. Younis, L. White, Q. Wu, E. Ryan, J. Burrows, D. Waterson, M. Witty, S. Wittlin, S. Charman, K. Chibale, J. Harris, D. Hill, W. Sheppard, J. Slater, W. Stouten, W. Trager, J. Jensen, C. Snyder, J. Chollet, J. Santo-Tomas, C. Scheurer, S. Wittlin, S. Hofer, R. Brun, S. Maerki, C. Scheurer, S. Wittlin, A. Dieckmann, A. Jung, D. Wilson, C. Langer, C. Goodman, G. McFadden, J. Beeson, H. Painter, J. Morrisey, A. Vaidya, E. Dahl, P. Rosenthal, S. Maerki, R. Brun, S. Charman, A. Dorn, H. Matile, S. Wittlin, Fast in vitro methods to

determine the speed of action and the stage-specificity of anti-malarials in Plasmodium falciparum, Malar. J. 12 (2013) 424.

[198] L.M. Sanz, B. Crespo, C. De-Cózar, X.C. Ding, J.L. Llergo, J.N. Burrows, J.F. García-Bustos, F.-J. Gamo, P. falciparum in vitro killing rates allow to discriminate between different antimalarial mode-of-action., PLoS One. 7 (2012) e30949.

[199] M. Linares, S. Viera, B. Crespo, V. Franco, M.G. Gómez-Lorenzo, M.B. Jiménez-Díaz, Í. Angulo-Barturen, L.M. Sanz, F.-J. Gamo, Identifying rapidly parasiticidal anti-malarial drugs using a simple and reliable in vitro parasite viability fast assay., Malar. J. 14 (2015) 441.

[200] Q.L. Fivelman, I.S. Adagu, D.C. Warhurst, Modified fixed-ratio isobologram method for studying in vitro interactions between atovaquone and proguanil or dihydroartemisinin against drug-resistant strains of Plasmodium falciparum., Antimicrob. Agents Chemother. 48 (2004) 4097–102.

[201] M. Ganter, J.M. Goldberg, J.D. Dvorin, J.A. Paulo, J.G. King, A.K. Tripathi, A.S. Paul, J. Yang, I. Coppens, R.H.Y. Jiang, B. Elsworth, D.A. Baker, R.R. Dinglasan, S.P. Gygi, M.T. Duraisingh, Plasmodium falciparum CRK4 directs continuous rounds of DNA replication during schizogony, Nat. Microbiol. 2 (2017) 17017.

[202] P. Rohrbach, O. Friedrich, H. Plattner, R.H.A. Fink, M. Lanzer, J. Hentschel, Quantitative Calcium Measurements in Subcellular Compartments of Plasmodium falciparum -infected Erythrocytes Quantitative Calcium Measurements in Subcellular Compartments of Plasmodium falciparum -infected Erythrocytes *, J. Biol. Chem. 280 (2005) 27960–27969.

[203] R.T. Eastman, D.A. Fidock, Artemisinin-based combination therapies: a vital tool in efforts to eliminate malaria., Nat. Rev. Microbiol. 7 (2009) 864–74.

[204] S. Krishna, S. Pulcini, C.M. Moore, B.H.-Y. Teo, H.M. Staines, Pumped up: reflections on PfATP6 as the target for artemisinins., Trends Pharmacol. Sci. 35 (2014) 4–11.

[205] S. Takala-Harrison, C.G. Jacob, C. Arze, M.P. Cummings, J.C. Silva, A.M. Dondorp, M.M. Fukuda, T.T. Hien, M. Mayxay, H. Noedl, F. Nosten, M.P. Kyaw, N.T.T. Nhien, M. Imwong, D. Bethell, Y. Se, C. Lon, S.D. Tyner, D.L. Saunders, F. Ariey, O. Mercereau-Puijalon, D. Menard, P.N. Newton, M. Khanthavong, B. Hongvanthong, P. Starzengruber, H.-P. Fuehrer, P. Swoboda, W.A. Khan, A.P. Phyo, M.M. Nyunt, M.H. Nyunt, T.S. Brown, M. Adams, C.S. Pepin, J. Bailey, J.C. Tan, M.T. Ferdig, T.G. Clark, O. Miotto, B. MacInnis, D.P. Kwiatkowski, N.J. White, P. Ringwald, C. V Plowe, Independent Emergence of Artemisinin Resistance Mutations Among Plasmodium falciparum in Southeast Asia., J. Infect. Dis. 211 (2014) 670–9.

[206] A. Bell, Antimalarial drug synergism and antagonism: mechanistic and clinical significance., FEMS Microbiol. Lett. 253 (2005) 171–84.

[207] S. David-Bosne, I. Florent, A.-M. Lund-Winther, J.B. Hansen, M. Buch-Pedersen, P. Machillot, M. le Maire, C. Jaxel, Antimalarial screening via large-scale purification of Plasmodium falciparum Ca2+-ATPase 6 and in vitro studies., FEBS J. 280 (2013) 5419–29.

[208] J.K. Pittman, Vacuolar Ca(2+) uptake., Cell Calcium. 50 (2011) 139–46.

[209] Z. Zhou, A.C. Poe, J. Limor, K.K. Grady, I. Goldman, A.M. McCollum, A.A. Escalante, J.W. Barnwell, V. Udhayakumar, Pyrosequencing, a high-throughput method for detecting single nucleotide polymorphisms in the dihydrofolate reductase and dihydropteroate synthetase genes of Plasmodium falciparum., J. Clin. Microbiol. 44 (2006) 3900–10.

[210] I. Petersen, S.J. Gabryszewski, G.L. Johnston, S.K. Dhingra, A. Ecker, R.E. Lewis, M.J. de Almeida, J. Straimer, P.P. Henrich, E. Palatulan, D.J. Johnson, O. Coburn-Flynn, C. Sanchez, A.M. Lehane, M. Lanzer, D.A. Fidock, Balancing drug resistance and growth rates via compensatory mutations in the Plasmodium falciparum chloroquine resistance transporter., Mol. Microbiol. 97 (2015) 381–95.

[211] S. Das, N. Hertrich, A.J. Perrin, C. Withers-Martinez, C.R. Collins, M.L. Jones, J.M. Watermeyer, E.T. Fobes, S.R. Martin, H.R. Saibil, G.J. Wright, M. Treeck, C. Epp, M.J. Blackman, Processing of Plasmodium falciparum Merozoite Surface Protein MSP1 Activates a Spectrin-Binding Function Enabling Parasite Egress from RBCs, Cell Host Microbe. 18 (2015) 433–444.

[212] T.N.C. Wells, R.H. van Huijsduijnen, W.C. Van Voorhis, Malaria medicines: a glass half full?, Nat. Rev. Drug Discov. 14 (2015) 424–442.

[213] J.N. Burrows, S. Duparc, W.E. Gutteridge, R. Hooft van Huijsduijnen, W. Kaszubska, F. Macintyre, S. Mazzuri, J.J. Möhrle, T.N.C. Wells, New developments in anti-malarial target candidate and product profiles, Malar. J. 16 (2017) 26.

[214] J.N. Burrows, R.H. van Huijsduijnen, J.J. Möhrle, C. Oeuvray, T.N.C. Wells, Designing the next generation of medicines for malaria control and eradication., Malar. J. 12 (2013) 187.

[215] Centers for Disease Control and Prevention (CDC), Published reports of delayed hemolytic anemia after treatment with artesunate for severe malaria worldwide, 2010-2012., MMWR. Morb. Mortal. Wkly. Rep. 62 (2013) 5–8.

[216] S. Jauréguiberry, P.A. Ndour, C. Roussel, F. Ader, I. Safeukui, M. Nguyen, S. Biligui, L. Ciceron, O. Mouri, E. Kendjo, F. Bricaire, M. Vray, A. Angoulvant, J. Mayaux, K. Haldar, D. Mazier, M. Danis, E. Caumes, M. Thellier, P. Buffet, French Artesunate Working Group, Postartesunate delayed hemolysis is a predictable event related to the lifesaving effect of artemisinins., Blood. 124 (2014) 167–75.

[217] T. Rolling, T. Agbenyega, S. Krishna, P.G. Kremsner, J.P. Cramer, Delayed haemolysis after artesunate treatment of severe malaria - review of the literature and perspective., Travel Med. Infect. Dis. 13 (2015) 143–9.

[218] Global report on antimalarial drug efficacy and drug resistance: 2000-2010, World Heal. Organ. (2000).

[219] T.E. Wellems, A. Walker-Jonah, L.J. Panton, Genetic mapping of the chloroquine-resistance locus on Plasmodium falciparum chromosome 7., Proc. Natl. Acad. Sci. U. S. A. 88 (1991) 3382–6.

[220] C. McNamara, E.A. Winzeler, Target identification and validation of novel antimalarials, Futur. Microbiol. 6 (2011) 693–704.

[221] P. Wang, M. Read, P.F. Sims, J.E. Hyde, Sulfadoxine resistance in the human malaria parasite Plasmodium falciparum is determined by mutations in dihydropteroate synthetase and an additional factor associated with folate utilization., Mol. Microbiol. 23 (1997) 979–86.

[222] I.K. Srivastava, J.M. Morrisey, E. Darrouzet, F. Daldal, A.B. Vaidya, Resistance mutations reveal the atovaquone-binding domain of cytochrome b in malaria parasites., Mol. Microbiol. 33 (1999) 704–11.

[223] M. Korsinczky, N. Chen, B. Kotecka, A. Saul, K. Rieckmann, Q. Cheng, Mutations in Plasmodium falciparum cytochrome b that are associated with atovaquone resistance are located at a putative drug-binding site., Antimicrob. Agents Chemother. 44 (2000) 2100–8.

[224] N.J. Spillman, K. Kirk, The malaria parasite cation ATPase PfATP4 and its role in the mechanism of action of a new arsenal of antimalarial drugs, Int. J. Parasitol. Drugs Drug Resist. 5 (2015) 149–162.

[225] E. Sonoiki, C.L. Ng, M.C.S. Lee, D. Guo, Y.-K. Zhang, Y. Zhou, M.R.K. Alley, V. Ahyong, L.M. Sanz, M.J. Lafuente-Monasterio, C. Dong, P.G. Schupp, J. Gut, J. Legac, R.A. Cooper, F.-J. Gamo, J. DeRisi, Y.R. Freund, D.A. Fidock, P.J. Rosenthal, A potent antimalarial benzoxaborole targets a Plasmodium falciparum cleavage and polyadenylation specificity factor homologue, Nat. Commun. 8 (2017) 14574.

[226] T. Paquet, C. Le Manach, D.G. Cabrera, Y. Younis, P.P. Henrich, T.S. Abraham, M.C.S. Lee, R. Basak, S. Ghidelli-Disse, M.J. Lafuente-Monasterio, M. Bantscheff, A. Ruecker, A.M. Blagborough, S.E. Zakutansky, A.-M. Zeeman, K.L. White, D.M. Shackleford, J. Mannila, J. Morizzi, C. Scheurer, I. Angulo-Barturen, M.S. Martínez, S. Ferrer, L.M. Sanz, F.J. Gamo, J. Reader, M. Botha, K.J. Dechering, R.W. Sauerwein, A. Tungtaeng, P. Vanachayangkul, C.S. Lim, J. Burrows, M.J. Witty, K.C. Marsh, C. Bodenreider, R. Rochford, S.M. Solapure, M.B. Jiménez-Díaz, S. Wittlin, S.A. Charman, C. Donini, B. Campo, L.-M. Birkholtz, K.K. Hanson, G. Drewes, C.H.M. Kocken, M.J. Delves, D. Leroy, D.A. Fidock, D. Waterson, L.J. Street, K. Chibale, Antimalarial efficacy of MMV390048, an inhibitor of Plasmodium phosphatidylinositol 4-kinase., Sci. Transl. Med. 9 (2017) eaad9735.

[227] I. Hastings, M. Donnely, The impact of antimalarial drug resistance mutations on parasite fitness, and its implications for the evolution of resistance, Drug Resist. Updat. 8 (2005) 43–50.

[228] C. Author, M. Fakruddin, A. Chowdhury, Pyrosequencing-An Alternative to Traditional Sanger Sequencing, Am. J. Biochem. Biotechnol. 8 (2012) 14–20.

[229] J. Yan, R. Zhang, C. Xiong, C. Hu, Y. Lv, C. Wang, W. Jia, F. Zeng, Pyrosequencing Is an Accurate and Reliable Method for the Analysis of Heteroplasmy of the A3243G Mutation in Patients with Mitochondrial Diabetes, J. Mol. Diagnostics. 16 (2014) 431–439.

[230] L.M. Berg, R. Sanders, A. Alderborn, Pyrosequencing™ technology and the need for versatile solutions in molecular clinical research, Expert Rev. Mol. Diagn. . 2 (2002) 361–369.

[231] H.M. Ismail, V.E. Barton, M. Panchana, S. Charoensutthivarakul, G.A. Biagini, S.A. Ward, P.M. O'Neill, A Click Chemistry-Based Proteomic Approach Reveals that 1,2,4-Trioxolane and Artemisinin Antimalarials Share a Common Protein Alkylation Profile, Angew. Chemie. 128 (2016) 6511–6515.

[232] H.M. Ismail, V. Barton, M. Phanchana, S. Charoensutthivarakul, M.H.L. Wong, J. Hemingway, G.A. Biagini, P.M. O'Neill, S.A. Ward, Artemisinin activity-based probes identify multiple molecular targets within the asexual stage of the malaria parasites *Plasmodium falciparum* 3D7, Proc. Natl. Acad. Sci. 113 (2016) 2080–2085.

[233] D.M. Penarete-Vargas, A. Boisson, S. Urbach, H. Chantelauze, S. Peyrottes, L. Fraisse, H.J. Vial, A Chemical Proteomics Approach for the Search of Pharmacological Targets of the Antimalarial Clinical Candidate Albitiazolium in Plasmodium falciparum Using Photocrosslinking and Click Chemistry, PLoS One. 9 (2014) e113918.

[234] R. Jambou, A. Martinelli, J. Pinto, S. Gribaldo, E. Legrand, M. Niang, N. Kim, L. Pharath, B. Volnay, M.T. Ekala, C. Bouchier, T. Fandeur, P. Berzosa, A. Benito, I.D. Ferreira, C. Ferreira, P.P. Vieira, M. das G. Alecrim, O. Mercereau-Puijalon, P. Cravo, Geographic Structuring of the Plasmodium falciparum Sarco(endo)plasmic Reticulum Ca2+ ATPase (PfSERCA) Gene Diversity, PLoS One. 5 (2010) e9424.

[235] S. Dahlström, M.I. Veiga, P. Ferreira, A. Mårtensson, A. Kaneko, B. Andersson, A. Björkman, J.P. Gil, Diversity of the sarco/endoplasmic reticulum Ca2+-ATPase orthologue of Plasmodium falciparum (PfATP6), Infect. Genet. Evol. 8 (2008) 340–345.

[236] K. Tanabe, S. Zakeri, N.M.Q. Palacpac, M. Afsharpad, M. Randrianarivelojosia, A. Kaneko, A.S.P. Marma, T. Horii, T. Mita, Spontaneous mutations in the Plasmodium falciparum sarcoplasmic/ endoplasmic reticulum Ca2+-ATPase (PfATP6) gene among geographically widespread parasite populations unexposed to artemisinin-based combination therapies., Antimicrob. Agents Chemother. 55 (2011) 94–100.

[237] G.N.S. Silva, D.C. Schuck, L.N. Cruz, M.S. Moraes, M. Nakabashi, G. Gosmann, C.R.S. Garcia, S.C.B. Gnoatto, Investigation of antimalarial activity, cytotoxicity and action mechanism of piperazine derivatives of betulinic acid, Trop. Med. Int. Heal. 20 (2015) 29–39.

[238] I.M. Vincent, D.E. Ehmann, S.D. Mills, M. Perros, M.P. Barrett, Untargeted Metabolomics To Ascertain Antibiotic Modes of Action, Antimicrob. Agents Chemother. 60 (2016) 2281–2291.

[239] D.J. CREEK, M.P. BARRETT, Determination of antiprotozoal drug mechanisms by metabolomics approaches, Parasitology. 141 (2014) 83–92.

[240] R.A. Cooper, D.J. Carucci, Proteomic Approaches to Studying Drug Targets and Resistance in Plasmodium, (n.d.).

[241] J.P. Rubio, A.F. Cowman, Plasmodium falciparum: the pfmdr2 protein is not overexpressed in chloroquine-resistant isolates of the malaria parasite., Exp. Parasitol. 79 (1994) 137–47.

[242] M.G. Zalis, C.M. Wilson, Y. Zhang, D.F. Wirth, Characterization of the pfmdr2 gene for Plasmodium falciparum., Mol. Biochem. Parasitol. 63 (1994) 311.

[243] E. Rosenberg, I. Litus, N. Schwarzfuchs, R. Sinay, P. Schlesinger, J. Golenser, S. Baumeister, K. Lingelbach, Y. Pollack, *pfmdr2* Confers Heavy Metal Resistance to *Plasmodium falciparum*, J. Biol. Chem. 281 (2006) 27039–27045.

[244] M. van der Velden, S.R. Rijpma, F. Russel, R.W. Sauerwein, J.B. Koenderink, PfMDR2 and PfMDR5 are dispensable for Plasmodium falciparum asexual parasite multiplication but change in vitro susceptibility to anti-malarial drugs, Malar. J. 14 (2015) 76.

[245] L. Steimer, D. Klostermeier, RNA helicases in infection and disease., RNA Biol. 9 (2012) 751–71.

[246] B.S. Crabb, M. Rug, T.-W. Gilberger, J.K. Thompson, T. Triglia, A.G. Maier, A.F. Cowman, Transfection of the human malaria parasite Plasmodium falciparum., Methods Mol. Biol. 270 (2004) 263–76.

7. Appendix I: DNA and proteins sequences

All the sequences displayed here were obtained from PlasmoDB, and processed on http://www.bioinformatics.org/sms2/ or http://www.ebi.ac.uk/Tools/msa/clustalo/ for display.

7.1. PF3D7_0106300 calcium-transporting ATPase (PfATP6)

7.1.1. Genomic DNA sequence

In lower case, non-coding DNA sequences; in red, A108 and A109 mutations loci; in green, F972 mutation locus; simply underlined, homology region A (HRA); doubly underlined, homology region B (HRB); in bold, guide 6 and guide 7.

```
   1 ATGGAAGAGG TTATTAAGAA TGCTCATACA TACGATGTTG AGGATGTACT
  51 AAAATTTTTG GATGTAAACA AAGATAATGG TTTAAAGAAT GAGGAATTGG
 101 ATGATAGAAG ATTAAAATAT GGTTTGAATG AATTAGAAGT AGAAAAGAAG
 151 AAAAGTATTT TTGAATTGAT ATTAAATCAA TTTGATGATT TATTAGTAAA
 201 GATATTATTA CTAGCTGCAT TCATTAGTTT CGTGTTAACT TTATTAGATA
 251 TGAAACATAA AAAAATAGAA ATATGTGATT TTATTGAACC ATTAGTTATA
 301 GTATTAATAT TAATATTAAA TGCTGCCGTA GGTGTATGGC AAGAATGTAA
 351 TGCTGAAAAA TCTTTAGAAG CTTTAAAAGA ATTACAACCT ACCAAAGCTA
 401 AAGTATTACG AGATGGGAAG TGGGAAATTA TTGATAGTAA ATATTTATAT
 451 GTTGGTGATA TTATTGAATT GAGTGTTGGT AATAAAACTC CCGCTGATGC
 501 AAGAATAATT AAAATATATT CAACAAGTTT AAAAGTTGAA CAGAGTATGT
 551 TAACAGGAGA ATCCTGTTCA GTTGACAAAT ATGCTGAAAA AATGGAAGAT
 601 AGTTATAAAA ATTGTGAAAT ACAGTTGAAA AAAAATATTT TATTTTCATC
 651 TACCGCTATT GTATGTGGTA GATGTATAGC TGTTGTAATC AACATAGGTA
 701 TGAAGACTGA AATAGGTCAT ATTCAGCATG CTGTTATAGA ATCAAATAGT
 751 GAAGATACTC AAACACCTTT ACAAATAAAA ATCGATTTAT TTGGTCAACA
 801 ATTATCAAAA ATCATTTTTG TAATATGTGT AACTGTATGG ATTATTAATT
 851 TTAAACATTT CTCAGATCCA ATTCATGGTT CATTTTTATA TGGTTGTTTA
 901 TATTATTTTA AAATTAGTGT TGCTTTAGCT GTTGCTGCTA TACCAGAAGG
 951 ATTGCCAGCA GTCATAACAA CTTGTTTAGC TTTAGGAACA AGAAGAATGG
1001 TAAAAAAAAA TGCTATAGTA AGAAAATTAC AAAGTGTTGA GACGTTAGGA
1051 TGTACAACGG TTATATGTTC TGATAAAACA GGTACCCTTA CAACAAATCA
1101 AATGACAACA ACCGTGTTTC ATTTGTTTAG AGAATCTGAT TCTTTAACAG
1151 AATACCAACT ATGTCAAAAA GGGGATACCT ATTACTTTTA TGAAAGTTCA
1201 AACTTAACAA ATGATATATA TGCAGGTGAA TCATCTTTTT TTAATAAATT
1251 AAAAGATGAA GGAAATGTTG AAGCTTTAAC GGATGATGGA GAAGAAGGAT
1301 CAATTGATGA AGCTGATCCA TATAGTGATT ATTTTTCTAG TGATAGTAAG
1351 AAAATGAAAA ATGATTTAAA CAACAACAAT AATAATAATA ATAATAGTAG
1401 TAGGAGTGGT GCTAAGAGGA ATATTCCTTT AAAAGAAATG AAATCAAATG
1451 AAAATACAAT AATAAGTAGA GGTAGTAAAA TATTAGAAGA TAAAATTAAT
1501 AAATATTGTT ATTCAGAATA TGATTATAAT TTTTATATGT GTTTAGTAAA
1551 TTGTAATGAA GCAAATATTT TCTGTAACGA TAATAGTCAA ATAGTAAAAA
1601 AATTTGGAGA CAGTACCGAA TTAGCTTTAT TACATTTTGT ACATAATTTT
1651 GATATATTAC CAACATTCTC TAAAAATAAT AAAATGCCAG CAGAATATGA
1701 AAAAAATACA ACACCTGTAC AATCATCAAA TAAGAAGGAT AAATCACCAA
1751 GGGGTATCAA CAAATTCTTT AGTTCAAAAA ATGATAACAG TCATATTACC
1801 AGTACATTGA ATGAAAATGA TAAGAATTTA AAGAATGCTA ACCATTCTAA
1851 TTATACTACA GCTCAGGCAA CAACAAATGG ATATGAAGCT ATAGGAGAAA
1901 ATACATTTGA GCATGGCACA AGTTTTGAAA ATTGTTTCCA CTCAAAATTG
1951 GGTAATAAAA TAAATACCAC ATCAACACAT AATAATAATA ACAACAATAA
2001 TAATAATAGT AATAGTGTTC CAAGTGAATG TATTTCTTCT TGGAGAAATG
2051 AATGTAAACA AATAAAAATT ATTGAATTCA CTAGAGAAAG GAAACTTATG
2101 AGTGTTATTG TTGAAAATAA AAAAAAAGAA ATAATATTGT ATTGTAAAGG
2151 TGCACCTGAG AATATAATAA AAAATTGTAA ATATTATTTA ACGAAAAATG
```

```
2201 ATATACGTCC ATTAAATGAA ACTTTAAAAA ATGAAATTCA TAATAAGATT
2251 CAAAATATGG GAAAAAGAGC ATTAAGAACA CTTAGCTTTG CTTATAAAAA
2301 ATTAAGTAGT AAAGATTTAA ATATTAAGAA TACAGATGAT TATTATAAAT
2351 TAGAACAAGA TTTAATTTAT TTAGGTGGAT TAGGTATTAT TGATCCACCA
2401 CGTAAATATG TAGGAAGAGC AATTAGATTA TGCCATATGG CTGGTATACG
2451 TGTATTTATG ATTACAGGTG ATAATATTAA TACGGCCAGA GCTATAGCTA
2501 AAGAAATTAA TATATTAAAT AAAAATGAAG GAGATGATGA AAAGGATAAT
2551 TATACAAATA ATAAAAATAC ACAAATATGT TGTTATAATG GAAGAGAATT
2601 TGAAGATTTT TCATTAGAAA AGCAAAAACA TATTTTAAAA AATACACCAA
2651 GAATTGTTTT CTGTAGAACT GAACCTAAAC ATAAAAAACA AATTGTAAAA
2701 GTATTAAAAG ACTTAGGAGA AACAGTTGCT ATGACAGGTG ATGGTGTAAA
2751 TGATGCACCA GCATTGAAAT CAGCTGACAT AGGAATAGCT ATGGGTATTA
2801 ATGGAACGGA GGTAGCTAAA GAAGCATCAG ATATTGTTTT AGCTGATGAT
2851 AATTTTAATA CTATAGTTGA AGCAATTAAA GAAGGAAGAT GTATATATAA
2901 TAATATGAAA GCATTTATCC GTTATCTAAT TAGTAGTAAT ATAGGAGAAG
2951 TTGCATCCAT TTTTATAACA GCCTTATTGG GTATACCTGA CAGTTTAGCT
3001 CCCGTTCAAT TATTGTGGGT AAATTTGGTT ACTGACGGAT TACCAGCAAC
3051 AGCACTAGgt aataacaata aaaaaaaaaa aaaaaaaaaa aaaaaaaaaa
3101 tatattatat attatatatt atatatatat atatgtatgt gtgttaattg
3151 tttgtcttat acatcctatt catcaattat ctttttttt aatttttta
3201 gGGTTCAATC CACCAGAACA TGACGTAATG AAGTGCAAGC CGAGACACAA
3251 AAACGACAAT TTAATAAACG GTCTAACTTT ATTAAGATAT ATAATTATTG
3301 GAACATATGT AGGAATAGCT ACAGTCTCAA TATTTGTGTA CTGGTTTTTA
3351 TTTTATCCAG ATTCAGATAT GCACACGTTG ATAAACTTTT ATCAATTATC
3401 ACATTATAAC CAATGTAAAG CATGGAATAA CTTCCGTGTA AATAAGGTTT
3451 ATGATATGTC TGAGGATCAC TGTTCATATT TTTCAGCAGG AAAAATTAAG
3501 gtaataaata tagtgcacac acacaaacat acacacacac atatatatat
3551 atatatatat atatatatat gtatatttac gtatatatgt atatatttat
3601 atatattcat ttatttatat atttttttat ttttagGCAA GCACCTTATC
3651 TTTATCCGTT TTAGTTTTAA TAGAAATGTT TAATGCTTTG AATGCCTTGA
3701 GTGAGTATAA TTCCTTATTT GAAATACCAC CATGGAGAAA TATGTACCTA
3751 GTATTAGCTA CTATAGGTTC CTTACTTTTA CATGTCTTAA TACTTTACAT
3801 TCCACCCTTA GCTCGTATTT TTGGTGTTGT TCCATTAAGT GCATATGACT
3851 GGTTCTTAGT ATTCTTGTGG TCCTTCCCAG TTATTATACT TGACGAAATT
3901 ATTAAATTCT ATGCAAAGAG GAAATTAAAG GAAGAGCAAA GAACCAAGAA
3951 AATTAAAATT GATTAA
```

7.1.2. Aminoacid sequence

In red, A108 and A109; in green, F972

```
   1 MEEVIKNAHT YDVEDVLKFL DVNKDNGLKN EELDDRRLKY GLNELEVEKK
  51 KSIFELILNQ FDDLLVKILL LAAFISFVLT LLDMKHKKIE ICDFIEPLVI
 101 VLILILNAAV GVWQECNAEK SLEALKELQP TKAKVLRDGK WEIIDSKYLY
 151 VGDIIELSVG NKTPADARII KIYSTSLKVE QSMLTGESCS VDKYAEKMED
 201 SYKNCEIQLK KNILFSSTAI VCGRCIAVVI NIGMKTEIGH IQHAVIESNS
 251 EDTQTPLQIK IDLFGQQLSK IIFVICVTVW IINFKHFSDP IHGSFLYGCL
 301 YYFKISVALA VAAIPEGLPA VITTCLALGT RRMVKKNAIV RKLQSVETLG
 351 CTTVICSDKT GTLTTNQMTT TVFHLFRESD SLTEYQLCQK GDTYYFYESS
 401 NLTNDIYAGE SSFFNKLKDE GNVEALTDDG EEGSIDEADP YSDYFSSDSK
 451 KMKNDLNNNN NNNNNSSRSG AKRNIPLKEM KSNENTIISR GSKILEDKIN
 501 KYCYSEYDYN FYMCLVNCNE ANIFCNDNSQ IVKKFGDSTE LALLHFVHNF
 551 DILPTFSKNN KMPAEYEKNT TPVQSSNKKD KSPRGINKFF SSKNDNSHIT
 601 STLNENDKNL KNANHSNYTT AQATTNGYEA IGENTFEHGT SFENCFHSKL
 651 GNKINTTSTH NNNNNNNNNS NSVPSECISS WRNECKQIKI IEFTRERKLM
 701 SVIVENKKKE IILYCKGAPE NIIKNCKYYL TKNDIRPLNE TLKNEIHNKI
 751 QNMGKRALRT LSFAYKKLSS KDLNIKNTDD YYKLEQDLIY LGGLGIIDPP
 801 RKYVGRAIRL CHMAGIRVFM ITGDNINTAR AIAKEINILN KNEGDDEKDN
 851 YTNNKNTQIC CYNGREFEDF SLEKQKHILK NTPRIVFCRT EPKHKKQIVK
```

```
 901 VLKDLGETVA MTGDGVNDAP ALKSADIGIA MGINGTEVAK EASDIVLADD
 951 NFNTIVEAIK EGRCIYNNMK AFIRYLISSN IGEVASIFIT ALLGIPDSLA
1001 PVQLLWVNLV TDGLPATALG FNPPEHDVMK CKPRHKNDNL INGLTLLRYI
1051 IIGTYVGIAT VSIFVYWFLF YPDSDMHTLI NFYQLSHYNQ CKAWNNFRVN
1101 KVYDMSEDHC SYFSAGKIKA STLSLSVLVL IEMFNALNAL SEYNSLFEIP
1151 PWRNMYLVLA TIGSLLLHVL ILYIPPLARI FGVVPLSAYD WFLVFLWSFP
1201 VIILDEIIKF YAKRKLKEEQ RTKKIKID
```

7.1.3. Alignment of pfatp6 coding sequence and the *S. cervisiae* codon optimized atp6 sequence

In green, 3xHA tag coding sequence.

78% identity between the sequences

```
pfatp6          ATGGAAGAGGTTATTAAGAATGCTCATACATACGATGTTGAGGATGTACTAAAATTTTTG
opt_atp6_HA     ATGGAAGAAGTTATTAAGAACGCCCACACCTACGATGTTGAAGATGTTTTGAAGTTCTTG
                ******** *********** ** ** ** *********** *****  * ** ** ***

pfatp6          GATGTAAACAAAGATAATGGTTTAAAGAATGAGGAATTGGATGATAGAAGATTAAAATAT
opt_atp6_HA     GACGTCAACAAGGATAACGGTTTGAAGAACGAAGAATTGGATGATAGAAGATTGAAGTAT
                ** ** ***** ***** ***** ***** ** ******************** ** ***

pfatp6          GGTTTGAATGAATTAGAAGTAGAAAAGAAGAAAAGTATTTTTGAATTGATATTAAATCAA
opt_atp6_HA     GGTTTGAACGAATTGGAAGTCGAAAAGAAGAAGTCCATCTTCGAATTGATCTTGAATCAA
                ******** ***** ***** ***********    ** ** ******** ** ******

pfatp6          TTTGATGATTTATTAGTAAAGATATTATTACTAGCTGCATTCATTAGTTTCGTGTTAACT
opt_atp6_HA     TTTGACGACTTGTTGGTTAAGATCTTGTTGTTGGCTGCCTTCATCTCTTTCGTTTTGACT
                ***** ** ** ** ** ***** ** **  * ***** *****   ****** ** ***

pfatp6          TTATTAGATATGAAACATAAAAAAATAGAAATATGTGATTTTATTGAACCATTAGTTATA
opt_atp6_HA     TTGTTGGATATGAAGCACAAAAAGATCGAAATCTGCGACTTCATCGAACCATTGGTTATC
                ** ** ******** ** ***** ** ***** ** ** ** ** ******** *****

pfatp6          GTATTAATATTAATATTAAATGCTGCCGTAGGTGTATGGCAAGAATGTAATGCTGAAAAA
opt_atp6_HA     GTCTTGATCTTAATTTTGAACGCTGCTGTTGGTGTTTGGCAAGAATGTAATGCTGAAAAG
                ** ** ** ***** ** ** ***** ** ***** **********************

pfatp6          TCTTTAGAAGCTTTAAAAGAATTACAACCTACCAAAGCTAAAGTATTACGAGATGGGAAG
opt_atp6_HA     TCTTTGGAAGCCTTGAAAGAATTGCAACCTACTAAGGCTAAGGTCTTGAGAGATGGTAAA
                ***** ***** ** ******** ******** ** ***** ** **  ******* **

pfatp6          TGGGAAATTATTGATAGTAAATATTTATATGTTGGTGATATTATTGAATTGAGTGTTGGT
opt_atp6_HA     TGGGAAATCATCGACTCTAAGTACTTGTACGTTGGTGACATCATCGAATTGTCTGTTGGT
                ******** ** **   *** ** ** ** ******** ** ** ******  *******

pfatp6          AATAAAACTCCCGCTGATGCAAGAATAATTAAAATATATTCAACAAGTTTAAAAGTTGAA
opt_atp6_HA     AACAAAACTCCAGCTGATGCCAGAATTATCAAGATCTACTCTACCTCCTTGAAGGTTGAA
                ** ******** ******** ***** ** ** ** ** ** **    ** ** ******

pfatp6          CAGAGTATGTTAACAGGAGAATCCTGTTCAGTTGACAAATATGCTGAAAAAATGGAAGAT
opt_atp6_HA     CAATCTATGTTGACTGGTGAATCTTGCTCCGTTGATAAGTACGCTGAAAAGATGGAAGAT
                **   ****** ** ** ***** ** ** ***** ** ** ******** *********

pfatp6          AGTTATAAAAATTGTGAAATACAGTTGAAAAAAAATATTTTATTTTCATCTACCGCTATT
opt_atp6_HA     TCCTACAAGAACTGCGAAATCCAATTGAAGAAGAACATCTTGTTCTCTTCCACCGCTATC
                   ** ** ** ** ***** ** ***** ** ** ** ** ** ** ** ********

pfatp6          GTATGTGGTAGATGTATAGCTGTTGTAATCAACATAGGTATGAAGACTGAAATAGGTCAT
opt_atp6_HA     GTTTGTGGTAGATGTATTGCTGTTGTTATCAACATCGGTATGAAGACCGAAATTGGTCAT
                ** ************** ******** ******** *********** ***** ******

pfatp6          ATTCAGCATGCTGTTATAGAATCAAATAGTGAAGATACTCAAACACCTTTACAAATAAAA
opt_atp6_HA     ATTCAACATGCCGTCATCGAATCCAATTCCGAAGATACTCAAACTCCATTGCAAATCAAG
                ***** ***** ** ** ***** ***   ************** ** ** ***** **

pfatp6          ATCGATTTATTTGGTCAACAATTATCAAAAATCATTTTTGTAATATGTGTAACTGTATGG
opt_atp6_HA     ATCGACTTGTTCGGTCAACAATTGTCCAAGATCATTTTCGTTATCTGCGTTACCGTTTGG
                ***** ** ** *********** ** ** ******** ** ** ** ** ** ** ***

pfatp6          ATTATTAATTTTAAACATTTCTCAGATCCAATTCATGGTTCATTTTTATATGGTTGTTTA
opt_atp6_HA     ATCATCAATTTCAAGCACTTCTCCGATCCAATCCATGGTTCTTTCTTGTATGGTTGCTTG
```

```
                ** ** ***** ** ** ***** ******** ******** ** ** ******** **

pfatp6          TATTATTTTAAAATTAGTGTTGCTTTAGCTGTTGCTGCTATACCAGAAGGATTGCCAGCA
opt_atp6_HA     TACTACTTCAAGATCTCTGTTGCTTTAGCTGTTGCTGCTATTCCAGAAGGTTTGCCAGCT
                ** ** ** ** **   ********************** ******** ********

pfatp6          GTCATAACAACTTGTTTAGCTTTAGGAACAAGAAGAATGGTAAAAAAAAAATGCTATAGTA
opt_atp6_HA     GTTATTACTACTTGTTTGGCTTTGGGTACTAGAAGAATGGTTAAGAAGAACGCCATCGTC
                ** ** ** ******** ***** ** ** ********** ** ** ** ** ** **

pfatp6          AGAAAATTACAAAGTGTTGAGACGTTAGGATGTACAACGGTTATATGTTCTGATAAAACA
opt_atp6_HA     AGAAAGTTGCAATCTGTTGAAACTTTGGGTTGCACCACCGTTATTTGTTCTGATAAGACT
                ***** ** ***  ****** ** ** ** ** ** ** ***** ********** **

pfatp6          GGTACCCTTACAACAAATCAAATGACAACAACCGTGTTTCATTTGTTTAGAGAATCTGAT
opt_atp6_HA     GGTACTTTGACCACCAATCAAATGACTACTACCGTTTTCCACTTGTTCAGAGAATCTGAT
                *****  * ** ** ********** ** ***** ** ** ***** ***********

pfatp6          TCTTTAACAGAATACCAACTATGTCAAAAAGGGGATACCTATTACTTTTATGAAAGTTCA
opt_atp6_HA     TCTTTGACCGAATACCAATTGTGCCAAAAGGGTGATACTTACTACTTCTACGAATCCTCT
                ***** ** ********* * ** ***** ** ***** ** ***** ** ***   **

pfatp6          AACTTAACAAATGATATATATGCAGGTGAATCATCTTTTTTTAATAAATTAAAAGATGAA
opt_atp6_HA     AACTTGACCAACGATATCTATGCTGGTGAAAGTTCCTTCTTCAACAAATTGAAAGACGAA
                ***** ** ** ***** ***** ******   ** ** ** ** ***** ***** ***

pfatp6          GGAAATGTTGAAGCTTTAACGGATGATGGAGAAGAAGGATCAATTGATGAAGCTGATCCA
opt_atp6_HA     GGTAACGTCGAAGCTTTGACTGATGATGGTGAAGAAGGTTCTATTGACGAAGCTGATCCA
                ** ** ** ******** ** ******** ******** ** ***** ***********

pfatp6          TATAGTGATTATTTTTCTAGTGATAGTAAGAAAATGAAAAATGATTTAAACAACAACAAT
opt_atp6_HA     TACTCTGATTACTTCTCATCCGACTCCAAAAAGATGAAGAATGACTTGAACAATAACAAC
                **   ****** ** **    **    ** ** ***** ***** ** ***** *****

pfatp6          AATAATAATAATAATAGTAGTAGGAGTGGTGCTAAGAGGAATATTCCTTTAAAAGAAATG
opt_atp6_HA     AACAACAATAACAACTCCTCCAGATCCGGTGCTAAGAGAAATATTCCATTGAAAGAAATG
                ** ** ***** **       **    ********** ******** ** *********

pfatp6          AAATCAAATGAAAATACAATAATAAGTAGAGGTAGTAAAATATTAGAAGATAAAATTAAT
opt_atp6_HA     AAGTCCAACGAAAACACCATTATCTCCAGAGGTTCCAAGATTTTGGAAGATAAGATCAAC
                ** ** ** ***** ** ** **    ******   ** ** ** ******** ** **

pfatp6          AAATATTGTTATTCAGAATATGATTATAATTTTTATATGTGTTTAGTAAATTGTAATGAA
opt_atp6_HA     AAGTACTGCTACTCCGAATACGACTACAACTTCTACATGTGTTTGGTCAACTGTAACGAA
                ** ** ** ** ** ***** ** ** ** ** ** ******** ** ** ***** ***

pfatp6          GCAAATATTTTCTGTAACGATAATAGTCAAATAGTAAAAAAATTTGGAGACAGTACCGAA
opt_atp6_HA     GCCAACATTTTCTGCAACGACAACTCTCAAATCGTCAAGAAATTCGGTGACTCTACTGAA
                ** ** ******** ***** **   ****** ** ** ***** ** ***  *** ***

pfatp6          TTAGCTTTATTACATTTTGTACATAATTTTGATATATTACCAACATTCTCTAAAAATAAT
opt_atp6_HA     TTGGCTTTGTTGCATTTCGTTCACAACTTCGATATTTTGCCAACCTTCTCCAAGAACAAC
                ** ***** ** ***** ** ** ** ** ***** ** ***** ***** ** ** **

pfatp6          AAAATGCCAGCAGAATATGAAAAAAATACAACACCTGTACAATCATCAAATAAGAAGGAT
opt_atp6_HA     AAAATGCCAGCAGAATACGAAAAGAACACTACCCCAGTTCAATCCTCCAACAAAAAAGAT
                ***************** ***** ** ** ** ** ** ***** ** ** ** ** ***

pfatp6          AAATCACCAAGGGGTATCAACAAATTCTTTAGTTCAAAAAATGATAACAGTCATATTACC
opt_atp6_HA     AAGTCTCCAAGAGGTATTAACAAGTTCTTCTCCTCCAAAAACGACAACAGTCATATTACC
                ** ** ***** ***** ***** *****    ** ***** ** ***************

pfatp6          AGTACATTGAATGAAAATGATAAGAATTTAAAGAATGCTAACCATTCTAATTATACTACA
opt_atp6_HA     TCTACCTTGAACGAAAACGATAAGAACTTGAAGAATGCCAACCACTCTAACTACACTACT
                  *** ***** ***** ******** ** ******** ***** ***** ** *****

pfatp6          GCTCAGGCAACAACAAATGGATATGAAGCTATAGGAGAAAATACATTTGAGCATGGCACA
opt_atp6_HA     GCTCAAGCTACTACTAATGGTTACGAAGCTATTGGTGAAAACACCTTCGAACATGGTACA
                ***** ** ** ** ***** ** ******** ** ***** ** ** ** ***** ***

pfatp6          AGTTTTGAAAATTGTTTCCACTCAAAATTGGGTAATAAAATAAATACCACATCAACACAT
opt_atp6_HA     TCTTTCGAAAACTGTTTCCACTCTAAGTTGGGTAACAAGATTAACACCACTTCCACCCAC
                  *** ***** ********** ** ******** ** ** ** ***** ** ** **


pfatp6          AATAATAATAACAACAATAATAATAATAGTAATAGTGTTCCAAGTGAATGTATTTCTTCT
opt_atp6_HA     AACAATAACAATAACAACAACAACAACAGTAACTCCGTCCCTTCTGAATGTATTTCTAGT
                ** ***** ** ***** ** ** ** *****    ** **   **************  *

pfatp6          TGGAGAAATGAATGTAAACAAATAAAAATTATTGAATTCACTAGAGAAAGGAAACTTATG
opt_atp6_HA     TGGAGAAACGAATGCAAGCAAATCAAAATTATCGAATTCACCAGAGAAAGAAAGTTGATG
```

```
                ******** ***** ** ***** ******** ******** ******** **  * ***

pfatp6          AGTGTTATTGTTGAAAATAAAAAAAAAGAAATAATATTGTATTGTAAAGGTGCACCTGAG
opt_atp6_HA     TCCGTTATCGTTGAAAACAAGAAGAAAGAAATCATCTTGTACTGCAAGGGTGCCCCAGAA
                   ***** ******** ** ** ******** ** ***** ** ** ***** ** **

pfatp6          AATATAATAAAAAATTGTAAATATTATTTAACGAAAAATGATATACGTCCATTAAATGAA
opt_atp6_HA     AACATTATCAAAAATTGCAAGTACTACTTGACTAAGAACGACATCAGACCTTTAAACGAA
                ** ** ** ******** ** ** ** ** ** ** ** ** **  * ** ***** ***

pfatp6          ACTTTAAAAAATGAAATTCATAATAAGATTCAAAATATGGGAAAAAGAGCATTAAGAACA
opt_atp6_HA     ACCTTGAAAAACGAAATCCATAACAAGATCCAAAACATGGGTAAGAGAGCTTTGAGAACT
                ** ** ***** ***** ***** ***** ***** ***** ** ***** ** *****

pfatp6          CTTAGCTTTGCTTATAAAAAATTAAGTAGTAAAGATTTAAATATTAAGAATACAGATGAT
opt_atp6_HA     TTGTCTTTCGCTTACAAGAAGTTGTCCTCCAAGGATTTGAACATCAAGAACACCGATGAT
                 *    ** ***** ** ** **       ** ***** ** ** ***** ** ******

pfatp6          TATTATAAATTAGAACAAGATTTAATTTATTTAGGTGGATTAGGTATTATTGATCCACCA
opt_atp6_HA     TACTACAAGTTGGAACAAGACTTGATCTACTTGGGTGGTTTGGGTATTATTGATCCACCA
                ** ** ** ** ******** ** ** ** ** ***** ** ******************

pfatp6          CGTAAATATGTAGGAAGAGCAATTAGATTATGCCATATGGCTGGTATACGTGTATTTATG
opt_atp6_HA     AGAAAGTATGTTGGTAGAGCCATTAGATTGTGTCATATGGCTGGTATCAGAGTTTTCATG
                 * ** ***** ** ***** ******** ** ***************  * ** ** ***

pfatp6          ATTACAGGTGATAATATTAATACGGCCAGAGCTATAGCTAAAGAAATTAATATATTAAAT
opt_atp6_HA     ATTACCGGTGATAACATTAACACCGCTAGAGCTATTGCCAAAGAAATCAACATCTTGAAC
                ***** ******** ***** ** ** ******** ** ******** ** ** ** **

pfatp6          AAAAATGAAGGAGATGATGAAAAGGATAATTATACAAATAATAAAAATACACAAATATGT
opt_atp6_HA     AAGAACGAAGGTGATGACGAAAAGGATAACTACACAAACAACAAGAATACCCAAATCTGC
                ** ** ***** ***** ********** ** ***** ** ** ***** ***** **

pfatp6          TGTTATAATGGAAGAGAATTTGAAGATTTTTCATTAGAAAAGCAAAAACATATTTTAAAA
opt_atp6_HA     TGCTACAACGGTAGAGAATTTGAAGATTTCTCCTTGGAAAAACAAAAGCACATTTTGAAA
                ** ** ** ** ***************** ** ** ***** ***** ** ***** ***

pfatp6          AATACACCAAGAATTGTTTTCTGTAGAACTGAACCTAAACATAAAAAACAAATTGTAAAA
opt_atp6_HA     AACACCCCAAGAATCGTTTTCTGTAGAACTGAACCTAAGCACAAGAAGCAAATTGTCAAG
                ** ** ******** ********************** ** ** ** ******** **

pfatp6          GTATTAAAAGACTTAGGAGAAACAGTTGCTATGACAGGTGATGGTGTAAATGATGCACCA
opt_atp6_HA     GTTTTGAAGGATTTGGGTGAAACTGTTGCTATGACAGGTGATGGTGTTAACGATGCTCCA
                ** ** ** ** ** ** ***** ********************** ** ***** ***

pfatp6          GCATTGAAATCAGCTGACATAGGAATAGCTATGGGTATTAATGGAACGGAGGTAGCTAAA
opt_atp6_HA     GCTTTGAAGTCTGCTGATATTGGTATTGCTATGGGTATCAACGGTACTGAAGTTGCTAAA
                ** ***** ** ***** ** ** ** ************ ** ** ** ** ** ******

pfatp6          GAAGCATCAGATATTGTTTTAGCTGATGATAATTTTAATACTATAGTTGAAGCAATTAAA
opt_atp6_HA     GAAGCTTCCGATATAGTTTTGGCCGATGATAACTTCAACACCATCGTTGAAGCTATCAAA
                ***** ** ***** ***** ** ******** ** ** ** ** ******** ** ***

pfatp6          GAAGGAAGATGTATATATAATAATATGAAAGCATTTATCCGTTATCTAATTAGTAGTAAT
opt_atp6_HA     GAAGGTAGATGCATATACAACAACATGAAGGCTTTCATCAGATACTTGATCTCCAGTAAC
                ***** ***** ***** ** ** ***** ** ** *** * **  * **    *****

pfatp6          ATAGGAGAAGTTGCATCCATTTTTATAACAGCCTTATTGGGTATACCTGACAGTTTAGCT
opt_atp6_HA     ATTGGTGAAGTTGCCTCTATTTTCATTACCGCCTTGTTAGGTATTCCAGATTCTTTGGCT
                ** ** ******** ** ***** ** ** ***** ** ***** ** **   *** ***

pfatp6          CCCGTTCAATTATTGTGGGTAAATTTGGTTACTGACGGATTACCAGCAACAGCACTAGGG
opt_atp6_HA     CCTGTCCAATTATTGTGGGTTAACTTGGTTACTGATGGTTTACCAGCTACTGCTTTGGGT
                ** ** ************** ** ********** ** ******** ** **  * **

pfatp6          TTCAATCCACCAGAACATGACGTAATGAAGTGCAAGCCGAGACACAAAAACGACAATTTA
opt_atp6_HA     TTTAATCCACCAGAACATGATGTTATGAAGTGCAAGCCAAGACACAAGAATGACAACTTG
                ** ***************** ** ************** ******** ** ***** **

pfatp6          ATAAACGGTCTAACTTTATTAAGATATATAATTATTGGAACATATGTAGGAATAGCTACA
opt_atp6_HA     ATCAATGGTTTGACCTTGTTAAGATATATCATTATCGGTACTTACGTCGGTATTGCCACC
                ** ** *** * ** ** ********** ***** ** ** ** ** ** ** ** **


pfatp6          GTCTCAATATTTGTGTACTGGTTTTTATTTTATCCAGATTCAGATATGCACACGTTGATA
opt_atp6_HA     GTTTCTATTTTTGTTTACTGGTTTTTGTTCTACCCAGACTCCGATATGCATACCTTGATT
                ** ** ** ***** ********** ** ** ***** ** ******** ** *****

pfatp6          AACTTTTATCAATTATCACATTATAACCAATGTAAAGCATGGAATAACTTCCGTGTAAAT
opt_atp6_HA     AACTTCTACCAATTGAGTCACTACAATCAATGCAAGGCTTGGAACAACTTCAGAGTAAAC
```

```
                 ***** ** *****    ** ** ** ***** ** ** ***** ****** * *****

pfatp6           AAGGTTTATGATATGTCTGAGGATCACTGTTCATATTTTTCAGCAGGAAAAATTAAGGCA
opt_atp6_HA      AAGGTTTACGATATGTCCGAAGATCACTGCTCTTATTTTTCCGCTGGTAAGATTAAGGCT
                 ******** ******** ** ******** ** ******** ** ** ** ********

pfatp6           AGCACCTTATCTTTATCCGTTTTAGTTTTAATAGAAATGTTTAATGCTTTGAATGCCTTG
opt_atp6_HA      TCTACCTTGTCTTTGTCCGTTTTGGTTTTGATCGAAATGTTCAATGCTTTGAACGCCTTG
                    ***** ***** ******** ***** ** ******** ********** ******

pfatp6           AGTGAGTATAATTCCTTATTTGAAATACCACCATGGAGAAATATGTACCTAGTATTAGCT
opt_atp6_HA      TCCGAATACAACTCCTTGTTTGAAATTCCACCTTGGAGAAATATGTACTTGGTTTTGGCT
                    ** ** ** ***** ******** ***** *************** * ** ** ***

pfatp6           ACTATAGGTTCCTTACTTTTACATGTCTTAATACTTTACATTCCACCCTTAGCTCGTATT
opt_atp6_HA      ACTATCGGTTCTTTGTTGTTGCACGTTTTGATCTTGTACATTCCACCATTGGCTAGAATC
                 ***** ***** **  * ** ** ** ** **  * *********** ** *** * **

pfatp6           TTTGGTGTTGTTCCATTAAGTGCATATGACTGGTTCTTAGTATTCTTGTGGTCCTTCCCA
opt_atp6_HA      TTTGGTGTTGTTCCATTGTCTGCTTACGATTGGTTCTTGGTTTTTTTGTGGTCTTTCCCA
                 *****************   *** ** ** ******** ** ** ******** ******

pfatp6           GTTATTATACTTGACGAAATTATTAAATTCTATGCAAAGAGGAAATTAAAGGAAGAGCAA
opt_atp6_HA      GTCATCATCTTGGACGAAATCATTAAGTTCTACGCCAAGAGAAAGTTGAAAGAAGAACAA
                 ** ** **  * ******** ***** ***** ** ***** ** ** ** ***** ***

pfatp6           AGAACCAAGAAAATTAAAATTGATTAA---------------------------------
opt_atp6_HA      AGAACTAAGAAAATCAAGATTGACGGTGGTGGTTACCCATATGATGTTCCAGATTATGCT
                 ***** ******** ** *****

pfatp6           ------------------------------------------------------------
opt_atp6_HA      TACCCTTACGATGTACCTGATTACGCATATCCATACGATGTCCCAGACTACGCTCATGGT

pfatp6           ----------------
opt_atp6_HA      GTTTAACCCGGGCGAT
```

7.1.4. Alignment of pfatp6 aminoacid sequence and the S. cervisiae codon optimized atp6 sequence

In green, 3xHA tag coding sequence.

```
PfATP6           MEEVIKNAHTYDVEDVLKFLDVNKDNGLKNEELDDRRLKYGLNELEVEKKKSIFELILNQ
opt              MEEVIKNAHTYDVEDVLKFLDVNKDNGLKNEELDDRRLKYGLNELEVEKKKSIFELILNQ
                 ************************************************************

PfATP6           FDDLLVKILLLAAFISFVLTLLDMKHKKIEICDFIEPLVIVLILILNAAVGVWQECNAEK
opt              FDDLLVKILLLAAFISFVLTLLDMKHKKIEICDFIEPLVIVLILILNAAVGVWQECNAEK
                 ************************************************************

PfATP6           SLEALKELQPTKAKVLRDGKWEIIDSKYLYVGDIIELSVGNKTPADARIIKIYSTSLKVE
opt              SLEALKELQPTKAKVLRDGKWEIIDSKYLYVGDIIELSVGNKTPADARIIKIYSTSLKVE
                 ************************************************************

PfATP6           QSMLTGESCSVDKYAEKMEDSYKNCEIQLKKNILFSSTAIVCGRCIAVVINIGMKTEIGH
opt              QSMLTGESCSVDKYAEKMEDSYKNCEIQLKKNILFSSTAIVCGRCIAVVINIGMKTEIGH
                 ************************************************************

PfATP6           IQHAVIESNSEDTQTPLQIKIDLFGQQLSKIIFVICVTVWIINFKHFSDPIHGSFLYGCL
opt              IQHAVIESNSEDTQTPLQIKIDLFGQQLSKIIFVICVTVWIINFKHFSDPIHGSFLYGCL
                 ************************************************************



PfATP6           YYFKISVALAVAAIPEGLPAVITTCLALGTRRMVKKNAIVRKLQSVETLGCTTVICSDKT
opt              YYFKISVALAVAAIPEGLPAVITTCLALGTRRMVKKNAIVRKLQSVETLGCTTVICSDKT
                 ************************************************************

PfATP6           GTLTTNQMTTTVFHLFRESDSLTEYQLCQKGDTYYFYESSNLTNDIYAGESSFFNKLKDE
opt              GTLTTNQMTTTVFHLFRESDSLTEYQLCQKGDTYYFYESSNLTNDIYAGESSFFNKLKDE
                 ************************************************************

PfATP6           GNVEALTDDGEEGSIDEADPYSDYFSSDSKKMKNDLNNNNNNNNNSSRSGAKRNIPLKEM
```

```
opt         GNVEALTDDGEEGSIDEADPYSDYFSSDSKKMKNDLNNNNNNNNNSSRSGAKRNIPLKEM
            ************************************************************

PfATP6      KSNENTIISRGSKILEDKINKYCYSEYDYNFYMCLVNCNEANIFCNDNSQIVKKFGDSTE
opt         KSNENTIISRGSKILEDKINKYCYSEYDYNFYMCLVNCNEANIFCNDNSQIVKKFGDSTE
            ************************************************************

PfATP6      LALLHFVHNFDILPTFSKNNKMPAEYEKNTTPVQSSNKKDKSPRGINKFFSSKNDNSHIT
opt         LALLHFVHNFDILPTFSKNNKMPAEYEKNTTPVQSSNKKDKSPRGINKFFSSKNDNSHIT
            ************************************************************

PfATP6      STLNENDKNLKNANHSNYTTAQATTNGYEAIGENTFEHGTSFENCFHSKLGNKINTTSTH
opt         STLNENDKNLKNANHSNYTTAQATTNGYEAIGENTFEHGTSFENCFHSKLGNKINTTSTH
            ************************************************************

PfATP6      NNNNNNNNNSNSVPSECISSWRNECKQIKIIEFTRERKLMSVIVENKKKEIILYCKGAPE
opt         NNNNNNNNNSNSVPSECISSWRNECKQIKIIEFTRERKLMSVIVENKKKEIILYCKGAPE
            ************************************************************

PfATP6      NIIKNCKYYLTKNDIRPLNETLKNEIHNKIQNMGKRALRTLSFAYKKLSSKDLNIKNTDD
opt         NIIKNCKYYLTKNDIRPLNETLKNEIHNKIQNMGKRALRTLSFAYKKLSSKDLNIKNTDD
            ************************************************************

PfATP6      YYKLEQDLIYLGGLGIIDPPRKYVGRAIRLCHMAGIRVFMITGDNINTARAIAKEINILN
opt         YYKLEQDLIYLGGLGIIDPPRKYVGRAIRLCHMAGIRVFMITGDNINTARAIAKEINILN
            ************************************************************

PfATP6      KNEGDDEKDNYTNNKNTQICCYNGREFEDFSLEKQKHILKNTPRIVFCRTEPKHKKQIVK
opt         KNEGDDEKDNYTNNKNTQICCYNGREFEDFSLEKQKHILKNTPRIVFCRTEPKHKKQIVK
            ************************************************************

PfATP6      VLKDLGETVAMTGDGVNDAPALKSADIGIAMGINGTEVAKEASDIVLADDNFNTIVEAIK
opt         VLKDLGETVAMTGDGVNDAPALKSADIGIAMGINGTEVAKEASDIVLADDNFNTIVEAIK
            ************************************************************

PfATP6      EGRCIYNNMKAFIRYLISSNIGEVASIFITALLGIPDSLAPVQLLWVNLVTDGLPATALG
opt         EGRCIYNNMKAFIRYLISSNIGEVASIFITALLGIPDSLAPVQLLWVNLVTDGLPATALG
            ************************************************************

PfATP6      FNPPEHDVMKCKPRHKNDNLINGLTLLRYIIIGTYVGIATVSIFVYWFLFYPDSDMHTLI
opt         FNPPEHDVMKCKPRHKNDNLINGLTLLRYIIIGTYVGIATVSIFVYWFLFYPDSDMHTLI
            ************************************************************

PfATP6      NFYQLSHYNQCKAWNNFRVNKVYDMSEDHCSYFSAGKIKASTLSLSVLVLIEMFNALNAL
opt         NFYQLSHYNQCKAWNNFRVNKVYDMSEDHCSYFSAGKIKASTLSLSVLVLIEMFNALNAL
            ************************************************************

PfATP6      SEYNSLFEIPPWRNMYLVLATIGSLLLHVLILYIPPLARIFGVVPLSAYDWFLVFLWSFP
opt         SEYNSLFEIPPWRNMYLVLATIGSLLLHVLILYIPPLARIFGVVPLSAYDWFLVFLWSFP
            ************************************************************

PfATP6      VIILDEIIKFYAKRKLKEEQRTKKIKID------------------------------
opt         VIILDEIIKFYAKRKLKEEQRTKKIKIDGGGYPYDVPDYAYPYDVPDYAYPYDVPDYAHG
            ****************************

PfATP6      --
opt         V*
```

7.2. PF3D7_0105800 conserved Plasmodium protein, unknown function

7.2.1. Genomic DNA sequence

In lower case, non-coding DNA sequences.

```
   1 ATGGCTACAA ATAGTAATAA TAACAACAGT AGTAATAATA ATAACAATTT
  51 AGAGAACATA AATTTGAGCC TACACAAAAT ATTTAATTGT CGTCATAGTG
 101 TTCCTAGTAA ATTTATTGAA GATGAAAAAG AAAATATAAG GAAACGTAGA
 151 TGCACAGTGG CTCATATGTA TGAGAAGAAT ATAAATTCAA AGAATACTAA
 201 TTATGATTAT TTAACCTATA ATTTTAATAA CTCGATAAGA AAGAGAAGAA
 251 AATATTCTCC TACTATTCAA ACCCAATTAT ATAAAAAATA TTCTCCTTTA
 301 AAAAGTAGAA TAGGATTAAG AAATAGTGTA GATGAGAGTA TTAAAAAAAG
 351 TGCATGTATA AGATCTATTG TTAATAATAC GATAAAGAAT AAAACTAGGG
 401 ATAGTAGTTA TATTCGAAAT GAAAATAAAA GTTGTTATAT TGGTGATAAA
 451 AATAATAAAA TAATATATGA AGGCTCTAAA TATAATGAAA AAAATAATTA
 501 TATAGATGAA AATATGAATG ATAGAAAAAT GTATATAAAT AAAAATTTAC
 551 ATGATACATA TATTATGAGT AATACTACAC AAAGCGATAA TTTTTTTAGA
 601 AGTAAAAATA TTAATAGAAT AAATAGTTTA ATAACGAATA GAGAAACGGC
 651 ACCTATATAT ATGAATTCTG AATCTACACT TTCAAGTTTT AATTTTGAAC
 701 CCAATGTAGA ACAAAAACAT TCTAAATTAA CATTAGATAT GAAAAGTACA
 751 ATTTATATAC CATCAGATAT GTCTTTATTT AATAAGAATA AATATTCTTT
 801 TATTTCAAAT ATGTCCTTAG AAGATTTAAA AAAAATGAAT AATGAATATA
 851 CATCTAAAAA TAATTACAAT GTAGAAATTA CAAATAAAAT AAATGAACAT
 901 TTACCTTTAA AAAGAAGACA CAGCACACAT GTGAGTAGTG AATATGATAA
 951 ATATAATAAT TCTCAATCAT TTCTTATGAA TAAGAGATTA AAAGACGATC
1001 AAAATTTATC TAAAAATAAT GTTCGTAGGT ATAGCGATAC ATTAGAATTA
1051 AATATGTTAA ATAATAATAT GGGACCTAAT GAAAAGAATA ATGAATATAT
1101 TTCGAAAATG AATAAAGATC ATTATATATT AAATCCCAAC AATTATAATA
1151 AATATAATAA TAACAACAAT TGTTTCAATA ATATGAAGAA CTCTTCCGTT
1201 TTATATGAAT ATAACAAAAA AAATCTTTCA CATATGAAAC AAAATGATAA
1251 TCATCTCAAT AAATCGGTCG CTTCACATTA TGAAGAAAAC AATCACCCTT
1301 TACTTCATAC CTGTTTTTTT AAAAATGCGG AAGATTTTGA GAACAACGAT
1351 ATTAAAAGGA AAGgtaacca ccacacacaa ataaatatat acatatatat
1401 aatatatata tatatatata tgtgtgtgtg tgtgtgtaca tgtttgtgtt
1451 tttatttgtg tttatatttt tgttatatgt gtaattattt atattattgt
1501 acaaaagtgg tatccacaaa atgaataatc cattaatatt atcttttatt
1551 ttatttttatt ttatttttatt tcattttatt ttatttttatt ttatttttatt
1601 tcattttaat ttaatttaat tttattattt ttttttttt ttagAAAAAG
1651 TCGAATCCAA CGAAGAAGAC GAATTTGTCA TGAAAAAGGA CGCGGAATAT
1701 GTGTTTAGTC AAAAGTTTTT TCAAGATATT TATTCTAATA TTAAGAGCAA
1751 AGGGGAATTA AATTTTATAG ACGAGTTGCT ACAATTAGAT GAAGAGAATT
1801 ATATTAGTAA AAGTAAGTTG AATAAAATTG TTGAGAATGC AAAGAATAAA
1851 GAAATGAAGT ATCATTATAT TGATAGGATG TTTTTATATC GACATGCAAA
1901 AAATGTTATA GATGATGCTG ATTATGAAAA TTACAAAAAT AAATGTAGAA
1951 GTGAATATAA ATATTTAGAT GTACCATTCC CAAATTTGTG TGATATTATG
2001 AATCTTAAAC GTATTAGTAA CGATGACGAA ATTGATGACA CAGACGAATT
2051 TTATGATGCA GAAGTTGCAT TATTAGAGGA ATATTATTCA AGATGTAATA
2101 GACAAAAACA AGGTAAAGGT AATGATATTT TCTTAGATAA CAAAAAACAC
2151 AAAAAAAATA TAGAAAAGCA AAAAGATAAA AAAGGAAAGG AAAAAATAAA
2201 AAAAAATCAA CAAGAATTAA ATGATGATCA TAATAATAAA ATTATTTTAA
2251 AAAATAATAA GCTACATTTC AATAAAAATA ATGTAACAGA AGATTTATCT
2301 TTATTAGAAA AAAGAGATAA ATTAATGCAT TTTATGAATA AAATGAAAAG
2351 ACAAAAAGAT TCCTTTTATG AATCTATTAT AGATGCTCCA GACTTTTCTA
2401 AATTACTAGA ACCTGTTTTC TCATTAAACG AAAGCTTCTT ATTATCACAT
2451 CAATTATTTA ATGTACAATA TGCAGCACAA TTAGGACCTG TTGTATATCT
2501 TACAAAAACG GAGGATGAAA ATTATATATA TAGAGCTATT GAGGTAAGTA
2551 GACTCTTTGA AGAAAAAGTG AAATCTATTC TTGATAATCA AAAAAATCAT
2601 TCGGGTATGA AAAATAAAAG TGATTCATAT GATTGTTTTA CAAATGAAAA
2651 AAATCCATTC TTACATGAAC TAGATGTCAA ATATTATCTT CGTATCCCAA
```

```
2701 TGAGTACTGG ATGGAATCAT TTCGGTTATT TAAAAAATCA AAATAATGTC
2751 CTATTTTTTA GACGACCTAA AAATAATTAA
```

7.2.2. Aminoacid sequence

```
   1 MATNSNNNNS SNNNNNLENI NLSLHKIFNC RHSVPSKFIE DEKENIRKRR
  51 CTVAHMYEKN INSKNTNYDY LTYNFNNSIR KRRKYSPTIQ TQLYKKYSPL
 101 KSRIGLRNSV DESIKKSACI RSIVNNTIKN KTRDSSYIRN ENKSCYIGDK
 151 NNKIIYEGSK YNEKNNYIDE NMNDRKMYIN KNLHDTYIMS NTTQSDNFFR
 201 SKNINRINSL ITNRETAPIY MNSESTLSSF NFEPNVEQKH SKLTLDMKST
 251 IYIPSDMSLF NKNKYSFISN MSLEDLKKMN NEYTSKNNYN VEITNKINEH
 301 LPLKRRHSTH VSSEYDKYNN SQSFLMNKRL KDDQNLSKNN VRRYSDTLEL
 351 NMLNNNMGPN EKNNEYISKM NKDHYILNPN NYNKYNNNNN CFNNMKNSSV
 401 LYEYNKKNLS HMKQNDNHLN KSVASHYEEN NHPLLHTCFF KNAEDFENND
 451 IKRKEKVESN EEDEFVMKKD AEYVFSQKFF QDIYSNIKSK GELNFIDELL
 501 QLDEENYISK SKLNKIVENA KNKEMKYHYI DRMFLYRHAK NVIDDADYEN
 551 YKNKCRSEYK YLDVPFPNLC DIMNLKRISN DDEIDDTDEF YDAEVALLEE
 601 YYSRCNRQKQ GKGNDIFLDN KKHKKNIEKQ KDKKGKEKIK KNQQELNDDH
 651 NNKIILKNNK LHFNKNNVTE DLSLLEKRDK LMHFMNKMKR QKDSFYESII
 701 DAPDFSKLLE PVFSLNESFL LSHQLFNVQY AAQLGPVVYL TKTEDENYIY
 751 RAIEVSRLFE EKVKSILDNQ KNHSGMKNKS DSYDCFTNEK NPFLHELDVK
 801 YYLRIPMSTG WNHFGYLKNQ NNVLFFRRPK NN
```

7.3. PF3D7_0105900 DNA binding protein, putative

7.3.1. Genomic DNA sequence

```
   1 ATGCTGAAAG GATTTAAGCA TATTTTAAAC ACATCACATA TTCTTTCATT
  51 AGATTTTTCT TTTGGCGCAC GTTTTTATAA ATCATGTTTT TCTTCGCGTA
 101 CAACATATGA AAATAATACA TATGAACAAT TGGAGGCTCT AAAATTTCCT
 151 GGGCTTGTTA TATATGTTAA TAAAGATAAT ATAGAAAAAT ATCAAGAGAA
 201 CATTTTGAAG TATTTCAATA CAAATGTTAT TGGATTCGAC ACGGAATTTA
 251 TTATTGATAT AAATGAAAAA GAGAATAATA ATGAGAACAG ATCAATAAGT
 301 TGTTATATTA AAAATGGAAA GGATAATAAT TATATAAATT CACAATTAAT
 351 AAATATATTT AAAAAAAAAA AAAAAAATTA TGCATATAAC TTATGTAATA
 401 ATGAAAAGAA TAAAATTTTA TGTTTAATTC AATTATGCTC TTCTGATTTA
 451 TGTTTTGTAT TTAATATTCA CAAATTAAAT GGACATATCC CTATAAGCGT
 501 AAAAAATATT CTAGAGAACG AAGAAATTAT AAAAGTTGCT CATGATATTA
 551 AAAATGAAAA GGATATGTTT CTATCAAATA ATATACAAAT AAAAAATGTT
 601 TTTGATTTAT ATAATTATGC CATTGATAAT TTTATATATC CTCCTTCATT
 651 ACAATCTTTA GTTAAAATAT ATCTTAACAA ATTCTTAGAT AAAAAATTTA
 701 GACTATCCAA CTGGTTAAAT TATTCCTTAT TACAAGAACA AATACTCTAT
 751 GCAGCAGTCG ATGCATATGC ATCTAGACAA ATATATTTTC ATTTGGACGA
 801 AAACAAAAAA AAAAGTCAAT CTTATATTCT TAATTATATC CTACAAGAAA
 851 ACCAAATAAA ATCATGTTAT CAAAAGTTTA ATAAATATAC ATATAAAAAA
 901 AAGGACCTCA ATAATGAAAA TATCATAAAA ATAGAAGAAA AAAACATACA
 951 AAATATCGAA TCTATCAATA ATACTATACA CAATCAAAAA AAAAAAAATA
1001 ATATAAACAA TCAACATCAA AATGAATATG ATTCAAATAT TAAACAATTA
1051 CAATCTTTCT ATACACATAG TAATCAAAAC AAGAAAAATT ATGAATTTGT
1101 AGAAAAATAC AAACTTCAAT TAATAAACAG TTTAAAAAAT GAAATTCATA
1151 ACAAGTGTAC TAATATGACT AATATCTCAT TTGTCCAAGA AATGACTTTC
1201 ACAAATAATA CTTATAAAAA TATTTTGTCC TTAAAACATA ATCAAAATAA
1251 TTATAATTTC ATAAAGTTCT CTTCGGTCAA TTATGATGAG GAAATAAATT
1301 CATGCTACCA AATTTTAACA TACCTTGATC ACACGCTCTG CACATAA
```

7.3.2. Aminoacid sequence

```
   1 MLKGFKHILN TSHILSLDFS FGARFYKSCF SSRTTYENNT YEQLEALKFP
```

```
  51 GLVIYVNKDN IEKYQENILK YFNTNVIGFD TEFIIDINEK ENNNENRSIS
 101 CYIKNGKDNN YINSQLINIF KKKKKNYAYN LCNNEKNKIL CLIQLCSSDL
 151 CFVFNIHKLN GHIPISVKNI LENEEIIKVA HDIKNEKDMF LSNNIQIKNV
 201 FDLYNYAIDN FIYPPSLQSL VKIYLNKFLD KKFRLSNWLN YSLLQEQILY
 251 AAVDAYASRQ IYFHLDENKK KSQSYILNYI LQENQIKSCY QKFNKYTYKK
 301 KDLNNENIIK IEEKNIQNIE SINNTIHNQK KKNNINNQHQ NEYDSNIKQL
 351 QSFYTHSNQN KKNYEFVEKY KLQLINSLKN EIHNKCTNMT NISFVQEMTF
 401 TNNTYKNILS LKHNQNNYNF IKFSSVNYDE EINSCYQILT YLDHTLCT
```

7.4. PF3D7_0106000 conserved Plasmodium protein, unknown function

7.4.1. Genomic DNA sequence

```
   1 ATGCGATCCA AATATTACAA GGAAGAAGAA AATAAAGGTT TTATAAAAAC
  51 GCATTATTTT CGTAAAATCG ATACAGAGAA AATCGACAAG AAATTAATAA
 101 GCCTTGAGAA TAATTTTAAT GGTGATGATG TATATTTAGA CATTGTAATA
 151 CATGATAAGG AACGAAATAA TTTTGATTTT TTCCTTATGA GAATAACAGA
 201 AAGTTCAAGT GTTAATAATA GTTTAGATGC ATGGAATCAT ATCGATATAA
 251 CTAATATATA TAATTATATA TTATATGATA ATAAATATTG TAGTGATATA
 301 ATAAATGAAA AAAAAGGATA TTTAATATTG AAATTAAAAT ATACGAATGA
 351 AAATAATATT ATTACATCTT ATTTTAAAGT TCATTGTAGA AATACAAAAT
 401 GGGAAAATGA TAAGAAAGTA TGGCATATAC CTTTATTTTA TATATTTGAA
 451 ATGTCTAAAC TTACCTTGTT TTTAGGGGGT ACCGTTAGTG ATACCGTTCT
 501 TTATTATTTA TGTAAATTAT TTCATCATTT TTCTAGTATC AAAAATGTAA
 551 ATAGCAATGT TAAAATGAAT GAATTATCTA AGGATCAGCT TATAAAAACG
 601 GATGAAATAT GTGACACTAC CCATAAGGAA AAAAAGAACA ACGATGATGA
 651 TAATACAGAT AATTATCACA ACAATAAAAA TAATAGTAAT AATAATAATA
 701 ATAATAATAA TAATAATCAA AACAACAACA ATAATAATAA TATTGCTGTT
 751 CAGGTTAATT GCAGGAAACA AGATAAATTT TATCCCAGTA ATAATGATGT
 801 AATAAGAAAT TCAAGTCCAA AAATTATTTT AGAAAACAAA AATGAAGAAA
 851 TAAATGTTAT AGAAAAGGAT TTAACCTTAA AGGATAACGG TGATGTATTA
 901 TACAAGGAGA AAAAAATAAG AAATGATGAT GACAGGAATT ACAACACCGA
 951 TGAGGACACA CATTATGGCA ATAATGATGA TACTTATTAT GATGATGAAA
1001 GTTGTGATAA TAAAAATGAT GATTCTGTTA ATAAAAATAA TATATGTGTT
1051 AATAAAAGTG ACGATTCTGT TAATAAAAGT AATGATTGTG ATAATAAAAA
1101 TGATGATGGT GTTAATAAAA ATGATCATTG TGATAATAAA AATGATCATT
1151 GTGATAATAA GAATGACCAT TGTGATAATA TAAATGACCA TTGTGATAAT
1201 AAGAATGACC ATTGTGATAA TAAAAATGAC CATTGTGATA ATAAAAATGA
1251 CCATTGTGAT AATAAGAATG ACCATTGTGA TAATAAGAAT GACCATTGTG
1301 ATAATAAGAA TGACCATTGT GATAATAAGA ATGACCATTG TGATAATATA
1351 AATGATCGTC ATACTAACCA AGAGAATAAT GTTTCGAAAG ACTGTAATAA
1401 GAATACAACA AATGAAATAA GTTTCAACTT GGATATTTTT ATAAAGGAAA
1451 ATAAATTAAA TTTTATAGAA TATATTAAGA ATGTAAGAAT GTTCAGGATT
1501 GAACACATCA TTATAAATAA TATTGTAAAA GGTGATACCA TGTATATAAA
1551 GATAATACCA TATAATGAAG ATATCGTTAC AAAAATAAAG CAAACAAATT
1601 TTATACAATG GAATAGAACG GAAAATATAT TATTAATAAA AAAAAGTAAT
1651 TTTAAAAATT TTTATATAAA TATAATAAAA GGTTTTAATT TCAAGTTATG
1701 TTCTTATTAT GATTATTTTA AATTATTTAG ACAAAAAATT ATGGAAAATG
1751 ATTCTAAATC GTTAAAAGGA AATTTTAGTG TCACAACAAA TATAACAATA
1801 AATACCGAAT ATTTAAGTAA GAAATTTAAT AAAAGAAAAA TGGATTTTCA
1851 TAATATAGAA GAAGAAATAA CCGATAAAGG AAATGTTCTA AAACATTCCA
1901 AAAAAAAGAA AAAATATAAA AATGAGTTTG GTTATGAGAG TACAGATTCA
1951 TGTAATTCAG ATGAATTATC GAATAATGTG GATTCAAGTT ATTATGAAGG
2001 TAGAGAATTA GTAAATAAAA TAAAATTAGT TGGTGCGGCA AATAATTATT
2051 ATAAAGAAGT TATATATAAT AAATTACATA AAATAAAACA TTTACGTCCA
2101 CCTAATTATA CATATGACCC TAAAGGATTA ATTACGAAAA ATGGAGCAGG
2151 TACCAAAGGT ATTGAAATTT TTGATATGCC TAGTGATATT AATGAATGGA
2201 ATAAAATAAG TTTTTGTATT GTACCTAATG AGAAAAAGGA TATCGATTTA
```

```
2251 TATGATCCAA AAATTTTATG TAGTTTAGTT AGTGATGTTT ATTTACTTAA
2301 AGAAAAAGCA TTAGATATAA TATTGAAAAA TTATAAAAAA TGGCCTGAAT
2351 ATACTGATGT GTTTTGGAAT ACGGTATGCT CCGAAAATGA ATTTATTGTA
2401 TGTAATAAAA ACTTTAATAC AAGACAAAAA TTAGCTCATG ATAGATTATT
2451 TAATAAACAA TACTTTTATA TTTTTAATAT GGAAAGTATT AAACATTCAA
2501 ATTATTATAA TCCATTATTT TTATGTAAAG TTTTAATTAC CTTAGGTGAA
2551 GGAATCCTTG TTCAACATCC ATATGATGCA GAGTATATCA TTATCTCAAA
2601 TTCTAATGAT TTTAATGCTA TACAATTCTA TAATTATCTT CATGAAAAAA
2651 AAAAAAAAAA AAAAAAATTA CCCTTATTTG TAACTCCAAA GTTTATATAT
2701 GATTGTATTT TAAACTATTC TATTTCTTAT CCTTCAAAAA ATAAAAACCA
2751 CTTTGCCTTC TCCTCCTAA
```

7.4.2. Aminoacid sequence

```
  1 MRSKYYKEEE NKGFIKTHYF RKIDTEKIDK KLISLENNFN GDDVYLDIVI
 51 HDKERNNFDF FLMRITESSS VNNSLDAWNH IDITNIYNYI LYDNKYCSDI
101 INEKKGYLIL KLKYTNENNI ITSYFKVHCR NTKWENDKKV WHIPLFYIFE
151 MSKLTLFLGG TVSDTVLYYL CKLFHHFSSI KNVNSNVKMN ELSKDQLIKT
201 DEICDTTHKE KKNNDDDNTD NYHNNKNNSN NNNNNNNNNQ NNNNNNNIAV
251 QVNCRKQDKF YPSNNDVIRN SSPKIILENK NEEINVIEKD LTLKDNGDVL
301 YKEKKIRNDD DRNYNTDEDT HYGNNDDTYY DDESCDNKND DSVNKNNICV
351 NKSDDSVNKS NDCDNKNDDG VNKNDHCDNK NDHCDNKNDH CDNINDHCDN
401 KNDHCDNKND HCDNKNDHCD NKNDHCDNKN DHCDNKNDHC DNKNDHCDNI
451 NDRHTNQENN VSKDCNKNTT NEISFNLDIF IKENKLNFIE YIKNVRMFRI
501 EHIIINNIVK GDTMYIKIIP YNEDIVTKIK QTNFIQWNRT ENILLIKKSN
551 FKNFYINIIK GFNFKLCSYY DYFKLFRQKI MENDSKSLKG NFSVTTNITI
601 NTEYLSKKFN KRKMDFHNIE EEITDKGNVL KHSKKKKKYK NEFGYESTDS
651 CNSDELSNNV DSSYYEGREL VNKIKLVGAA NNYYKEVIYN KLHKIKHLRP
701 PNYTYDPKGL ITKNGAGTKG IEIFDMPSDI NEWNKISFCI VPNEKKDIDL
751 YDPKILCSLV SDVYLLKEKA LDIILKNYKK WPEYTDVFWN TVCSENEFIV
801 CNKNFNTRQK LAHDRLFNKQ YFYIFNMESI KHSNYYNPLF LCKVLITLGE
851 GILVQHPYDA EYIIISNSND FNAIQFYNYL HEKKKKKKKL PLFVTPKFIY
901 DCILNYSISY PSKNKNHFAF SS
```

7.5. PF3D7_0106100 V-type proton ATPase subunit C, putative

7.5.1. Genomic DNA sequence

```
  1 ATGAGTGAAA TTCCCATGTG TTTGTTCATA GCTTGTTCAA CACGAGATAA
 51 TACAAGCCGT GAATATATTT ATACTATATT GAAGAATCGT CTTTTAGGTA
101 GTCATATATG TATAGATACG AATATATTGG ATGTGCCTAC GAATATAAAA
151 TTTTGTTCAT TTGATGATTT ATTAAAGTGT GCTGATGATT TACAGAAATA
201 TGATAGTTAC GCATATGGTT GTTTAAAAAA GATAGAAAAA ATAGCAAAAG
251 AATATGATGA AAATATTGAA TTGAAAATAA TATATCAACG TCAACATATA
301 AATATAGATC AATATATAAG AAGATTTACT TGGGATGATG CAAAATATCC
351 AAGGAGTAGA TCTTTAACGG ATACTATTGA TGTTATGATA AATAATATTA
401 CAAAATTATC TGATGAAATT CAAATAAAGT CAAGTATGTT AAATGATTTA
451 AAAGAAAAGA AAAAAAAAGA AGTACCAAAA AATGATTCCA ATAATTTCTT
501 TTTAAGAAAT TTGAATGAAA TATTAACTCC ACAAACTGTT AGCGAAACCG
551 ATTTTATAGA AACAGAATAT CTAACAACAC TTATAGCTTA TGTACCTAAA
601 AATTCTATAG ATGATTGGTT AAATAATTAT GAAAAATTTT CATCCTATGT
651 TGTACCTAGA TCTACAGAAC AATTTAAAGA TTTAATAGAT AAAGATGGAA
701 ATACATTATG GAAAGTTTTT GTTTTTAAGA AATTTGCAGA AGATTTTAAA
751 AAAGAAGCAA AAGTTAAAAA ATTTGTTGTA AAATCATTTA AATATGATGA
801 AAAACAATAT AATGATATGA TGGAATCGAG AACAAAAGTA GAAGCAGAAA
851 TCATAAGACA AGAAACTTTT CTAAGACGCA TGTGCTTAGC CGCTTTTTCA
901 GATATATTTA TTGCATTCAT TCATATTAAT ATACTTCGAG TCTTTTGTGA
```

```
 951 ATCTGTATTA CGATTTGGTG TTCCACCTAA TTTTGCTTCA TTTAGTATAA
1001 GAATTAATGG AGAAAGTAAA GAAAAAAAAG TCAGAAAAAA ATTATACGAC
1051 ATTTTTTCAT CATCTGATTC TATAGGAAAG AATTATATAA AAAGATCTGA
1101 TGAAAATGAT GAAGAAATAT ATCCCTACGT TTCGGTGTCC TTTAAAATAT
1151 GA
```

7.5.2. Aminoacid sequence

```
   1 MSEIPMCLFI ACSTRDNTSR EYIYTILKNR LLGSHICIDT NILDVPTNIK
  51 FCSFDDLLKC ADDLQKYDSY AYGCLKKIEK IAKEYDENIE LKIIYQRQHI
 101 NIDQYIRRFT WDDAKYPRSR SLTDTIDVMI NNITKLSDEI QIKSSMLNDL
 151 KEKKKKEVPK NDSNNFFLRN LNEILTPQTV SETDFIETEY LTTLIAYVPK
 201 NSIDDWLNNY EKFSSYVVPR STEQFKDLID KDGNTLWKVF VFKKFAEDFK
 251 KEAKVKKFVV KSFKYDEKQY NDMMESRTKV EAEIIRQETF LRRMCLAAFS
 301 DIFIAFIHIN ILRVFCESVL RFGVPPNFAS FSIRINGESK EKKVRKKLYD
 351 IFSSSDSIGK NYIKRSDEND EEIYPYVSVS FKI
```

7.6. PF3D7_0106200 conserved Plasmodium protein, unknown function

7.6.1. Genomic DNA sequence

In lower case, non-coding DNA sequences.

```
   1 ATGGAAAATA TAAATAGAGT AAATAAATAT GACAACCCAA ATGAAGCTAT
  51 CAAAAATATG GTTGACAAAA TAATAAATAA GTTGAATAAG ACACAGAAAG
 101 ATTCTTCTAA AAGGATATAT TATAGCAGgt ttttatattt ttataaatta
 151 taatataata aaattaatta tatatatata tatatttata aacacataat
 201 gtacttatgt atgtgaaatg aaaacataat tattttgtgc atttatatat
 251 atatatatgt atatttattt atatttatat ttatgatttg tttttgtatt
 301 atatttcttt tgcttatttg atgtacattt taatttttt tttatgaatt
 351 gaaaccactc ttagGAAGGA AATGATGAAG TACTTTTTAG ATGCTCAGGA
 401 TATATTTGAA TATCATGATG TGGGGAAAAA AGGAGAAGTT GATATAACAT
 451 TATTTCCTAA AATGGCTAGA CAATTAAAAC AAGTATATGA TATAAGAGAT
 501 ATAAATAATT TTAAAAAAGA AATGAAAATT AAAAAAATTT ATAAGATGGA
 551 TTTACAATTA TTTTTTACTT TATTAAAAAG AAAAATACTT TATTCCATAA
 601 ATAATAGTAA TAATAATGAA AATGACAATT CATCCTTTAG ACAACATTAT
 651 GACATTTTAG ATATGAAAAA AAAACAATTA TTAGATGTAG ACGAATTAAG
 701 AACTTATTTA GGATTAATGG GTGATAAAAT AAATCCAGAT GATTTTAATA
 751 TTTTATTAAG ATATAACTTG ATAAATAATC ACAGAATAAA TAAAGATGAT
 801 ATTGTATTAG ATGAAAATAA AGAAATTAAA AATATATCTT TTAATGCGTA
 851 CGTTGACATG TTAACATGTT ATAAATATAT ATGA
```

7.6.2. Aminoacid sequence

```
   1 MENINRVNKY DNPNEAIKNM VDKIINKLNK TQKDSSKRIY YSRKEMMKYF
  51 LDAQDIFEYH DVGKKGEVDI TLFPKMARQL KQVYDIRDIN NFKKEMKIKK
 101 IYKMDLQLFF TLLKRKILYS INNSNNNEND NSSFRQHYDI LDMKKKQLLD
 151 VDELRTYLGL MGDKINPDDF NILLRYNLIN NHRINKDDIV LDENKEIKNI
 201 SFNAYVDMLT CYKYI
```

8. Appendix II: Plasmid maps

8.1. pUF1-CAS9

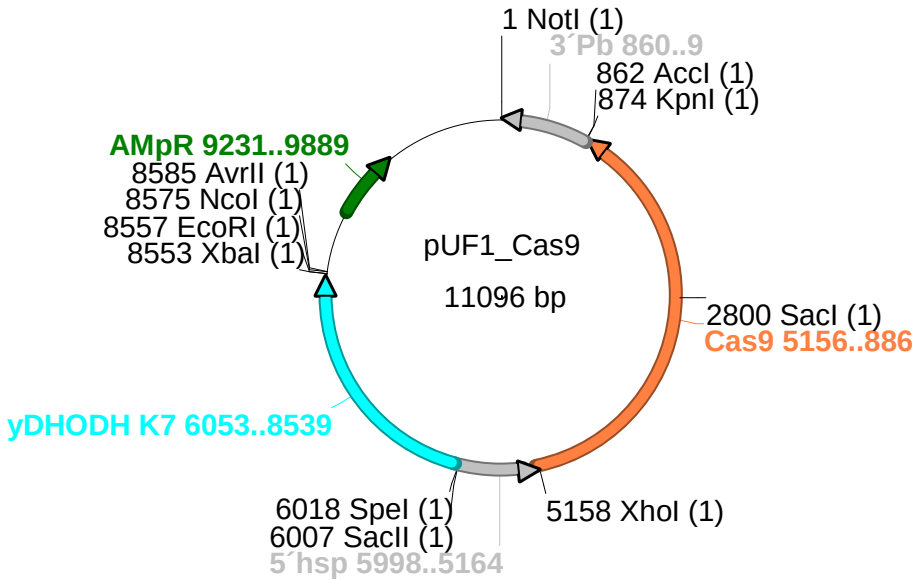

The vector pUF1-Cas9 encodes the sequence of the *Cas9* endonuclease flanked by nuclear localization signals (NLS). Its expression is regulated by the promoter region of the heat shock protein 86 (5' hsp) and the 3'UTR region of the *P. berghei* dhfr (3' Pb dhfr). The selection marker of the plasmid is the yeast dihydroorotate dehydrogenase gene (*ydhodh*). This plasmid kindly was provided by Dr. José Juan Lopez Rubio [78].

8.2. pL6 plasmids

The pL6 plasmid bears the sgRNA-expression cassette. The expression of the sgRNA is regulated by the promoter and the 3'UTR region of the *P. falciparum* U6 snRNA polymerase III (5' U6). Positive selection is achieved with the selection marker human dihydrofolate reductase gene (*hdhfr*) and negative selection marker with the bifunctional yeast cytosine deaminase and uridyl phosphoribosyl transferase (*yfcu*). The original pL6 vector was kindly provided by Dr. José Juan Lopez Rubio [78].

8.2.1. pL6-HRA-guide6

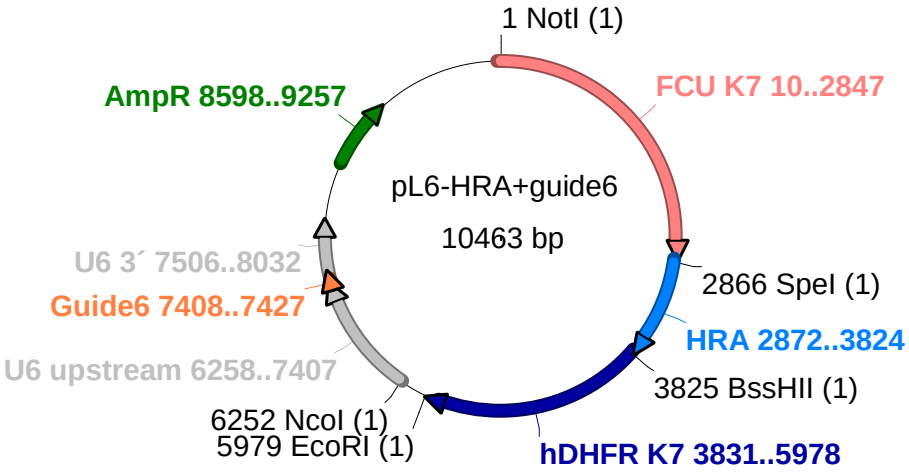

The original pL6 vector was digested with the enzyme BtgZI and the PfATP6 guide 6 sequence was cloned into the vector using the In Fusion cloning approach (primers [49] and [50]). The pfatp6 homology region containing the single nucleotide polymorphisms coding for the double mutations A108T and A109T (HRA) was amplified from Dd2 cDNA with the primers ATPase6-HRA(-79)-SpeI-for (39), ATPase6-HRA-855-BssHII-rev (40), ATPase6-620-1080-for (2) (43) and ATPase6- 620-1080-rev (2) (44) and cloned into the vector using the restriction enzymes SpeI and BssHII.

8.2.2. pL6-HRAsi-guide6

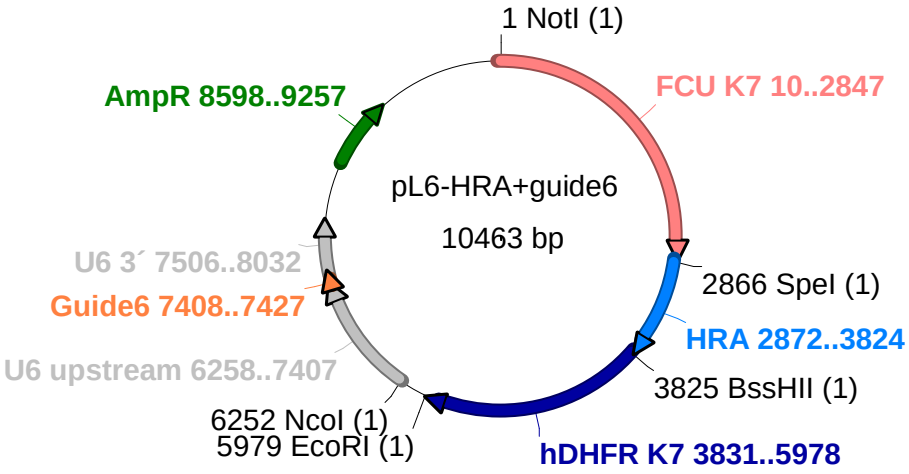

The original pL6 vector was digested with the enzyme BtgZI and the PfATP6 guide 6 sequence was cloned into the vector using the In Fusion cloning approach (primers (49) and

(50)). The pfatp6 homology region containing the silent mutations coding for the aminoacids residues A108 and A109 (HRA) was amplified from Dd2 cDNA with the primers ATPase6-HRA(-79)-SpeI-for (39), ATPase6-HRA-855-BssHII-rev [40], ATP6 HRA sil-for (47) and ATP6 HRA sil-rev (48) cloned into the vector using the restriction enzymes SpeI and BssHII. This vector was generated to test the efficacy of the guide 6.

8.2.3. pL6-HRB-guide7

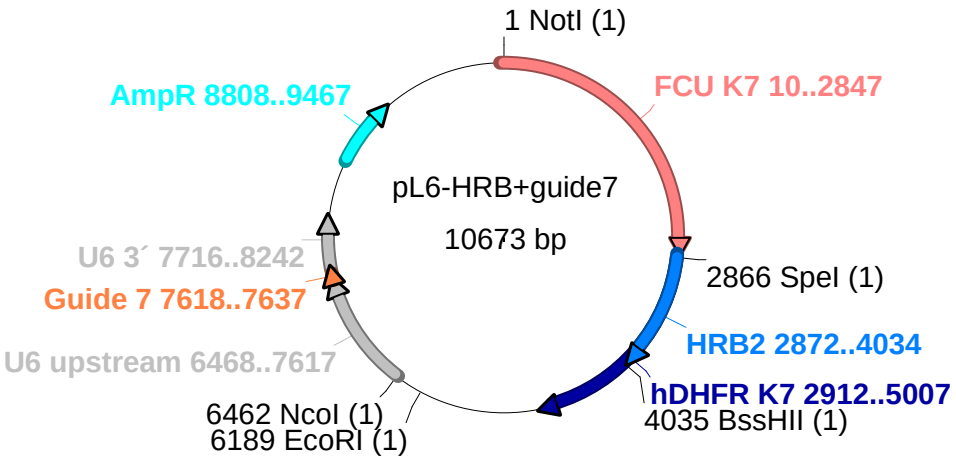

The original pL6 vector was digested with the enzyme BtgZI and the PfATP6 guide 7 sequence was cloned into the vector using the *In Fusion* cloning approach (primers [51] and [52]). The pfatp6 homology region containing the single nucleotide polymorphism coding for the mutation F972Y, as well as shield mutations (HRB) was amplified from Dd2 cDNA with the primers ATPase6-HRB-2269-SpeI-for (41), ATPase6-HRB-3409-BssHII-rev (42), ATPase6-shield(guide7)-for (45) and ATPase6-shield(guide7)-rev (46) and cloned into the vector using the restriction enzymes SpeI and BssHII

8.3. pARL-gene-HA plasmids

The coding sequence of the genes present in the DNA locus amplified in the Dd2 parasites resistant to 1 µM SC83288 were amplified from Dd2 cDNA and cloned into a pARL-3xHA tag (provided by Dr. Sonia Moliner Cubel) using the restriction enzymes XhoI and AvrII. The expression is regulated by the PfCRT promoter and the 3'UTR region of the *P. berghei* DT. The original pARL1a+ vector was kindly provided by Prof. Tim Gilberger [246].

8.3.1. pARL-0105800

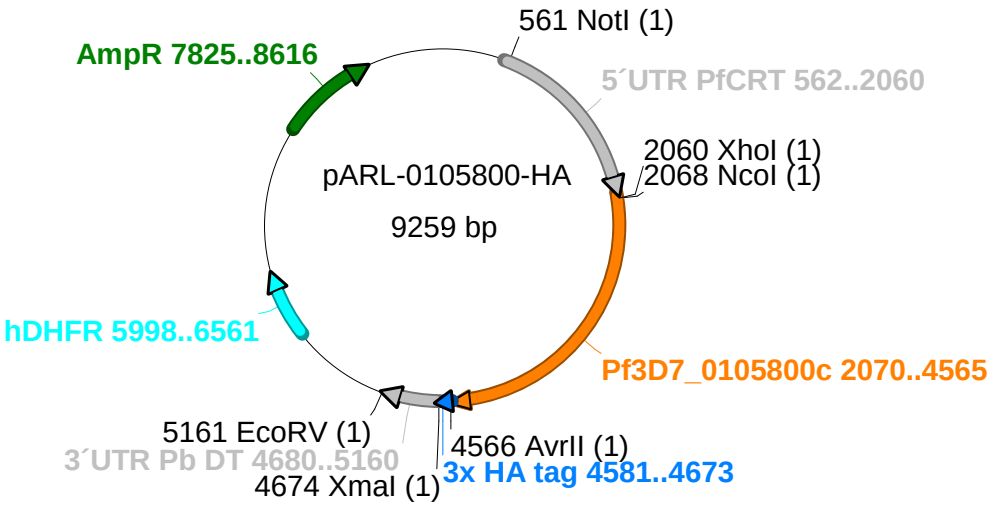

The primers 800-XhoI-for (25) and 800-AvrII-rev (26) were used for the amplification of the gene coding sequence.

8.3.2. pARL-0105900-HA

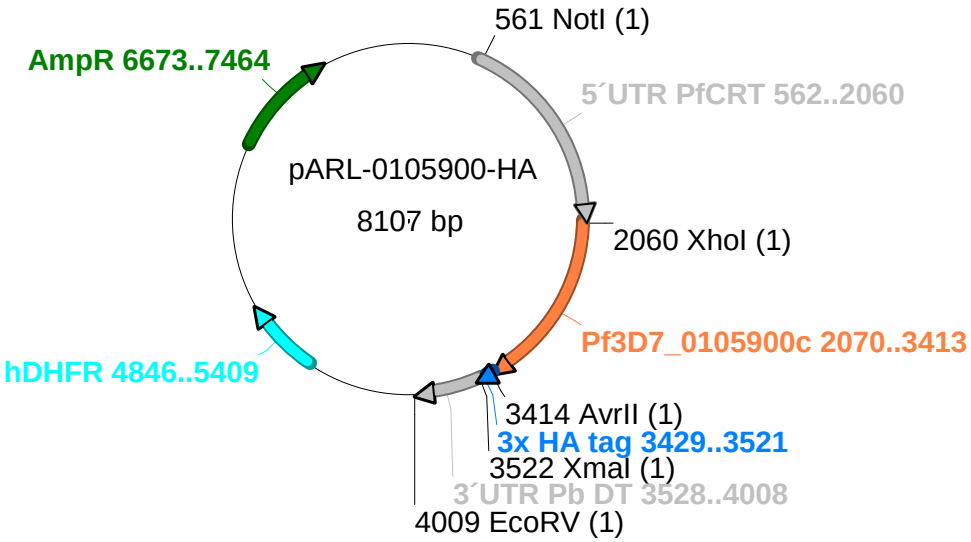

The primers 900-XhoI-for (27) and 900-AvrII-rev (28) were used for the amplification of the gene coding sequence.

8.3.3. pARL-0106000-HA

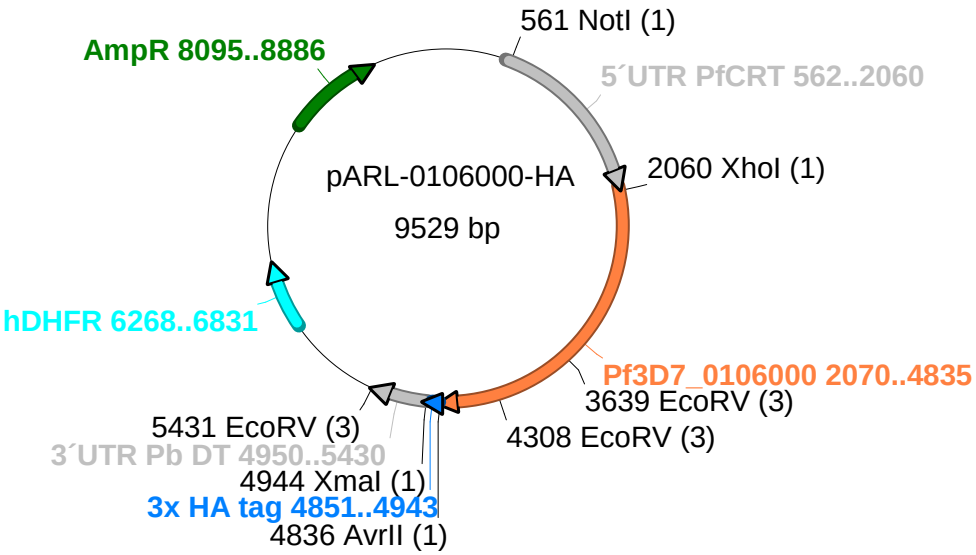

The primers 000-XhoI-for (29) and 000-AvrII-rev (30) were used for the amplification of the gene coding sequence.

8.3.4. pARL-0106100-HA

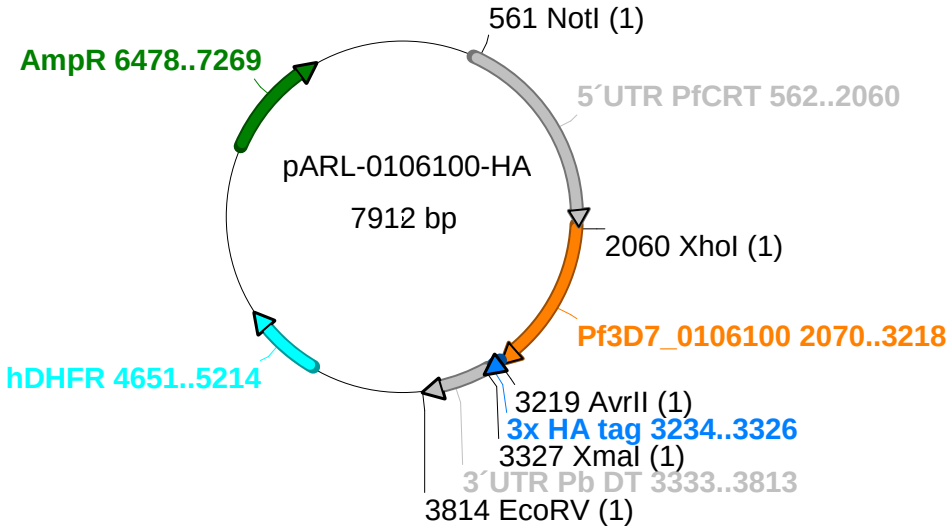

The primers 100-XhoI-for (31) and 100-AvrII-rev (32) were used for the amplification of the gene coding sequence.

8.3.5. pARL-0106200-HA

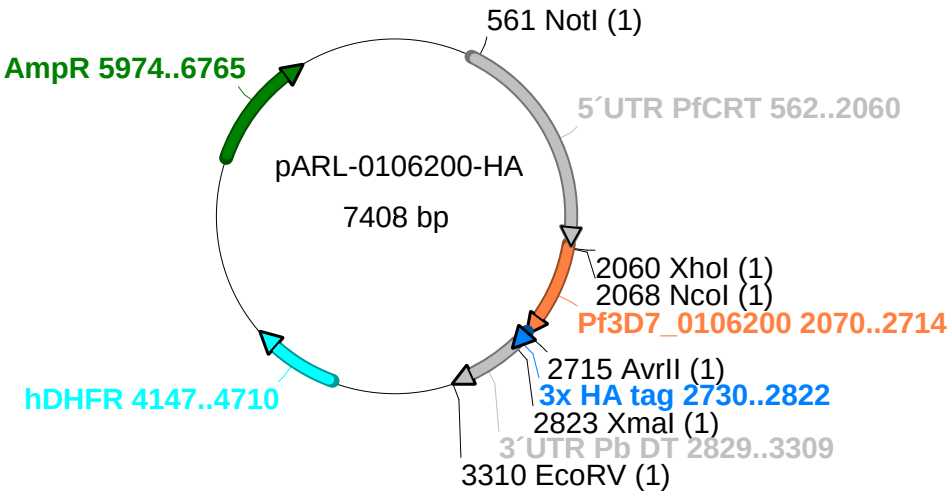

The primers 200-XhoI-for (33) and 200-AvrII-rev (34) were used for the amplification of the gene coding sequence.

8.4. pHBIRH-ATP6(WT)-HA

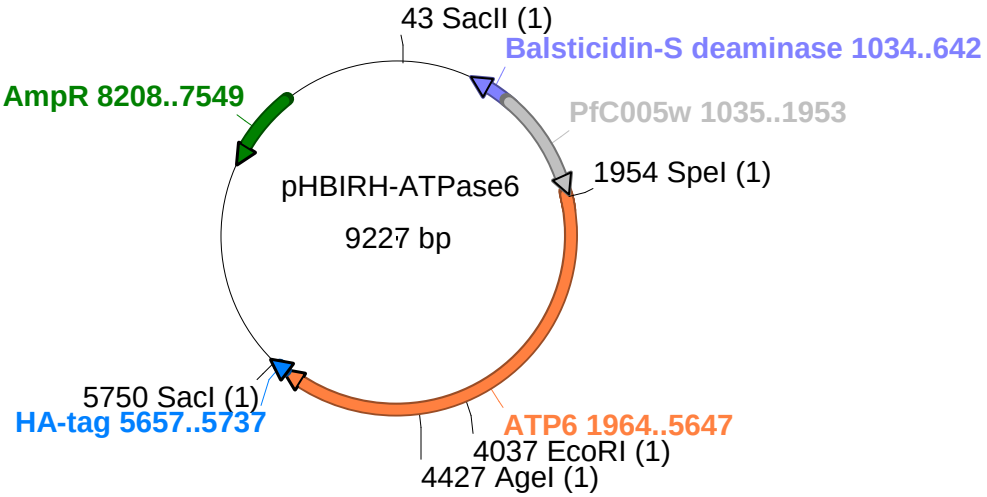

The coding sequence of ATP6 was amplified from a Geneart plasmid containing the *Saccharomyces cerevisiae* codon optimized version of pfatp6, tagged with a sequence coding for 3xHA tags on the c-terminal end, using the primers ScATPase6-SpeI-for (35) and ScATPase6-SacI-rev (36). This fragment was cloned in the pHBIRH vector using the restriction enzymes SpeI and SacI. A bi-directional P. falciparum promoter (the intron of PlasmoDB: PFC0005w) drives expression of the blasticidin- S-deaminase gene and atp6. The original pHBIRH vector was kindly provided by Dr. Christian Epp [211].

8.5. pHBIRH-ATP6(A108T, A109T)-HA

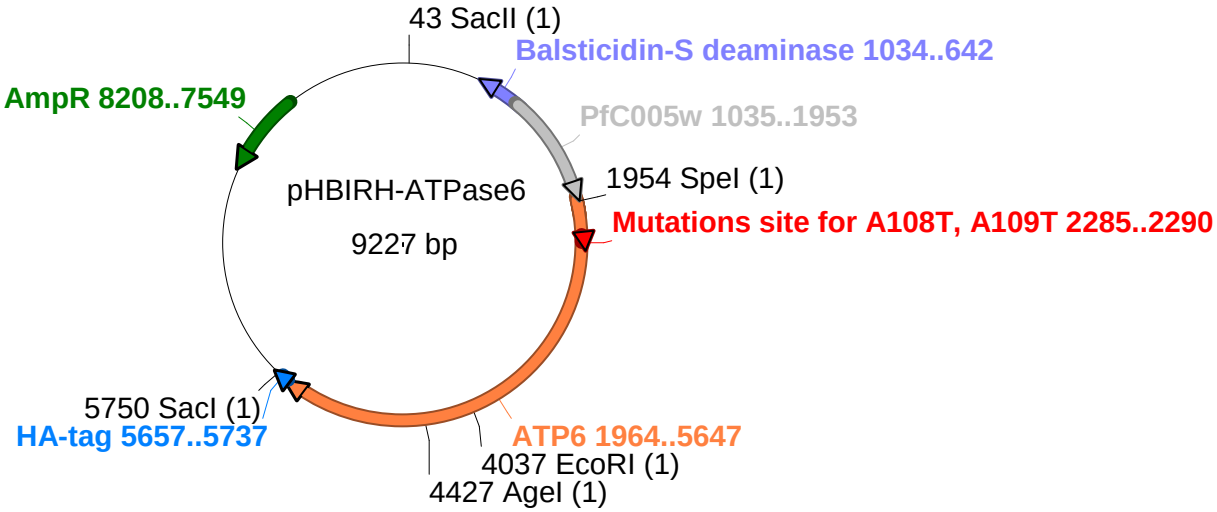

A similar approach was use as for the generation of the pHBIRH-ATP6(WT)-HA vector. The primers ScATPase6-mut1/2-for (37) and ScATPase6-mut1/2-rev (38) were used to generate the atp6 fragment bearing the single nucleotide polymorphisms coding for the double mutation A108T and A109T.

9. Appendix III

To investigate the possible inhibitory effect of SC83288 on protein synthesis, a [^{35}S]-methionine incorporation assay was performed, together with Dr. Chaitali Chakraborty (Zentrum für Molekular Biologie (ZMHB) in Heidelberg, in Prof. Christine Clayton´s lab). Treatment with SC83288 for 1 hour at concentrations corresponding to different multiples of the IC_{50} value (0.01x, 0.1x, 1x, 10x and 100x) showed no difference in [^{35}S]-methionine incorporation (Figure 3.35).

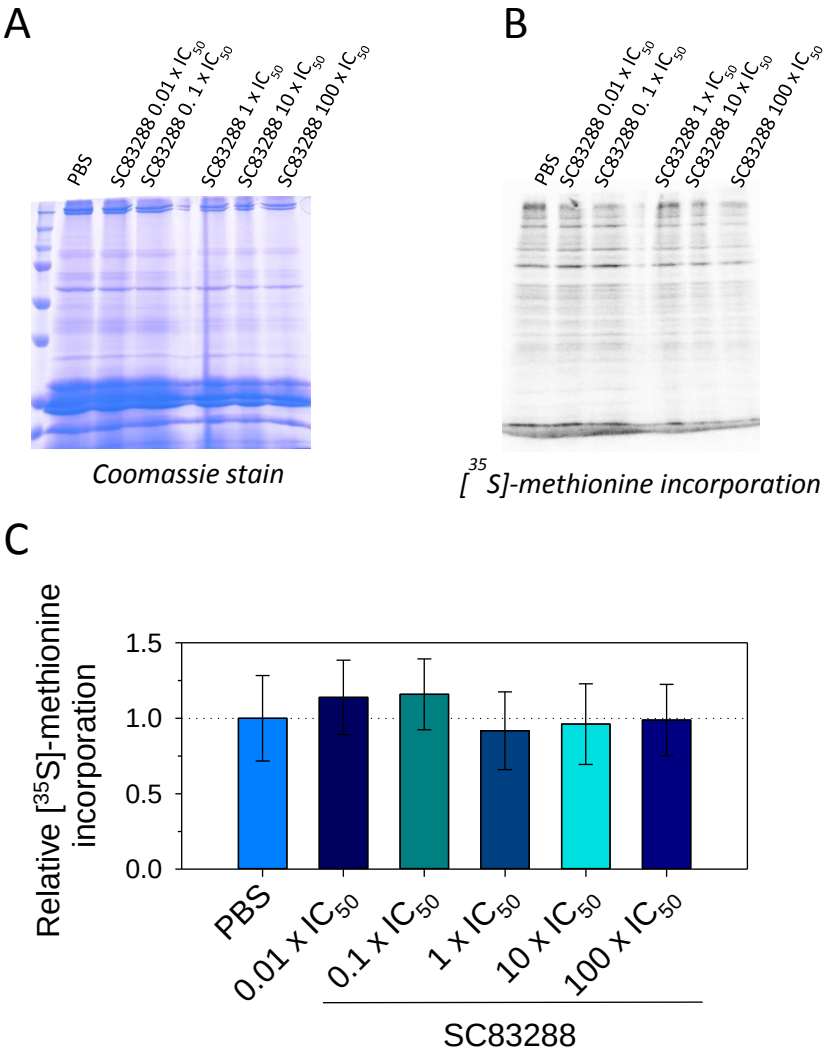

Figure 9.1: [^{35}S]-methionine incorporation assay in *P. falciparum* 3D7 in presence of SC83288. Parasites were starved in labeling medium (DMEM without methionine) and treated with various concentrations of SC83288 (0.01x, 0.1x, 1x, 10x or 100x IC_{50}) for 1 hour at 37°C, before addition of [^{35}S]-methionine and further incubation for 30 minutes at 37°C. Proteins were separated by SDS-PAGE and the total amount was visualized using Coomassie staining (**A**) and [35S]-methionine incorporation was visualized by autoradiography (**B**). (**C**) Quantification of the [^{35}S]-methionine incorporation in newly synthetized proteins. Mean ± SD of 1 experiment, based on quantification on 3 protein bands.

10. Publications and Conference presentations

The following publications emerged/will emerge from this work:

Pegoraro S, **Duffey M**, Otto TD, Wang Y, Rösemann R, Baumgartner R, Fehler SK, Lucantoni L, Avery VM, Moreno-Sabater A, Mazier D, Vial HJ, Strobl S, Sanchez CP, Lanzer M. SC83288 is a clinical development candidate for the treatment of severe malaria. *Nat Commun.* 2017 Jan 31;8:14193. *doi: 10.1038/ncomms14193*.

Duffey M, Lanzer M. Profiling the antimalarial drug candidate SC83288 against artemisinins in *Plasmodium falciparum. Manuscript under in review in Malaria Journal*.

Duffey M, Staines HM, Krishna S, Lanzer M. The endoplasmic Ca^{2+} pump (PfATP6) mediates resistance to the antimalarial drug candidate SC83288. *Manuscript in preparation.*

The results of this work were presented in the following scientific conferences:

BioMalPar XII: Biology and Pathology of the Malaria Parasite (Heidelberg, Germany). 18th -20th May 2016. Poster: “SC83288, a novel clinical development candidate for the treatment of severe malaria”.

German Center for Infectious Research (DZIF) Annual Meeting (Köln, Germany). 24th - 26th November 2016. Poster: “SC83288, a novel clinical development candidate for the treatment of severe malaria”.

28th Annual Molecular Parasitology Meeting (MPM) (Woods Hole, MA, USA). 10th – 14th September 2017. Poster: “The endoplasmic Ca^{2+} pump (PfATP6) mediates the resistance to the preclinical drug development candidate SC83288”.